THE ECONOMICS OF FUEL DEPLETION IN FAST BREEDER REACTOR BLANKETS

by

Shelby Templeton Brewer

B.A., Columbia University (1959)
B.S., Columbia University (1960)
M.S., Massachusetts Institute of Technology (1966)

Submitted in Partial Fulfillment

of the Requirements for

the Degree of Doctor

of Philosophy

at the

Massachusetts Institute of Technology

October 1972 (i.e. Feb. 1973)

PART I

Signature of Author _____

Department of Nuclear Engineering, October 1972

Certified by _____

Thesis Supervisor

Certified by _____

Thesis Supervisor

Accepted by _____

Chairman, Departmental Committee on Graduate Studies

THE ECONOMICS OF FUEL DEPLETION IN FAST BREEDER REACTOR BLANKETS

by

SHELBY TEMPLETON BREWER

Submitted to the Department of Nuclear Engineering on October 24, 1972 in partial fulfillment of the requirements for the degree of Doctor of Philosophy.

ABSTRACT

A fast breeder reactor fuel depletion-economics model was developed and applied to a number of 1000 MWe LMFBR case studies, involving radial blanket-radial reflector design, radial blanket fuel management, and sensitivity of energy costs to changes in the economic environment.

Choice of fuel cost accounting philosophy, e.g. whether or not to tax plutonium revenue, was found to have significant effect on absolute values of energy costs, without, however, distorting design rankings, comparative results, and irradiation time optimization.

A single multigroup physics computation, to obtain the flux shape and local spectra for depletion calculations, was found to be sufficient for preliminary design and sensitivity studies. The major source of error in blanket depletion results was found to be the assumption of a fixed flux shape over an irradiation cycle; spectrum hardening in the radial blanket with irradiation is of minor importance.

The simple depletion-economics model was applied to several 1000 MWe LMFBR case studies. Advantages of a moderating reflector were found to increase as blanket thickness was reduced. For a 45 cm radial blanket, a beryllium metal reflector offered little improvement, in blanket fuel economics, over sodium; for a 15 cm blanket, beryllium increased net blanket revenue by about 60%. An improvement of about 50% in net blanket revenue resulted when each radial blanket annular region was assumed to be exposed to its own local optimum radiation time. Optimum radial blanket irradiation time and the net blanket revenue (mills/KWHe) at this optimum were found to be approximately linear in the unit fuel cycle costs, i.e. fabrication and reprocessing costs ($/kgHM) and fissile market value ($/kg).

Thesis Supervisor: Edward A. Mason
Title: Professor of Nuclear Engineering

Thesis Supervisor: Michael J. Driscoll
Title: Associate Professor of Nuclear Engineering

ACKNOWLEDGEMENTS

The author is indebted to his supervisors, Professors Michael J. Driscoll and Edward A. Mason, for their guidance in the course of this work.

Financial support from the U.S. Atomic Energy Commission under contract AT(30-1)-4105 is gratefully acknowledged.

Computer calculations were performed at the MIT Information Processing Center.

Dr. W. W. Little and Mr. R. W. Hardie of Battelle Northwest graciously provided the computer program 2DB and cross section data used as a starting point in this work.

This thesis was ably typed by Mrs. Rosemarie Wilkes and Mrs. Linda Ilsley. Their patience and conscientiousness in completing this task are appreciated.

Several MIT faculty members provided encouragement and counsel during the author's career at MIT. They are Professor Edward A. Mason, the late Professor and USAEC Commissioner Theos J. Thompson, Professor Michael J. Driscoll, Professor Norman C. Rasmussen, Professor Manson Benedict, and Professor Thomas Olson.

Thanks are due the author's wife, Marie Anesten, whose patience and fortitude were invaluable. Finally, the author recognizes his little son Jens whose "help" in arranging drafts of this report provided a measure of comic relief.

TABLE OF CONTENTS

LIST OF FIGURES

LIST OF TABLES

CHAPTER 1

INTRODUCTION AND SUMMARY

1.1 INTRODUCTION

A Fast Breeder Reactor blanket performs several functions: fertile-to-fissile converter, reflector, shield. In addition, it produces some power, thereby relieving, slightly, the power burden on the core. Of these functions, the fissile breeding objective is considered paramount. For current 1000 MWe designs, a fast reactor without blankets is not a breeder; although most of the conversion is accomplished in the core (internal breeding ratio ~ 0.8), a fertile blanket is required to achieve overall breeding ratios above unity.

An AEC sponsored program is underway at MIT using the Fast Reactor Blanket Test Facility (BTF) to investigate blanket neutronics for the LMFBR effort (60, 61). To guide the selection of blanket mock-up experiments, comparative studies have been made of the fuel economics of several LMFBR blanket-reflector configurations.

Objectives of the work reported here were twofold: (1) to develop a simple depletion-economics calculational tool for survey evaluations of LMFBR blanket configurations; and (2) to perform several comparative studies around a 1000 MWe reference LMFBR configuration. The 1000 MWe case studies involve choice of radial reflector material (Be-metal vs. sodium), radial blanket thickness, advantages of local fuel management in the radial blanket, and the sensitivity of LMFBR fuel energy costs to changes in the economic environment.

1.2 OUTLINE OF THE REPORT

Calculational methods for FBR fuel depletion economics are developed in Chapters 2 and 3. Chapter 2 deals with the accounting details involved in determining energy costs by reactor region (core, axial blanket, radial blanket). The depletion method is developed in Chapter 3.

In Chapter 4, the energy cost and depletion methods are combined to form a computational tool for evaluating the fuel economic performance - in units of mills/KWHe or $/kg HM/year - of regions under either batch or scatter fuel management schemes. (Appendix C describes a computer program, SPPIA, developed to perform the depletion-economics computations.) A reference LMFBR configuration is selected, and the integrated depletion-economics model is applied to this reactor, in a reference economic environment.

In Chapter 5, the fuel depletion-economics model is applied to a series of case studies in which the radial blanket thickness, radial reflector material, fuel management scheme, and economic environment are varied around the reference.

Chapter 6 summarizes major conclusions of the study and lists several recommendations for future efforts.

Appendix B describes a preliminary scoping study examining the economic viability of FBR blankets as reactor unit size increases.

1.3 QUALITATIVE DISCUSSION OF FBR BLANKET DESIGN CONSIDERATIONS AND LITERATURE SURVEY

The major economic objective[1] of FBR blanket design is to maximize the

---

1 Another objective frequently adopted is the maximization of blanket breeding ratio. This objective, which is usually not consistent with the net revenue (or minimum power cost) objective, is macro-economic in nature, and is keyed to national fuel resource conservation considerations.

net blanket fissile revenue, that is, to maximize the fissile credit less fabrication, reprocessing, and carrying charges. At the same time thermal-hydraulic engineering design seeks to minimize the effects of the blanket power swing over a refueling cycle interval and to minimize the power gradient across the blanket. Other engineering considerations are the shielding role of the blanket, and possible material constraints on blanket exposure.

The blanket designer has several design variables and options to work with in meeting these objectives while satisfying the constraints. Some of the major variables and options are discussed qualitatively below. Studies which have addressed these considerations are referenced.

Blanket Thickness

Selection of blanket thickness involves a tradeoff between the fissile plutonium production rate and fuel cycle costs - fabrication, reprocessing, and associated carrying charges. An incremental increase in blanket thickness imposes additional fabrication and reprocessing costs while providing some additional fissile production. The incremental increase in fissile production decreases with blanket thickness because of flux attenuation. An incremental increase in thickness beyond some point is unprofitable - the added fissile revenue is not sufficient to offset the added fabrication and reprocessing costs.

The "optimum" thickness depends on the economic environment - fissile value ($/kg Pu_f), fabrication cost ($/kg HM) and reprocessing cost ($/kgHM). Thick blankets are indicated when fissile value is high and/or fabrication and reprocessing costs are low. Thicker blankets may also be in order when leakage flux to the blanket is increased due to changes in core design.

The Westinghouse LMFBR Follow-On Studies (73), Task I, have shown that the optimum radial blanket thickness is not sharp, that is, the

blanket profit is a weak function of blanket thickness. This conclusion is borne out in the present study. The Westinghouse optimum thickness is between 25 and 30 cm, again consistent with the present study.

Blanket Irradiation Time

Below some irradiation time, T_1, the bred fissile inventory in the blanket is not sufficient to offset the blanket fabrication, reprocessing, and carrying charges. At T_1, the "breakeven point", the revenue from bred fissile is just equal to fabrication, reprocessing, and carrying charges. Beyond T_1, the blanket produces a net profit. As irradiation time, T, is further increased, Pu239 is produced at a decreasing rate, because of the burnup of both fertile U238 and fissile Pu239, and the fissile credit averaged over irradiation time, T, decreases. Also, as irradiation time T increases, carrying charges increase, and direct fabrication and reprocessing charges decrease. Taken together, these opposing effects result in an optimum irradiation time, Topt, at which the net revenue in $/kg HM/year (or in mills/KWHe) is a maximum.

Local optimum irradiation time decreases, and local net revenue at the optimum increases, with increased local flux. Thus regions near the blanket-core interface reach their optima sooner and produce more revenue than regions deeper in the blanket. For pancaked cores, the axial blanket optimum irradiation time is less than that of the radial blanket. Thinner blankets enjoy shorter optimum irradiation times.

Several studies have assessed optimum blanket irradiation times for particular designs (1, 4, 12, 70). Typical local optima range from about two to about eight years across the radial blanket.

Engineering considerations such as burnup, power swing, corrosion, and irradiation damage of cladding may tend to limit feasible irradiation time.

Blanket Fuel Management Scheme

Axial blanket fuel management is constrained to that of the core since axial blanket fuel assemblies are merely extensions of core assemblies in present LMFBR designs. The core-axial blanket fuel management scheme adopted in the 1000 MWe LMFBR Follow-on Studies (69, 70,71,72,73) can be described as a region-scatter scheme. In this scheme, the core-axial blanket is divided into annular regions. At each refueling event, fractions g_1, g_2, ... of regions 1, 2, ... are discharged and replaced with fresh fuel. Fuel sees only one position in the reactor. The discharge fractions g_1, g_2, ... decrease with distance from the core centerline, implying that irradiation times increase with distance from the core centerline. This procedure enhances flux flattening and discharge burnup uniformity.

Radial blanket fuel management is independent of that of the core-axial blanket, with the restriction, of course, that blanket refueling dates coincide with those of the core-axial blanket, to minimize reactor shutdowns for refueling. With the exception of Westinghouse (73) the scheme selected in the 1000 MWe Follow-on Studies is region-scatter. Again, irradiation time increases and discharge fraction decreases with distance of the region from the core-blanket interface, thus implementing flux flattening across the blanket. Batch management is the special case of scatter management in which the discharge fractions are set equal to unity, i.e. at each refueling event for a given region, 100% of the fuel is discharged and replaced with fresh fuel.

Other schemes proposed for the radial blanket are out-in, in-out, and fuel assembly rotation. The Westinghouse Follow-on design (73) specifies in-out. In this scheme, fresh fuel is loaded in the innermost blanket

region, and is moved outward in subsequent refuelings, remaining in each annular region for one or more cycles. Fuel is discharged, finally, from the outermost region. Advantages (10) of the in-out management are power flattening, reduction of local power swing, and burnup uniformity. An earlier study (4) argued qualitatively that in-out management would be uneconomic due to the prolonged holdup of bred fissile. This was not demonstrated quantitatively.

In the out-in scheme, fresh fuel is loaded in the outermost region, moved inward, and discharged from the innermost region. The scheme has the advantage of achieving uniform burnup, and would tend to reduce the power swing over an irradiation cycle. However, out-in would tend to aggravate the power tilt across the blanket. Out-in management was compared (4) to fixed element management (batch or scatter) and was found to have only a few percent profit advantage.

A recent study (17) has investigated the optimum out-in throughput for a 1000 MWe LMFBR radial blanket. The study determined the effect of throughput on 10-year fuel cycle costs. Halving of the radial blanket out-in throughput increased fuel cycle costs (from optimal) by less than 5%. Increasing the throughput by a factor of about 1.5 increased the 10 year fuel cycle cost by about 1%.

The optimum throughput analysis reported in this (17) study was used as an illustration of a computational method for selecting optimal FBR fuel management strategies in a changing economic environment. The method permits changing fuel management during plant life (in response to changes in the economic environment) in order to minimize fuel costs during the remainder of plant life. In the radial blanket illustration cited, remaining plant life is 10 years.

Fuel element rotation has been studied by Westinghouse (10). Rotation may be considered a sub-fuel management scheme in that it may be used in conjunction with the other schemes. During a refueling, fuel assemblies are simply rotated in place, thus moving fuel with high fissile content deeper into the blanket. Advantages of rotation are power-flattening and reduction of local power swing over an irradiation cycle. Westinghouse has shown that the maximum (with time) rod peaking factor for a radial blanket rod adjacent to the core can be reduced by about 20% by rotation. The reduction in power peaking across the blanket was not reported. Also, the effect of rotation on breeding economics was not reported.

Inner Radial Moderator

Insertion of a layer of moderating material between core and blanket would offer the advantage of softening the leakage flux entering the blanket, improving the fertile capture rate per incident neutron. On the other hand, the incident flux (entering the blanket) would be diminished due to absorption and reflection by the moderating layer. Thus the net effect of inner radial moderator configuration on blanket breeding is not qualitatively clear. Furthermore, one might expect the moderating layer to return more neutrons to the core and to degrade the returning spectrum. The net effect (on critical mass and internal breeding ratio) of the improved reflection plus degraded core spectrum is also not intuitively evident.

Perks and Lord (5) have performed survey calculations on the inner radial moderator concept, using a variety of moderating materials and thicknesses. Candidate materials were graphite (82% graphite), graphite-steel (41% graphite, 51% stainless steel) and sodium (100% sodium). The inner radial moderator configuration consistently resulted in a small reduction in critical mass, an increase in internal breeding ratio, a

reduction in blanket breeding ratio,and a net reduction in total breeding ratio. Their (5) cost results show that the core fissile inventory reduction does not offset the breeding revenue reduction; thus, the inner radial moderator concept does not appear economically attractive.

Moderated Blankets

Replacing some blanket fuel with moderator material would tend to soften the blanket spectrum, enhancing the conversion rate per unit of fuel. Opposing this effect is the lessened gross breeding occasioned by the diminished fuel content. Some candidate moderating materials are graphite, ZrH_2, and BeO.

Two studies (4, 12) have investigated the breeding economics of moderated blankets. Hasnain (4) considered graphite in an LMFBR radial blanket, while Mayer (12) considered graphite, ZrH_2, and BeO in a steam-cooled fast reactor (SCFR) radial blanket. In all cases, the inclusion of moderating materials (at the expense of fuel volume) led to a reduction in breeding ratio. Core parameters (k_{eff}, critical mass) were only slightly affected. Both studies concluded that moderated blankets offered no significant economic advantages.

Another study (17) has shown that seeding a typical LMFBR radial blanket with carbon leads to a slight improvement in the breeding performance of the inner radial blanket: about 10% increase in inner radial blanket fissile concentration. The outer radial blanket was found to be practically unaffected.

Radial Reflector

Functions of the radial reflector are: (1) to enhance radial blanket performance by flattening blanket flux, and, possibly, by softening the return spectrum; and (2) to provide a neutron shield for structural materials outside the reactor. Two major design decisions are choice of radial reflector composition and choice of radial reflector thickness.

In the Westinghouse LMFBR Follow-On work (73), Fe, C, Ni, and Na (reference case) reflectors were compared for a 10.5 inch thick radial blanket. Maximum improvement (over the Na reflected case) in radial blanket fuel economic performance was only 0.008 mills/KWHe (the 12 inch graphite reflector). A 3 inch Fe reflector provided minimum improvement (0.002 mills/KWHe). A 3 inch Ni reflector resulted in 0.007 mills/KWHe savings. Choice of radial reflector material and thickness was found to have little effect on power ratios across the blanket. Nickel provided a significant improvement in flux attenuation and was selected as the preferred reflector material.

Using the BR-1 reactor, Russian experimenters (6) have studied the effect of reflector composition on radial blanket breeding. Be, C, Ni, Fe, Cu, 1 Kh 18N9T steel, water, and extended blanket material were compared. The thicknesses of these reflectors were chosen such that any further increase in thickness resulted in negligible increase in blanket U238 (n,γ) captures. "Reflector efficiency" was defined as

$$B_i = A_i / A_{xB}$$

where

A_i = additional U238 (n,γ) captures resulting from addition of reflector of material i.

A_{xB} = additional U238 (n,γ) captures resulting from extending the blanket.

The base radial blanket thickness was not given, nor could it be inferred. Two types of blankets - uranium carbide and metallic uranium - were used.

Table 1.1 summarizes the results. The reflector efficiency for the extended blanket case was unity, by definition. All other efficiencies were less than unity, indicating that an extended blanket is preferable if fabrication and reprocessing costs are ignored. The results show that

TABLE 1.1

EFFECT OF RADIAL REFLECTOR ON RADIAL BLANKET BREEDING, RUSSIAN EXPERIMENTAL RESULTS (6)

Reflector Material	Reflector Thickness (cm)	Bi	
		Uranium Carbide Blanket	Metallic Uranium Blanket
Be	140	0.54	0.86
C	600	0.50	-
Ni	192	0.47	0.51
Fe	184	0.42	0.28
Steel	160	0.33	0.40
Cu	184	0.24	0.41
Water	144	0.23	0.49
UC		1.00	-
U-met.		-	1.00

moderating reflectors (Be, water) are significantly more effective for metallic blankets than for carbide blankets, owing to the harder spectrum in metallic blankets and the potential for improved U238 (n,γ) capture. For both carbide and metallic blankets, Be is the preferred reflector.

The study included no analysis of the fissile revenue-fuel cycle cost tradeoff in extending the blanket. Thus from their results, Table 1.1, it is not possible to reach a firm economic judgement vis-a-vis replacement of blanket material with reflector.

In an analytic study at MIT (61) it was found that for an 18 inch blanket, no improvement in blanket breeding was accomplished by increasing the reflector (Fe) thickness beyond 18 inches. Similarly, no improvement was noted in extending an unreflected 18 inch blanket by more than an additional 18 inches, i.e. beyond a total unreflected thickness of 36 inches. Thus an 18 inch iron reflector and a 36 inch radial blanket are effectively infinite.

A German study (12) has evaluated radial reflector materials for steam cooled FBRs. Candidate materials were steam, water, ZrH_2, BeO, graphite, steel, UO_2 (extended blanket), and U metal. The radial blanket in all cases, was 35 cm thick, and composed of 56 v/o UO_2 and 18 v/o structural material. Reflectors, in all cases, were 80 v/o reflector material, 10 v/o steel, and 10 v/o coolant.

The reflector materials were first ranked by their effect on "breeding rate" (undefined). Optimum reflector thickness was selected such that further increase in thickness increased the breeding rate by less than 1%. Table 1.2 summarizes the results of the breeding rate ranking.

The moderating reflectors are ZrH_2, BeO, and graphite. Of these, ZrH_2 has the strongest moderating effect, but it is also the strongest absorber and thus the weakest net reflector. It has the least beneficial effect on blanket breeding. The less-thermalizing and less-absorbing BeO and graphite return more neutrons, albeit at higher energies, and result in higher blanket breeding.

TABLE 1.2

EFFECT OF RADIAL REFLECTOR ON RADIAL BLANKET BREEDING, GERMAN STUDY (12)

Reflector Material	Optimum Reflector Thickness (cm)	B^{1}
BeO	12-16	0.023
graphite	12-16	0.021
steel	6-8	0.015
UO_2	6-8	0.013
U-metal	6-8	0.013
ZrH_2	4	0.011

1/ B = radial breeding rate - radial breeding rate with no reflector

The shielding effectiveness of the materials was also considered. In these studies, reflector thickness was held constant at 8 cm. Flux values (in arbitrary units) at the outer edge of the reflectors are shown in Table 1.3. If the objective is to minimize high energy flux, ZrH_2 would be the preferred reflector. The other moderating reflectors, BeO and graphite, are somewhat poorer attenuators.

The breeding rate and shielding effectiveness surveys described above were based on "snapshot" multigroup physics computations. In a further study, the same author (12) evaluated the blanket revenues, with the various reflectors, at optimum irradiation times. Fabrication costs of the blanket were ignored entirely. Also portions of the blanket which would not yield a net profit (after reprocessing) were not counted. That is, these unprofitable regions did not burden the blanket with any cost whatever; they were simply not considered to be reprocessed. Table 1.4 summarizes the percent revenue improvements (over the case with no reflector) resulting from the addition of the various reflectors. The oversimplified economic assumptions apparently account for the inconsistency in reflector rankings between Tables 1.2 and 1.4.

Metallic vs. Oxide Blankets

The economics of metallic and oxide blankets have been compared by Klickman (1). Core design was held fixed. Optimum thickness for the metallic blanket (~20 cm) was about one half that of the oxide blanket (~40 cm). For these thicknesses, the two blankets had approximately the same breeding ratio, uranium content, and flux attenuation characteristics. Burnup limitations were assumed to be 5000 MWD/MT for the metallic blanket and 25,000 MWD/MT for the oxide blanket. The study showed that the low burnup limitation severely disadvantages the metallic blanket - its regional optimum irradiation times cannot be achieved. The oxide blanket's ir-

TABLE 1.3

SHIELDING PERFORMANCE OF REFLECTORS,

GERMAN STUDIES (12)

Reflector Material	Flux at Outer-Edge of an 8 cm Reflector: Fast Flux 0.8-10.5 Mev (arbitrary units)	Flux at Outer-Edge of an 8 cm Reflector: Total Flux 0-10.5 Mev (arbitrary units)
BeO	1.63	49.66
graphite	2.68	53.30
steel	2.77	39.14
UO_2	2.41	33.28
U-metal	2.00	25.46
ZrH_2	1.09	33.24

TABLE 1.4

EFFECT OF RADIAL REFLECTOR ON BLANKET REVENUE, GERMAN STUDIES (12)

Reflector Material	Blanket Revenue Improvement with respect to reference [1]
BeO	11.6%
graphite	12.9
steel	6.8
UO_2	4.0
U-metal	3.2
ZrH_2	9.8

1/ Reference = no reflector

radiation time was not so-limited. Even without the burnup limitations, the oxide blanket was found to be economically preferable.

1.4 SUMMARY

1.4.1 Objectives

The objectives of this work were twofold:

(1) to develop a simple depletion-economics calculational tool for survey evaluations of LMFBR blanket configurations; and

(2) to perform several comparative studies around a 1000 MWe reference LMFBR configuration.

The 1000 MWe case studies (2), to which model (1) was applied, dealt with (a) effect of choice of radial reflector material (Be-metal vs. Na) and radial blanket thickness on radial blanket fuel economics, (b) the advantage of operating each radial blanket region on its own local optimum irradiation schedule, and (c) the sensitivity of LMFBR fuel energy costs to the economic environment.

A preliminary study examined the economic viability of FBR blankets as reactor size is increased. The reactor size-blanket economics study used only the economics equations developed in task (1) above. Depletion information was obtained from simple, one energy group, spherical geometry breeding ratio expressions. Three cases were compared over a range of core sizes: (a) a spherical core surrounded by a breeding blanket, with no fissile burnup in the blanket; (b) a spherical core surrounded by a sodium reflector (no blanket); and (c) a spherical core surrounded by a breeding blanket, with blanket burnup (power) accounted for.

1.4.2 The Depletion-Economics Model (Chapters 2,3)

The depletion-economics model has two parts: (a) the cost analysis

model which yields the fuel components of energy cost , given unit fabrication and reprocessing costs ($/kgHM), plutonium market values ($/kg$Pu_f$), money costs (discount and tax rates), and the nuclide balance data; and (b) the physics-depletion model, which yields the nuclide balance data - load and discharge masses of fertile and fissile materials - used in the cost analysis model. The depletion economics model is programmed in the computer code SPPIA, described in Appendix C. Given local physics data (local flux and flux-averaged cross sections) from a single multigroup physics computation, and given the economic parameters, the code yields fuel costs locally (or for an annular region) in $/kgHM/year, and energy costs by major region (core, axial blanket, radial blanket) in mills/KWHe.

1.4.2.1 Cost Analysis Model

Despite attempts to standardize nuclear fuel cost accounting methodology (21,22,23,24), a casual review of methods actually used in design evaluations and tradeoff studies reveals substantial inconsistencies. Furthermore, FBR blankets impose several unique accounting problems: blanket fuel appreciates with irradiation, raising certain tax questions; and the long irradiation times in the radial blanket make the treatment of blanket carrying charges important. For these reasons, a cash flow method (CFM) was adopted in the present work.

A general CFM expression for the levelized cost of electricity (mills/KWHe) was derived and applied to FBR fuel costs. When applied to a region (core, axial blanket, or radial blanket) or subregion under fixed-element (batch or scatter) management, the equations reduce to forms giving local fuel economic performance, e.g. in an annular zone, or at a "point", in mills/KWHe or $/kgHM/year:

$$\bar{e} = \frac{1000}{E} M_{HM}^{0} \left[\frac{C_{fiss} \epsilon_0 F^{mp}(T)}{T} \right.$$ material purchase

$$+ \frac{C_{fab} F^{fab}(T)}{T}$$ fabrication

$$+ \frac{C_{repr} F^{repr}(T)}{T}$$ reprocessing

$$\left. - \frac{C_{fiss} \epsilon(T) F^{mc}(T)}{T} \right]$$ material credit (1-1)

where $\bar{e}$ is the local levelized fuel component of the energy cost (mills/KWhe), E is the electrical energy produced by the reactor in one year (kwhe/yr), T is the local irradiation time (yr.), C_{fab} and C_{repr} are the unit fabrication and reprocessing costs ($/kgHM), C_{fiss} is the fissile plutonium price ($/kg), ϵ_0 is the initial enrichment, $\epsilon(T)$ is the discharge enrichment (kg fissile discharged per kg of heavy metal loaded), $F^q(T)$ is the carrying charge factor for cost component q, and M_{HM}^{0} is the mass of heavy metal loaded. The term in brackets [ ] may be regarded as a figure of merit representing local fuel economic performance, having units of dollars per year per local kilogram of heavy metal loaded.

The carrying charge factors, $F^q(T)$, are given by

$$F^q(T) = \frac{1}{1-\tau} \left[\frac{1}{(1+x)^{Tq}} - \tau \right]$$ for capitalized costs or revenues

$$= \frac{1}{(1+x)^{Tq}}$$ for non-capitalized costs or revenues (expensed cost or taxed revenue) (1-2)

where

$$x = (1-\tau)r_b f_b + r_s f_s = \text{"discount rate"} \qquad (1\text{-}3)$$

and where τ is the income tax rate, f_b and f_s are the debt and equity fractions, r_b and r_s are the debt and equity rates of return, and T^q is the time between the cash flow transaction q and the irradiation midpoint.

The "front end" components, fabrication and material purchase, are normally capitalized. The "backend" components, reprocessing and material credit, may be capitalized or not, according to tax interpretation. If they are not capitalized, then revenue from the sale of plutonium is taxed as ordinary income, along with electricity revenue, and reprocessing charges are treated as tax deductible expenses in the year in which they occur. The two methods, capitalizing and not capitalizing backend transactions, were compared and were found to have a significant effect on absolute values of energy costs. However, choice of method does not distort comparative or incremental results, e.g. design rankings, optimum blanket irradiation time, sensitivity studies. In the case studies to which the depletion-economics model was applied, material credit was consistently taxed and reprocessing charges were consistently expensed.

The CFM treatment of carrying charges is embodied in Equations (1-2) above. Two approximate methods, here labeled "Simple Interest Method" (SIM) and "Compound Interest Method" (CIM), were identified in the literature:

$$F^q = 1 + y_q T^q \qquad \text{(SIM)} \qquad (1\text{-}4)$$

and

$$F^q = (1 + y_q)^{T^q} \qquad \text{(CIM)} \qquad (1\text{-}5)$$

where

$$y_q = x/1-\tau \qquad \text{for capitalized costs or revenues}$$

$$= x \qquad \text{for non-capitalized costs or revenues (expensed costs or taxed revenues)} \qquad (1\text{-}6)$$

The CFM expressions were shown, through series expansions, to reduce to SIM and CIM for small $T^q y_q$. SIM underpredicts, while CIM overpredicts, the carrying charge factor. Because radial blanket irradiation times are typically long, the CFM method was selected for use in the case studies of this report.

1.4.2.2 Physics-Depletion Model

The function of the physics-depletion model is to furnish discharge fuel composition, $\epsilon(T)$, to the cost analysis model for use in computing material credit.

In the method developed for this work, the "Semi-Analytic Method" (SAM), local physics data (fluxes and spectrum-weighted cross sections) from a single multigroup calculation are used in the analytic solutions of the reaction rate equations to obtain discharge fissile content:

$$\epsilon = \frac{M_{49} + M_{41}}{M^0_{HM}} \qquad (1\text{-}7)$$

$$M_{49} = N_{49} V \frac{\tilde{M}_{49}}{N_{av}}, \quad M_{41} = N_{41} V \frac{\tilde{M}_{41}}{N_{av}} \qquad (1\text{-}8)$$

$$N_{49} = N^0_{28} A \exp(-\sigma^{28}_a \theta) [1 - \exp(-(\sigma^{49}_a - \sigma^{28}_a)\theta)] + N^0_{49} \exp(-\sigma^{49}_a \theta) \qquad (1\text{-}9)$$

$$N_{41} = N^0_{28} AB_1C_1 \exp(-\sigma^{28}_a \theta) - N^0_{28} AB_2C_2 \exp(-\sigma^{49}_a \theta)$$
$$+ N^0_{49} B_2C_2 \exp(-\sigma^{49}_a \theta) + \beta_1 C_3 \exp(-\sigma^{40}_a \theta) + \beta_2 \exp(-\sigma^{41}_a \theta) \quad (1\text{-}10)$$

$$A = \sigma^{28}_c / (\sigma^{49}_a - \sigma^{28}_a)$$

$$B_1 = \sigma^{49}_c / (\sigma^{40}_a - \sigma^{28}_a) \qquad B_2 = \sigma^{49}_c / (\sigma^{40}_a - \sigma^{49}_a)$$

$$C_1 = \sigma^{40}_a / (\sigma^{41}_a - \sigma^{28}_a) \quad C_2 = \sigma^{40}_c / (\sigma^{41}_a - \sigma^{49}_a) \quad C_3 = \sigma^{40}_c / (\sigma^{41}_a - \sigma^{40}_a)$$

$$\beta_1 = N^0_{40} - (N^0_{28} AB_1 - N^0_{28} AB_2 + N^0_{49} B_2)$$

$$\beta_2 = N^0_{41} - (N^0_{28} AB_1C_1 - N^0_{28} AB_2C_2 + N^0_{49} B_2C_2 + \beta_1 C_3) \quad (1\text{-}11)$$

$$\theta = \int^T \phi(T')dT' = \text{local flux time} \quad (1\text{-}12)$$

M_{49}, M_{41} = discharge masses of Pu239, Pu241 respectively

N_{49} , N_{41} = discharge atom density of Pu239, Pu241 respectively

$\tilde{M}_{49}$, $\tilde{M}_{41}$ = atomic masses of Pu239, Pu241 respectively

N_{av} = Avogadro's Number

V = volume of the zone (1-13)

Local flux and local spectrum-weighted cross sections are taken from a single multigroup physics computation, and are assumed constant over a fueling cycle.

Several effects complicate the physics-depletion characteristics of FBR blankets: (1) spectrum softening with distance from the core-blanket interface; (2) spectrum hardening with irradiation time, due to the

relatively large buildup of fissile plutonium in the blanket; (3) flux shift, i.e. increase in blanket flux with irradiation time, due to buildup of fissile plutonium in the blanket; and (4) heterogeneity effects occasioned by the soft blanket spectrum,and aggravated, in the case of radial blankets, by larger pin diameters.

Effect (1) requires that cross sections be input to the depletion calculation with sufficient spatial detail, i.e. a separate cross section set, properly flux weighted, for each of many blanket regions. Since the accurate spatial description of blanket physics is a prime concern in the Blanket Test Facility work, no attempt was made to determine potential savings in computational effort through reduced spatial detail. Instead, attention was concentrated on effects (2) and (3).

Effects (2) and (3) suggest that static physics calculations be performed sufficiently often, during a depletion calculation, to correct the local fluxes and cross sections. Since most of the computational effort is absorbed by the multigroup calculations, computer expense can be significantly reduced by minimizing their frequency, that is by maximizing the irradiation time intervals over which flux shape and local spectra are assumed constant. For this reason, studies were performed to assess the effects of item (2), spectrum hardening, and item (3) flux shift, on depletion calculation results. Qualitatively, the two effects operate in opposite directions, spectrum hardening tending to decrease blanket discharge fissile inventory, flux shift tending to increase blanket discharge fissile inventory.

Three parallel depletion calculations were performed for a reference 1000 MWe LMFBR:

(a) a 26 energy group time step depletion calculation (26G-TSD), which accounted for both spectrum changes and flux shift;

(b) a 1 energy group time step depletion calculation (1G-TSD), which accounted only for flux shift; and

(c) a "semi-analytic method" (SAM) calculation, which accounts for neither spectrum change nor flux shift with irradiation.

The two approximate methods, (b) and (c), used local spectrum-weighted cross sections from the initial (time zero) method (a) solution. In addition, method (c) used local fluxes from the initial method (a) solution. The computer program 2DB (26) was used for calculations (a) and (b). Method (a) used the Bondarenko 26 group cross section set (48), heterogeneity-corrected by the program 1DX (27).

The calculations assumed batch management of both core (plus axial blanket) and radial blanket. Core and axial blanket fuel was assumed replaced after two years irradiation, corresponding to an average burnup of 100,000 MWD/MT. Radial blanket fuel was assumed irradiated to four years. The use of batch management in these calculations imposes a severe test of the constant flux, constant spectrum assumptions. For the same irradiation time, the variations of composition, flux shape, and spectra over a cycle interval are greater for batch management than for scatter management.

Principal findings of the methods study described above are listed below.

(1) For the core, the discharge fissile inventories from the three calculations were practically in exact agreement (errors less than 0.1%).

(2) For the axial blanket, 1G-TSD overpredicted[1] discharge fissile inventory by less than 4%, while SAM underpredicted[1] by less than 4%.

1. Compared to the 26G-TSD calculation.

(3) For the radial blanket, 1G-TSD overpredicted[1] discharge fissile inventory by about 10%, due to its soft cross sections. SAM underpredicted[1] discharge fissile inventory by around 10%, in spite of its soft cross sections, because of its low flux values.

(4) Of the two effects examined in this exercise, spectrum hardening and flux shift, the latter was found to be dominant.

The SAM calculation, performed by the program SPPIA, resulted in computer time savings (over the 26G-TSD, performed by 2DB) of on the order of 90%, while the 1G-TSD (2DB) led to about 60% time savings. In addition to depletion results, the SPPIA computation obtained fuel costs by region, as functions of irradiation time.

The effect of heterogeneity corrections (i.e. U238 resonance, spatial self-shielding) on radial blanket depletion results was examined. Heterogeneity influences blanket fissile production in two opposing ways: (a) the lower effective U238 microscopic capture cross section, σ_c^{28}, depresses the conversion rate, tending to decrease bred fissile inventory; (b) viewing blanket neutronics as an attenuation process, the lower σ_c^{28} results in higher blanket fluxes, tending to increase the conversion rate and bred fissile inventory. Of these two opposing effects, (a) dominates and heterogeneity leads to a net adverse effect on blanket breeding.

Two multigroup physics computations were performed using, respectively, 26 group infinitely dilute cross sections and 26 group heterogeneity - corrected cross sections in the blanket. Local fluxes and one group cross sections from these two computations were then input to SAM to obtain depletion results with and without heterogeneity corrections. Comparison of the two SAM results showed that blanket heterogeneity reduced fissile discharge inventory by about 10% for irradiation times of interest (2-7 years). A similar study (30) showed that heterogeneity corrections for a

1. Compared to the 26G-TSD calculation.

typical LMFBR axial blanket diminished calculated axial blanket Pu239 discharge mass by as much as 3%.

1.4.3 1000 MWe LMFBR Case Studies (Chapter 5)

The depletion-economics model established above was applied to case studies involving radial blanket thickness, choice of radial reflector material, radial blanket fuel management, and the sensitivity of LMFBR fuel energy costs to the economic environment.

1.4.3.1 Radial Blanket Thickness and Radial Reflector Material

Combinations of three radial blanket thicknesses (15, 30, 45 cm) and two radial reflector materials (sodium, beryllium metal) were evaluated. The total radial dimension (blanket plus reflector) was held fixed at 95 cm, since even the thinnest (50 cm) reflector is effectively infinite (6,61). The core and axial blanket configuration was also held fixed. Core volume was 4908 liters, core height-to-diameter ratio was 0.4 and the axial blanket was 40 cm thick. Core and axial blanket fuel economics were found to be insensitive to radial blanket/reflector design changes. A solid beryllium metal reflector (no coolant, no structural material) was selected as a limiting case, i.e. as the reflector apt to provide maximum improvement in radial blanket fuel economics.

Figure 1.1 and Table 1.5 summarize the results of the blanket thickness-reflector material survey. "Reference" and "more favorable" economic environments, for radial blankets, are defined in Table 1.6. Principal findings are listed below.

1. The relative advantage of the moderating reflector, Be-metal, increases as the reflector is moved nearer the high flux zones of the blanket, that is, as the blanket thickness decreases. For a thick

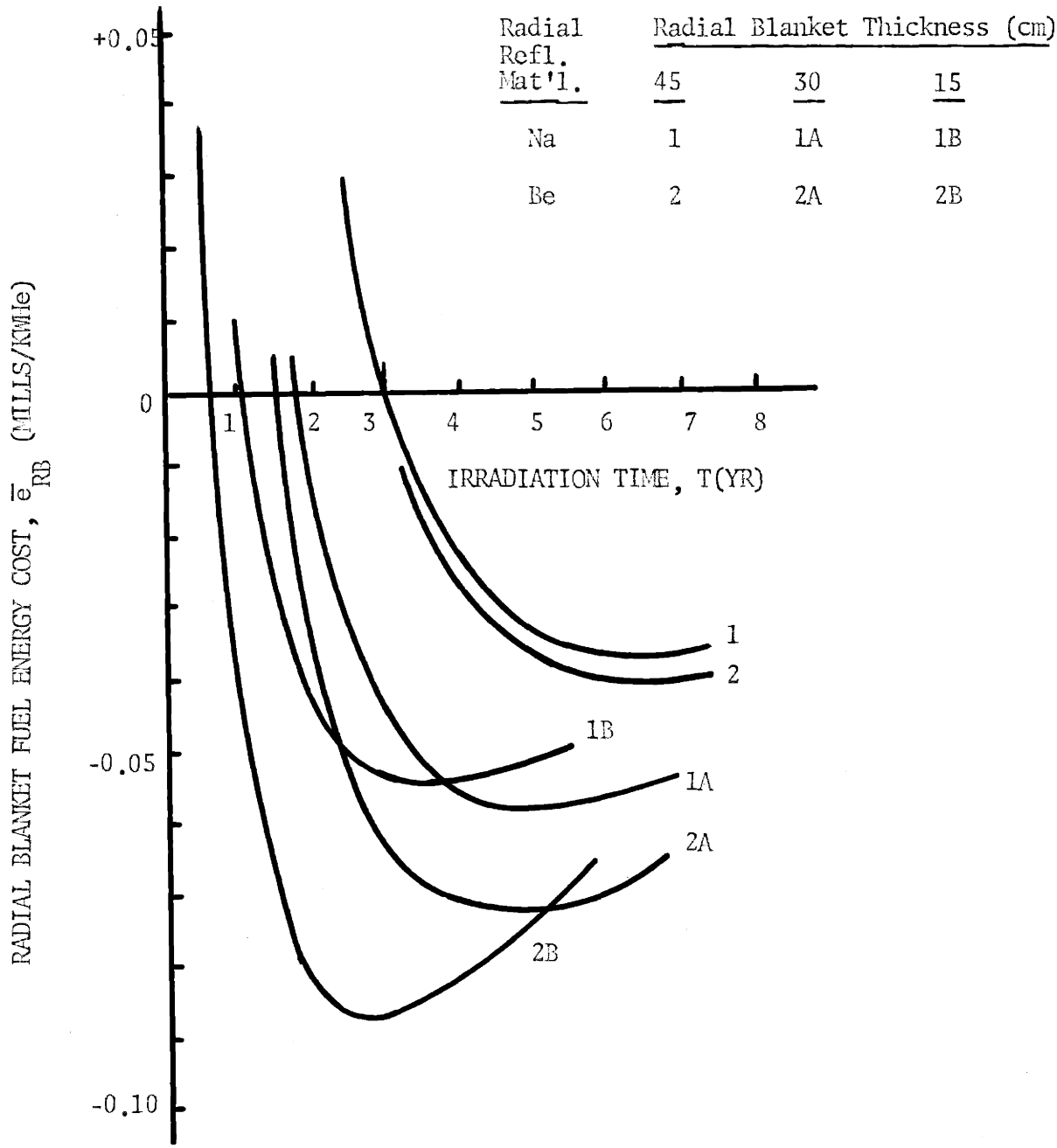

FIG. 1.1 EFFECT OF RADIAL BLANKET THICKNESS AND RADIAL REFLECTOR MATERIAL ON RADIAL BLANKET FUEL ECONOMICS

TABLE 1.5 EFFECT OF RADIAL BLANKET THICKNESS AND RADIAL REFLECTOR MATERIAL ON RADIAL BLANKET FUEL ECONOMICS

				Reference Economic Environment			More Favorable Economic Environment		
Configuration #	Radial Blanket Thickness (cm)	Radial Reflector Material	M_{49}/T @ T=2yr. (kg/yr.)	Topt (yr)	$\bar{e}_{RB}$ @Topt (mills/KWHe)	M_{49} @Topt(kg)	Topt (yr)	$\bar{e}_{RB}$ @Topt (mills/KWHe)	M_{49} @Topt(kg)
1	45	Na	158	6-1/2	-0.037	825	3-1/2	-0.237	512
2	45	Be-metal	160	6-1/2	-0.040	845	3-1/2	-0.243	521
1A	30	Na	141	4-3/4	-0.058	596	2-1/2	-0.242	342
2A	30	Be-metal	157	4-1/2	-0.072	610	2-1/2	-0.279	380
1B	15	Na	97	3-1/2	-0.055	304	2	-0.188	194
2B	15	Be-metal	130	2-3/4	-0.087	308	1-1/2	-0.276	205

TABLE 1.6

RADIAL BLANKET ECONOMIC ENVIRONMENT

	Reference	More Favorable
Fabrication, $/kgHM	69	40
Reprocessing, $/kgHM	31	31
Fissile Market Value, $/kg	10,000	20,000
Discount Rate, %	8	8

(45 cm) blanket, the effect of radial reflector material choice is only slight.

2. For either reflector, reducing the blanket thickness always reduces the bred plutonium inventory of the blanket, that is, the plutonium forfeited in the region eliminated is greater than the additional plutonium bred in the remaining region as a result of improvement of its breeding performance ($\overline{\sigma_c^{28}\phi}$).

3. Optimum irradiation time decreases as the radial blanket thickness decreases and as the economic environment improves. The effect of the choice of radial reflector material on optimum irradiation time is more pronounced the thinner the blanket.

4. Radial blanket thickness optimization is weak, that is, net blanket revenue does not display a sharp peak as radial blanket thickness is reduced from 3 rows to 2 rows to 1 row (15 cm per row). Thick blankets are indicated when fabrication and reprocessing costs decrease and/or fissile market value increases.

1.4.3.2 Advantage of Local Fuel Management

Fuel management schemes addressed in this study are characterized as "fixed fuel" schemes, i.e. fuel sees only one position in the reactor. During a refueling event a fraction, g, of a region's fuel is discharged and replaced with fresh fuel ("scatter" management). If all of the region's fuel (g=1.0) is replaced, the region is said to be "batch" managed.

The entire radial blanket may be batch or scatter managed, in which case all fuel experiences the same irradiation time. Alternatively, the blanket may be divided into annular regions (rows), with each irradiated to its own local optimum irradiation time, again in a batch or scatter

management scheme. The advantage of operating each radial blanket annular region on its own local optimum irradiation schedule was estimated for the reference LMFBR configuration (45 cm blanket,Na radial reflector). Net radial blanket revenue in mills/KWHe was found to be about 30% higher when local management was assumed. The local optimum irradiation time ranged from 2.5 years (at the core blanket interface) to about 12 years (at the blanket-reflector interface),while the optimum irradiation time for the blanket as a whole was 6.5 years.

Another advantage of local fuel management, not quantified in the present studies, is the power flattening effect.

1.4.3.3 Sensitivity of LMFBR Fuel Energy Costs to the Economic Environment

Costs generated throughout the fuel cycle are ultimately transferred to the utility company and borne, along with the utility company's carrying charges, by the electricity consumer via the fuel component of the levelized cost (price) of electricity in mills/KWHe. Economic environment is defined here as the unit costs for fabrication[1] and reprocessing ($/kgHM), the fissile Pu market value ($/kgPu fissile) and the utility company discount rate(%). The sensitivity of reference LMFBR fuel energy costs (mills/KWHe) to components of the economic environment was examined by varying each parameter around the reference values given in parentheses in Table 1.7. Sensitivity of region "s" fuel cost ($\bar{e}_s$) to cost component "q", about reference environment "o",is represented by the "sensitivity coefficient", $(A_{q,s})_o$, defined by

$$(A_{q,s})_o = (C_{q,s} / \bar{e}_s)_o \; (\partial \bar{e}_s / \partial C_{q,s}) \qquad (1\text{-}14)$$

1. Carrying charges of the fuel cycle industries are included in their unit costs($/kgHM). Carrying charge components of energy costs refer to utility company carrying charges.

TABLE 1.7

RANGES OF ECONOMIC ENVIRONMENT PARAMETERS

Unit Processing Costs [$/kgHM]	
Fabrication	
Core	150-(314)-330
Axial Blanket	20-(80)-314
Radial Blanket	20-(69)-100
Reprocessing	
Core	15-(31)- 60
Axial Blanket	15-(31)- 60
Radial Blanket	15-(31)- 60
Nuclide Market Values ($/kg)	
Fertile (C_{28}, C_{40})	0
Fissile (C_{49}, C_{41})	5000-(10,000)-25,000
Utility Company Financial Parameters	
Income Tax Rate (τ)	(0.5)
Discount Rate (x)	0.06-(0.08)-0.10

( ) indicates reference value

Table 1.8 summarizes the sensitivity coefficients for the reference core, axial blanket, and radial blanket. Fabrication and reprocessing components include their respective carrying charges. The material component is the net direct fissile material cost (fissile material purchase less fissile material credit) plus the material carrying charges (inventory). For all three regions, the energy costs for fuel are seen to be most sensitive to unit fissile value and least sensitive to unit reprocessing cost.

For the core and axial blanket, irradiation time is set by the burnup limit of the core. Thus, for these regions, Equation (1-1) reduces to simple linear relations of the unit costs:

$$\bar{e}_s = a_{fab,s} C_{fab,s} + a_{repr,s} C_{repr,s} + a_{mat,s} C_{fiss} \qquad (1\text{-}15)$$

where

$$a_{q,s} = \frac{1000}{ET} M^0_{HM} g(T) = \text{constant.}$$

Hence, for these regions, sensitivity coefficients simply represent the fractions of the regional cost, $\bar{e}_s$, contributed by the respective components:

$$(A_{q,s})_o = \left(\frac{\bar{e}_{q,s}}{\bar{e}_s} \right)_o \qquad (1\text{-}16)$$

where

$$\bar{e}_{q,s} = a_{q,s} C_{q,s}$$

The radial blanket energy cost of interest is the fuel cost at the optimum irradiation time, $(\bar{e}_{RB})_{Topt}$. Since the optimum irradiation time is an implicit function of the economic environment parameters, the Equation (1-1) for the radial blanket does not reduce exactly to a simple linear form. However, sensitivity results from the SPPIA program,

TABLE 1.8

SENSITIVITY COEFFICIENTS, $(A_{q,s})_o^*$, FOR REFERENCE LMFBR CORE, AXIAL BLANKET, AND RADIAL BLANKET

q s	Core	Axial Blanket	Radial Blanket
Fabrication	0.357	-0.495**	-2.15**
Reprocessing	0.025	-0.140**	-0.44**
Material	0.628	1.635	+3.59
	1.000	1.000	1.00

* $$(A_{q,s})_o = \frac{\Delta \bar{e}_s/(\bar{e}_s)_o}{\Delta C_{q,s}/(C_{q,s})_o}$$

** These terms are negative because the $(\bar{e}_s)_o$ for the blankets are negative.

Figures 1.2, 1.3 and 1.4, showed that $(\bar{e}_{RB})_{Topt}$ is practically linear in C_{fab}, C_{repr}, and C_{fiss} over the expected ranges of these parameters. Thus, Equations (1-15) and (1-16) are applicable to the radial blanket near reference economic conditions.

Figures 1.2, 1.3, and 1.4 also show that Topt is approximately linear in C_{fab}, C_{repr}, and C_{fiss}, and that Topt decreases with improvement in the radial blanket's economic environment.

Figure 1.5 shows the regional (core, axial blanket, and radial blanket) and total fuel costs as functions of fissile plutonium value. Several features are noted:

(a) Due to the core fissile inventory component, the total reactor fuel energy cost, $\bar{e}_{reactor}$, increases with C_{fiss} despite the fact that the reactor produces more fissile plutonium than it consumes.

(b) The axial blanket is more profitable than the radial blanket, because the axial blanket sees more neutrons in this particular, but typical, design (H/D = 0.4).

(c) The axial blanket breakeven point occurs at about 3.9 $/gm.

(d) The radial blanket breakeven point occurs at about 7.25 $/gm.

(e) As fissile price increases, the blankets become more viable, substantially offsetting the higher core inventory costs.

It is unlikely that the disparity between axial blanket profit and radial blanket profit would be diminished significantly by reasonable changes in the thickness or composition of either blanket. The axial blanket advantage is largely inherent: the axial blanket enjoys a higher flux, and higher fissile generation rate per unit of heavy metal loaded, and a short optimum irradiation time close to that set by the core burnup limit, (2 years). Hence axial blanket fissile credit is not threatened by overwhelming processing and material carrying charges.

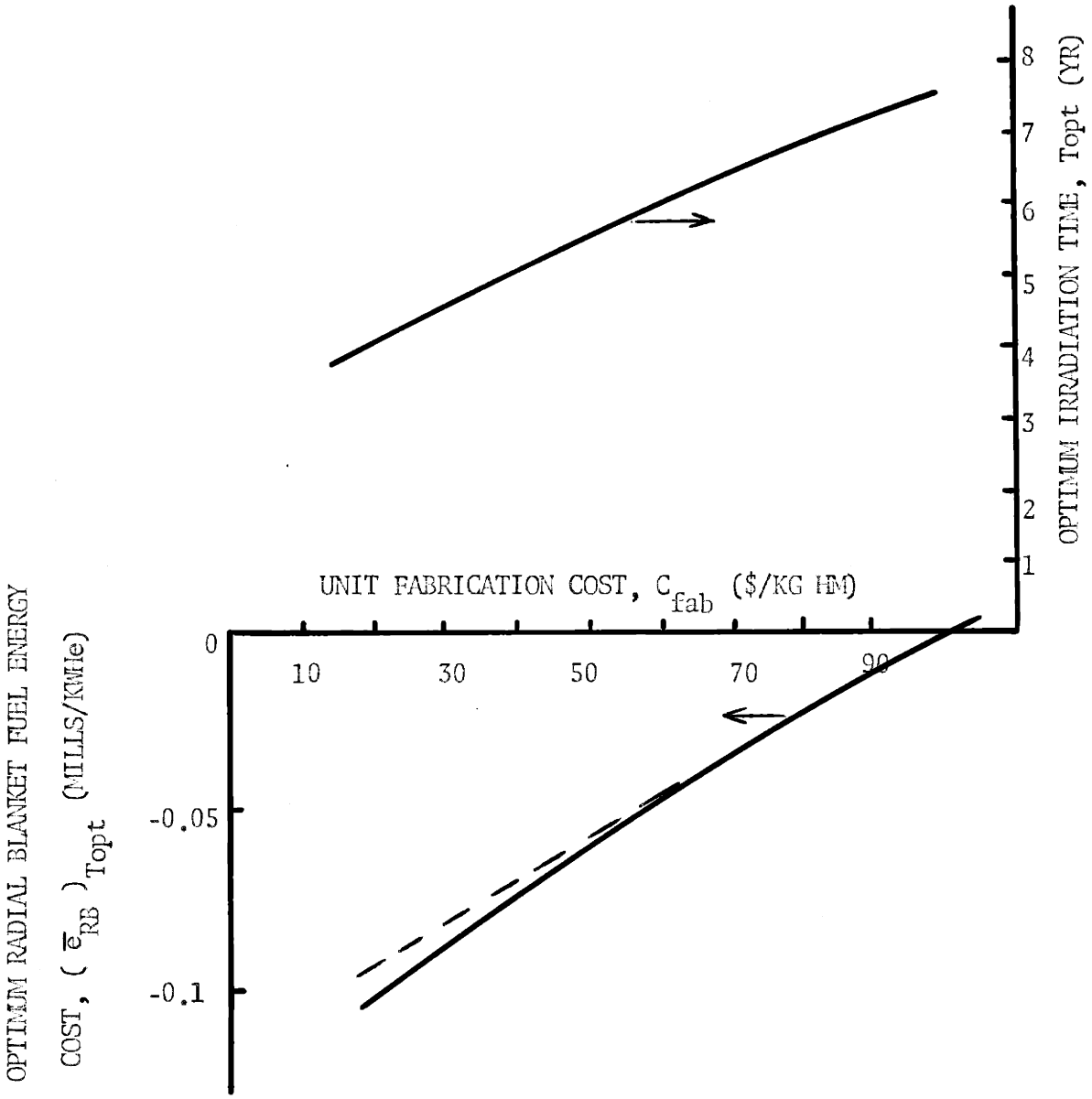

FIG. 1.2 SENSITIVITY OF OPTIMUM RADIAL BLANKET FUEL ENERGY COST TO UNIT FABRICATION COST

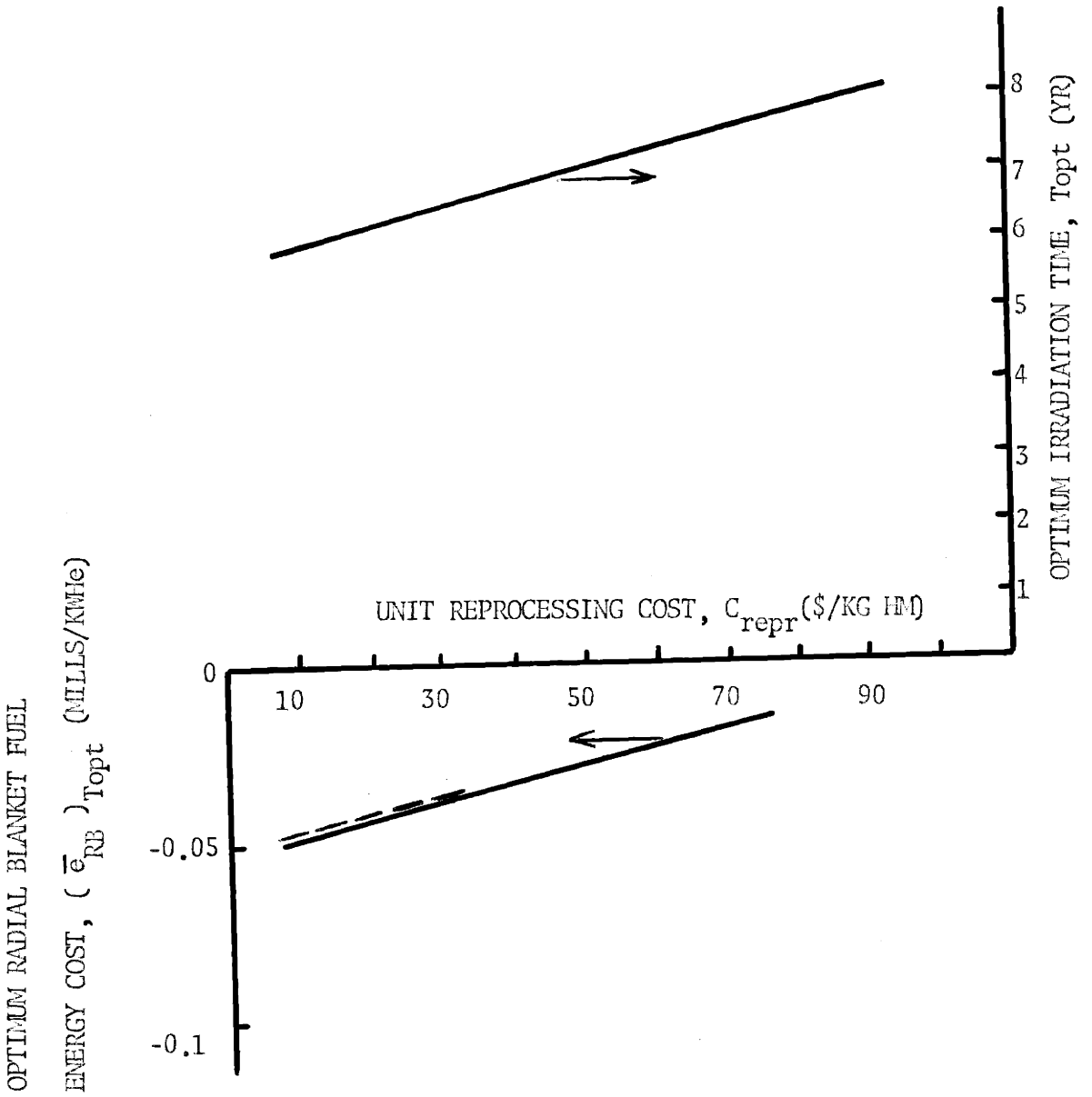

FIG. 1.3 SENSITIVITY OF OPTIMUM RADIAL BLANKET FUEL ENERGY COST TO UNIT REPROCESSING COST

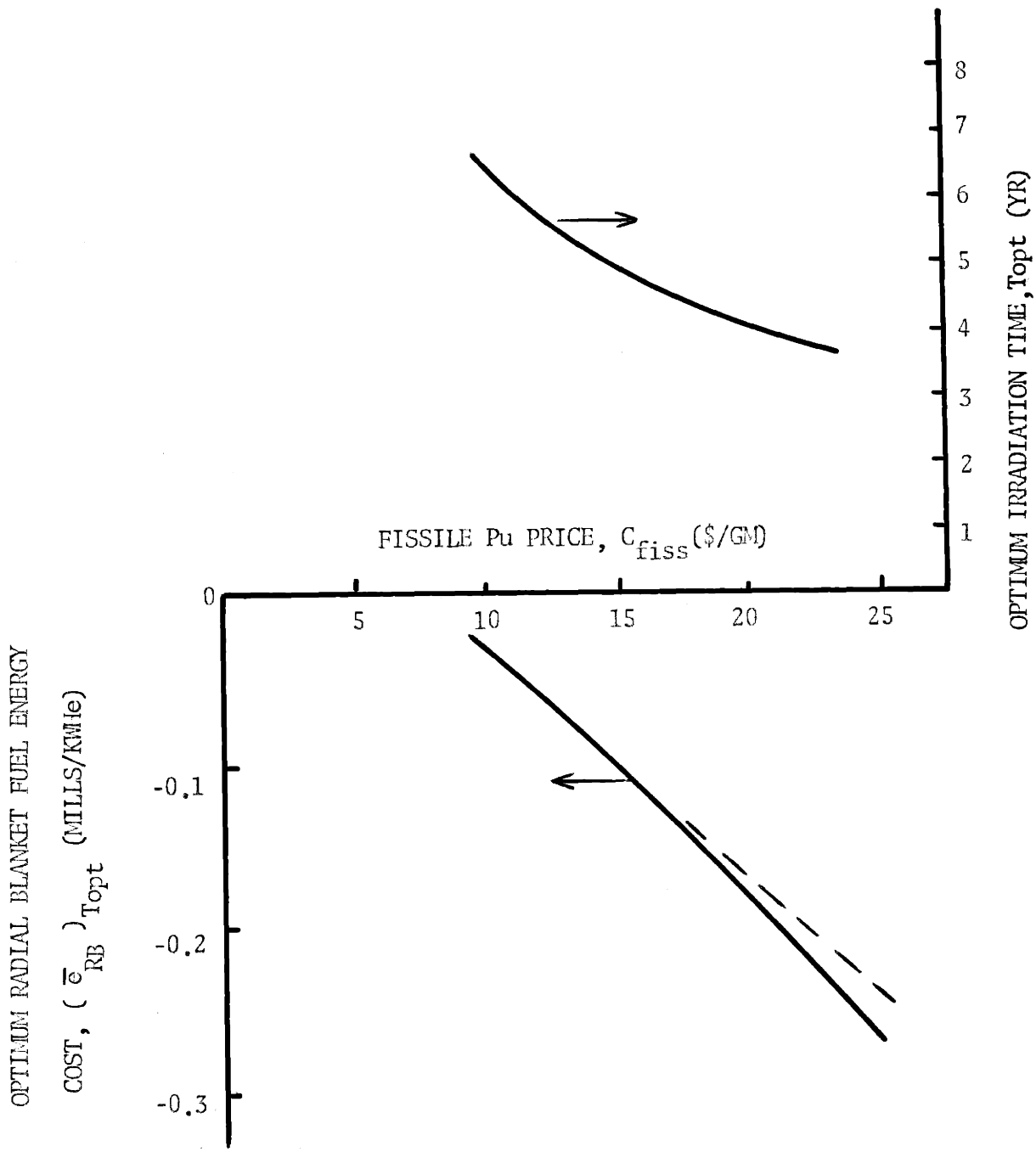

FIG. 1.4 SENSITIVITY OF OPTIMUM RADIAL BLANKET FUEL ENERGY COST TO FISSILE PLUTONIUM PRICE

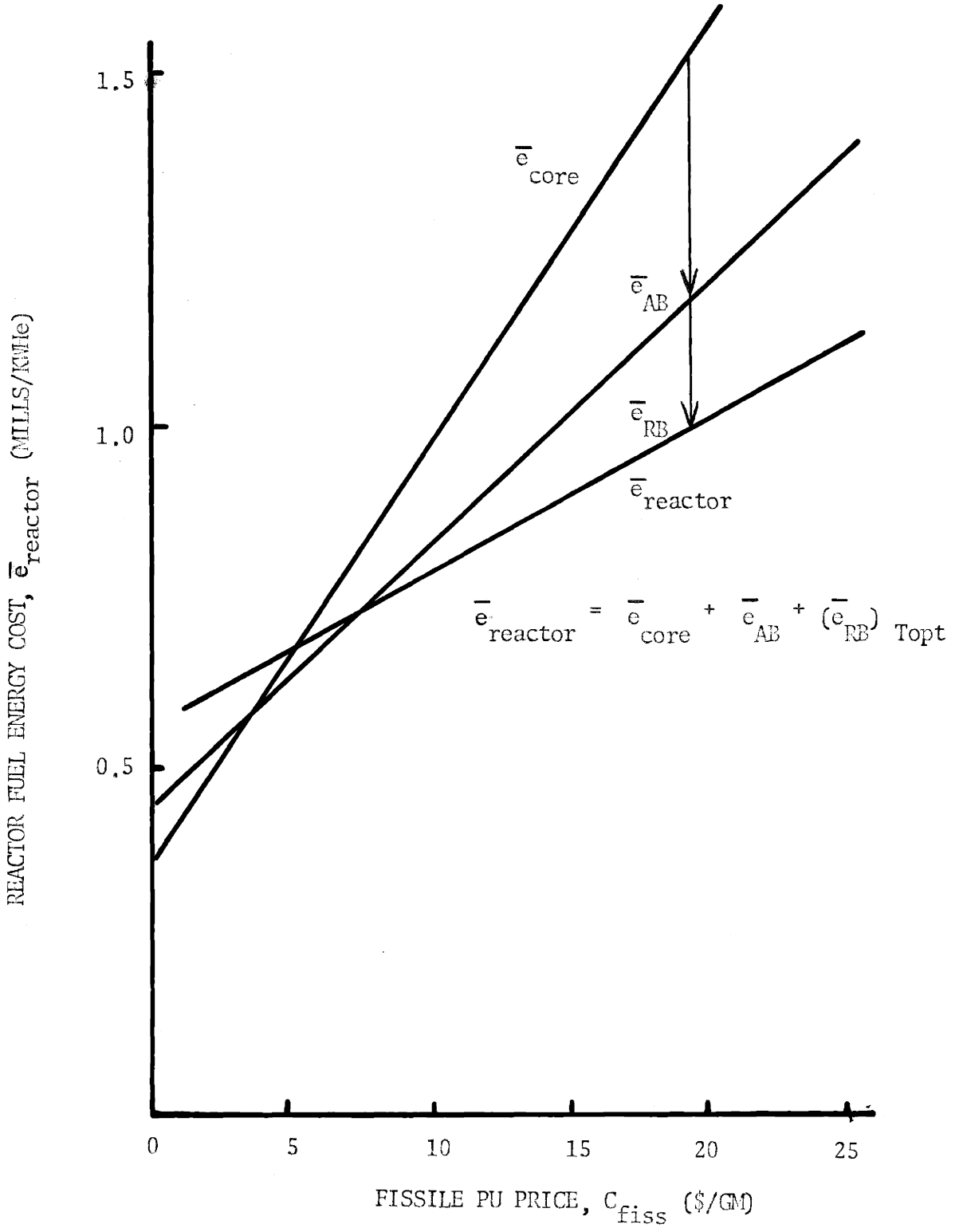

FIG. 1.5 EFFECT OF FISSILE PU PRICE ON TOTAL REACTOR FUEL ENERGY COST

1.4.4 Reactor Size and Blanket Fuel Economics

A semiquantitative scoping study was performed to examine the effect of reactor unit rating on the economic viability of blankets. As core size increases (holding core shape fixed), core fuel economics improve due to the decreased critical enrichment and increased internal breeding ratio. At the same time, core surface-to-volume ratio and external breeding ratio diminish, and blanket fuel economics degenerate.

All of the major assumptions in this preliminary study penalized the blanket. A spherical core was assumed throughout the range of core size, that is, core geometry spoiling to maintain negative sodium void coefficients was not accounted for. A one-zone core was assumed, whereas a graded enrichment scheme would have enhanced blanket economics. The increased control requirements, and associated costs, involved in increasing the internal breeding ratio much above unity,were ignored.

Figure 1.6 shows that in spite of these (and other) penalties, the blanket concept is economically preferable to a non-breeding reflector (Na) for reactor ratings well over 1000 MWe. Beyond the "indifference point", the advantage of the "no-blanket" configuration is only very slight. Thus, it is likely that blanketswill remain an important part of LMFBR design for the foreseeable future.

1.5 CONCLUSIONS AND RECOMMENDATIONS

The most significant findings and recommendations are summarized in the following paragraphs.

Choice of fuel cost accounting method has a significant effect on absolute values of energy costs (mills/KWHe), but does not distort comparative and incremental results, design rankings, optimization of fuel residence times, etc. Choice of taxing method can, however, affect the

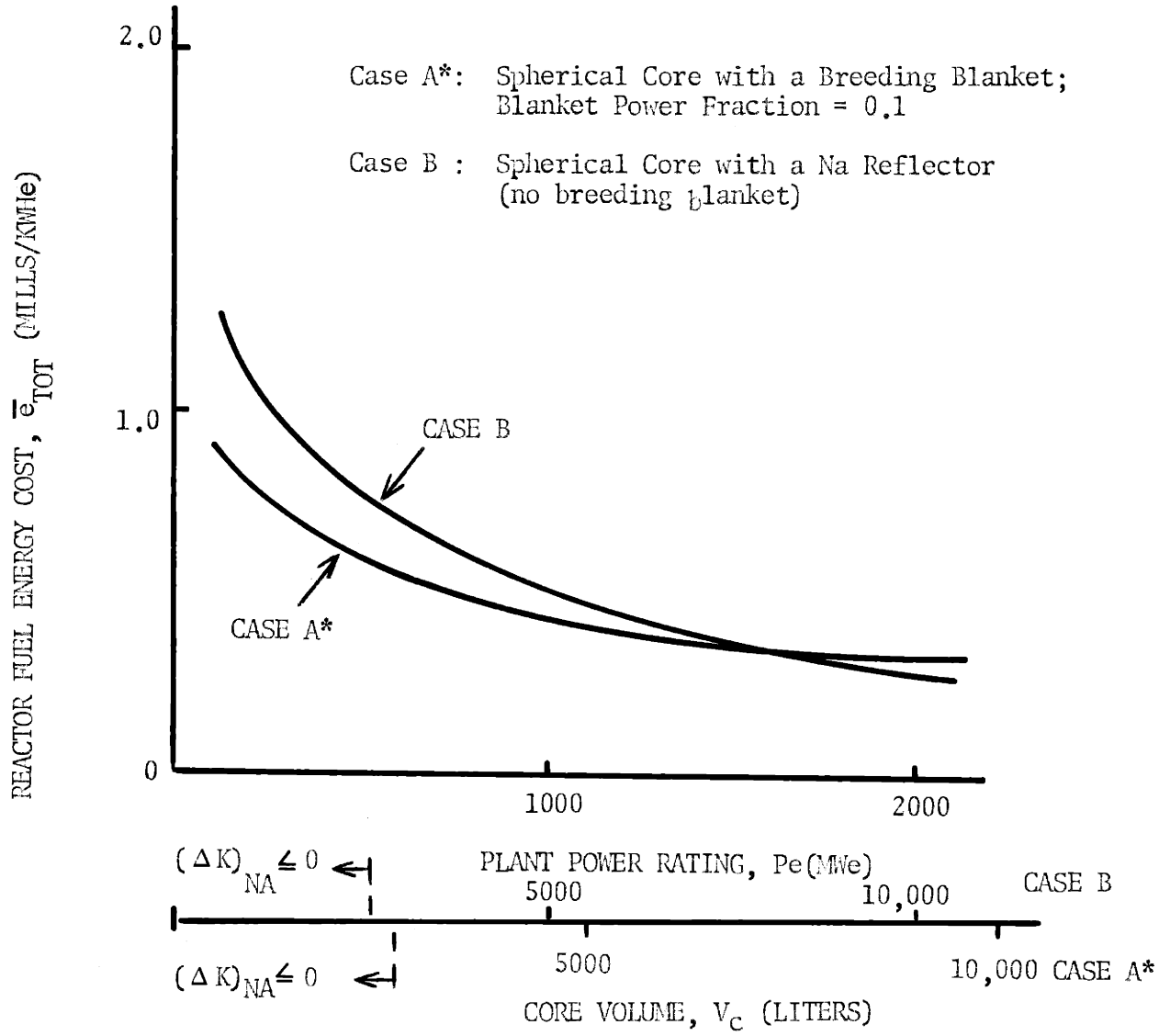

FIG. 1.6 REACTOR FUEL ENERGY COSTS WITH AND WITHOUT A BREEDING BLANKET

optimized thickness of blankets.

A single multigroup physics computation, to obtain the flux shape and local spectra for depletion calculations, is sufficient for evaluating blanket/reflector design changes and for scoping and sensitivity studies. The major source of error in depletion results is the assumption of constant local flux over an irradiation cycle.

Choice of radial reflector material is important for radial blankets of one or two rows of subassemblies (15-30 cm). The relative advantage of a moderating reflector increases as the reflector is moved nearer the high flux zones of the blanket, that is, as the blanket thickness decreases from three (45 cm) rows to two (30 cm) rows to one (15 cm) row of subassemblies.

Radial blanket thickness optimization is weak, i.e. net blanket revenue does not display a sharp peak as radial blanket thickness is reduced from three rows to two rows to one row. Significant improvement (~30% increase in net blanket revenue) results from irradiating each radial blanket region to its own, local optimum irradiation time.

Both the optimum radial blanket irradiation time and the corresponding radial blanket net revenue are approximately linear functions of the unit costs in dollars per kilogram for fabrication, reprocessing, and fissile material. For increased fissile costs, both blankets (axial and radial) become more important in offsetting the increased core fissile inventory costs.

Based on a simple examination of reactor size versus blanket fuel economics, blankets are expected to remain an important part of LMFBR design for the foreseeable future.

Fast breeder reactor blanket design and fuel management has not received attention, in the open literature, commensurate with its importance. Design and fuel management study results tend to be highly specialized and fragmentary, making normalizations and comparisons difficult. A comparative evaluation of scatter, batch, out-in, and in-out equilibrium radial blanket fuel management schemes, for a fixed reactor configuration, is recommended.

The flexibility of radial blanket fuel management, after the reactor is in operation, presents the opportunity of optimizing reload strategies in accordance with the current and projected economic environments. Further effort in this area is recommended.

Interactions between engineering design and fuel management parameters should be examined with the aim of better understanding and characterizing the blanket. Radial blanket fuel management directly influences the degree of power flattening across the blanket, the power swing over an irradiation cycle, and the core-blanket power split. The associated economic trade offs are not well understood. In particular, an analysis of the benefits and penalties of blanket fissile seeding is recommended.

In brief, the most important recommendation is that, whatever aspects of blanket fuel management are subjected to further scrutiny, this be done on a more global basis, at the minimum taking into consideration the strong interaction of management schemes and the flow orificing pattern adopted.

Since unit sizes are projected to increase to 2000 MWe and beyond after the year 2000, a more thorough parametric study of blanket performance versus reactor rating is recommended.

CHAPTER 2

FUEL COST ANALYSIS METHOD

2.1 INTRODUCTION

2.1.1 Objectives of the Chapter

The purpose of this chapter is to establish a fuel cost analysis method, for fast breeder reactors, capable of

(a) ranking major technological alternatives, e.g. choice of blanket and reflector materials,

(b) optimizing certain design and fuel management variables, e.g. optimum blanket thickness, optimum blanket irradiation time(s), and

(c) determining the sensitivity of fuel cost to changes in the economic environment, e.g. changes in unit fabrication and reprocessing costs, sale value of fissile nuclides, and cost of money parameters.

A secondary purpose of the chapter is to compare alternative fuel cost accounting methods. While alternative methods frequently yield significantly different absolute values of power costs in mills/KWHe, choice of accounting method should not distort the ranking of design alternatives, the values of optimized parameters nor the results of the sensitivity studies.

2.1.2 Background: Utility Company Economics

In non-regulated industries, the objective function used in measuring performance is profit (to be maximized), i.e. the stockholders' return on investment. By contrast, the objective function in utility company economics is usually the cost of electricity to the customer (to be minimized), or price, since a ceiling is imposed on investors' rate of return by regulatory

agencies. Hence, in utility economic analyses, investors' rate of return is treated as an expense to the customer, is fixed in the calculations, and the cost (price) of electricity to the customer must be such that the company's revenue from the sale of electricity balances all of its costs in generating and delivering that electricity, including payment of investors' principal and return, taxes ,and direct expenses.

For purposes of selecting generating plant type, design studies, etc., the electricity generated by a given plant is normally burdened with the costs associated with that plant alone. For purposes of preparing financial statements and setting electricity rates, however, the costs of different plants are, of course, mixed.

Generation costs are normally divided into three categories: plant capitalization, fuel, and operating and maintenance costs. Only LMFBR fuel costs are considered in this report. Costs generated throughout the nuclear fuel cycle are ultimately transferred to the utility company, burdened to the production of electricity, and borne by the customer, along with the company's costs of capital associated with the fuel, in the form of a levelized price (cost) of electricity (mills/KWHe).

2.1.3 Scope of the Cost Analysis Model

Figure 2.1 illustrates the scope of the cost analysis model established for the present work. The model has the features and restrictions listed below.

1. The model is restricted to fuel costs. It excludes the other major cost categories:plant capitalization, and operating and maintenance.

2. The model treats costs associated with an individual plant or class of plant, i.e. LMFBR, in a given economic environment. Other concerns such as the mix of plant types (capacity planning),coupling effects,

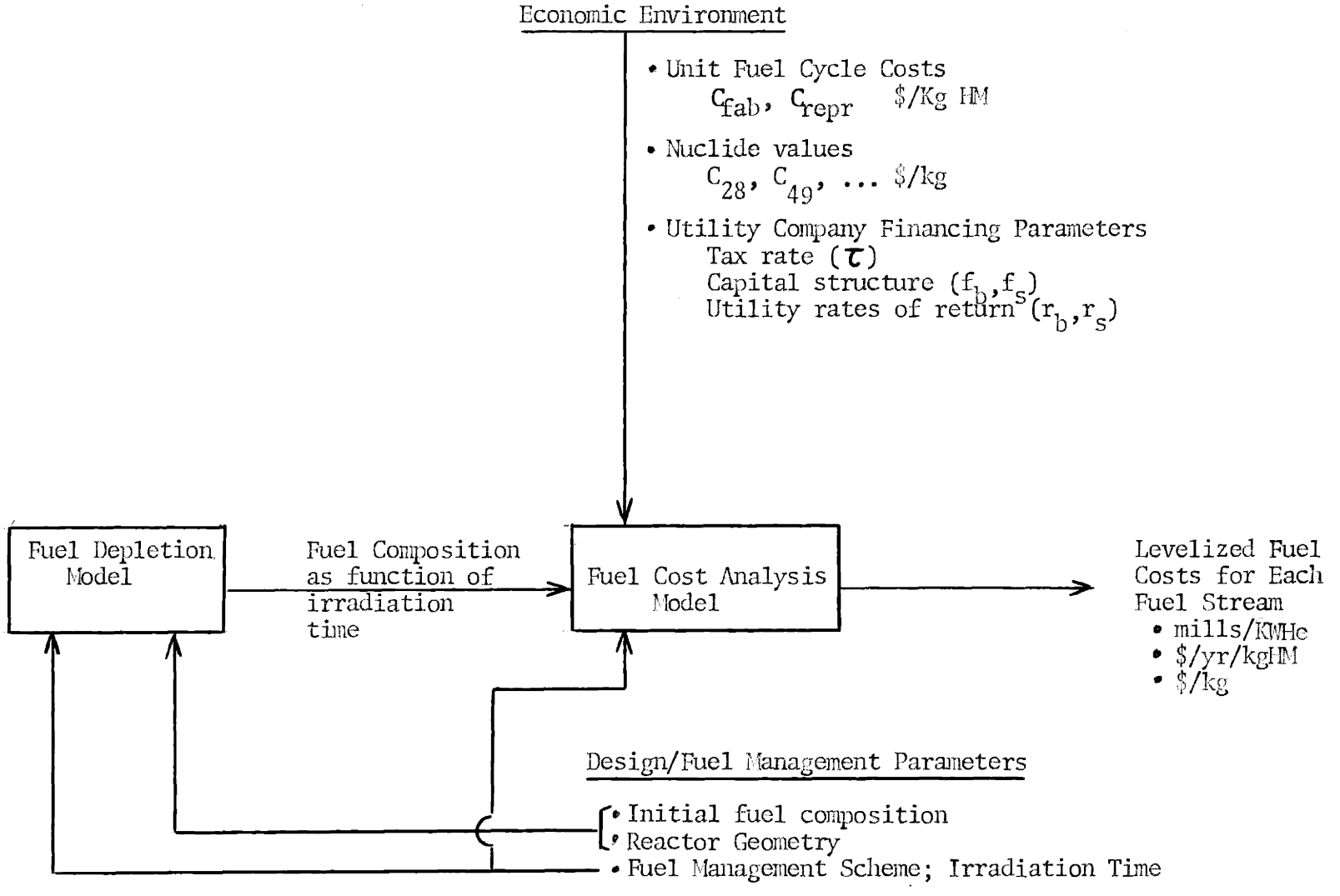

FIG. 2.1 SCOPE OF THE FBR FUEL COST ANALYSIS MODEL

generating schedules (dispatching) are not treated.

3. The "economic environment" is set, in parametric fashion, outside the cost analysis, and is assumed to be constant throughout plant life. The"economic environment" is defined here as the market value of fuel materials, prices of fuel cycle processing services, and the utility company's cost of money parameters. Such macroeconomic concerns as supply-demand effects in the market place (value of fissile isotopes), allocation of national resources, and effects of total processing industry throughput on processing prices, are not treated by the model.

4. As shown in Figure 2.1, the cost analysis model requires irradiation-depletion data from a fuel depletion model. (Fuel depletion models for LMFBR's are discussed in Chapter 3.) Output of the cost analysis model includes the following:

* fuel component of electricity costs, in mills per kilowatt hour (electric), by major region, i.e. core, axial blanket, radial blanket; and

* local annual fuel costs, in units of dollars per year per kilogram of heavy metal loaded, by major region, subregion (an annulus of fuel), or at a point.

2.1.4 Outline of the Chapter

A general expression for the levelized cost of electricity is derived in Section 2.2. This formulation, labeled here as the "cash flow method" (CFM), is applicable to all categories of costs: plant capitalization, fuel, and operating and maintenance costs. The derivation presented in Section 2.2 follows that of Vondy (19), with the following exception: an option is included for taxing revenue from sources other than the sale of electricity.

The CFM expression is applied to fast breeder reactor fuel costs in Section 2.4. Two methods for the tax treatment of post-irradiation transactions are derived.

In Section 2.4, the CFM expressions are specialized for fixed-fuel management schemes, in which fuel assumblies "see" only one irradiation position. A figure of merit representing local fuel economic performance ($/year/local kg heavy metal) is derived.

In Section 2.5, several fuel cost accounting methods are compared. The effect of post-irradiation tax assumptions is shown. The cash flow method (CFM) is related to and numerically compared with two other methods: the simple-interest method (SIM) and the compound interest method (CIM).

A sample CFM calculation is present in Section 2.6. Major features of the blanket fuel cost vs. irradiation time characteristic are shown, i.e. the breakeven point and the optimum irradiation time.

2.2 DERIVATION OF A GENERAL EXPRESSION FOR THE LEVELIZED COST OF ELECTRICITY (CASH FLOW METHOD)

A general expression for the levelized cost of electricity, $\overline{e}$(mills/KWHe) - applicable to plant capitalization costs, fuel costs and operating and maintenance costs - is derived in this section. The general expression is applied to FBR fuel costs in Section 2.3.

An electric utility company interacts financially with

* customers (electricity revenue, $\overline{e}\, E_j$);
* capital equipment suppliers (capitalized costs, Z_j);
* fuel suppliers, fabricators, reprocessors (capitalized costs Z_j, expensed costs, O_j)
* federal, state and local governments (income tax, T_j, property tax, π_j)

* investors, including stockholders (owners) and bondholders (Y_j)
* and others.

Nomenclature is given in Appendix A.

Figure 2.2 illustrates the detailed accounting treatment of utility company cash flows in year j.

Book value (liability to investors) at the end of year j is the book value, Y_j, in effect during year j plus any new capitalization which occured during year j. Residual revenue for year j (revenue after taxes, current expenses, and return to investors have been subtracted), R_j, is applied against end-of-year book value to obtain the book value in effect for the following year, j + 1, i.e.

$$Y_{j+1} = Y_j - R_j + Z_j \tag{2-1}$$

Residual revenue, R_j, is a function of the levelized price (cost) of electricity, $\bar{e}$. Application of the boundary conditions

$$Y_1 = Z_0 \tag{2-2}$$

and

$$Y_{N+1} = 0 \tag{2-3}$$

to equation (2-1) yields an expression for $\bar{e}$, as is shown below.

Residual revenue, R_j, is given by

$$\begin{aligned} R_j = {} & (\text{taxable revenue} + \text{non-taxable revenue}) \\ & - (\text{current expenses}) \\ & - (\text{investors return}) \\ & - (\text{income tax}) \\ = {} & \frac{\bar{e}E_j}{1000} + V_j + V_j' \\ & - O_j - (r_b f_b Y_j + r_s f_s Y_j) - T_j \end{aligned} \tag{2-4}$$

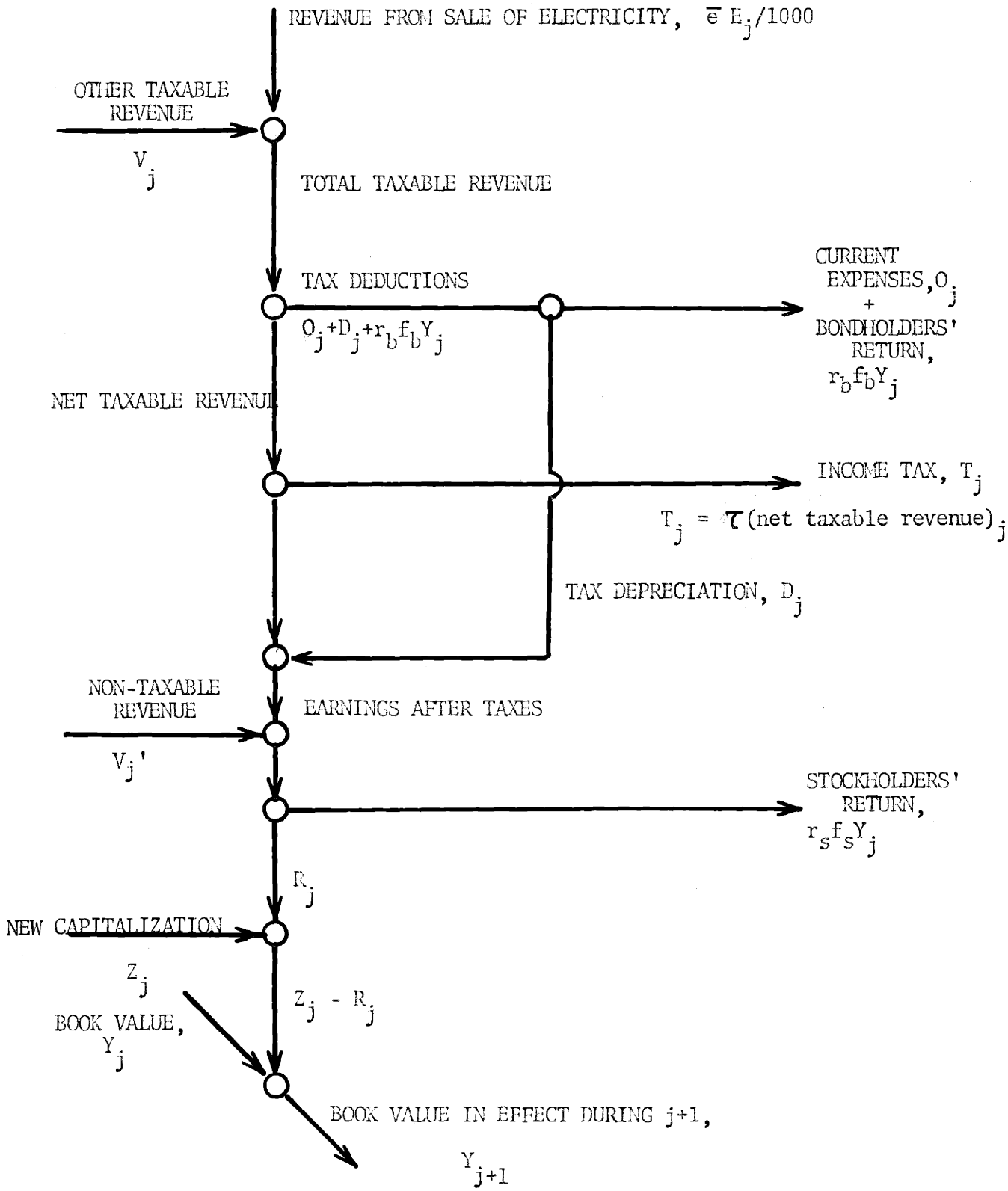

FIG. 2.2 UTILITY COMPANY CASH FLOW ACCOUNTING

Income tax, T_j, is computed by applying an income tax rate (τ) to the net taxable revenues, i.e.

$$\begin{aligned} T_j &= \tau[\text{net taxable revenues, } j] \\ &= \tau[(\text{taxable revenue})_j - (\text{tax deductions})_j] \end{aligned} \tag{2-5}$$

Taxable revenue is given by

$$(\text{taxable revenue})_j = \frac{\bar{e}\, E_j}{1000} + V_j \tag{2-6}$$

The second term V_j (taxable revenue from sources other than the sale of electricity) is included for flexibility and generality.

Allowed tax deductions are:

current (non-capitalized) costs, O_j ;

return on debt capital (bonds), $r_b\, f_b\, Y_j$; and

depreciation of capitalized costs, D_j :

$$(\text{tax deductable expenses})_j = O_j + r_b f_b Y_j + D_j \,. \tag{2-7}$$

Thus income tax for year j is given by

$$T_j = \tau\left[\frac{\bar{e}\, E_j}{1000} + V_j - O_j - r_b f_b Y_j - D_j\right] \tag{2-8}$$

Substituting Equation (2-8) into Equation (2-4) for T_j, one obtains

$$\begin{aligned} R_j &= \frac{\bar{e}\, E_j}{1000} + V_j + V_j' - O_j - r_b f_b Y_j - r_s f_s Y_j \\ &\quad - \tau\left[\frac{\bar{e}\, E_j}{1000} + V_j - O_j - r_b f_b Y_j - D_j\right] \\ &= (1-\tau)\left[\frac{\bar{e}\, E_j}{1000} + V_j - O_j\right] + \tau D_j \\ &\quad - [(1-\tau) r_b f_b + r_s f_s]\, Y_j + V_j' \end{aligned} \tag{2-9}$$

The residual revenue R_j is available to pay back the bondholders' and stockholders' principal, as shown in (2-1), and may be thought of as a book depreciation payment. Substituting Equation (2-9) into Equation (2-1) for R_j,

$$Y_{j+1} = Y_j + Z_j - (1-\tau)\left[\frac{\bar{e}\,E_j}{1000} + V_j - O_j\right] + \tau D_j + V'_j - [(1-\tau)r_b f_b + r_s f_s]\,Y_j \qquad (2\text{-}10)$$

Defining

$$A_j = Z_j - (1-\tau)\left[\frac{\bar{e}\,E_j}{1000} + V_j - O_j\right] - \tau D_j + V'_j \qquad (2\text{-}11)$$

and collecting terms on Y_j, one obtains

$$Y_{j+1} = \left[1 + (1-\tau)\,r_b f_b + r_s f_s\right] Y_j + A_j \qquad (2\text{-}12)$$

Defining

$$x \equiv (1-\tau)\,r_b f_b + r_s f_s\ , \qquad (2\text{-}13)$$

Equation (2-12) becomes

$$Y_{j+1} = (1+x)\,Y_j + A_j\ . \qquad (2\text{-}14)$$

The quantity x defined in Equation (2-13) will presently be identified as the appropriate discount rate for present value calculations.

The recursive relation (2-14), together with the boundary conditions (2-2), (2-3) and the definition of A_j, Equation (2-11), leads to a closed form expression for levelized price of electricity, E. Equation (2-14) is applied repeatedly, as follows, subject to the boundary conditions:

$$Y_1 = Z_o = A_o \qquad (2\text{-}2)$$

$$Y_2 = (1+x)Y_1 + A_1 = (1+x)\,A_o + A_1$$

$$Y_3 = (1+x)^2 A_o + (1+x)A_1 + A_2$$

.

.

.

$$Y_i = \sum_{j=0}^{i-1} (1+x)^{i-1-j} A_j$$

.

.

.

$$Y_{N+1} = \sum_{j=0}^{N} (1+x)^{N-j}\, A_j = 0 \qquad (2\text{-}3)$$

$$= (1+x)^N \sum_{j=0}^{N} (1+x)^{-j}\, A_j = 0 \qquad (2\text{-}15)$$

Substituting Equation (2-11) for A_j into Equation (2-15), and solving for $\bar{e}$,

$$\bar{e} = 1000\, \frac{\sum_{j=0}^{N} (1+x)^{-j} \left[\frac{Z_j}{1-\tau} - \frac{V_j'}{1-\tau} - \frac{\tau}{1-\tau} D_j - V_j + O_j \right]}{\sum_{j=0}^{N} (1+x)^{-j}\, E_j} \,. \qquad (2\text{-}16)$$

The factor $(1+x)^{-j}$ is seen to be the "discount factor", or "present value factor",

$$w(j) = (1+x)^{-j} \qquad (2\text{-}17)$$

and x, defined by

$$x = (1-\tau) r_b f_b + r_s f_s \qquad (2\text{-}13)$$

is identified as the "discount rate".

The derivation above assumes that the capital structure (f_b, f_s) and rates of return (r_b, r_s) are fixed.

The cash flow approach used in deriving Equation (2-16) has many advantages. First, Equation (2-16) is exact; that is, it avoids the tax iteration of methods which treat income taxes as costs to be present-valued separately. In the cash flow method derived above, allowance for income taxes is implicit in the coefficients of the present values ($1/1-\tau$, $\tau/1-\tau$, 1) and in the discount rate.

Another advantage is that vagaries in the interpretation of the discount rate are circumvented. The discount rate is defined within the cash flow derivation above. It may be calculated once the tax rate (τ), capital structure (f_b, f_s), and debt and equity rates of return (r_b, r_s) are set.

Further, the cash flow method (CFM) is flexible. A broad range of financial conventions may be accommodated within the CFM structure. Whether to "capitalize" (Z, V') or "expense" (O, V) a given transaction is the user's decision, subject to IRS and state regulations. Equation (2-16) specifies how these transactions are treated. Different classes of transactions must be treated in different ways, when taxes are present, and the CFM specifies how.

Finally, in other methods (20) two depreciation schedules sometimes appear (depreciation for tax purposes, and depreciation for computing investors' return), leading to confusion. In the CFM described above, depreciation enters the calculation only in the tax computation. The depreciation of investors principal is set by the assumption that residual revenue R_j is applied toward paying back this principal. This restriction imposes a standard convention, of sorts, but permits alternative designs to be evaluated on a standard basis, free of accounting artifices.

2.3 APPLICATION TO FBR FUEL COSTS

A general expression for the levelized cost of electricity, Equation (2-16), was developed in Section 2.3. In the present section, that formulation is specialized to treat FBR fuel costs.

2.3.1 Separation of Costs

For convenience and flexibility, one wishes the costs to be as separable and additive as possible. They are made additive, in this report, by burdening the total reactor energy with each cost item individually, as opposed to charging the energy released by a single fuel stream with costs associated with that stream.

The reactor fuel costs are separated, or classified, as follows:

(a) by fuel stream. A fuel stream is a distinct sequence of fuel lots which sees one (batch or scatter management) or more (e.g. in-out, out-in management, etc.) positions in the reactor. A fuel stream can normally be identified with a major region (core, axial blanket, or radial blanket), and may be characterized by features such as pin diameter, initial isotope composition, etc.

(b) by component , for each stream. Each fuel lot of each stream incurs certain "component" costs as it proceeds through the fuel cycle, i.e. material purchase, fabrication, reprocessing, and material credit.

(c) as direct costs or carrying charges. Each component of each stream includes direct and carrying charge subcomponents. Thus there are eight (8) cost items per fuel stream.

If S is the number of fuel streams, there are SX8 separate cost items in mills/KWHe which may be added directly to obtain total reactor fuel cost. These cost items may be regrouped as desired to assist technological economic insight, to make results comparable with other studies, etc.

For example, direct material purchase and direct material credit may be combined to form "burnup" cost. Their carrying charges may be combined to form "inventory" cost.

2.3.2 Application to FBR Fuel Costs

The cost expressions associated with an arbitrary fuel stream are developed below. Total reactor fuel cost may be found by summing the costs of the individual streams, provided the denominator of Equation (2-16), discounted total plant electricity, is retained in each of the stream equations. For the moment, attention is focused on the numerator.

For an arbitrary fuel stream, the numerator of Equation (2-16) may be expressed as a sum over the fuel lots (m) rather than over years (j):

$$\text{(numerator)} = \sum_{j=0}^{N} w(j) \left[\frac{Z_j}{1-\tau} - \frac{V_j}{1-\tau} - \frac{\tau}{1-\tau} D_j - V_j - O_j \right]$$

$$= \sum_{m=1}^{n} \left\{ \frac{Z_m}{1-\tau} w(t^Z_m) - \frac{V'_m}{1-\tau} w(t^{V'}_{m,k}) \right.$$

$$- \frac{\tau}{1-\tau} \sum_k (D_m)_k \, w(t^D_{m,k})$$

$$\left. - V_m \, w(t^V_m) + O_m \, w(t^O_m) \right\} \qquad (2\text{-}18)$$

where the t's are the times, in years, from beginning of plant life to the indicated transactions.

For each fuel lot m, four direct cash flows are identified, as shown in Figure 2.3:

material purchase, z_m^{mp};

fabrication cost, z_m^{fab} ; [$/lot]

reprocessing cost, z_m^{repr} ; and

material credit, $-z_m^{mc}$.

Each of these transactions is to be assigned to one of the classes of transactions appearing in Equation (2-16) and Equation (2-18).

These classes of transactions and two methods of assigning the lot's costs to them are summarized in Table 2.1. In both methods, the pre-irradiation transactions (material purchase and fabrication) are capitalized. Method A treats post-irradiation transactions as non-capitalized; that is, revenue from the sale of valuable isotopes is taxed as ordinary income, along with revenue from the sale of electricity, and reprocessing cost is written off as a tax deductable expense in the year that it occurs. Method B capitalizes the post-irradiation transactions.

Method B is strictly applicable, or at least conceptually correct, in cases of depreciating fuel, such as thermal reactor fuel, which experiences no net fissile gain during irradiation. For depreciating fuel,

$$D = (z_m^{fab} + z_m^{mp}) - (z_m^{mc} - z_m^{repr}) > 0 \qquad (2\text{-}19)$$

and the interpretation of the tax depreciation credit, $\tau D/(1-\tau)$, is clear and correct. On the other hand, if fuel appreciates, as in a fast breeder reactor blanket,

$$D < 0, \qquad (2\text{-}20)$$

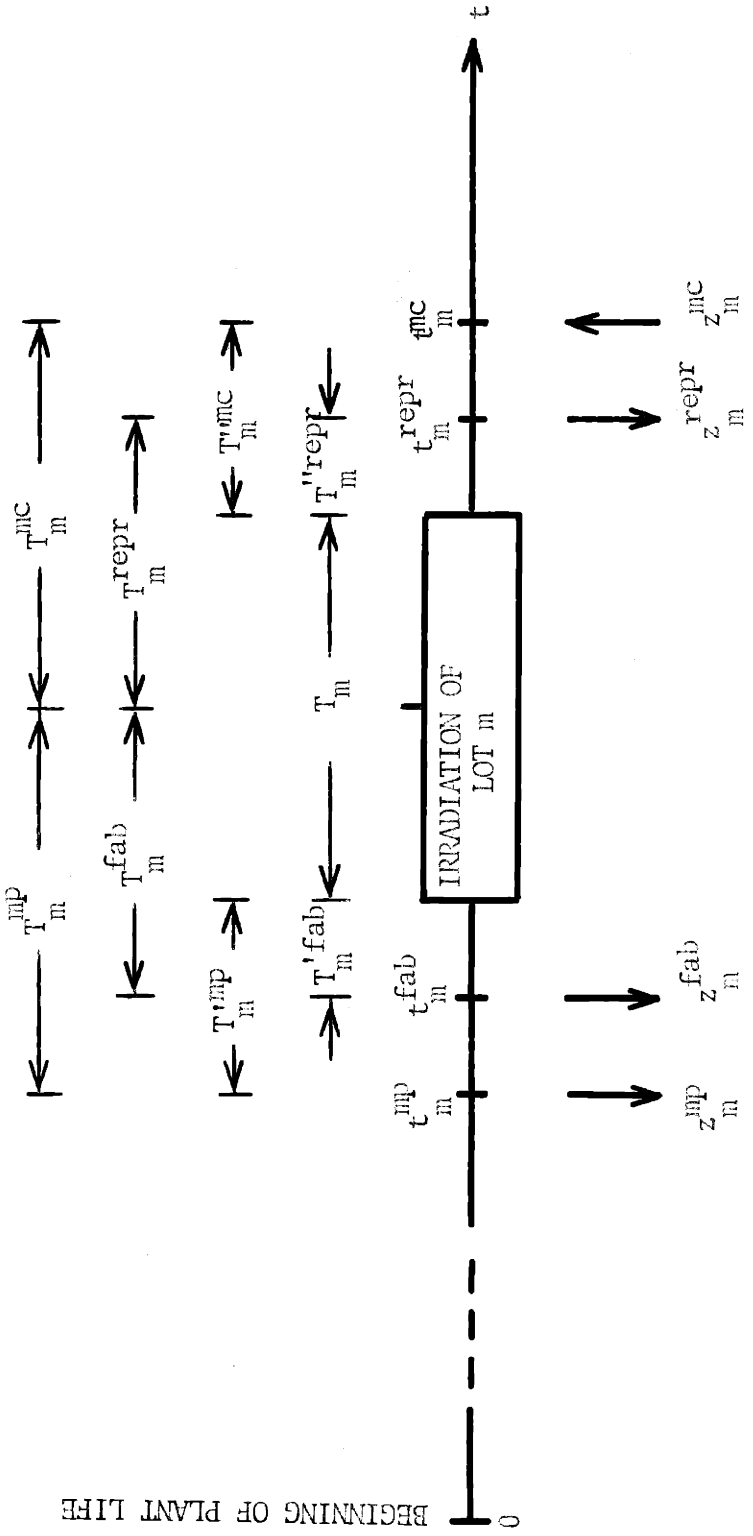

FIG. 2.3 TIMING OF CASH FLOWS ASSOCIATED WITH A FUEL LOT

TABLE 2.1 TAX TREATMENT OF FUEL TRANSACTIONS

Transaction Type	Description	Tax Factor	Method A	Method B
Z	capitalized cost	$1/1-\tau$	material purchase; fabrication	material purchase; fabrication; reprocessing
O	expensed cost	1	reprocessing	
V'	capitalized (non-taxable) revenue from sources other than sale of electricity	$1/1-\tau$		material credit
V	non-capitalized (taxable) revenue from sources other than sale of electricity	1	material credit	
D	depreciation for tax purposes; fictitious; for each Z-type cost, there must appear a depreciation term	$\tau/1-\tau$	material purchase and fabrication	(material purchase and fabrication) -(material credit -reprocessing)

and the tax depreciation credit reverses sign. This would imply a "tax appreciation debit", an entity not recognized in accounting nor allowed by taxing authorities. There is no symmetry with regard to tax depreciation: appreciation is not the opposite, or mirror image, of depreciation, for tax purposes.

Tax regulations require that ordinary income - that from the sale of the firm's ordinary product - be taxed at the corporate rate, τ, at the time that the income is realized (product exchanged for cash). Other regulations and rates cover extraordinary income, capital gains, losses, etc. The "ordinary" product of electric utility companies is electricity. It is conceivable that fissile material could become another ordinary product for utilities operating breeders, and that this new income will be taxed in the same manner as that from the sale of electricity.

How or whether this income is to be taxed, and the details of the fuel account structure, are beyond the scope of this report, and must await resolution by tax and regulatory agencies, or by common usage. Methods A and B are compared in Section 2.5. Choice of method has a significant effect on absolute values of levelized fuel cost, particularly in the radial blanket, but does not distort the economic ranking of design alternatives, nor does it significantly affect optimized parameters such as exposure. Method A was selected and used consistently in the case studies of Chapter 5.

2.3.2.1 Method A

Under Method A, Equation (2-18) becomes

$$\text{(numerator)} = \sum_{m}^{n} \left\{ \frac{z_m^{mp}}{1-\tau} \, w(t_m^{mp}) + \frac{z_m^{fab}}{1-\tau} \, w(t_m^{fab}) \right.$$

$$+ z_m^{repr} \, w(t_m^{repr}) - z_m^{mc} \, w(t_m^{mc})$$

$$\left. - \frac{\tau}{1-\tau} (z_m^{mp} + z_m^{fab}) \sum_{k}^{K} g_k \, w(t_m^k) \right\} , \qquad (2\text{-}21)$$

where the inner summation is taken over the tax depreciation credits, k, for lot m, and the g_k are fractional coefficients determined by the tax depreciation schedule used.

Capitalized costs associated with the fuel lot m are amortized (depreciated for tax purposes) over the time the lot is in productive use, i.e. the time it spends in the reactor. Except for tax purposes, the depreciation schedule is immaterial; only the initial and discharge values of the fuel are relevant. Tax depreciation need not be consistent with the actual change of fuel value during irradiation since the IRS permits certain fictitious tax depreciation schedules. For consistency, simplicity, and because actual fuel value changes are practically linear, straight line depreciation of fuel is frequently used in utility accounting(80).

With straight line tax depreciation, the tax depreciation term for lot m becomes

$$\frac{\tau}{1-\tau} (z_m^{mp} + z_m^{fab}) \sum_{k}^{K} g_k \, w(t_m^k)$$

$$= \frac{\tau}{1-\tau} \frac{(z_m^{mp} + z_m^{fab})}{K} \sum_{k}^{K} w(t_m^k)$$

$$= \frac{\tau}{1-\tau} \frac{(z_m^{mp} + z_m^{fab})}{K} \, w(t_m) \sum_{k}^{K} w(T_m^k) , \qquad (2\text{-}22)$$

where

$t_m \equiv$ time from beginning of plant life to midpoint of irradiation of lot m,

$T_m^k \equiv t_m^k - t_m$

$t_m^k \equiv$ time of depreciation credit k.

Little accuracy is lost if only one tax depreciation credit is assumed and it occurs at the irradiation midpoint. Table 2.2 illustrates the effect of this assumption for an irradiation time of five years. With this assumption, Equation (2-21) becomes

$$\text{(numerator)} = \sum_m^n \left\{ \frac{z_m^{mp}}{1-\tau} \, w(t_m^{mp}) + \frac{z_m^{fab}}{1-\tau} \, w(t_m^{fab}) + z_m^{repr} \, w(t_m^{repr}) - z_m^{mc} \, w(t_m^{mc}) - \frac{\tau}{1-\tau} (z_m^{mp} + z_m^{fab}) \, w(t_m) \right\} \qquad (2\text{-}23)$$

Grouping the terms by component (mp, fab, repr, mc) and recalling Equation (2-16), the contribution of the fuel stream ($\bar{e}$) to the total reactor fuel cost is given by

$$\bar{e} = \bar{e}_{mp} + \bar{e}_{fab} + \bar{e}_{repr} + \bar{e}_{mc}$$

$$\bar{e}_{mp} = 1000 \, \frac{\sum_m^n z_m^{mp} \left[\frac{w(t_m^{mp})}{1-\tau} - \frac{\tau}{1-\tau} \, w(t_m) \right]}{\sum_j^N w(j) \, E_j}$$

TABLE 2.2 EFFECT OF ASSUMING A SINGLE TAX DEPRECIATION CREDIT

	K = 5 "exact"			K = 1 "approx."		
k	T_m^k	$w(T_m^k)$	k	T_m^k (yr)	$w(T_m^k)$
1	-2	1.1664			
2	-1	1.08000			
3	0	1.00000	1	0	1.00000
4	+1	0.92593			
5	+2	0.85754			
$\frac{1}{K}\sum_{k}^{K} w(T_m^k) =$		1.00594			1.00000

$$\bar{e}_{fab} = 1000 \frac{\sum_m^n z_m^{fab} \left[\frac{w(t_m^{fab})}{1-\tau} - \frac{\tau}{1-\tau} w(t_m) \right]}{\sum_j^N w(j) E_j}$$

$$\bar{e}_{repr} = 1000 \frac{\sum_m^n z_m^{repr} w(t_m^{repr})}{\sum_j^N w(j) E_j}$$

$$\bar{e}_{mc} = -1000 \frac{\sum_m^n z_m^{mc} w(t_m^{mc})}{\sum_j^N w(j) E_j} \qquad (2\text{-}24)$$

Defining

$$T_m^{mp} \equiv t_m - t_m^{mp} = T_m'^{mp} + 1/2\, T_m$$

$$T_m^{fab} \equiv t_m - t_m^{fab} = T_m'^{fab} + 1/2\, T_m$$

$$T_m^{repr} \equiv t_m - t_m^{repr} = -(T_m''^{repr} + 1/2\, T_m)$$

$$T_m^{mc} \equiv t_m - t_m^{mc} \equiv -(T_m''^{mc} + 1/2\, T_m)\,, \qquad (2\text{-}25)$$

observing that

$$w(a)\, w(b) = w(a+b), \qquad (2\text{-}26)$$

one obtains, for the fuel stream in question,

$$\bar{e}_{mp} = 1000 \frac{\sum_{m}^{n} w(t_m)\, z_m^{mp} \left[\frac{w(-T_m^{mp})}{1-\tau} - \frac{\tau}{1-\tau} \right]}{\sum_{j}^{n} w(j) E_j}$$

$$\bar{e}_{fab} = 1000 \frac{\sum_{m}^{n} w(t_m)\, z_m^{fab} \left[\frac{w(-T_m^{fab})}{1-\tau} - \frac{\tau}{1-\tau} \right]}{\sum_{j}^{N} w(j) E_j}$$

$$\bar{e}_{repr} = 1000 \frac{\sum_{m}^{n} w(t_m)\, z_m^{repr} \left[w(-T_m^{repr}) \right]}{\sum_{j}^{N} w(j)\, E_j}$$

$$\bar{e}_{mc} = -1000 \frac{\sum_{m}^{n} w(t_m)\, z_m^{mc} \left[w(-T_m^{mc}) \right]}{\sum_{j}^{N} w(j)\, E_j} \qquad (2\text{-}27)$$

2.3.2.2 Direct and Carrying Charge Contributions

Each fuel stream component can further be separated into direct and carrying charge subcomponents. For component q(mp, fab, repr, or mc), of lot m, the direct dollar cost is z_m^q . Let $(z_m^q)^{**}$ be the carrying charge component. Then the total dollar cost, $(z_m^q)^*$, is given by

$$(z_m^q)^* \equiv (\text{direct})_m^q + (\text{Ca.Chg.})_m^q$$

$$= z_m^q + (z_m^q)^{**}$$

$$= z_m^q + f_m^q z_m^q$$

$$= z_m^q \quad F_m^q \qquad (2\text{-}28)$$

where

$$F_m^q \equiv 1 + f_m^q$$

The carrying charge factors (F_m^q) are readily identified as the bracketed [ ] terms in Equation (2-27), and are summarized in Table 2.3.

Levelized cost of electricity associated with the fuel stream's component q is therefore

$$\bar{e}_q = (\pm)\ 1000\ \frac{\sum_m^n w(t_m)\ z_m^q\ F_m^q}{\sum_j^N w(j)\ E_j}$$

$$= 1000\ \frac{\sum_m^n w(t_m)\ z_m^q}{\sum_j^N w(j)\ E_j} + 1000\ \frac{\sum_m^n w\ (t_m)\ z_m^q\ f_m^q}{\sum_j^N w(j)\ E_j}$$

$$= \bar{e}_{q,\text{direct}} + \bar{e}_{q,\text{CaChg}} \qquad (2\text{-}29)$$

2.3.2.3 Method B

In Method B, the reprocessing and material credit transactions are capitalized. Only the reprocessing and material credit carrying charge factors differ between Methods A and B.

TABLE 2.3 SUMMARY OF EXPRESSIONS FOR CARRYING CHARGE FACTORS, F_m^q, BY CASH FLOW METHOD

Component q	Method A	Method B
material purchase	$\frac{1}{1-\tau}[w(-T_m^{mp}) - \tau]$	$\frac{1}{1-\tau}[w(-T_m^{mp}) - \tau]$
fabrication	$\frac{1}{1-\tau}[w(-T_m^{fab}) - \tau]$	$\frac{1}{1-\tau}[w(-T_m^{fab}) - \tau]$
reprocessing	$w(-T_m^{repr})$	$\frac{1}{1-\tau}[w(-T_m^{repr}) - \tau]$
material credit	$w(-T_m^{mc})$	$\frac{1}{1-\tau}[w(-T_m^{mc}) - \tau]$

Following a derivation parallel to Equation (2-21) through Equation (2-29), the Method B carrying charge factors shown in Table 2.3 are found. Equations (2-29) are common to both methods.

2.3.2.4 Direct Dollar Costs Per Lot

A fuel lot's direct costs are given in terms of unit costs ($/kg) as follows:

$$z_m^{mp} = C_{28}M_{28}^0 + C_{49}M_{49}^0 + C_{40}M_{40}^0 + C_{41}M_{41}^0 + C_{42}M_{42}^0$$

$$z_m^{fab} = C_{fab}\, M_{HM}^0$$

$$z_m^{repr} = C_{repr}\, M_{HM}^0 \qquad (2\text{-}30)$$

$$z_m^{mc} = C_{28}M_{28}(T) + C_{49}M_{49}(T) + C_{40}M_{40}(T) + C_{41}M_{41}(T) + C_{42}M_{42}(T)$$

where

$$M_{HM}^0 \equiv M_{28}^0 + M_{49}^0 + M_{40}^0 + M_{41}^0 + M_{42}^0$$

The M's are masses of the isotopes U238, Pu239, Pu240, Pu241, Pu242 contained in the lot m in kilograms. Isotope values (C_{28}, C_{49}, ...) have units of dollars per kilogram of the isotope in question. Processing unit costs (C_{fab}, C_{repr}) have units of dollars per kilogram of heavy metal (U, Pu) loaded, and depend, of course, on the region for which the lot is intended (core, axial blanket, radial blanket).

The unit costs (C_{fab}, C_{repr}, C_{28}, C_{49}, . . .) together with the cost of money parameters (τ, f_b, r_b, f_s, r_s) are regarded in this report as forming the "economic environment," and are set parametrically, external to the present fuel costing model. Economic environment is varied in the sensitivity studies of Chapter 5.

2.4 SIMPLIFICATIONS FOR BATCH AND SCATTER FUEL MANAGEMENT SCHEMES; LOCAL FUEL ECONOMIC PERFORMANCE

2.4.1 Batch Fuel Management

"Batch" fuel management of a region (core, axial blanket or radial blanket) is defined here as a scheme in which the region's fuel is discharged and replaced as a whole, and the fuel associated with the region or fuel stream sees only one position in the reactor.

If plant load factor remains approximately constant throughout plant life, and if physics-depletion characteristics of the stream are insensitive to the fuel management of the remainder of the reactor, then the fuel lots in the stream are identical: the load and discharge compositions of all lots are the same, the irradiation times for the lots are the same, and for the fuel stream in question, there are no beginning-of-plant-life and end-of-plant-life transients. For such a fuel stream, Equation (2-29) becomes

$$\bar{e}_q = 1000 \frac{z^q F^q \sum_m^n w(t_m)}{E \sum_j^N w(j)} \qquad (2\text{-}31)$$

where $\bar{e}_q$ is the levelized energy cost (mills/KWHr) for cost component q, F^q is the carrying charge factor for component q, E is the annual electricity produced in KWHr, n is the number of fuel lots in the fuel stream throughout plant life, N is the number of years of plant life, and z^q is the direct cost in dollars for component q associated with a fuel lot, that is, associated with the total fuel volume of the batch-managed region.

The expression may be further simplified by noting that

$$\frac{\sum_{m}^{n} w(t_m)}{\sum_{j}^{N} w(j)} \simeq \frac{n}{N} = \frac{1}{T} \qquad (2\text{-}32)$$

where T is the irradiation time of a fuel lot in years.

Equation (2-32) is exact for n = N (T = 1 year). Error in the approximation (2-32) increases with decrease in n (increase in T). Irradiation times of interest are about six years (radial blanket fuel) or less. Table 2.4 shows that the error, for a six year irradiation time and an 8% discount rate, is less than 1%.

The factor 1/T may be thought of as the fuel throughput in lots per year, for the fuel stream in question.

Equation (2-31) becomes

$$\bar{e}_q = \frac{1000}{ET} z^q F^q \qquad (2\text{-}33)$$

and the total cost associated with the stream is

$$\bar{e} = \frac{1000}{ET} \sum_{q} z^q F^q \qquad (2\text{-}34)$$

2.4.2 Scatter Fuel Management

"Scatter" fuel management of a region or subregion is a scheme in which a fraction g of the region's fuel is discharged and replaced during a refueling event. As in batch management, the fuel sees only one position in the reactor.

Because a fraction 1-g of the initial load is incompletely irradiated, the region experiences a beginning of plant life fuel transient. Once in

TABLE 2.4 EFFECT OF THE APPROXIMATION $\dfrac{\sum_{m}^{n} w(t_m)}{\sum_{j}^{N} w(j)} \simeq \dfrac{1}{T}$

T(yr)	n	N	$\dfrac{\sum_{m}^{n} w(t_m)}{\sum_{j}^{N} w(j)}$	$\dfrac{n}{N}$	Error
1	30	30	1.00000	1.00000	0
6	5	30	0.1653066	0.166666	less than 1%

equilibrium, the fuel lots' irradiation times and load and discharge compositions are identical, and assuming plant load factor remains constant, Equation (2-31) modified for equilibrium scatter fueling is:

$$(\bar{e}_q)_{EQ} = \frac{1000 \; g \; z^q \; F^q \; \sum_m^n w(t_m)}{E \sum_j^N w(j)} \quad , \tag{2-31A}$$

where the fuel lot size is one-gth of the total fuel volume of the region.

The expression corresponding to Equation (2-32) for equilibrium scatter management is:

$$\frac{\sum_m^n w(t_m)}{\sum_j^N w(j)} \simeq \frac{n}{N} = \frac{1}{gT} \tag{2-32A}$$

Thus,

$$(\bar{e}_q)_{EQ} = \frac{1000}{ET} \; z^q \; F^q \tag{2-33A}$$

and the total equilibrium fuel cost associated with the stream is

$$(\bar{e})_{EQ} = \frac{1000}{ET} \sum_q z^q \; F^q \quad . \tag{2-34A}$$

Comparison of Equations (2-33), (2-34), (2-33A) and (2-34A) shows that the functional forms of the batch and equilibrium scatter cost equations are identical. Indeed, the processing costs - fabrication, reprocessing - are numerically equal as well, for the same irradiation time. Only the material costs

$$z^{mp} = C_{28}M_{28}^0 + C_{49}M_{49}^0 + \ldots$$

$$z^{mc} = C_{28}M_{28}(T) + C_{49}M_{49}(T) + \ldots \tag{2-30}$$

may differ, owing to the possibly-differing physics-depletion characteristics of the two management schemes.

For the same irradiation time (T), the time averaged composition, e.g. fissile plutonium content, of a region managed by scatter refueling is qualitatively the same as if it were batch managed. In scatter management, however, the composition varies within a smaller range, since its cycle time is shorter - one gth that of the batch managed region.

2.4.3 Local Fuel Economic Performance

It is useful to display the fuel economic performance as a function of position in one of the major regions (core, axial blanket, radial blanket), under batch or scatter management. For example, one may wish to know the performance of the third row of fuel assemblies in the radial blanket, and how it compares to that of the second row, etc. For purposes of comparing these subregions, a figure of merit independent of their volumes is desired.

From Equation (2-34), the fuel costs associated with a stream (region or subregion) is

$$\bar{e} = \bar{e}_{mp} + \bar{e}_{fab} + \bar{e}_{repr} + \bar{e}_{mc}$$

$$= \frac{1000}{E}\left[\frac{z^{mp}F^{mp}(T)}{T} + \frac{z^{fab}F^{fab}(T)}{T} + \frac{z^{repr}F^{repr}(T)}{T} - \frac{z^{mc}(T)\ F^{mc}(T)}{T}\right] \qquad (2\text{-}35)$$

where the carrying charge factors and direct material credit have been expressed as functions of irradiation time, T.

Using Equations (2-30) to express the direct dollar costs in terms of unit costs, one obtains

$$\bar{e} = \frac{1000}{E}\left[\frac{(C_{28}M^0_{28} + C_{49}M^0_{49} + \ldots)\,F^{mp}(T)}{T} + \frac{C_{fab}\,M^0_{HM}\,F^{fab}(T)}{T} + \frac{C_{repr}\,M^0_{HM}\,F^{repr}(T)}{T} - \frac{(C_{28}M_{28}(T) + C_{49}M_{49}(T) + \ldots)\,F^{mc}(T)}{T}\right] \quad (2\text{-}36)$$

The contribution of fertile material (U238, Pu240) to the value of fuel is insignificant. For core fuel

$$C_{fert}M^0_{fert} << C_{fiss}M^0_{fiss}, C_{fab}M^0_{HM}, C_{repr}M^0_{HM}$$

$$C_{fert}M_{fert}(T) << C_{fiss}M_{fiss}(T), C_{fab}M^0_{HM}, C_{repr}M^0_{HM} \quad (2\text{-}37)$$

For blanket fuel,

$$C_{fert}M^0_{fert} << C_{fiss}M_{fiss}(T), C_{fab}M^0_{HM}, C_{repr}M^0_{HM}$$

$$C_{fert}M_{fert}(T) << C_{fiss}M_{fiss}(T) \quad (2\text{-}38)$$

In either case, the assumption

$$\text{a)}\quad C_{fert} \simeq 0 \quad (2\text{-}39)$$

has a negigible effect on results. In addition, the following assumption is made:

b) $C_{fiss} = C_{49} = C_{41}$ (2-40)

With assumptions a) and b), Equation (2-36) reduces to

$$\bar{e} = \frac{1000}{E} \left[\frac{C_{Fiss}(M^0_{49} + M^0_{41})\, F^{mp}(T)}{T} + \frac{C_{fab}\, M^0_{HM}\, F^{fab}(T)}{T} + \frac{C_{repr}\, M^0_{HM}\, F^{repr}(T)}{T} - \frac{C_{fiss}(M_{49}(T) + M_{41}(T))\, F^{mc}(T)}{T} \right] \quad (2\text{-}41)$$

Multiplying and dividing by M^0_{HM},

$$\bar{e} = \frac{1000}{E} M^0_{HM} \left[\frac{C_{fiss}\, \epsilon_0\, F^{mp}(T)}{T} + \frac{C_{fab}\, F^{fab}(T)}{T} + \frac{C_{repr}\, F^{repr}(T)}{T} - \frac{C_{fiss}\, \epsilon(T)\, F^{mc}(T)}{T} \right] \quad (2\text{-}42)$$

where

$$\epsilon_0 = (M^0_{49} + M^0_{41}) / M^0_{HM}$$

$$\epsilon(T) = (M_{49}(T) + M_{41}(T))/M^0_{HM} \quad (2\text{-}43)$$

The term in brackets may be regarded as a figure of merit representing local fuel performance, having units of dollars per year per local kilogram of heavy metal. Normalizing to kilograms of initial heavy metal in this manner removes the volume effect in comparing regions or subregions. Except through the discharge composition, $\epsilon(T)$, in the material credit term, the local performance is independent of reactor power level, or load factor.

2.5 COMPARISON OF FUEL COST ACCOUNTING METHODS

2.5.1 Effect of Tax Assumptions in the Cash Flow Method

In Section 2.3, two tax interpretations were applied to the treatment of post-irradiation transactions:

Method A: The post-irradiation transactions are not capitalized i.e. reprocessing cost is written off as a tax deductable expense in the year that it occurs, and material credit is taxed as ordinary income, along with the sale of electricity.

Method B: The post-irradiation transactions are capitalized.

Choice of Method A or B affects only the carrying charges associated with reprocessing and material credit. All direct costs and the carrying charges on pre-irradiation costs remain the same.

For a tax rate of 50%, the carrying charges on material credit and reprocessing under Method B are double those from Method A, i. e.

$$\frac{(\bar{e}^{repr})^{**}_B}{(\bar{e}^{repr})^{**}_A} = \frac{(F^{repr})_B - 1}{(F^{repr})_A - 1}$$

$$= \frac{\frac{1}{1-\tau}\left[w(-T^{repr}) - \tau\right] - 1}{w(-T^{repr}) - 1} = 2 \quad ; \qquad (2\text{-}44)$$

and similarly,

$$\frac{(\bar{e}^{mc})^{**}_{B}}{(\bar{e}^{mc})^{**}_{A}} = 2 \qquad (2\text{-}45)$$

Thus,

$$\frac{(\bar{e}^{mc})^{**}_{B} + (\bar{e}^{repr})^{**}_{B}}{(\bar{e}^{mc})^{**}_{A} + (\bar{e}^{repr})^{**}_{A}} = 2 \qquad (2\text{-}46)$$

The carrying charges on reprocessing and material credit are but two of the eight subcomponents making up the total cost of the fuel lot. Also, the carrying charges on reprocessing and material credit are of opposite sign, tending to cancel.

The discrepancy between total costs of the lot, as calculated by Methods A and B, increases with irradiation time as carrying charges in general become more important, and as the material credit (plutonium buildup) from blanket fuel further overshadows blanket reprocessing costs.

Figures 2.4, 2.5 and 2.6 compare the two methods as applied to core, axial blanket and radial blanket fuel costs, respectively, of the reference LMFBR (Chapter 4). Method A is seen to result in lower total fuel costs in all three regions. The discrepancy in core fuel costs is about 10% at the design residence time of two years. In the axial blanket, the discrepancy is about 20% at two years. For the radial blanket, the discrepancy is quite severe, although the two methods yield comparable optimum residence times - 6 years in Method B, 6.5 years in Method A.

2.5.2 Relationship of the Cash Flow Method to Two Other Accounting Methods

For cost component q, lot m, the carrying charge in dollars, $(z_m^q)^{**}$, and the total cost in dollars, $(z_m^q)^{*}$, are given by

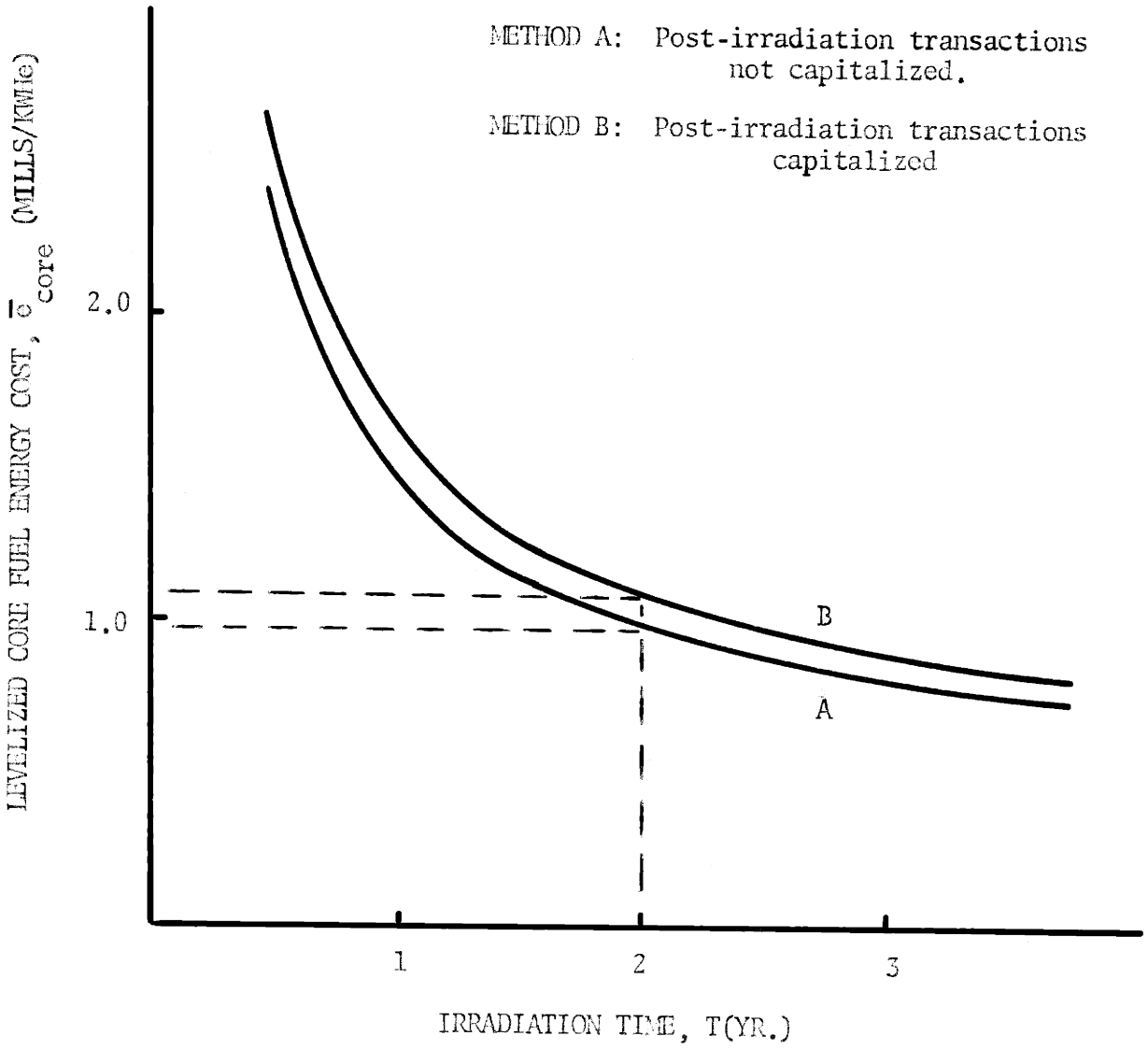

FIG. 2.4 EFFECT OF POST-IRRADIATION TAX ASSUMPTION ON LEVELIZED CORE FUEL ENERGY COST

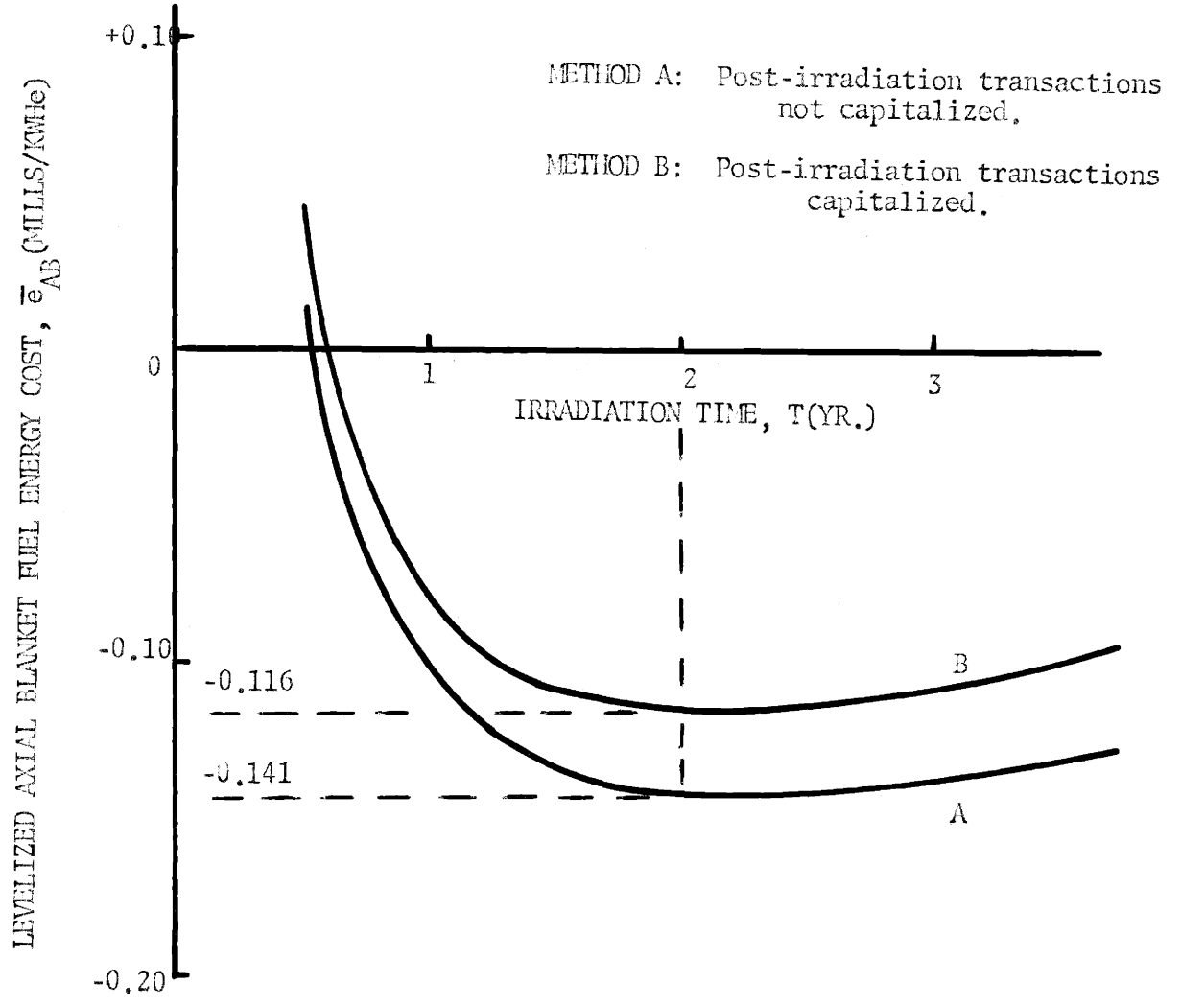

FIG. 2.5 EFFECT OF POST-IRRADIATION TAX ASSUMPTION ON LEVELIZED AXIAL BLANKET FUEL ENERGY COST.

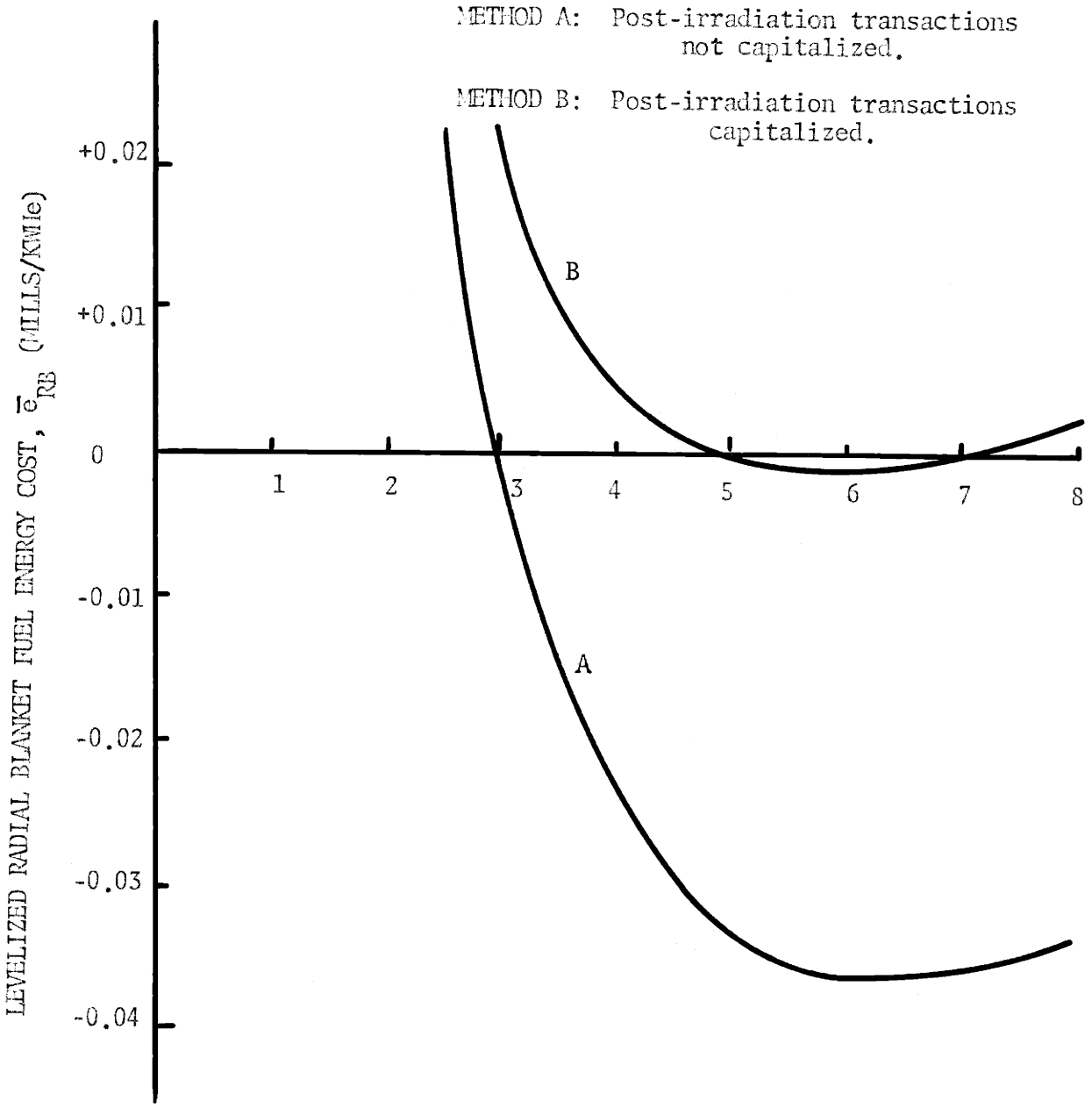

FIG. 2.6 EFFECT OF POST-IRRADIATION TAX ASSUMPTION ON LEVELIZED RADIAL BLANKET FUEL ENERGY COST

$$(z_m^q)^{**} = z_m^q f_m^q$$

and

$$(z_m^q)^{*} = z_m^q F_m^q$$

where

$$F_m^q \equiv 1 + f_m^q \,. \tag{2-28}$$

2.5.2.1 Cash Flow Method (CFM)

The cash flow method (CFM) of Sections 2.2 and 2.3 showed that for capitalized costs or capitalized revenues the carrying charge factor F_m^q takes the form

$$(F_m^q)_{CFM} = \frac{1}{1-\tau}\left[w\,(-T_m^q) - \tau\right] \qquad \text{(capitalized)} \tag{2-47}$$

while for expensed costs and taxed revenues the factor is

$$(F_m^q)_{CFM} = w(-T_m^q) \qquad \text{(expensed costs; taxed revenues)} \tag{2-48}$$

where

$$w(-T_m^q) \equiv \frac{1}{(1+x)^{-T_m^q}} = (1+x)^{T_m^q} \equiv \text{discount factor} \tag{2-49}$$

$$x \equiv (1-\tau)\, r_b\, f_b + r_s\, f_s \equiv \text{discount rate} \tag{2-50}$$

Two other methods of treating nuclear fuel carrying charges are commonly used:

(a) Simple Interest Method (SIM), (20, 22, 23)

(b) Compound Interest Method (CIM), (83)

The cash flow method (CFM) is related to these "approximate" methods below.

2.5.2.2 Simple Interest Method (SIM)

The SIM associates carrying charges with areas under a fuel lot's value histogram. Figure 2.7 shows the general appearance of such histograms for (a) depreciating core fuel and (b) appreciating blanket fuel, and how they may be constructed from the cash flows. Figures 2.8 and 2.9 are value histograms for the reference reactor core and radial blanket, respectively, defined in Chapter 4. Pre-irradiation transactions (material purchase and fabrication are assumed to occur simultaneously, as are the post-irradiation transactions (reprocessing and material credit).

In the SIM, the carrying charge and total dollar costs for component q of lot m are given by

$$(z_m^q)^{**}_{SIM} = (z_m^q)\ T_m^q\ y_q \qquad (2\text{-}51)$$

and

$$(z_m^q)^{*}_{SIM} = (z_m^q)\ (1 + T_m^q\ y_q) \qquad (2\text{-}52)$$

respectively, where

$$T_m^q = T'^q_m + 1/2\ T_m \quad \text{(pre-irradiation cash flows)} \qquad (2\text{-}53)$$

$$= -(T_m^q + 1/2\ T_m) \quad \text{(post-irradiation cash flows)}$$

$y_q \equiv$ carrying charge rate applicable to component q.

Thus the carrying charge factors F_m^q for the SIM are given by

$$(F_m^q)_{SIM} = 1 + T_m^q\ y_q\ . \qquad (2\text{-}54)$$

The factors $(F_m^q)_{CFM}$, given by Equations (2-47) and (2-48), reduce to $(F_m^q)_{SIM}$ for small $T_m^q\ y_q$. Expanding the discount factor in Equation (2-47) in a binomial series, one finds, for capitalized costs or capitalized revenues,

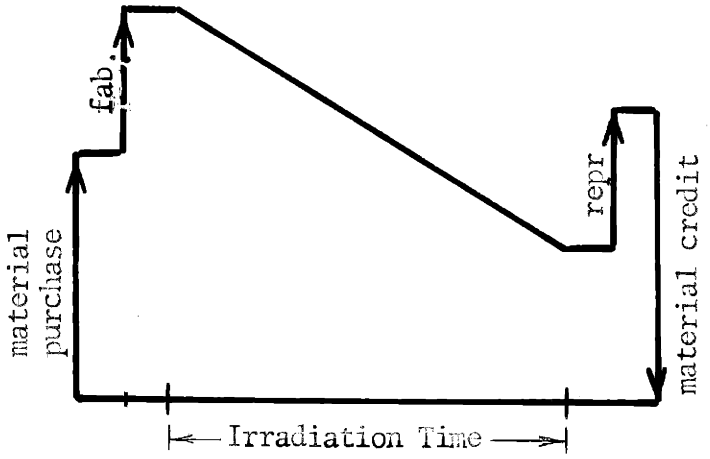

(a) FBR CORE FUEL

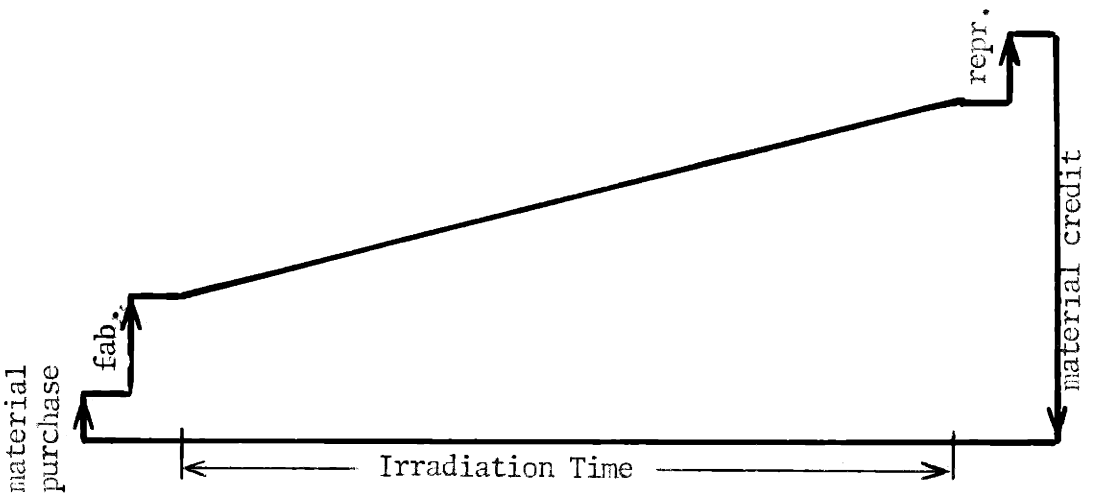

(b) FBR BLANKET FUEL

FIG. 2.7 CONSTRUCTION OF VALUE-TIME PLOTS FROM FUEL LOT CASH FLOWS

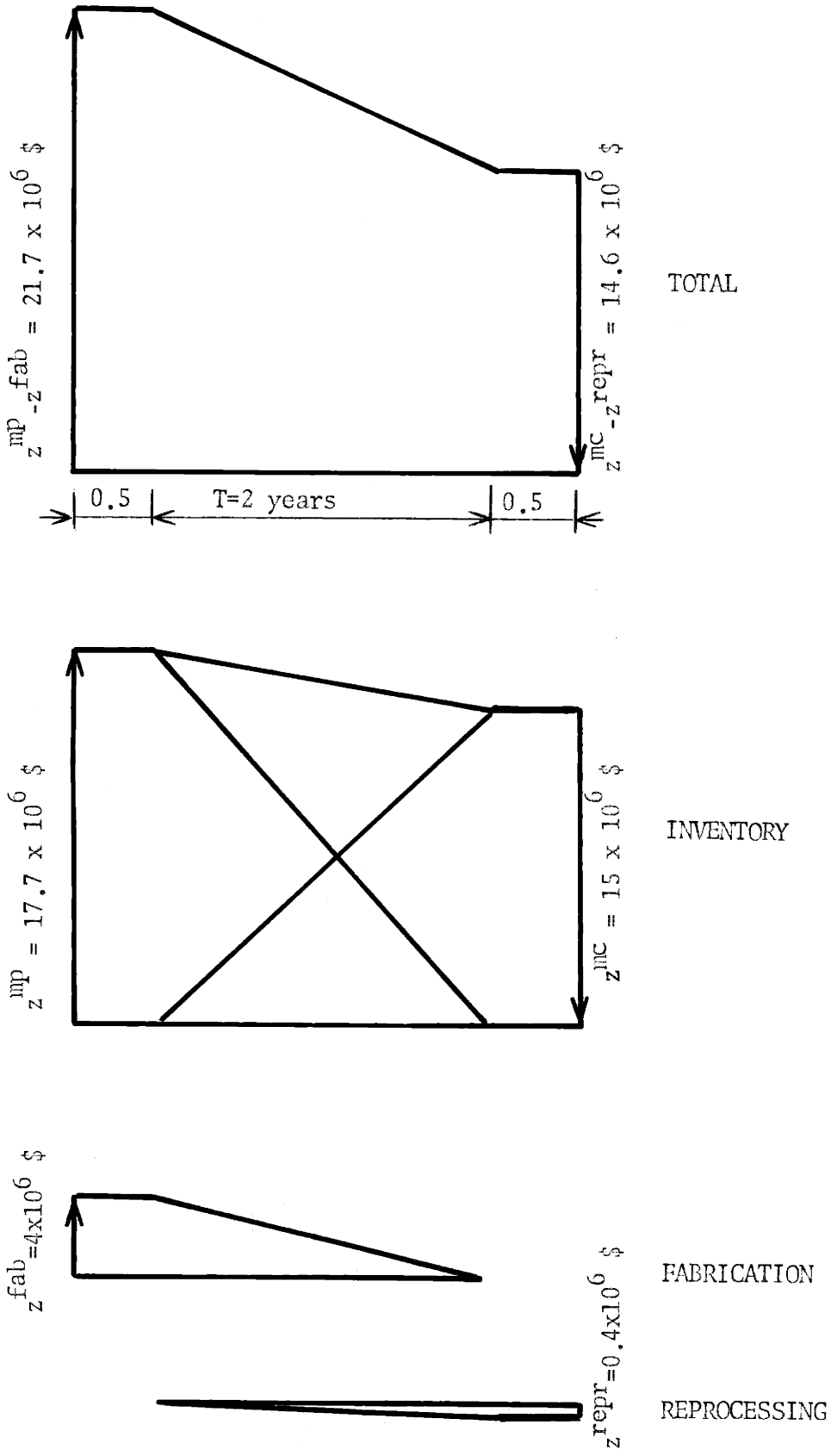

FIG. 2.8 VALUE-TIME PLOTS FOR A CORE FUEL BATCH

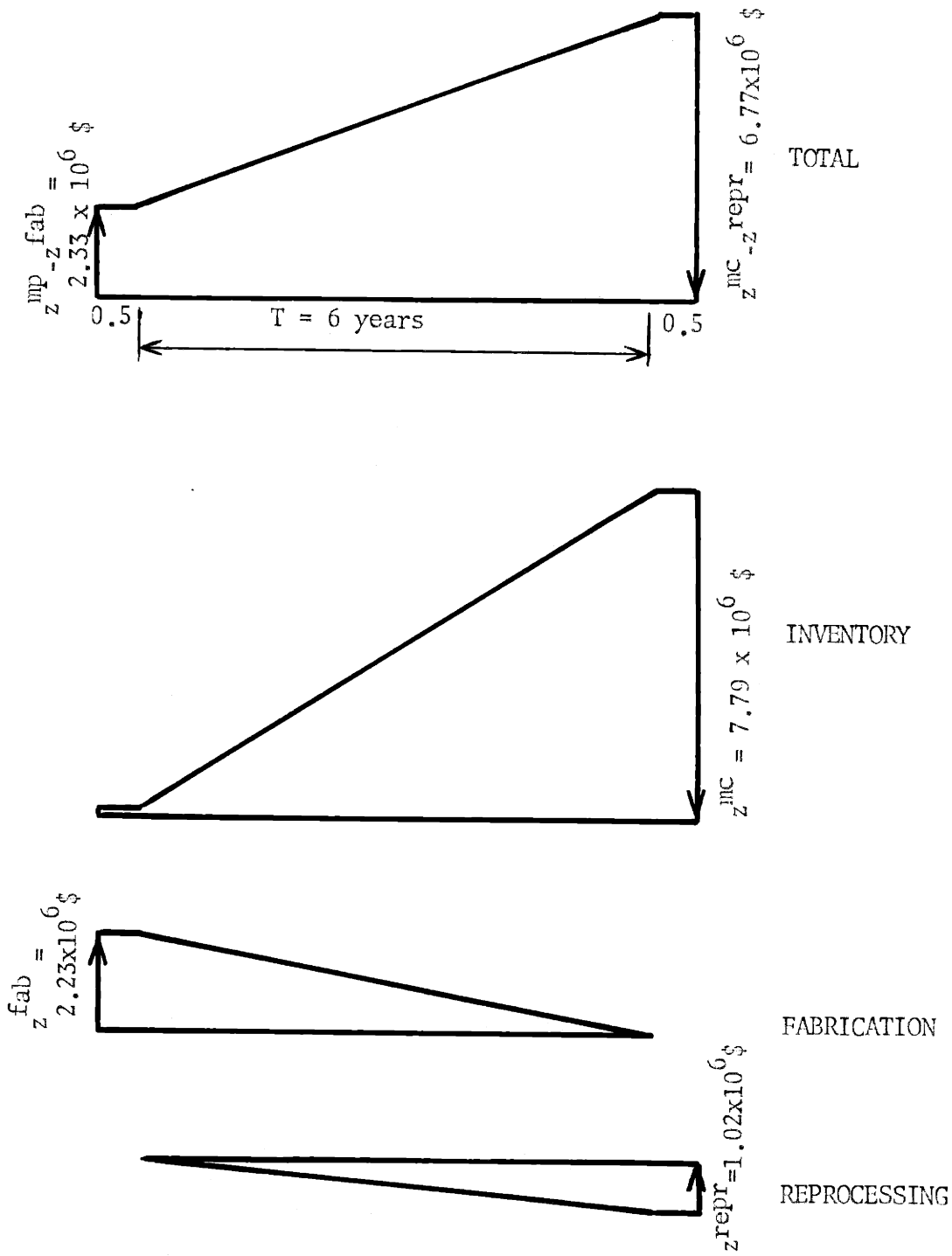

FIG. 2.9 VALUE-TIME PLOTS FOR A RADIAL BLANKET FUEL BATCH

$$(F_m^q)_{CFM} = \frac{1}{1-\tau}\,[w(-T_m^q) - \tau\,]$$

$$= \frac{1}{1-\tau}\,[(1+x)^{T_m^q} - \tau\,]$$

$$= \frac{1}{1-\tau}\,[\,1-\tau + T_m^q\,x + \frac{T_m^q\,(T_m^q - 1)x^2}{2!} + \ldots]$$

$$= 1 + T_m^q\,\frac{x}{1-\tau} + \frac{T_m^q\,(T_m^q - 1)}{2!}\,\frac{x^2}{1-\tau} + \ldots \qquad (2\text{-}55)$$

For small $T_m^q\,x/\,1-\tau$ Equation (2-55) reduces to the approximate form

$$(F_m^q)_{CFM} \simeq 1 + T_m^q\,\frac{x}{1-\tau} \equiv 1 + T_m^q\,y_q = (F_m^q)_{SIM} \qquad (2\text{-}56)$$

Thus for capitalized costs and capitalized revenues (not taxed), the correct carrying charge rate y_q for the SIM is

$$y_q = \frac{x}{1-\tau} \qquad \text{(capitalized costs or capitalized revenues)} \qquad (2\text{-}57)$$

where the discount rate (x) is given by (2-50).

Similarly, for expensed costs and taxed revenues,

$$(F_m^q)_{CFM} = w(-T_m^q) = (1+x)^{T_m^q}$$

$$= 1 + T_m^q\,x + \frac{T_m^q\,(T_m^q - 1)\,x^2}{2!} + \ldots . \qquad (2\text{-}58)$$

For small $T_m^q\,x$,

$$(F_m^q)_{CFM} \simeq 1 + T_m^q\,x = 1 + T_m^q\,y_q = (F_m^q)_{SIM}. \qquad (2\text{-}59)$$

Thus for expensed costs and taxed revenues the correct carrying charge

rate y_q in the SIM is

$$y_q = x \qquad \text{(expensed costs or taxed revenues)} \tag{2-60}$$

where, as before, the discount rate (x) is given by Equation (2-50).

2.5.2.3 Compound Interest Method (CIM)

The restriction on SIM Equations (2-56) and (2-57) that $T_m^q y_q$ be small suggests that SIM may be improved by continuing (2-56) in a series of powers of y_q:

$$(F_m^q)_{CIM} = 1 + T_m^q y_q + \frac{T_m^q (T_m^q - 1)}{2!} y_q^2 + \ldots$$

$$= (1 + y_q)^{T_m^q} \tag{2-61}$$

Thus for the compound interest method (CIM),

$$(z_m^q)^{**}_{CIM} = (z_m^q)\,[(1+y_q)^{T_m^q} - 1] \tag{2-62}$$

and

$$(z_m^q)^{*} = (z_m^q)\,(1 + y_q)^{T_m^q} \tag{2-63}$$

where, again,

$$y_q = \frac{x}{1-\tau} \qquad \text{(capitalized costs or capitalized revenues)} \tag{2-57}$$

$$= x \qquad \text{(expensed costs or taxed revenues)} \tag{2-60}$$

The $(F_m^q)_{SIM}$ factors reduce, of course, to the $(F_m^q)_{CIM}$. Comparing Equations (2-61) and (2-60) with Equation (2-48), one observes that the $(F_m^q)_{CIM}$ and $(F_m^q)_{CFM}$ are identical for expensed costs and taxed revenues.

However, the $(F_m^q)_{CIM}$ and $(F_m^q)_{CFM}$ are not identical for capitalized costs and capitalized revenues, as can be seen by comparing the expansions (2-61) and (2-55): their first order terms are identical, but a CIM term of order $k>1$ is in error by a factor of $(1-\tau)^{k-1}$. The CIM overpredicts the true (CFM) factor F_m^q, for capitalized transactions.

2.5.2.4 Summary

Table 2.5 summarizes the distinction between the three methods of computing carrying charge factors, F_m^q.

Figure 2.10 illustrates the discrepancies between the three methods of computing F_m^q for a capitalized transaction. A discount rate of 8% and a tax rate of 50% are assumed in Figure 2.10. The SIM underpredicts F_m^q, while CIM overpredicts F_m^q. In both cases, errors are significant only for large T_m^q, or large y_q, or both. Since radial blanket fuel may be irradiated as long as ten years, the CFM derived in Sections 2.2 and 2.3 was selected.

2.6 SAMPLE CALCULATION: BEHAVIOR OF BLANKET FUEL COSTS WITH IRRADIATION TIME

Results using the fuel cost model derived in this Chapter exhibit features one would expect qualitatively. Figures 2.5 and 2.6 show the levelized fuel costs of the reference reactor's axial and radial blankets, respectively, as functions of irradiation time. Two major characteristics are noted.

(1) A "breakeven" exposure point exists, at which material credit just balances the material purchase, fabrication, and reprocessing costs:

$$\text{m.c.} = \text{m.p.} + \text{fab.} + \text{repr.} \qquad (2\text{-}64)$$

For blanket irradiation times below this point, fissile material produced

TABLE 2.5 SUMMARY OF EXPRESSIONS FOR CARRYING CHARGE FACTOR (F_m^q) BY CFM, CIM AND SIM

Transaction Type	Expression for Carrying Charge Factor, F_m^q		
	CFM	CIM	SIM
Capitalized Costs (Z) and Revenues (V')	$\frac{1}{1-\tau}\left[(1+x)^{T_m^q} - \tau\right]$	$(1+y_q)^{T_m^q}$	$1+y_q T_m^q$
		$y_q = \frac{x}{1-\tau}$	$y_q = \frac{x}{1-\tau}$
Non-Capitalized Transactions: Expensed Costs (O) Taxed Revenues (V)	$(1+x)^{T_m^q}$	$(1+y_q)^{T_m^q}$	$1+y_q T_m^q$
		$y_q = x$	$y_q = x$

Discount Rate: $x = (1-\tau)\, r_b f_b + r_s f_s$

Discount Intervals:

$T_m^q \equiv T_m'^q + 1/2\ T_m$ (pre-irradiation transactions)

$\equiv -(T_m''^q + 1/2\ T_m)$ (post irradiation transactions)

$(F_m^q)_{SIM} < (F_m^q)_{CFM} < (F_m^q)_{CIM}$

For $T_m^q y_q << 1$,

$(F_m^q)_{CFM} \longrightarrow (F_m^q)_{SIM}$

$(F_m^q)_{CIM} \longrightarrow (F_m^q)_{SIM}$

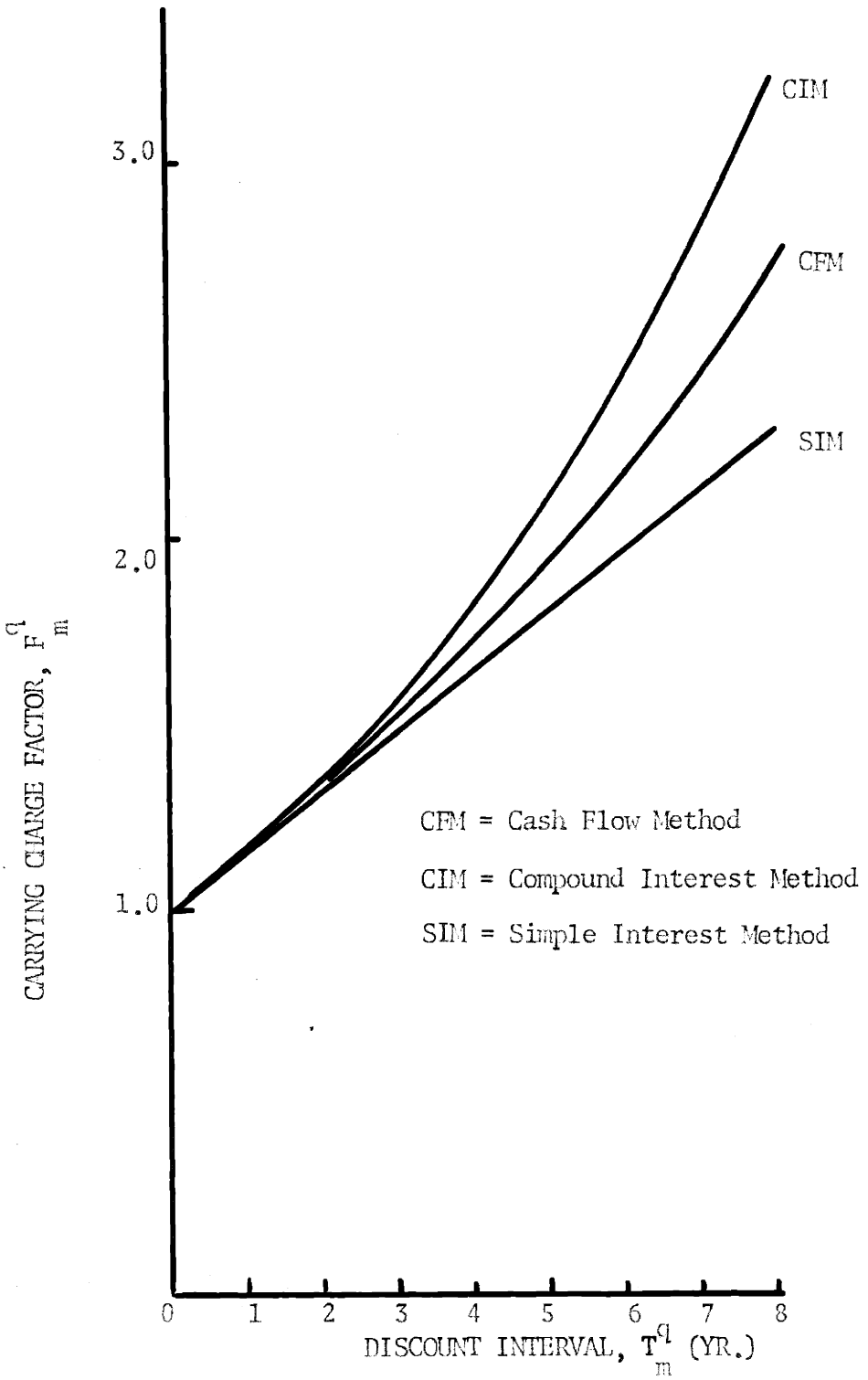

FIG. 2.10 COMPARISON OF CARRYING CHARGE FACTORS FOR CAPITALIZED TRANSACTIONS COMPUTED BY CFM, CIM, AND SIM

is not sufficient to yield a net revenue.

(2) An optimum exposure point exists, at which the cost is a minimum (most negative).

Figures 2.11 and 2.12 display radial blanket cost components as functions of irradiation time, under Method A. Material purchase (U238) has been ignored in both plots since its contribution is an order of magnitude below other components. Direct material credit is the only negative component; positive costs are shown netted against material credit in both figures. Carrying charges on fabrication and reprocessing components have been combined in "processing carrying charges".

In Figure 2.11 levelized costs are in units of dollars per kilogram of heavy metal (U + Pu) loaded. Total reactor energy released during irradiation of the radial blanket, is shown at the top of the figure. Direct material credit, $\left|C_{fiss} \in (T)\right|$, is seen to increase (become more negative) as irradiation time increases, but at a decreasing rate. (The depletion model used in generating $\in(T)$ is described in Chapter 3.) Inventory cost, $C_{fiss} \in (T)\ [F^{mc}(T) - 1]$, is seen to increase with irradiation time. Direct processing costs, C_{fab}, C_{repr} are, of course, constant, while their carrying charge, $C_{fab}[F^{fab}(T)-1] + C_{repr}[F^{repr}(T)-1]$, increases with irradiation time.

The costs of Figure 2.11, in dollars per kilogram of heavy metal, are to be assigned to the total reactor energy released during radial blanket irradiation, $E(KWH_e/year)T(year)$. Since E is constant, one may divide the costs of Figure 2.11 by blanket irradiation time T to obtain the radial blanket fuel costs in units of dollars per year per kilogram of heavy metal, Figure 2.12. This is the term in brackets in Equation (2.42), applied to the entire radial blanket. Figure 2.12 also includes a scale indicating the radial blanket levelized power costs in mills/KWHr.

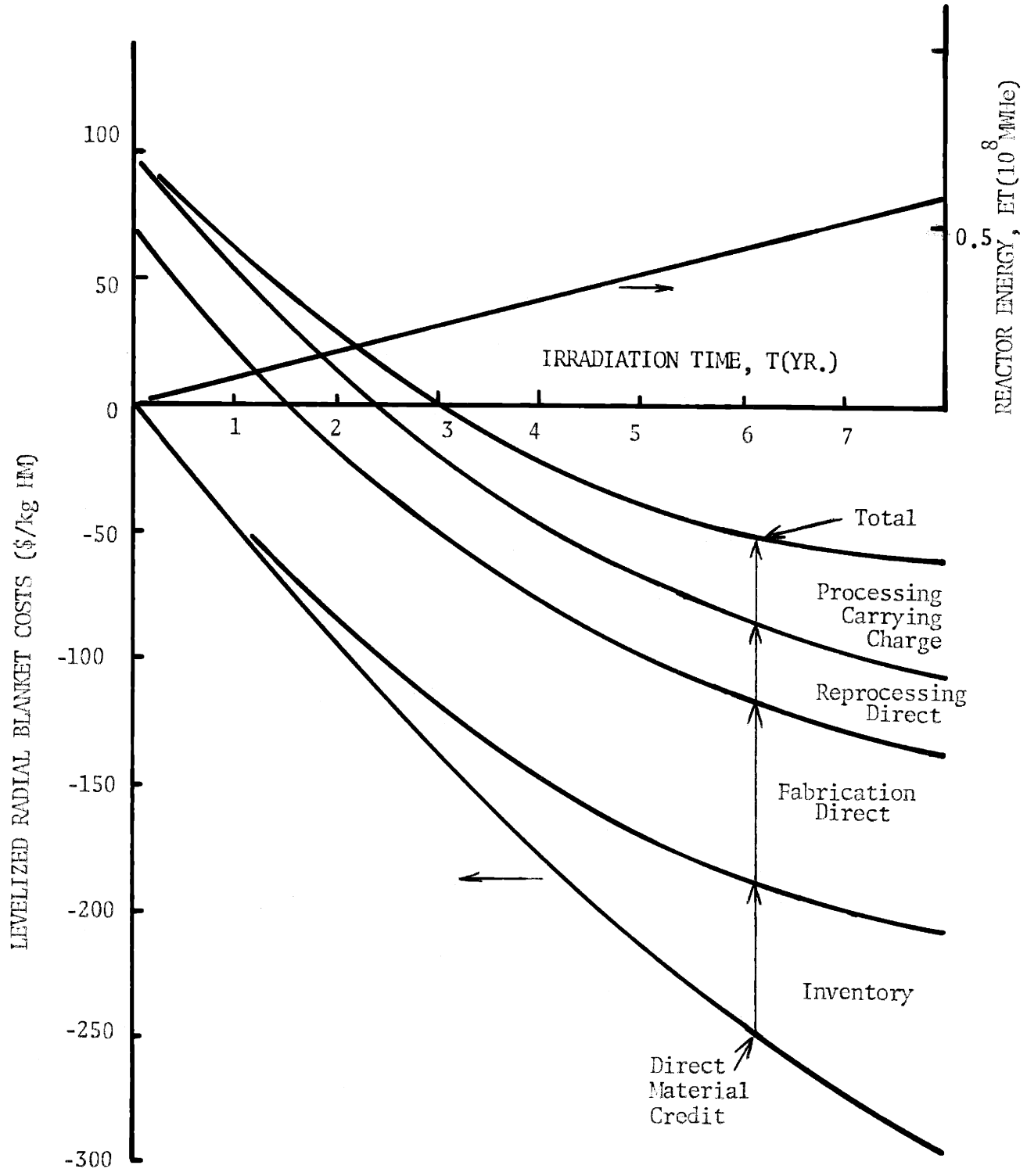

FIG. 2.11 COMPONENTS OF RADIAL BLANKET LEVELIZED COSTS AS FUNCTIONS OF IRRADIATION TIME

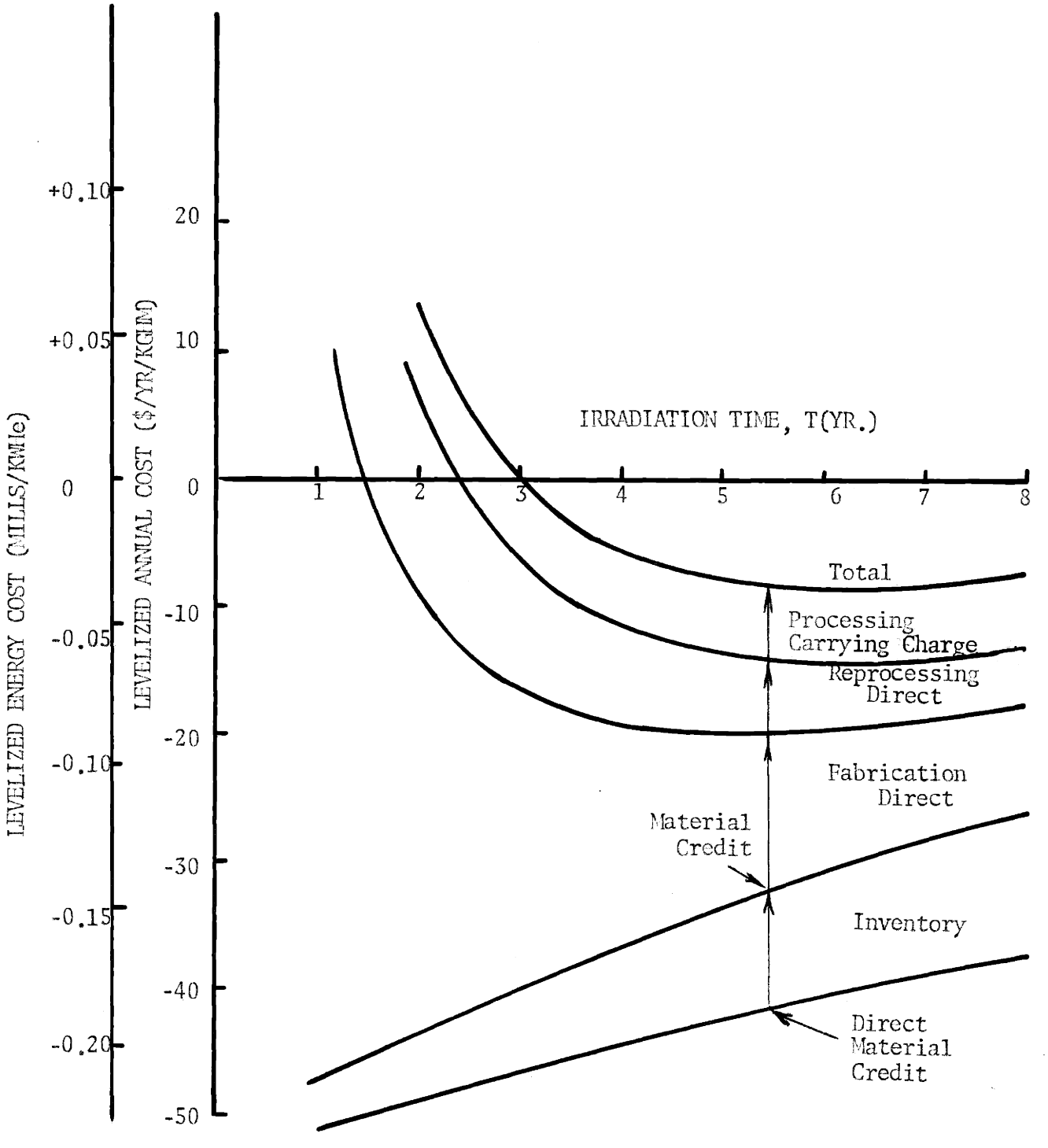

FIG. 2.12 COMPONENTS OF RADIAL BLANKET FUEL LEVELIZED ANNUAL COSTS AND ENERGY COSTS AS FUNCTIONS OF IRRADIATION TIME

From Figure 2.12, an optimum radial blanket irradiation time is seen to exist because of the opposing behavior of material credit and processing costs with irradiation time. Material credit decreases (becomes less negative) while processing cost decreases (become less positive).

2.7 SUMMARY

A general expression for levelized cost (price) of electricity is derived in Section 2.2. This formulation, labeled the "Cash Flow Method" (CFM) is applied to FBR fuel costs in Section 2.3. When applied to a region (core, axial blanket, or radial blanket) under batch or scatter fuel management, Section 2.4, the equations reduce to forms giving local fuel economic performance, e.g. in an annular fuel region or at a point. Table 2.6 below summarizes the CFM fuel cost equations.

Effects of the choice of accounting methods are examined in Section 2.5. Within the CFM, two options for treating post-irradiation transactions are identified:

Method A. Tax revenue from the sale of fissile material (material credit) as ordinary income, along with electricity revenue; treat reprocessing costs as tax deductable expenses.

Method B. Capitalize the revenue from the sale of fissile material; capitalize the reprocessing cost.

Choice between these two tax interpretations has a significant effect on absolute values of power costs (mills/KWHr), but does not distort comparative and incremental results, e.g. design rankings, optimization of radial blanket residence time, sensitivity studies.

The CFM is related to and compared with two approximate methods of treating carrying charges in Section 2.5: The "Compound Interest Method" (CIM); and the "Simple Interest Method" (SIM). For both capitalized and

TABLE 2.6 SUMMARY OF FBR FUEL COST ANALYSIS EQUATIONS (CASH FLOW METHOD)

1. Total Reactor Fuel Cost: $\bar{e}(\text{reactor}) = \sum_s (\bar{e})_s \ldots\ \frac{\text{mills}}{\text{KWHe}}$ s≡ fuel stream index

2. Fuel Stream Cost: $(\bar{e})_s = \sum_q (\bar{e}_q)_s \ldots\ \frac{\text{mills}}{\text{KWHe}}$ q ≡ cost component index = mp, fab, repr, mc

3. Component Costs of a Stream: $(\bar{e}_q)_s = (\bar{e}_{q,\text{direct}})_s + (\bar{e}_{q,\text{CaChg}})_s \ldots\ \frac{\text{mills}}{\text{KWHe}}$

$$= 1000\left(\frac{\sum_m^n w(t_m) z^q{}_m}{\sum_j^N w(j) E_j} + \frac{\sum_m^n w(t_m) z^q{}_m f^q{}_m}{\sum_j^N w(j)\ E_j} \right)_s$$

$$= 1000 \left(\frac{\sum_m^n w(t)_m z^q{}_m F^q{}_m}{\sum_j^N w(j)\ E_j} \right)_s$$

m ≡ fuel lot index, stream s

TABLE 2.6 - continued

4. Carrying Charge Factors:

$F_m^q \equiv 1 + f_m^q \equiv$ carrying charge factor, component q, fuel lot m of a given fuel stream

$= \frac{1}{1-\tau} [w(-T_m^q) - \tau] \ldots$ for q capitalized

$= w(-T_m^q) \ldots$ for q not capitalized (expensed cost or tax revenues)

where

$w(t) \equiv (1+x)^{-t} \equiv$ discount factor

$x \equiv (1-\tau) r_b f_b + r_s f_s \equiv$ discount rate

T_m^q as defined in Figure 2.3.

$\tau \equiv$ tax rate

$f_b \equiv$ bond fraction

$f_s \equiv$ stock fraction

$r_b \equiv$ rate of return to bondholders

$r_s \equiv$ rate of return to stockholders

5. Tax Assumptions

Component, q	Method A	Method B
material purchase	capitalized	capitalized

TABLE 2.6 - continued

Component, q	Method A	Method B
fabrication	capitalized	capitalized
reprocessing	not capitalized (expensed)	capitalized
material credit	not capitalized (taxed)	capitalized

6. Direct Dollar Costs (per lot, per stream)

material purchase . . $z_m^{mp} = C_{28}M_{28}^0 + C_{49}M_{49}^0 + C_{40}M_{40}^0 + C_{41}M_{41}^0 + C_{42}M_{42}^0$ ... \$/lot

fabrication . . $z_m^{fab} = C_{fab} M_{HM}^0$

reprocessing . . $z_m^{repr} = C_{repr} M_{HM}^0$

material credit . . $z_m^{mc} = C_{28}M_{28}(T) + C_{49}M_{49}(T) + C_{40}M_{40}(T) + C_{41}M_{41}(T) + C_{42}M_{42}(T)$

7. For batch or scatter fuel management of fuel stream s:

$$(\bar{e})_s = \frac{1000}{E} M_{HM}^0 \left[\frac{C_{fissile} \epsilon_o F^{mp}(T)}{T} + \frac{C_{fab} F^{fab}(T)}{T} + \frac{C_{repr} F^{repr}(T)}{T} - \frac{C_{fissile} \epsilon(T) F^{mc}(T)}{T} \right] \frac{\text{mills}}{\text{KWHe}}$$

[ ] = figure of merit, local fuel performance . . . $\frac{\$/\text{yr.}}{\text{kg HM loaded}}$

noncapitalized costs, the carrying charge factors of CIM and CFM are identical. Errors in carrying charge factors, introduced by use of CIM or SIM , are slight for typical core and axial blanket irradiation times - about one percent for an irradiation time of two years. At six years, representative of radial blanket batch irradiation, the errors are about +10% for the CIM, and -10% for the SIM.

The CFM with tax treatment method A is used consistently in the case studies of Chapter 5.

Chapter 3

PHYSICS - DEPLETION MODEL

3.1 INTRODUCTION

Fuel cost analysis requires that fuel discharge composition be known as a function of irradiation time. The objective of the present chapter is to establish a fast breeder reactor fuel depletion model suitable for fuel economic scoping, survey, ranking and sensitivity studies, but sufficiently simple to permit its use, in the form of a computer code, without incurring excessive computer time or capacity requirements.

Effects of spectral, spatial and time detail on FBR physics-depletion calculations have been the subject of several recent studies (28), (29), (30), (37), (44). In particular, Little et.al. (28) have found that little detail is required for accurate core depletion calculations. This is due to the spatial uniformity of spectrum in the core, and the slow variations of flux magnitude and spectrum with irradiation time.

Blanket physics-depletion is considerably more complex, due to the following:

(1) spectrum softening with distance from the core-blanket interfact;

(2) spectrum hardening with irradiation time due to the relatively large buildup of fissile plutonium in the blanket;

(3) flux shift, i.e. increase in blanket flux with irradiation time, due to the buildup of fissile plutonium in the blanket; and

(4) spatial self-shielding (heterogeneity) effects occasioned by the softer blanket spectrum, and aggravated, in the case of radial

blankets, by larger fuel pin diameters.

Effect (1) requires that cross-sections be input to the calculation with sufficient spatial detail, i.e. a separate cross-section set, properly flux weighted, for each of many blanket regions. Effects (2) and (3) suggest that physics calculations be performed sufficiently often, during a time step depletion calculation, to correct the local cross-sections and fluxes.

Parametric and survey studies commonly require the evaluation of numerous cases involving different configurations and compositions, and if models are unnecessarily complex, the computation costs may be prohibitive. In physics-depletion calculations, practically all of the computer time is absorbed by the static physics computations (neutron balances) which yield flux magnitudes and spectra at discrete points in irradiation time and space. The calculations of composition changes between these points in time, using the nuclide depletion equations, require negligible effort in terms of computer time. Hence, computer expense can be significantly reduced by decreasing the number of static physics calculations, i.e. maximizing the length of the irradiation time intervals over which flux magnitudes and spectra are treated as being constant. For this reason, studies were performed, Section 3.4, to assess the effects of item (2), spectrum hardening, and item (3), flux shift, on depletion calculation results.

Conventional multigroup time step depletion (MG-TSD) methods (26), against which simpler methods are to be judged, permit local fluxes and spectra to vary with irradiation. One group time step depletion calculations (1G-TSD) permit local fluxes (flux shape) but not spectra, to vary with irradiation. Both MG-TSD and 1G-TSD models yield reactivity behavior with irradiation, or, alternatively, may involve performing

criticality searches on control poison concentrations. Time step depletion methods are described in Section 3.2.

A simpler (and less expensive) depletion model, the "Semi-Analytic Depletion Method"(SAM), has been developed in this study, and is introduced in Section 3.3. This method is based on the assumptions that both flux (local) and spectrum (local) are constant with irradiation time (or exposure), thus requiring only one multigroup neutron balance for a given reactor configuration. The assumptions of constant local flux and local spectrum, while suitable for the core, may be questionable for the blankets, due to the rapid buildup of fissile plutonium in the blankets. Effects of these assumptions on core, axial blanket, and radial blanket depletion results are evaluated in Section 3.4 by comparing results of three parallel depletion calculations (26G-TSD, 1G-TSD, and SAM).

In SAM, only one multigroup physics calculation is performed. Thus SAM does not provide the k_{eff} behavior with irradiation. This limitation is discussed in Section 3.5.

Effects of spatial self-shielding on blanket depletion results are estimated in Section 3.7.

3.2. DESCRIPTION OF TIME STEP DEPLETION (TSD) CALCULATIONS

Depletion calculations are central to several reactor design functions, yielding space-time-dependent power densities for thermal design, reactivity and criticality information for control system design and absorber management, and fuel discharge compositions for fuel management.

Conventional time step depletion (TSD) calculations may be characterized as one or more neutron balance (in space and energy) computations ("physics"), separated in the irradiation time domain by depletion ("burnup") computations

describing the changes in nuclide populations at each point or region. This process is shown schematically in Figure 3.1. Preparation for the TSD calculation includes the selection of a standard multigroup cross-section set, e.g. the Russian Set (48), the Yiftah-Okrent-Moldauer Set (49), the Hansen-Roach Set (50), or cross-section file, e.g. ENDF/B. More refined calculations may require corrections to this parent cross-section data. Such corrections may be performed by a "cross-section generating program", such as 1DX (27), MC^2 (39), or TDOWN (40). For example, given a reactor configuration (geometry, composition) and the parent cross-section data, 1DX performs resonance and spatial shielding corrections by region, and collapses to regional few group sets if desired. The resulting multigroup set is then used as input to the TSD calculation, which may be performed by a computer program such as 2DB (26), PHENIX (31), PYRE (34), or CITATION (47).

With reactor geometry and initial compositions, $\left\{N_i\ (\bar{r},0)\right\}$, as input, the TSD begins with a physics calculation at time zero. This calculation yields initial flux shapes and position-dependent spectra, $\phi(\bar{r}, E, 0)$, and the initial effective multiplication constant $k_{eff}(0)$. (Some programs provide the option of performing a "criticality search" on compositions or dimensions to obtain $k_{eff} = 1$ at each physics calculation.) The flux profile is normalized to the reactor power specified.

Flux shape and spectrum, $\phi(\bar{r}, E,0)$, serve as input to the depletion calculation and are assumed constant over the next time interval, that is, until the next physics calculation. Depletion calculations are performed individually for each specified zone. Each zone normally consists of several spatial mesh points; zone fluxes are obtained by appropriate spatial averaging, and nuclide composition is assumed uniform over the zone. The zone depletion equation for nuclide j is

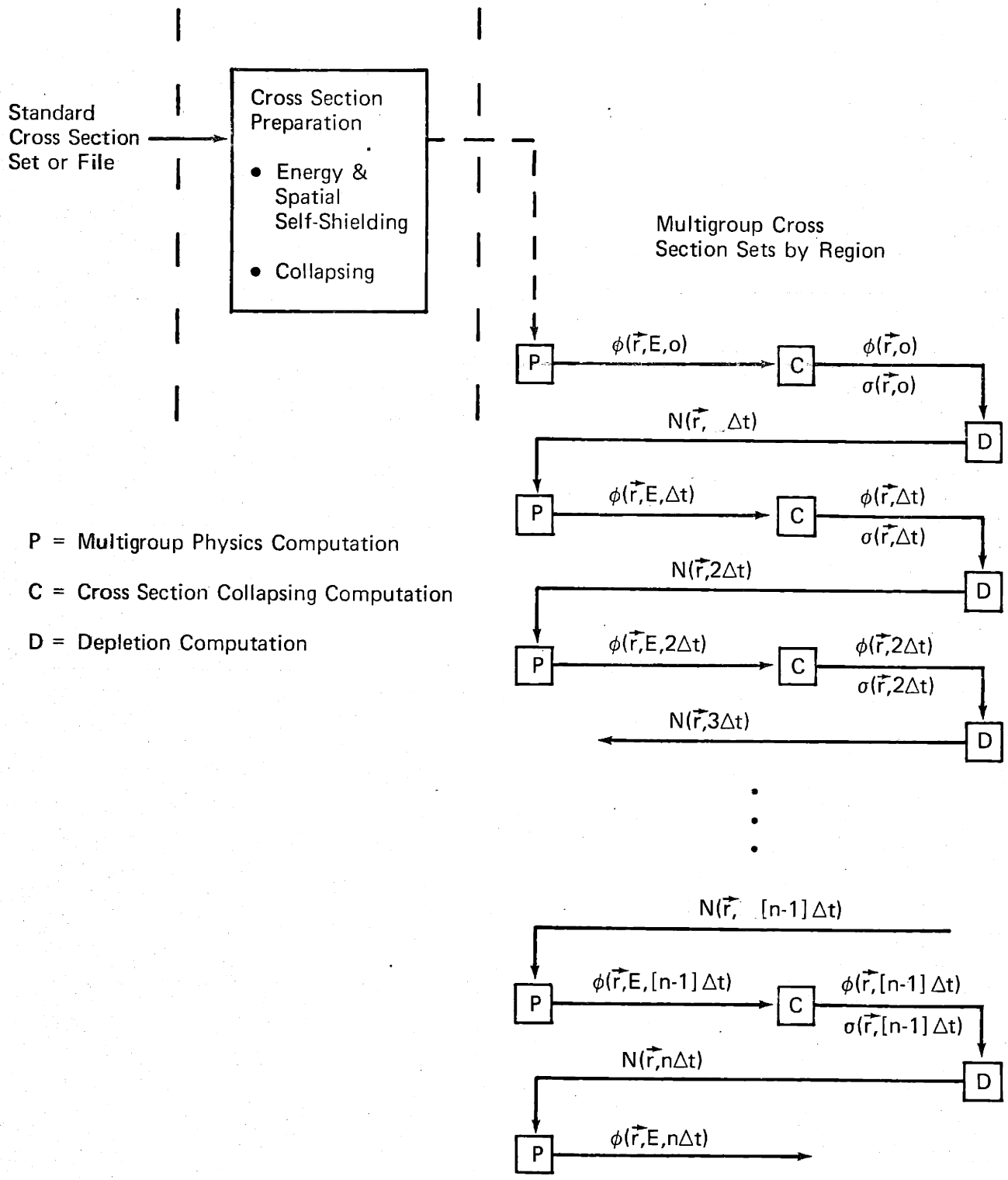

FIG. 3.1 MULTIGROUP TIME STEP DEPLETION CALCULATION

$$\frac{dN_j}{dt} = -\lambda_j N_j \qquad \text{(decay loss)}$$

$$- N_j \sum_{k=1}^{n} \phi_k \sigma^j_{k,a} \qquad \text{(absorption loss)}$$

$$+ \lambda_i N_i \qquad \text{(decay source)}$$

$$+ \sum_m N_m \sum_{k=1}^{n} \phi_k \sigma^m_{k,c} \qquad \text{(capture source)}$$

$$+ \sum_q N_q y_{q,j} \sum_{k=1}^{n} \phi_k \sigma^q_{k,f} \qquad \text{(fission source)} \qquad (3\text{-}1)$$

where

j≡ nuclide index

k= energy group index

m= capture parent index

i≡ decay parent index

q≡ fission parent index

N_j ≡ atom density, nuclide j, in the zone (atoms/cm^3)

ϕ_k ≡ group k neutron flux in the zone (n/cm^2sec)

$\sigma^j_{k,e}$ ≡ microscopic cross-section for event e, group k, nuclide j (cm^2)

e = a, absorption

= c, capture

= f, fission

λ_j ≡ decay constant, nuclide j (sec^{-1})

t ≡ time (sec)

$y_{q,j}$ ≡ yield of nuclide j per fission of nuclide q

Rates of neutron-induced reactions may be expressed in terms of spectrum-weighted cross sections (collapsed to one group) by noting that, in the zone in question,

$$\sum_{k=1}^{n} \phi_k \sigma^y_{k,x} = \frac{\left(\sum_{k=1}^{n} \phi_k\right)\left(\sum_{k=1}^{n} \phi_k \sigma^y_{k,x}\right)}{\left(\sum_{k=1}^{n} \phi_k\right)} \qquad (3\text{-}2)$$

$$= \phi \sigma^y_x$$

where

$$\phi \equiv \text{total flux} \equiv \sum_{k=1}^{n} \phi_k \qquad (3\text{-}3)$$

$$\sigma^y_x \equiv \text{spectrum averaged one group cross-section, nuclide y, event x} \equiv \frac{\sum_{k=1}^{n} \phi_k \sigma^y_{k,x}}{\sum_{k=1}^{n} \phi_k} \qquad (3\text{-}4)$$

Coefficients of the nuclide depletion equation are thus seen to be one group microscopic cross-sections, collapsed in the zone spectrum, and Equation (3-1) takes the form

$$\frac{dN_j}{dt} = -\lambda_j N_j - N_j \phi \sigma_a^j + \lambda_i N_i + \sum_m N_m \phi \sigma_c^m + \sum_q N_q y_{q,i} \phi \sigma_f^q \qquad (3\text{-}5)$$

The collapsing implied in going from Equation (3-2) to Equation (3-5) does not represent any further approximation or loss of generality.

With the flux information $\phi(\bar{r}, E, 0)$ from the initial physics calculations, zone fluxes and cross-sections are computed with Equations (3-3), (3-4) and used in equations of the form of Equation (3-5) to determine zone

compositions at the end of the time interval Δt, assuming the ϕ and σ are constant over Δt. Equations (3-5) may be solved analytically, if the important nuclide chains are simple and known, or in a finite difference fashion, if more flexibility in programming is desired.

The reactor composition thus computed, $\{N_j(\bar{r},t)\}$ at $t= \Delta t$, is used in the next physics calculation to obtain $\phi(\bar{r}, t, E)$ and k_{eff} at $t= \Delta t$. Again, the flux is normalized to the specified constant reactor power. Zone fluxes and cross-sections collapsed in zone spectra are then used in the depletion calculation for the second time step, yielding $\{N_j(\bar{r},t)\}$ at $t= 2\Delta t$. This cycle of "physics-collapse-deplete" is repeated until the specified end of the calculation is reached.

The procedure just described accounts for variations in flux shape with irradiation since physics calculations are performed periodically. If these physics calculations are of two or more energy groups, variations in spectra (with irradiation) are also account for. The TSD computation may be made more refined by decreasing the irradiation time interval between physics calculations and increasing the number of energy groups. One group TSD calculations will assess the flux shape variation, but not spectrum variations.

3.3 SEMI-ANALYTIC DEPLETION METHOD (SAM)

3.3.1 Introduction

If local flux and local spectrum are assumed constant over the entire irradiation time, then only one multigroup physics calculation is necessary. The local ϕ's and σ's from this "snapshot" may be used in the analytic solutions of the coupled depletion equations of the form (3-5) to obtain the local fuel composition as a function of irradiation time. Such a procedure will be labeled the "Semi-Analytic Depletion Method (SAM)".

3.3.2 Analytic Solution of Depletion Equations

For a uranium-plutonium fueled FBR, the important nuclides (for fuel economics) are U238, Pu239, Pu240, Pu241, Pu242. Their coupled depletion equations are:

$$\underline{\text{U238:}} \quad \frac{dN_{28}}{dt} = -N_{28}\,\phi\,\sigma_a^{28} \tag{a}$$

$$\underline{\text{Pu239:}} \quad \frac{dN_{49}}{dt} = N_{28}\,\phi\,\sigma_c^{28} - N_{49}\,\phi\,\sigma_a^{49} \tag{b}$$

$$\underline{\text{Pu240:}} \quad \frac{dN_{40}}{dt} = N_{49}\,\phi\,\sigma_c^{49} - N_{40}\,\phi\,\sigma_a^{40} \tag{c}$$

(3-6)

$$\underline{\text{Pu241:}} \quad \frac{dN_{41}}{dt} = N_{40}\,\phi\,\sigma_c^{40} - N_{41}\,\phi\,\sigma_a^{41} - \lambda_{41}\,N_{41} \tag{d}$$

$$\underline{\text{Pu242:}} \quad \frac{dN_{42}}{dt} = N_{41}\,\phi\,\sigma_c^{41} - N_{42}\,\phi\,\sigma_a^{42} \tag{e}$$

where

$$\phi\,\sigma_x^y = \sum_{k=1}^{n} \phi_k \cdot \frac{\sum_{k=1}^{n} \phi_k\,\sigma_{k,x}^y}{\sum_{k=1}^{n} \phi_k}$$

Without decay terms, nuclide depletion equations and their solutions may be expressed in more convenient form with flux time (θ),

$$\theta(t) \equiv \int^t \phi(t')\,dt'$$

$$d\theta(t) \equiv \phi(t)\,dt \tag{3-7}$$

as the independent variable. Of the nuclides involved, only Pu241 suffers

a significant decay loss (half life 14 years). Assuming for the moment that Pu241 decay may be neglected, Equations (3-6) take the following form:

$$\underline{\text{U238}}: \quad \frac{dN_{28}}{d\theta} + \sigma_a^{28} N_{28} = 0$$

$$\underline{\text{Pu239}}: \quad \frac{dN_{49}}{d\theta} + \sigma_a^{49} N_{49} = \sigma_c^{28} N_{28}$$

$$\underline{\text{Pu240}}: \quad \frac{dN_{40}}{d\theta} + \sigma_a^{40} N_{40} = \sigma_c^{49} N_{49} \qquad (3\text{-}8)$$

$$\underline{\text{Pu241}}: \quad \frac{dN_{41}}{d\theta} + \sigma_a^{41} N_{41} = \sigma_c^{40} N_{40}$$

$$\underline{\text{Pu242}}: \quad \frac{dN_{42}}{d\theta} + \sigma_a^{42} N_{42} = \sigma_c^{41} N_{41}$$

Assuming the cross-sections $\{\sigma\}$ are independent of flux time (θ), the solutions of the set (3-8), to be applied locally, are

$$\underline{\text{U238}}: \quad N_{28} = N_{28}^0 \exp(-\sigma_a^{28} \theta) \qquad (a)$$

$$\underline{\text{Pu239}}: \quad N_{49} = N_{28}^0 A \exp(-\sigma_a^{28} \theta)\,[1-\exp(-(\sigma_a^{49} - \sigma_a^{28})\theta)] + N_{49}^0 \exp(-\sigma_a^{49}\theta) \qquad (b)$$

$$\underline{\text{Pu240}}: \quad N_{40} = N_{28}^0 AB \exp(-\sigma_a^{28}\theta) - N_{28}^0 AB_2 \exp(-\sigma_a^{49}\theta)$$

$$+ N_{49}^0 B_2 \exp(-\sigma_a^{49}\theta) + \beta_1 \exp(-\sigma_a^{40}\theta) \qquad (c)$$

$$\underline{\text{Pu241}}: \quad N_{41} = N_{28}^0 AB_1C_1 \exp(-\sigma_a^{28}\theta) - N_{28}^0 AB_2C_2 \exp(-\sigma_a^{49}\theta)$$

$$+ N_{49}^0 B_2C_2 \exp(-\sigma_a^{49}\theta) + \beta_1 C_3 \exp(-\sigma_a^{40}\theta) \qquad (d)$$

$$+ \beta_2 \exp(-\sigma_a^{41}\theta)$$

$$\underline{\text{Pu242:}} \quad N_{42} = N_{28}AB_1C_1D_1\exp(-\sigma_a^{49}\theta) - N_{28}^0AB_2C_2D_2\exp(-\sigma_a^{49}\theta) \qquad (e)$$

$$+ N_{49}^0 B_2C_2D_2\exp(-\sigma_a^{49}\theta) + \beta_1 C_3D_3\exp(-\sigma_a^{40}\theta)$$

$$+ \beta_2 D_4\exp(-\sigma_a^{41}\theta) + \beta_3\exp(-\sigma_a^{42}\theta) \qquad (3\text{-}9)$$

where

$$A \equiv \frac{\sigma_c^{28}}{\sigma_a^{49} - \sigma_a^{28}}$$

$$B_1 \equiv \frac{\sigma_c^{49}}{\sigma_a^{40} - \sigma_a^{28}} \qquad B_2 \equiv \frac{\sigma_c^{49}}{\sigma_a^{40} - \sigma_a^{49}}$$

$$C_1 \equiv \frac{\sigma_c^{40}}{\sigma_a^{41} - \sigma_a^{28}} \qquad C_2 \equiv \frac{\sigma_c^{40}}{\sigma_a^{41} - \sigma_a^{49}} \qquad C_3 \equiv \frac{\sigma_c^{40}}{\sigma_a^{41} - \sigma_a^{40}}$$

$$D_1 \equiv \frac{\sigma_c^{41}}{\sigma_a^{42} - \sigma_a^{28}} \qquad D_2 \equiv \frac{\sigma_c^{41}}{\sigma_a^{42} - \sigma_a^{49}} \qquad D_3 \equiv \frac{\sigma_c^{41}}{\sigma_a^{42} - \sigma_a^{40}} \qquad D_4 \equiv \frac{\sigma_c^{41}}{\sigma_a^{42} - \sigma_a^{41}}$$

$$\beta_1 \equiv N_{40}^0 - (N_{28}^0AB_1 - N_{28}^0AB_2 + N_{49}^0B_2)$$

$$\beta_2 \equiv N_{41}^0 - (N_{28}^0AB_1C_1 - N_{28}^0AB_2C_2 + N_{49}^0B_2C_2 + \beta_1C_3)$$

$$\beta_3 \equiv N_{42}^0 - (N_{28}^0AB_1C_1D_1 - N_{28}^0AB_2C_2D_2 + N_{49}^0B_2C_2D_2 + \beta_1C_3D_3 + \beta_2D_4)$$

In expressing Equation (3-6d) in terms of flux time, Equation (3-8d), Pu241 decay was neglected. Without this assumption, the details of the flux history and out of pile processing and cooling schedules would be required

for estimates of Pu241 and Pu242 populations.

Using the representative FBR blanket reaction rate

$$\sigma_a^{41}\phi \simeq 1.8 \times 10^{-8}\ \text{sec}^{-1}\ , \tag{3-11}$$

the Pu 241 decay rate is seen to be about 10% of its absorption loss rate:

$$\frac{\lambda_{41}}{\sigma_a^{41}\phi} \simeq \frac{1.57 \times 10^{-9}\ \text{sec}^{-1}}{1.8 \times 10^{-8}\ \text{sec}^{-1}} = 0.087 \simeq 10\% \tag{3-12}$$

The solution of Equation (3-6d) assuming constant N_{40}, ϕ, and σ's is

$$N_{41} = \frac{N_{40}^0\ \sigma_c^{40}}{\sigma_a^{41}\left(\frac{\lambda_{41}}{(1+\sigma^{41}\phi)}\right)}\ [\,1-\exp(-\sigma_a^{41}\phi(1+\frac{\lambda_{41}}{\sigma_a^{41}\phi})\ t\,)]$$

$$+\ N_{41}^0\ \exp(-\sigma_a^{41}\phi(1+\frac{\lambda_{41}}{\sigma_a^{41}\phi})\ t\,) \tag{3-13}$$

Letting N_{41}^* denote the Pu241 concentration calculated by ignoring decay, and assuming no initial Pu241, one finds that for an irradiation time of 10 years,

$$\frac{N_{41}}{N_{41}^*} \simeq 0.97 \tag{3-14}$$

Under these conditions, the assumption of no Pu241 decay results in an over-prediction of about 3% in N_{41}.

3.3.3 Summary

The semi-analytic depletion method (SAM) assumes that local spectra and local flux magnitudes do not change with irradiation time. The assump-

tion of constant local fluxes contains another assumption: that the reactor flux shape does not change with irradiation time.

SAM differs from the time step depletion method in that only one multigroup physics computation is performed. Local fluxes and local spectrum-weighted cross-sections from this single physics computation are used as input to Equation (3-7) and Equations (3-9) to obtain local fuel compositions as functions of irradiation time.

3.4 EFFECTS OF THE ASSUMPTIONS OF CONSTANT LOCAL FLUX AND SPECTRUM

3.4.1 Description

The semi-analytic method (SAM) uses neutronic data (local σ's and ϕ's) from a single multigroup neutron balance to obtain local fuel composition as a function of irradiation time. These local σ's and ϕ's are assumed constant throughout the irradiation life of the fuel. The constant ϕ and constant σ assumptions produce opposing errors in calculations of blanket discharge fissile inventory.

The effects of these assumptions were estimated by comparing results of three parallel depletion calculations (Methods a, b and c) described in Table 3.1 and Figure 3.2. Two sets of comparisons were made:

(1) Reactor #1: Reference Reactor (sodium radial reflector); no fission products included in the TSD methods; comparison of methods a, b, and c.

(2) Reactor #2: Identical in all respects to reactor #1, except that Be metal is used as the radial reflector; fission products included in the TSD method; comparison of methods a and c.

The reference reactor (#1) configuration is described in Figure 3.3. Selection of this reactor as a reference is discussed in Chapter 4. The Be-reflected reactor (#2) is obtained by replacing the Na of zone 24 with

TABLE 3.1 DEPLETION CALCULATIONAL METHODS TO DETERMINE EFFECTS OF CONSTANT FLUX, CONSTANT SPECTRUM

			ASSUMPTIONS	Allowed to Vary	
Method	Description	Program	Input Data Source	Local ϕ's	Local σ's
a	26G-TSD	2DB*	σ (E)'s from 1DX	yes	yes
b	1G-TSD	2DB*	σ's from a at t=0	yes	no
c	SAM	SPPIA**	ϕ's and σ's from a at t=0	no	no

* Ref. (26)

** SPPIA is a program written to perform SAM calculations, and is described in Appendix C.

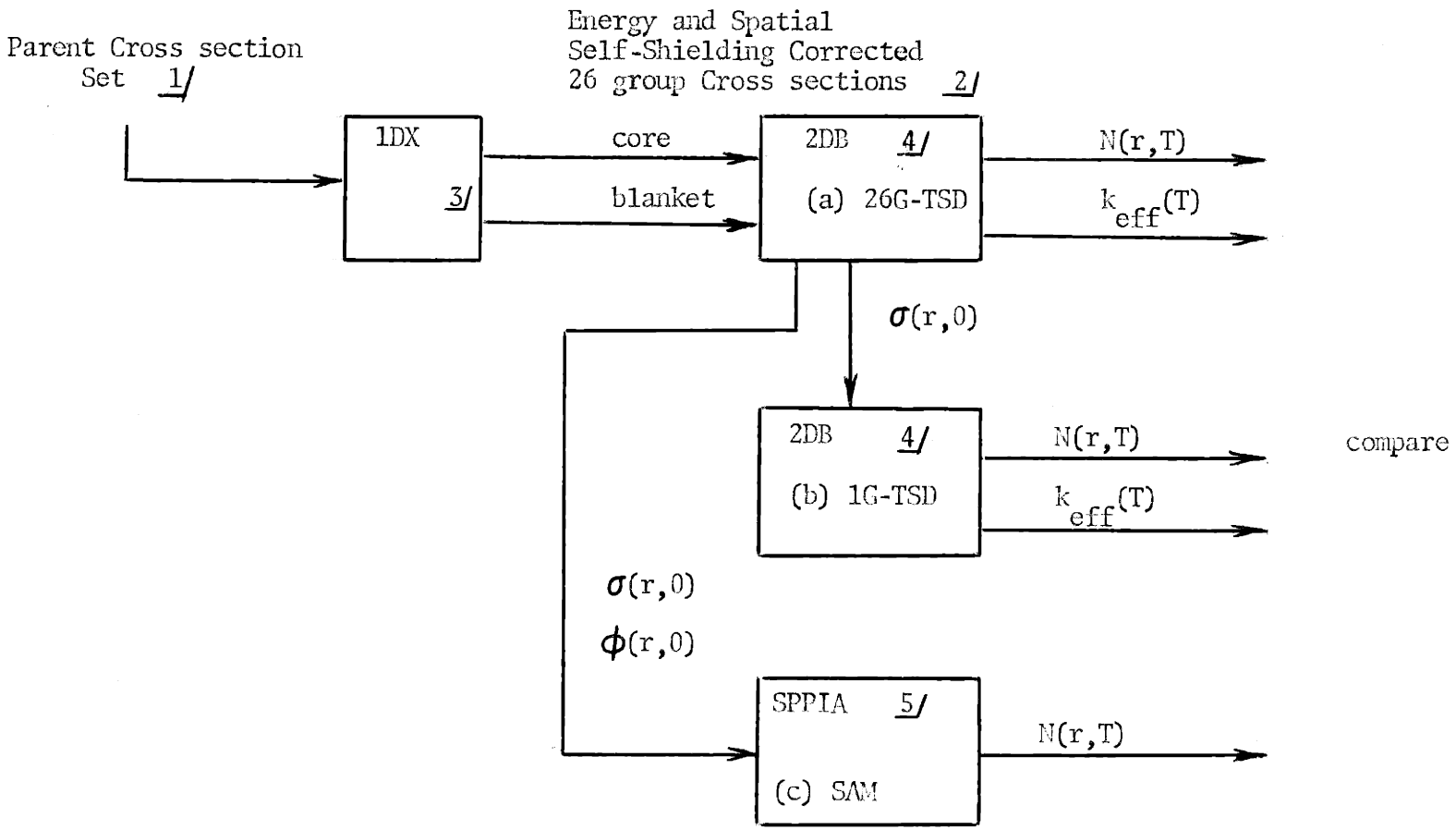

1 Ref. 48
2 Ref. 81
3 Ref. 27
4 Ref. 26
5 SPPIA is a program written to perform SAM calculations, and is described in Appendix C.

FIG. 3.2 PROCEDURE FOR METHODS COMPARISONS: 26G-TSD vs. 1G-TSD vs. SAM

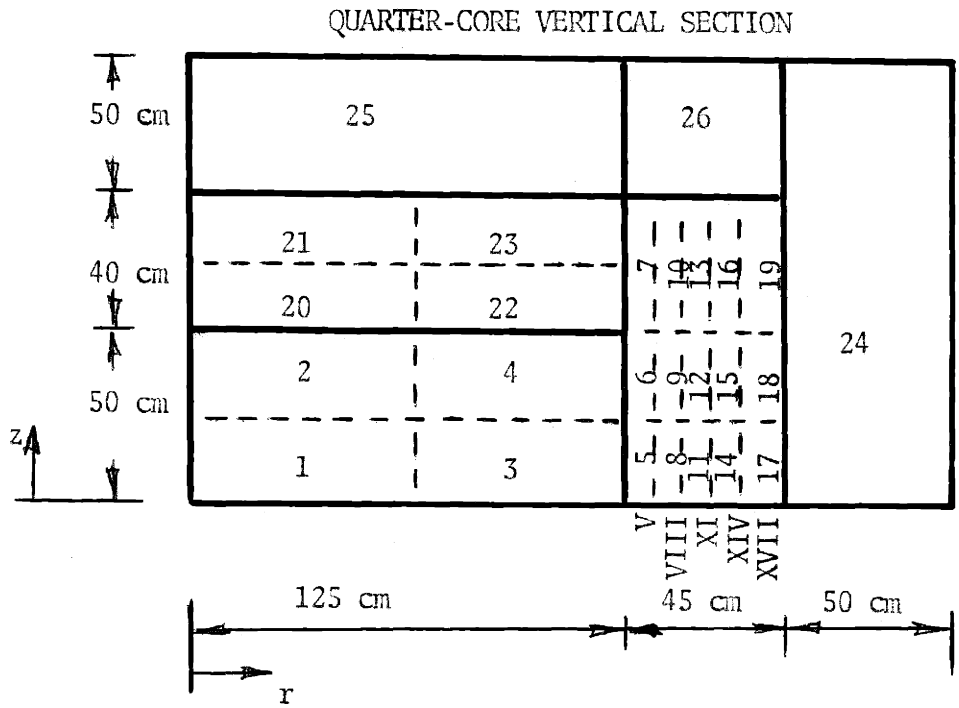

VOLUME FRACTIONS

REGION	CORE	RADIAL BLANKET	AXIAL BLANKET	RADIAL REFL.	AXIAL REFL.	AX.REFL. FOR RAD. BKT.
ZONE	1-4	5-19	20-23	24	25	26
SODIUM	0.50	0.30	0.50	1.00	0.50	0.30
OXIDE	0.30*	0.50	0.30	0	0	0
SS CR-FE-NI	0.20	0.20	0.20	0	0.50	0.70

* INITIAL CORE ENRICHMENT = 14%

FIG. 3.3 REFERENCE LMFBR CONFIGURATION (REACTOR #1).

Be metal.

Zone definitions are also shown in Figure 3.3. In all three methods, each burnable zone (1, 2, ..., 23) was depleted individually, that is, a zone was the basic volume unit over which number densities were "smeared" at each time step. The same zone definitions were used for inputting the space-dependent one group cross-sections for methods b(1G-TSD) and c(SAM) and the flux shape for method c (SAM).

For purposes of displaying results, and for use in fuel economic analysis (but not in the physics-depletion calculations) zone compositions were combined to form "region" compositions. For example, the inner-most radial blanket region ("V") is the sum of zones 5, 6 and 7, and

$$M_{49}^{V}(t) = M_{49}^{5}(t) + M_{49}^{6}(t) + M_{49}^{7}(t) \quad ,$$

$$\epsilon_{49}^{V}(t) = M_{49}^{V}(t) \; / \; M_{HM}^{V}(0) \qquad (3\text{-}15)$$

The TSD calculations (a, b) allowed k_{eff} to vary with burnup; that is, criticality searches were not performed. Effects of this simplification (neglect of flux shape and spectral perturbations introduced by control poison) are considered negligible (29).

In the TSD runs (a, b), physics computations were performed at 150 equivalent full power day (EFPD) intervals. Each of these physics computations yielded the current k_{eff}, the current flux shape, and in the case of the multigroup run (a), the local spectra. After each physics computation, the flux was normalized to a total reactor power of 2576 MW_t, corresponding to 1000 MW_e and a plant thermal efficiency of 39%.

In the TSD calculations, the core and axial blanket were assumed discharged at 600 EFPD, corresponding to an average core burnup of 100,000

MWD_t/MT. At a plant load factor of 82%, this is consistent with a core residence time of two years. The radial blanket remained in situ until the end of the depletion calculation at 1200 EFPD (4 years). Batch fuel management of the radial blanket and the core-axial blanket combination was assumed, which imposes a more severe test of constant flux, constant spectrum assumptions than scatter management.

3.4.2 Results (with Time as the Independent Variable)

The results of the methods-comparisons are reported below by major region (core, axial blanket, radial blanket).

Core

Tables 3.2 and 3.3 show the core depletion results (fissile plutonium population) for reactors #1 and #2 respectively. Excellent agreement between methods a, b and c is noted: at two years irradiation (100000 MWD_t/MT), discrepancies in fissile masses are about 0.03% for Pu239 and about 1% for Pu241. Zone spectra remain practically constant, accounting for the success of method b. This, together with the result that zone fluxes were fairly constant, explains the close agreement of method c with the other two methods.

The second core load (600 to 1200 EFPD) shows a very slight increase in discharge Pu239 and decrease in discharge Pu241, compared to the first core load. This results from the flux shift to the radial blanket, which is not replaced at two years. As fissile Pu builds up in the radial blanket, the radial blanket provides a greater fraction of total reactor power, decreasing somewhat the powerload, and flux, in the core.

Axial Blanket

Axial blanket depletion results for reactors #1 and #2 are shown in

TABLE 3.2

COMPARISON OF CORE DEPLETION RESULTS FOR

REACTOR #1 (REFERENCE REACTOR)

Equiv. Reactor Full Power Time (D)	Core Res. Time (Yr.)		Method (a) 26G-TSD	Method (b) 1G-TSD	Method (c) SAM
0	0	ϵ_{49}	14.05	14.05	14.05
		ϵ_{41}	0	0	0
300	1	ϵ_{49}	12.89	12.89	12.89
		ϵ_{41}	0.062	0.062	0.062
600	2	ϵ_{49}	11.90	11.90	11.90
		ϵ_{41}	0.175	0.174	0.175
600+	0	ϵ_{49}	14.05	14.05	14.05
		ϵ_{41}	0	0	0
900	1	ϵ_{49}	12.93	12.93	12.89
		ϵ_{41}	0.058	0.058	0.062
1200	2	ϵ_{49}	11.97	11.98	11.90
		ϵ_{41}	0.168	0.165	0.175

$\epsilon_{49} = 100 \times M_{49}/M^0_{HM}$ (%) $\quad M_{49}$ = Pu239 mass

$\epsilon_{41} = 100 \times M_{41}/M^0_{HM}$ (%) $\quad M_{41}$ = Pu241 mass

M^0_{HM} = mass of heavy metal loaded (kg) = 12623 kg

TABLE 3.3

COMPARISON OF CORE DEPLETION RESULTS FOR REACTOR #2 (Be-RADIAL REFLECTOR)

Equiv. Reactor Full Power Time (D)	Core Res. Time (Yr.)		Method (a) 26G-TSD	Method (c) SAM
0	0	ϵ_{49}	14.05	14.05
		ϵ_{41}	0	0
300	1	ϵ_{49}	12.89	12.90
		ϵ_{41}	0.062	0.062
600	2	ϵ_{49}	11.94	11.91
		ϵ_{41}	0.168	0.175
600+	0	ϵ_{49}	14.05	14.05
		ϵ_{41}	0	0
900	1	ϵ_{49}	12.93	12.90
		ϵ_{41}	0.058	0.062
1200	2	ϵ_{49}	12.02	11.91
		ϵ_{41}	0.159	0.175

$\epsilon_{49} = 100 \times M_{49}/M^0_{HM}$ (%) $\quad M_{49}$ = Pu239 mass

$\epsilon_{41} = 100 \times M_{41}/M^0_{HM}$ (%) $\quad M_{41}$ = Pu241 mass

M^0_{HM} = mass of heavy metal loaded (kg) = 12623 kg

Tables 3.4 and 3.5 respectively.

The 1G-TSD method b, which assumes constant spectra but accounts for flux shape changes, overpredicts the discharge Pu239 content at two years by about 4%, relative to method a. This occurs because the cross-sections input to method b, obtained by collapsing the spectra from method a's solution at time zero, are too soft. (Blanket spectra harden with irradiation due to the fissile buildup.) Method c, SAM, underpredicts Pu239 content by about 4%, in spite of its soft cross-section set, because its input zone fluxes, from the method a time zero solution, are too low. (Blanket flux increases with irradiation due to fissile buildup in the blanket.)

The second axial blanket batch (600 + to 1200 EFPD) suffers a slight decrease (~3%)in discharge fissile content, compared to the first batch. The second axial blanket batch experiences a lower flux than the first, owing to the buildup of flux and power in the radial blanket.

Fission product buildup in the blanket tends to diminish plutonium breeding, by competing with U238 resonance capture and by generally hardening the spectrum. Comparison of 26G-TSD axial blanket results for Reactor #1 (no fission products) and Reactor #2 (with fission products) shows that this is not a discernable effect.

Radial Blanket

Figures 3.4 and 3.5 display the radial blanket depletion method comparisons for reactors #1 and #2 respectively. Results for the innermost annular region (zones 5,6,7) and outermost annular region (zones 17,18,19), as well as for the entire radial blanket, are shown.

As in the axial blanket, the 1G-TSD method consistently overpredicts Pu239 content, while SAM consistently underpredicts Pu239 content. The cross-sections input to 1G-TSD and SAM were obtained by collapsing in the

TABLE 3.4

COMPARISON OF AXIAL BLANKET DEPLETION RESULTS

FOR REACTOR #1 (REFERENCE LMFBR)

Equiv. Reactor Full Power Time (D)	Axial Blanket Res.Time (Yr.)		Method (a) 26G-TSD	Method (b) 1G-TSD	Method (c) SAM
0	0	ϵ_{49}	0	0	0
		ϵ_{41}	0	0	0
300	1	ϵ_{49}	2.09	2.15	2.08
		ϵ_{41}	0.0019	0.0019	0.0019
600	2	ϵ_{49}	3.85	4.00	3.71
		ϵ_{41}	0.0113	0.0148	0.0119
600+	0	ϵ_{49}	0	0	0
		ϵ_{41}	0	0	0
900	1	ϵ_{49}	2.03	2.08	2.08
		ϵ_{41}	0.0017	0.0018	0.0019
1200	2	ϵ_{49}	3.74	3.89	3.71
		ϵ_{41}	0.01006	0.01312	0.0119

$\epsilon_{49} = 100 \times M_{49}/M^0_{HM}$ (%) $\quad M_{49}$ = Pu239 mass

$\epsilon_{41} = 100 \times M_{41}/M^0_{HM}$ (%) $\quad M_{41}$ = Pu241 mass

M^0_{HM} = mass of heavy metal loaded (kg) = 10093 kg

TABLE 3.5

COMPARISON OF AXIAL BLANKET DEPLETION RESULTS

FOR REACTOR #2(Be-RADIAL REFLECTOR)

Equiv. Reactor Full Power Time (D)	Axial Blanket Res. Time (yr)		Method (a) 26G-TSD	Method (c) SAM
0	0	ϵ_{49}	0	0
		ϵ_{41}	0	0
300	1	ϵ_{49}	2.0884	2.0794
		ϵ_{41}	0.0019	0.0019
600	2	ϵ_{49}	3.8836	3.6887
		ϵ_{41}	0.0112	0.0121
600+	0	ϵ_{49}	0	0
		ϵ_{41}	0	0
900	1	ϵ_{49}	2.0278	2.0794
		ϵ_{41}	0.00167	0.0019
1200	2	ϵ_{49}	3.7702	3.6887
		ϵ_{41}	0.0098	0.0121

$\epsilon_{49} = 100 \times M_{49}/M^0_{HM}$ (%) $\quad M_{49}$ = Pu239 mass

$\epsilon_{41} = 100 \times M_{41}/M^0_{HM}$ (%) $\quad M_{41}$ = Pu241 mass

M^0_{HM} = mass of heavy metal loaded (kg) = 10093 kg

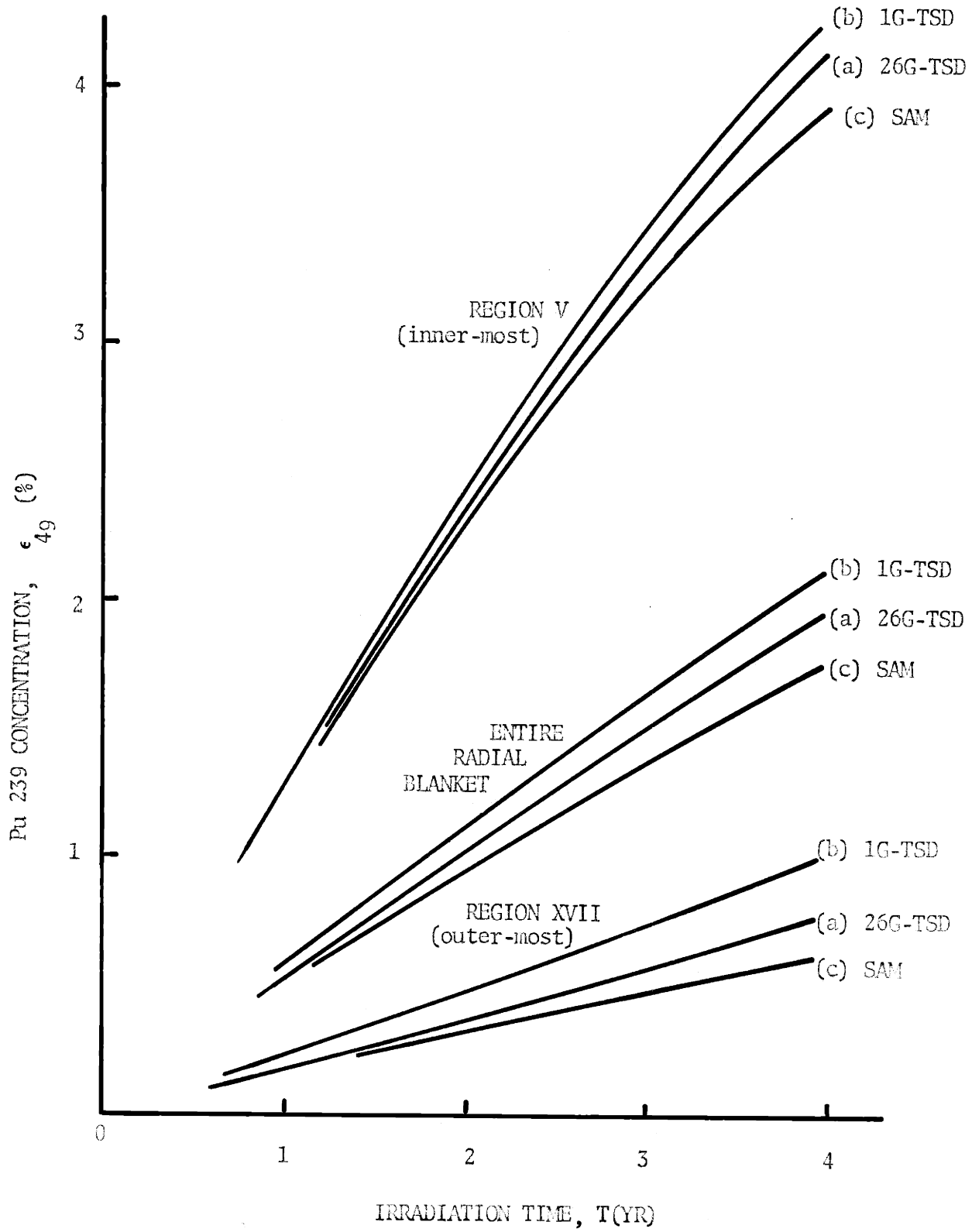

FIG. 3.4 COMPARISON OF RADIAL BLANKET DEPLETION RESULTS FOR REACTOR #1 (REFERENCE LMFBR)

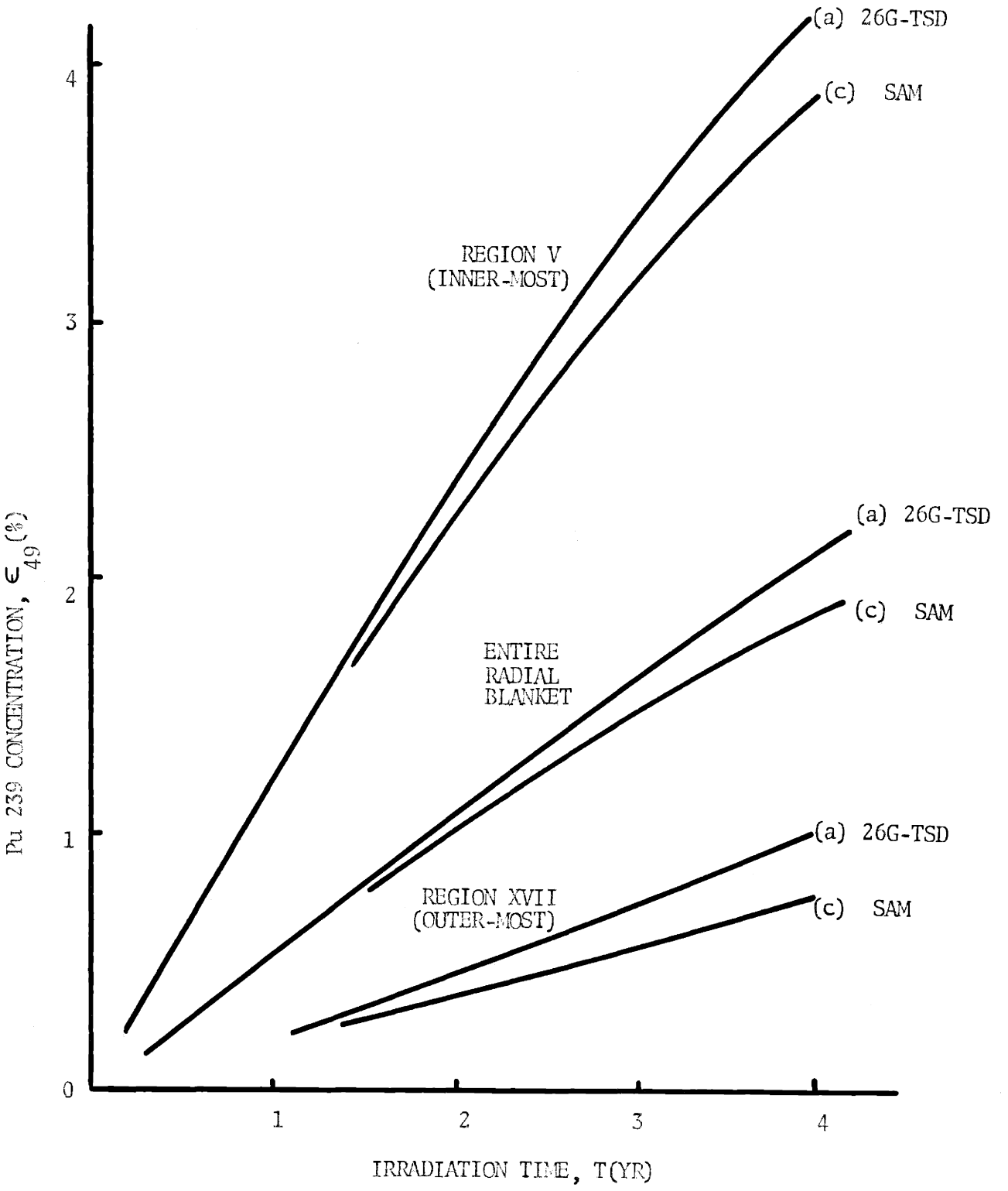

FIG. 3.5 COMPARISON OF RADIAL BLANKET DEPLETION RESULTS FOR REACTOR #2 (BE-RADIAL REFLECTOR)

26G-TSD time zero local spectra. Blanket spectra harden with irradiation due to fissile buildup. This accounts for the 1G-TSD overprediction. The zone fluxes input to SAM were taken from the 26G-TSD time zero solution. Blanket flux increases with irradiation, also because of fissile buildup. This explains SAM's underprediction, despite its soft cross-sections. Evidently the flux shift effect overrides the spectrum hardening effect.

At four years (1200 EFPD), SAM underpredicts the Pu239 content in the innermost region by about 5%, and that in the outermost region by about 20%. Since regions deep in the blanket produce relatively little plutonium, the relatively large error there has little effect on overall radial blanket Pu239 content, which SAM underpredicts by about 10% at 4 years.

The core's nearly constant flux and spectra has greatest influence on blanket fuel near the core-blanket interface, tending to validate SAM's assumptions there. SAM's error increases with distance from the core.

Fission product buildup in the blanket tends to diminish plutonium breeding rate, by competing with U238 resonance capture and by hardening the spectrum. Comparison of 26G-TSD radial blanket results for Reactor #1 (no fission products) and Reactor #2 (with fission products) shows that this is not a discernable effect.

Use of initial fluxes and spectrum-weighted cross-sections as input to SAM resulted in SAM's underprediction of blanket Pu239 inventories. Better agreement between SAM and 26G-TSD results would be expected if the fluxes and cross-sections for SAM were generated by a multigroup physics calculation in which a "representative" amount of fissile material were included in the blanket. Choice of the "representative" amount of fissile material would involve a guess, and perhaps an iteration, for each irradiation time to be evaluated. For example, for a 4 year irradiation, the "representative" amount might be the fissile inventory at 2 years; for an

8 year irradiation, it might be the fissile inventory at 4 years, etc.

To test these ideas, a SAM calculation (SAM_4) was performed using radial blanket fluxes and cross-sections from the 26G physics solution at 4 years. Results of the SAM_4 calculation were compared to those of SAM_0 and the 26G-TSD "truth" calculation, as shown schematically in Figure 3.6. Figure 3.7 displays this comparison.

As expected, SAM_4 overpredicts $\epsilon_{48}(T)$ while SAM_0 underpredicts $\epsilon_{49}(T)$. Table 3.6 shows that the discrepancy between SAM_4 and SAM_0 is about 24% (of SAM_4), independent of irradiation time. Comparing the two SAM calculations with the 26G-TSD "truth", one notes that SAM_0 error increase with irradiation time, while SAM_4 error decreases. Although the two SAM calculations disagreed in ϵ_{49}, and therefore radial blanket material credit (mills/KWHr) by about 24%, they both yielded an optimum blanket irradiation time of about 6 years.

In the case studies of Chapter 5, clean (initial) conditions are used consistently in SAM,tending to underestimate the economic value of all blanket cases considered.

3.4.3 Results (With Burnup as the Independent Variable)

Depletion method comparisons in Section 3.4.2 were presented with time as the independent variable. With time as the independent variable, SAM requires that one assume constant local flux (and therefore flux shape) throughout the fuel irradiation, or that one use a time-averaged local flux. Table 3.4 and Figure 3.4 of Section 3.4.2 show that the constant flux assumption is the dominant source of error in SAM blanket depletion

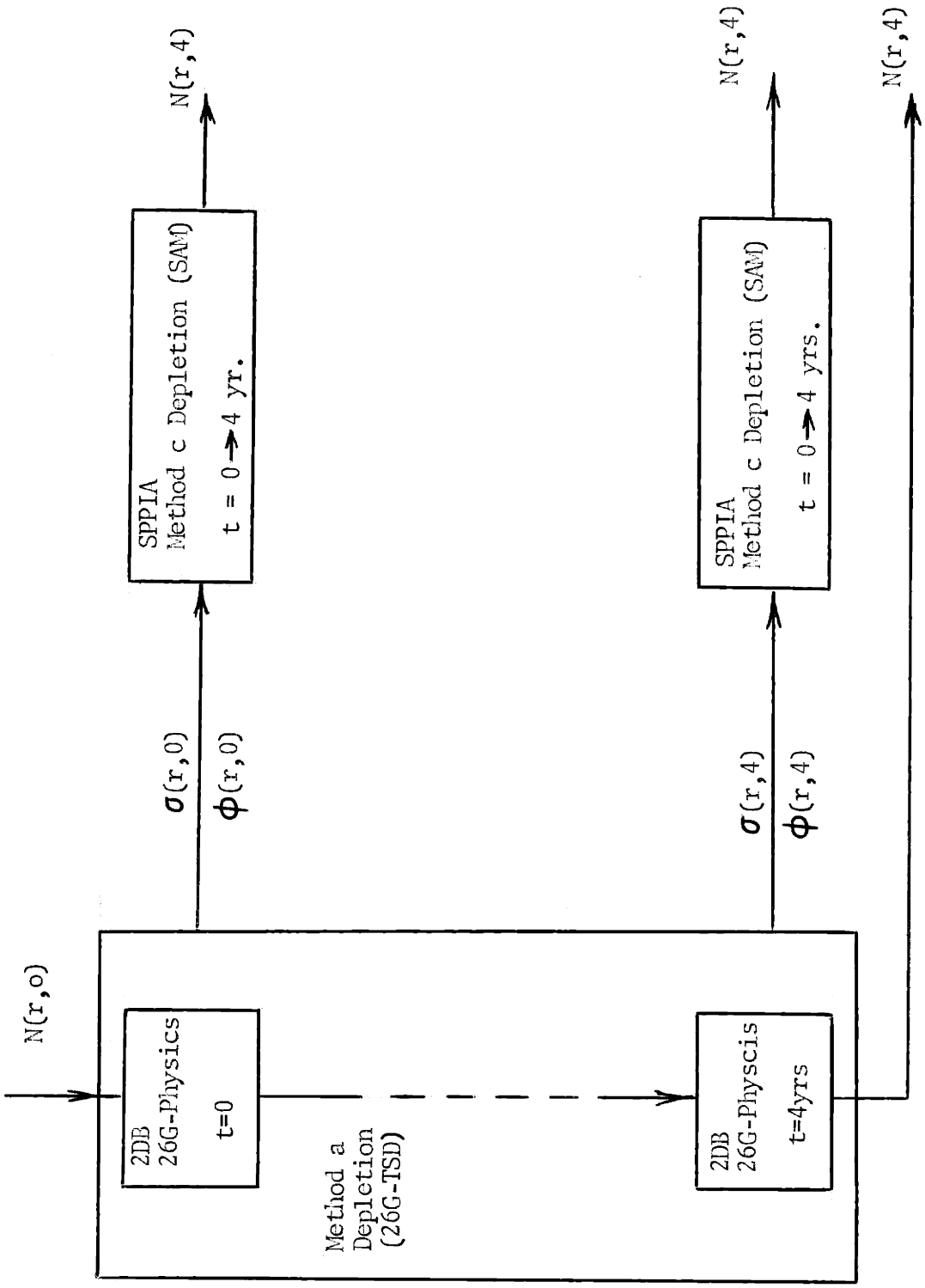

FIG. 3.6 PROCEDURE FOR COMPARING SAM RESULTS USING CLEAN AND IRRADIATED FUEL NEUTRONIC DATA

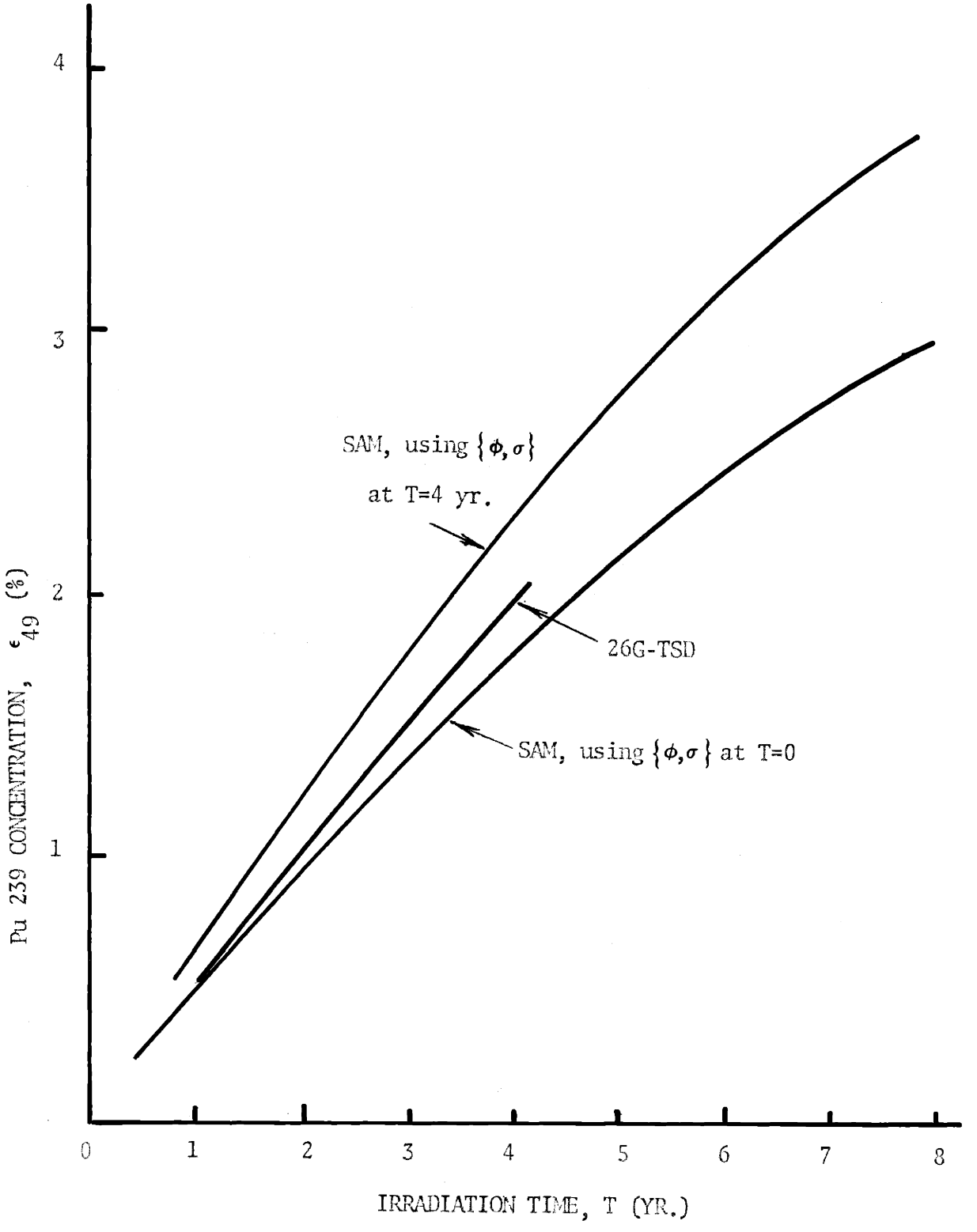

FIG. 3.7 COMPARISON OF SAM RADIAL BLANKET RESULTS USING CLEAN AND IRRADIATED FUEL NEUTRONIC DATA

TABLE 3.6

COMPARISON OF SAM_0, SAM_4, and 26G-TSD
RADIAL BLANKET DEPLETION RESULTS

		Irradiation Time (years)		
		2	4	8
ϵ_{49} (%)	(1) SAM_0	0.975	1.764	2.942
	(2) SAM_4	1.295	2.329	3.838
	(3) 26G-TSD	1.030	1.972	-
Error	(3)-(1)/(3)	0.05	0.10	-
	(3)-(2)/(3)	0.25	0.18	-
	(2)-(1)/(2)	0.24	0.24	0.24

calculations[1]. This assumption may be relaxed if, instead of time, a time integral property at a point or zone is selected as the independent variable representing degree of exposure, eg. flux-time (θ),

$$\theta \equiv \int \phi \, dt \tag{3-16}$$

or burnup (B),

$$B = \frac{CV}{M^0_{HM}} \int_\theta \{N_F(\theta')\ \ \sigma_f\}\ d\theta' \tag{3-17}$$

where the brackets $\{\ \ \}$ represent a summation over fissionable materials, V is the zone volume, C is energy released per fission, and M^0_{HM} is the mass of heavy metals (U + Pu) loaded in the zone.

This section presents a comparison of 26G-TSD and SAM results for reactor #2 (Be-reflected), with burnup as the independent variable. Having "normalized out" the local flux variation, any discrepancy between 26G-TSD and SAM results should be attributable to SAM's assumption of constant local spectra. Further, part of the spectral variation is ameliorated since burnup ($\sim \sigma_f \int d\theta\ \ N_F(\theta)$), as well as composition $N_F(\theta)$, is affected by the spectrum, and in the same direction.

Zone burnup in the 26G-TSD was calculated from fission product inventories. In SAM, the $N(\theta)$ equations (3-9) were integrated and solved directly for burnup.

Figures 3.4 and 3.5 showed the largest discrepancy between 26G-TSD and SAM depletion results (vs. time) to be in the outermost region of the

---

1. The constant flux and constant spectrum assumptions produce opposing errors in $\epsilon_{fissile}$. Refer to Table 3.4 and Figure 3.4. The effect of the constant spectrum assumption is seen by comparing the 1G-TSD and 26G-TSD results, while comparison of 1G-TSD and SAM results shows the influence of the constant flux assumption.

radial blanket. This comparison, together with the burnup-normalized results are shown in Figure 3.8. With burnup as the independent variable, the two methods yield practically identical results. Similar agreement was found in all radial blanket, axial blanket, and core regions and zones.

Figure 3.9 displays overall radial blanket depletion results by the two methods, with both time and overall radial blanket burnup as independent variables. Again, excellent agreement is noted when burnup is the independent variable.

The excellent agreement in depletion results, when burnup is the independent variable, reinforces the conclusion of Section 3.2.2 that flux shift is more important than spectral variations with irradiation time. Unfortunately, fuel economic analysis requires time as the independent variable in order to assess carrying charges. With time as the independent variable, SAM requires that constant local fluxes and fixed flux shape be assumed. Future work in developing FBR blanket calculational tools should be aimed at predicting the flux shift to the radial blanket, by simple, inexpensive methods.

Composition - Burnup Characteristics

Figure 3.10 shows the ϵ_{49} - burnup characteristics for the innermost and outermost annular regions of the radial blanket. Characteristic curves for the interior regions lie in the shaded area. The curve for the outermost region lies above the others because this region enjoys the softest spectrum in the radial blanket. Data for Figure 3.10 was generated by SAM.

Figure 3.11 compares the depletion characteristics of radial blanket, axial blanket, and core. The axial blanket curve lies above that of the radial blanket because of its softer spectrum (more Na). Core Pu239 fraction decreases with burnup, e.g. the internal breeding ratio is less than unity.

FIG. 3.8 DEPLETION RESULTS FOR OUTER-MOST RADIAL BLANKET REGION: TIME VERSUS BURNUP AS THE INDEPENDENT VARIABLE

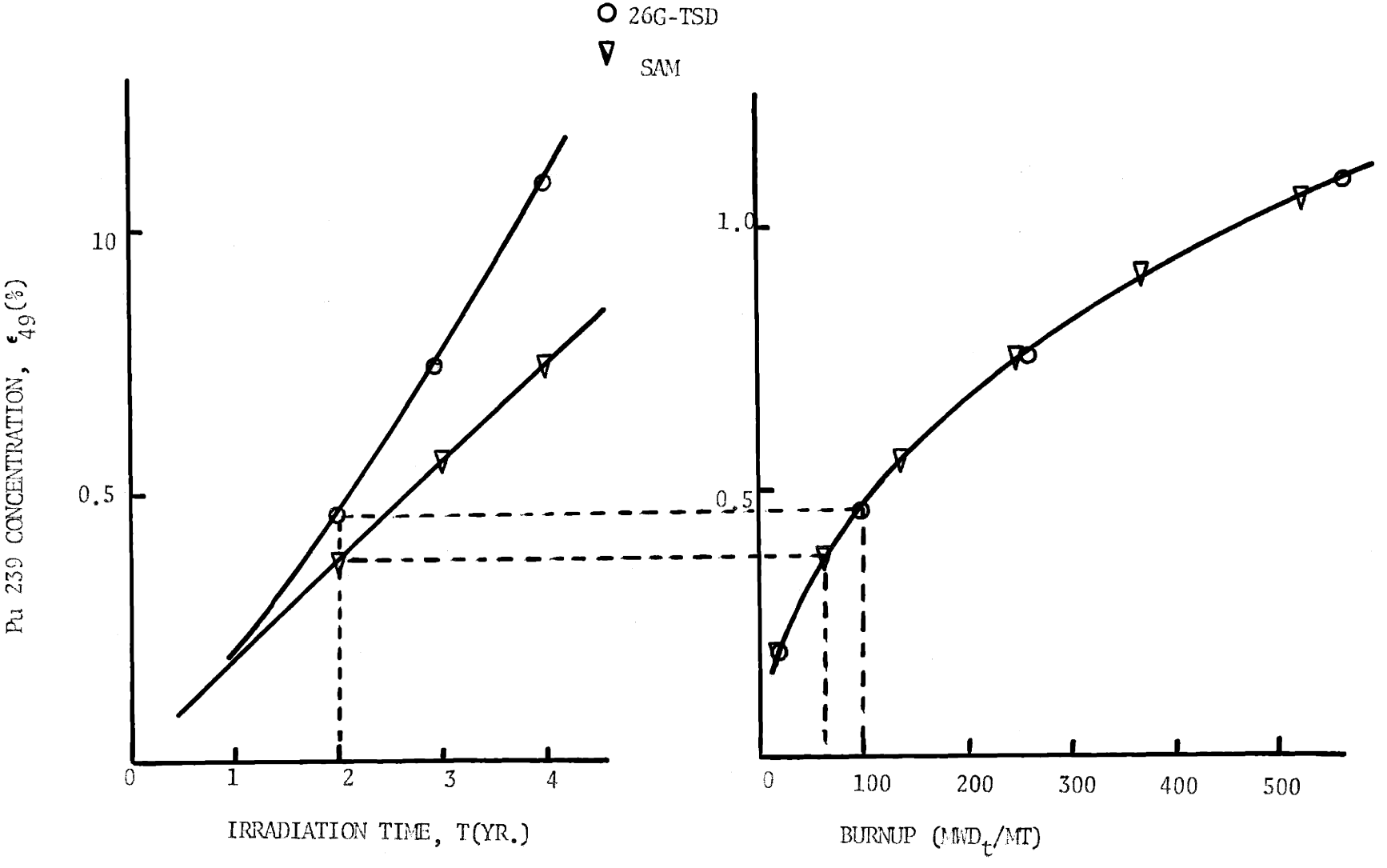

FIG. 3.9 DEPLETION RESULTS FOR THE ENTIRE RADIAL BLANKET: TIME VERSUS BURNUP AS THE INDEPENDENT VARIABLE

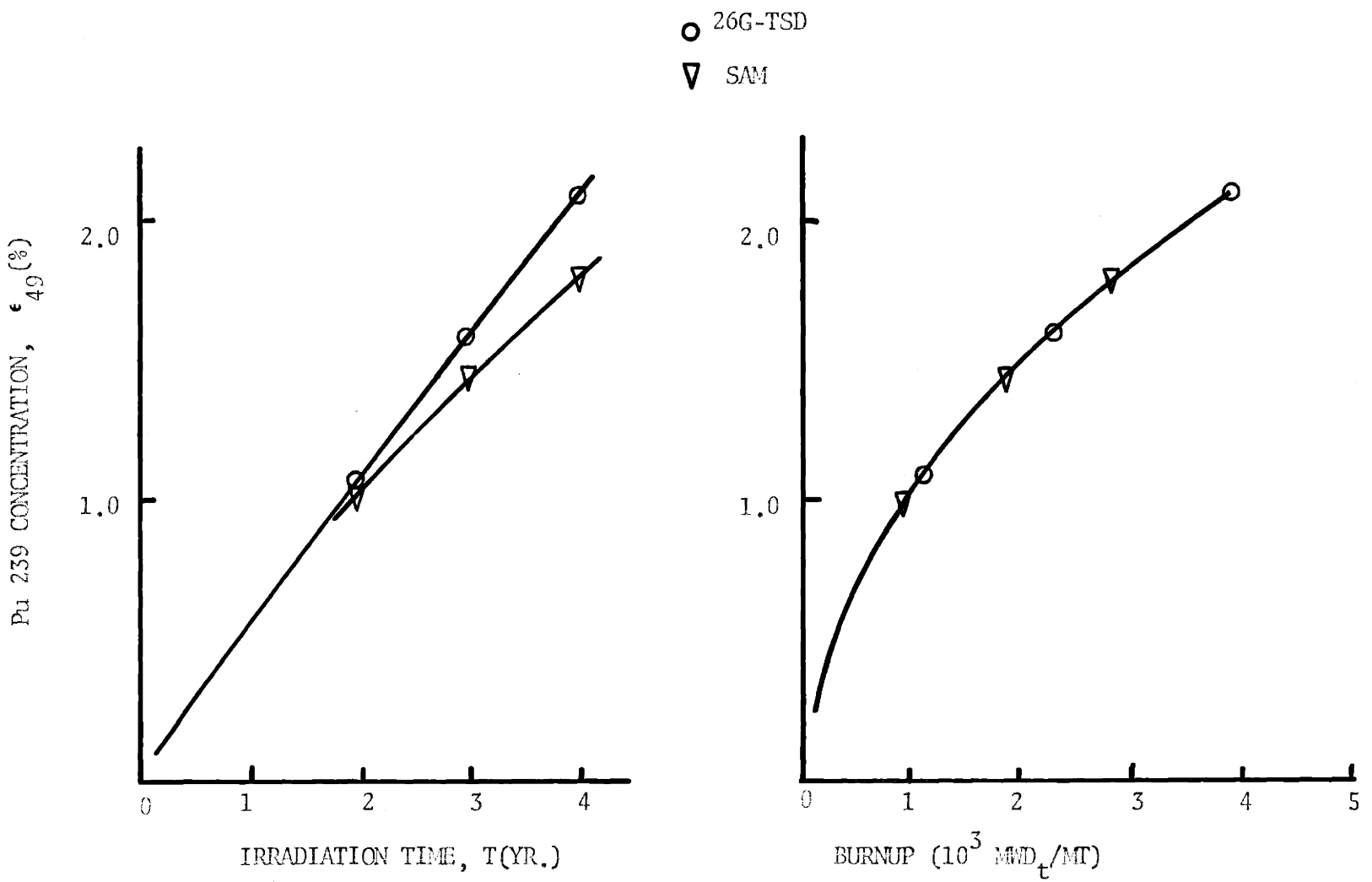

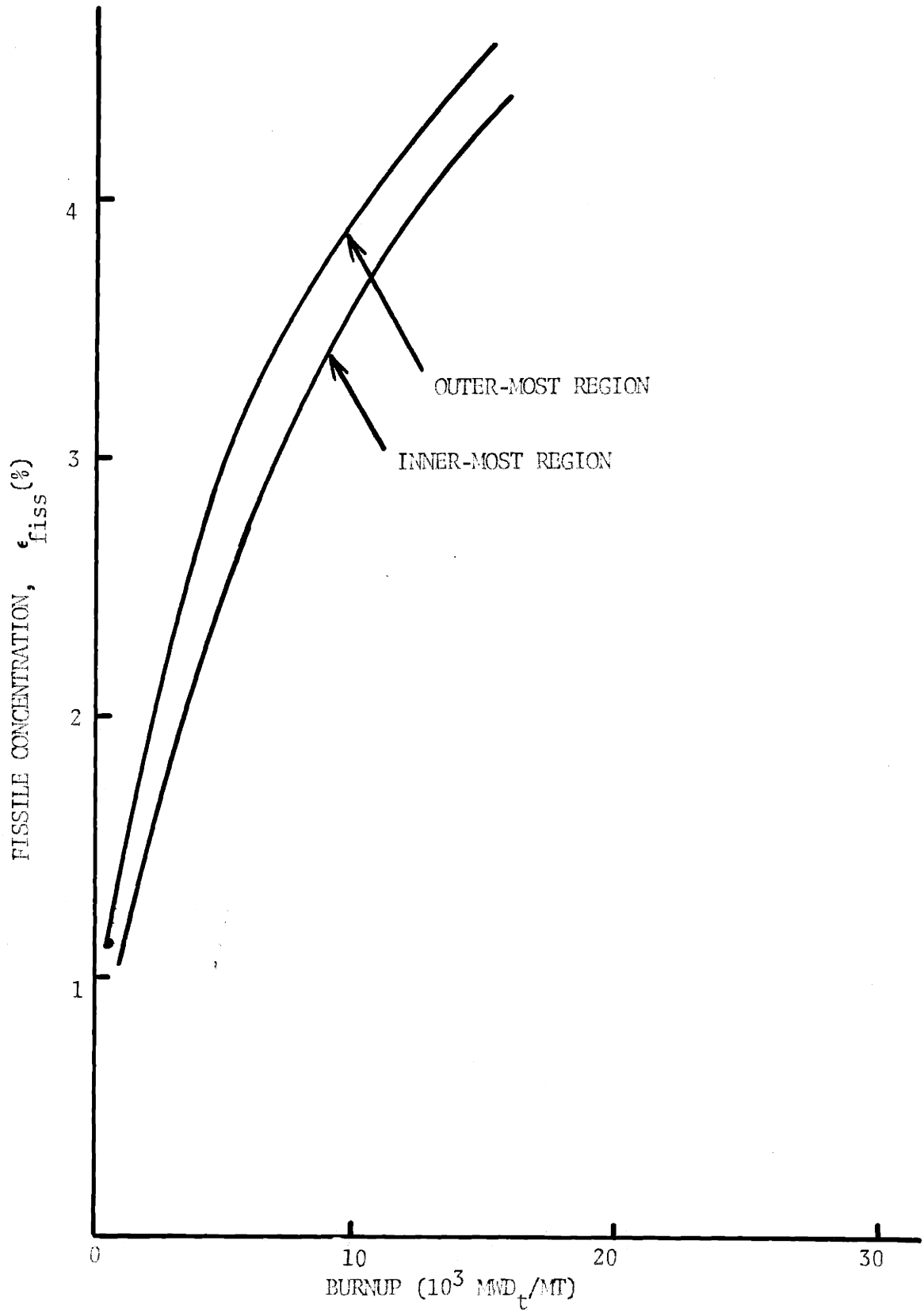

FIG. 3.10 BURNUP-FISSILE CONCENTRATION CHARACTERISTICS FOR INNER-MOST AND OUTER-MOST RADIAL BLANKET REGIONS

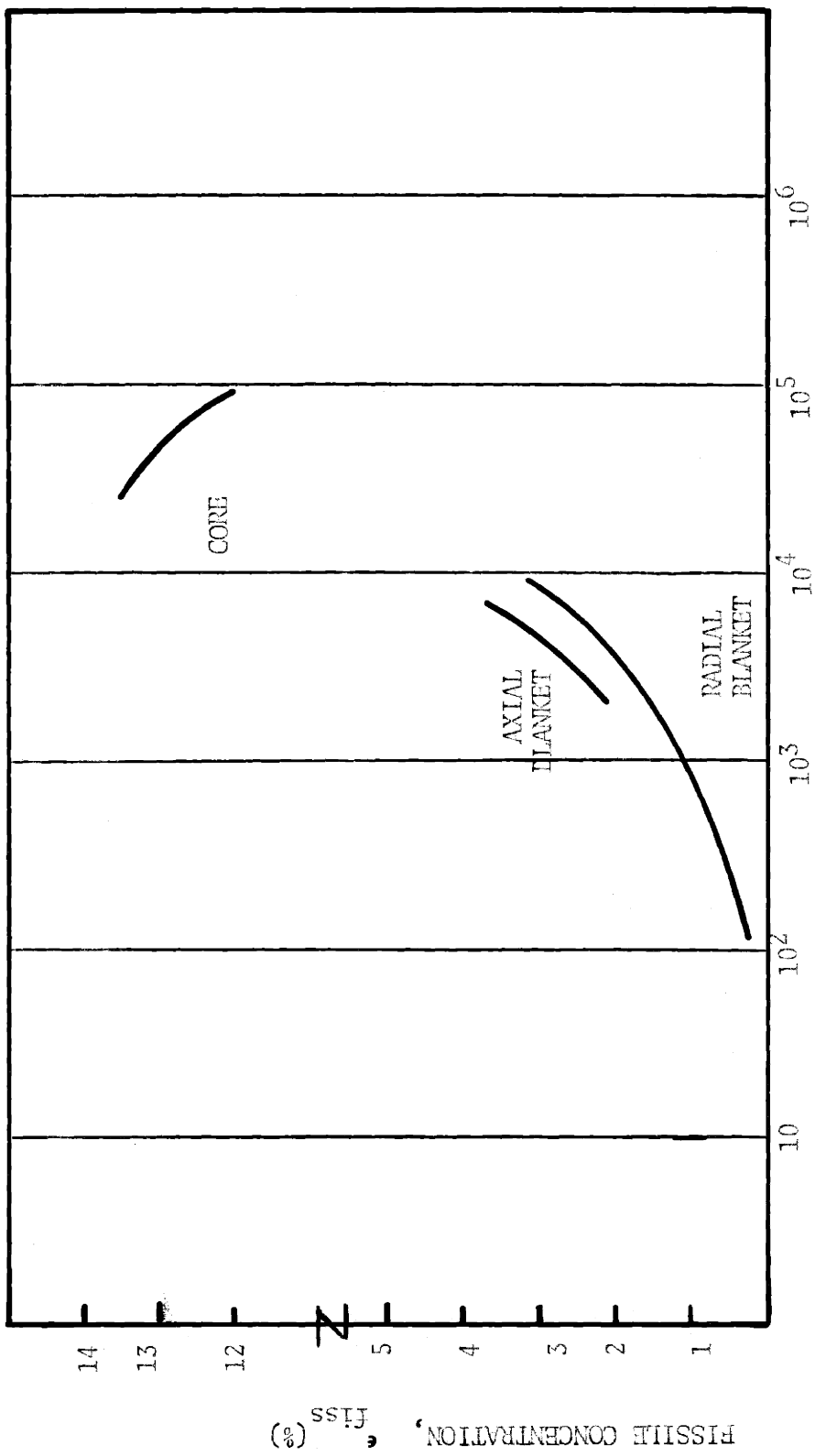

FIG. 3.11 COMPARISON OF BURNUP-FISSILE CONCENTRATION CHARACTERISTICS OF CORE, AXIAL BLANKET, AND RADIAL BLANKET

3.5 CRITICALITY AND REACTIVITY

In fuel economic analysis, two major functions of a physics-depletion model are (1) to provide fuel composition as a function of irradiation exposure, and (2) to provide criticality and reactivity information. The first is required for computing direct material costs ("burnup costs"), for core and blanket fuel. The second is closely related to core material carrying charges ("inventory cost"), i.e. carrying charges associated with the excess fissile material required to maintain criticality throughout fuel life.

Effects of simplifying assumptions (constant local fluxes and constant local spectra) on irradiated fuel composition results were estimated in Section 3.4 by comparing results of three depletion methods (26G-TSD, 1G-TSD and SAM). The present section concerns criticality and reactivity information (or lack of it) from the two simplified methods (1G-TSD, SAM).

3.5.1 SAM

The SAM procedure as outlined in Section 3.3 includes only one neutron balance computation — to obtain the flux shape, spectra and k_{eff}. Thus the lifetime behavior of k_{eff} is not determined in SAM. However, this is not considered a serious restriction in economic sensitivity and scoping studies.

A rigorous model would include the constraint that enough excess reactivity be loaded to ensure criticality at the desired discharge burnup. Computationally, this may require several complete depletion iterations (at various load enrichments, ϵ_0), as suggested in Figure 3.12, to determine the correct ϵ_0.

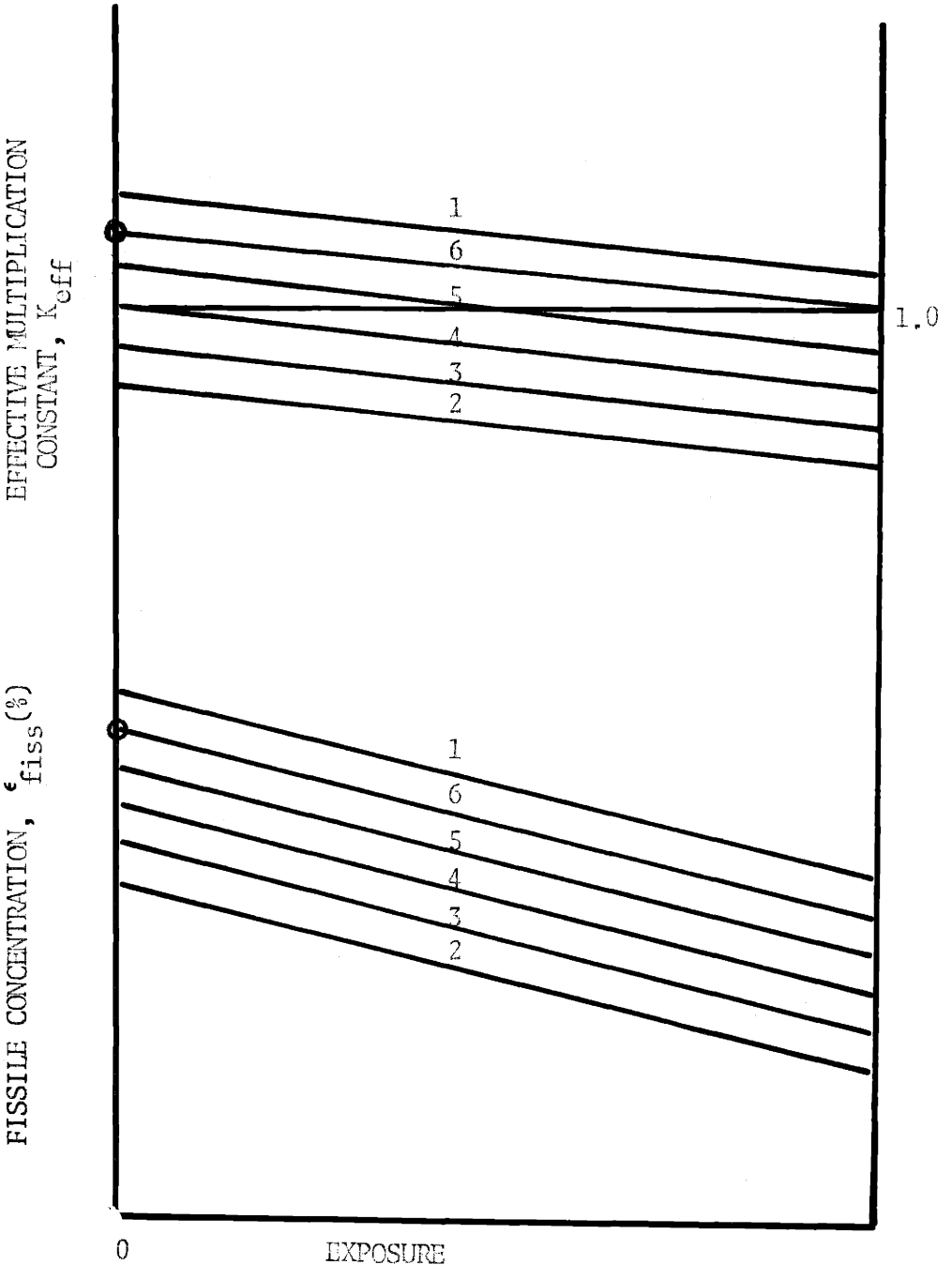

FIG. 3.12 ILLUSTRATION OF DEPLETION ITERATION TO SELECT INITIAL CORE ENRICHMENT

Load enrichment ϵ_0 affects FBR fuel costs through the material components: direct material purchase, direct material credit, and their associated carrying charges (inventory charges).

Effect of ϵ_0 on Direct Material Costs (Core)

Direct material cost ("burnup cost") represents the difference between direct material purchase costs and direct material credits. The direct material purchase component of FBR core fuel cost is directly proportional to load enrichment, ϵ_0. (By contrast, the same component in light water reactors increases in a parabolic fashion with ϵ_0, because of the separative work cost.) With flux and cross-sections held constant, Equation (3-9) shows that material credit is also proportional to ϵ_0, though with a lower constant of proportionality than direct material purchase because higher ϵ_0 implies less fertile material available for breeding. Thus changes in direct material purchase cost and material credit, due to adjustments in ϵ_0, tend to cancel.

Effect of ϵ_0 on Material Inventory Costs (Core)

The effect of ϵ_0 on core inventory costs is illustrated in Fig. 3.13. Two cases are shown: (1) reactor critical at beginning of fuel life; and (2) reactor critical at end of fuel life. Assuming simple interest, inventory cost is proportional to the area under the fissile fraction (ϵ) plot. The difference in inventory costs between the two cases is represented by the shaded area, $iT\,\Delta\epsilon$. Both plots are practically linear, and have approximately the same slope, i.e. about 2% in two years, representative of 100,000 MWD_t/MT core burnup. The discrepancy in inventory costs for this simple example is thus

$$\frac{(inv)_2 - (inv)_1}{(inv)_2} = \frac{iT\Delta\epsilon}{iT\epsilon_c + 1/2\ iT\Delta\epsilon} \simeq 12\% \quad (3\text{-}18)$$

The discussion above ignores the slight perturbation of core spectrum

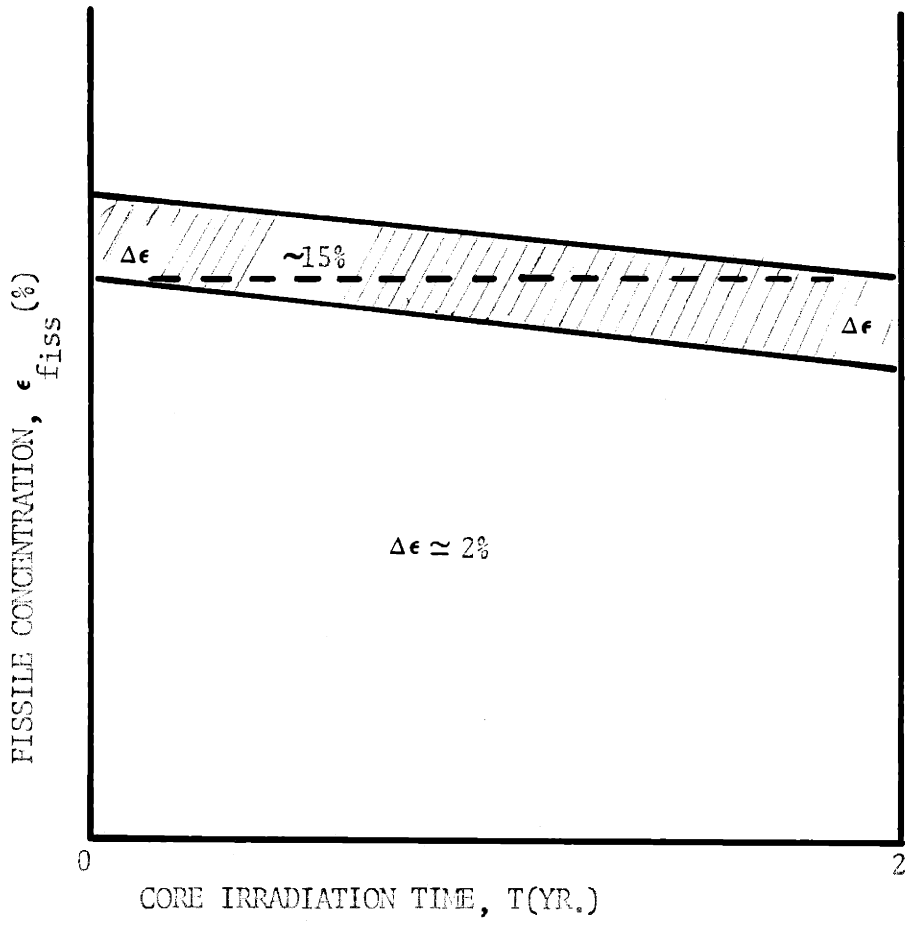

FIG. 3.13 ILLUSTRATION OF THE EFFECT OF CORE INITIAL ENRICHMENT ON MATERIAL INVENTORY COST

and flux level (for the same power) due to the changes in ϵ_0. Results of 26G-TSD calculations, Section 3.4, show that core spectrum and flux were practically constant over a two year irradiation which resulted in a fissile fraction decrease of $\Delta\epsilon \simeq 2\%$. This suggests that ϵ_0 adjustments near criticality, to obtain the desired BOL excess reactivity, would have little effect on core spectrum, flux, and therefore, on discharge compositions.

The discussion above also ignores the perturbation of core spectrum and flux shape due to control poisons. Other studies (29) have concluded that the inclusion of control poisons in TSD calculations (criticality search option) has little effect on depletion results.

The SAM procedure is used in Chapter 5 to compare the fuel economics of various radial blanket sizes (45,30,and 15 cm) and radial reflector materials. It was found that changing the radial blanket-radial reflector configuration had negligible effect on critical enrichment.

To summarize, the inability of SAM to provide the lifetime behavior of reactivity is not a serious limitation for survey-type, comparative economic studies, provided, of course, that the one shapshot physics calculation is performed at conditions near criticality.

3.5.2 1G-TSD

Comparison of 1G-TSD versus 26G-TSD reactivity information is shown in Table 3.7. Using the expression[1]

$$\frac{\delta K}{K} \simeq 0.2 \quad \frac{\delta \epsilon}{\epsilon},$$

the 1G-TSD method would result in an "error" of about 15% in critical mass (or inventory cost). The discrepancy in reactivity swing over one core lifetime is negligible.

---

1. From the 26G-TSD calculation for Reactor #1 (no fission products).

TABLE 3.7

COMPARISON OF MULTIPLICATION CONSTANT VALUES

FROM 26G-TSD AND 1G-TSD CALCULATIONS

Method	k^0_{eff}	Δk_{eff} (per core life)
(a) 26G-TSD	1.0004	0.0245
(b) 1G-TSD	0.9631	0.0248
	$\delta K^0_{eff} = 0.0363$	$\delta(\Delta K_{eff}) = -0.0003$

$\delta \equiv$ (a) - (b)

The 1G-TSD method requires one multigroup physics computation, anyway, to generate its position-dependent cross-sections, and the k_{eff} from this computation is presumably available. This, together with the ΔK-lifetime data from the 1G-TSD calculation, may be used to obtain excess reactivity requirements, fissile loading, and inventory costs.

3.6 COMPARISON OF COMPUTER TIME REQUIREMENTS FOR 26G-TSD, 1G-TSD AND SAM

Table 3.8 compares the MIT IBM 360/65 computer time requirements for the 26G-TSD, 1G-TSD, and SAM calculations discussed in Sections 3.4 and 3.5. All physics and TSD calculations were performed by 2DB.

The reactor configuration was the reference LMFBR described in Figure 3.3, with 1232 mesh points (44 x 28) and 23 active burnup zones. Depletion calculations spanned 1200 EFPD with 150 EFPD time steps for the TSD methods.

3.7 EFFECT OF HETEROGENEITY ON BLANKET DEPLETION RESULTS

Among the effects making irradiated blanket compositions difficult to predict is spatial self-shielding of resonance capture (heterogeneity effects) resulting from the relatively soft blanket spectrum and, for radial blankets, aggravated by the large pin diameters (30).

Figure 3.14 shows the heterogeneity-corrected core and blanket U238 absorption cross-sections as functions of energy group index. These cross-sections were generated by the 1DX code (27) using the Russian 26 group set (48) as input. The 1DX run (a) changed the cross-section format from Russian format to DTF format, (b) corrected group definitions (lethargy interval) from the Russian definitions to uniform lethargy widths of 0.5, commencing with the upper boundary of group 1 at 10.5 Mev, and (c) performed heterogeneity corrections for a typical FBR composition and geometry.

TABLE 3.8

COMPARISON OF COMPUTER TIME* REQUIREMENTS

FOR 26G-TSD, 1G-TSD, and SAM

26G-TSD Method	
ten 26G static physics calculations (@ 30 min.per)	300 min.
eight depletion step calculations	negligible
Total 26G-TSD method	300 min.
1 G-TSD Method	
one 26G static physics calculation	30 min.
ten 1G static physics calculations (@ 25 min.per)	25 min.
eight depletion step calculations	negligible
Total, attributable to 1G-TSD method	55 min.
SAM	
one 26G static physics calculation	30 min.
one depletion step calculation	negligible
Total attributable to SAM	30 min.

* IBM 360/65

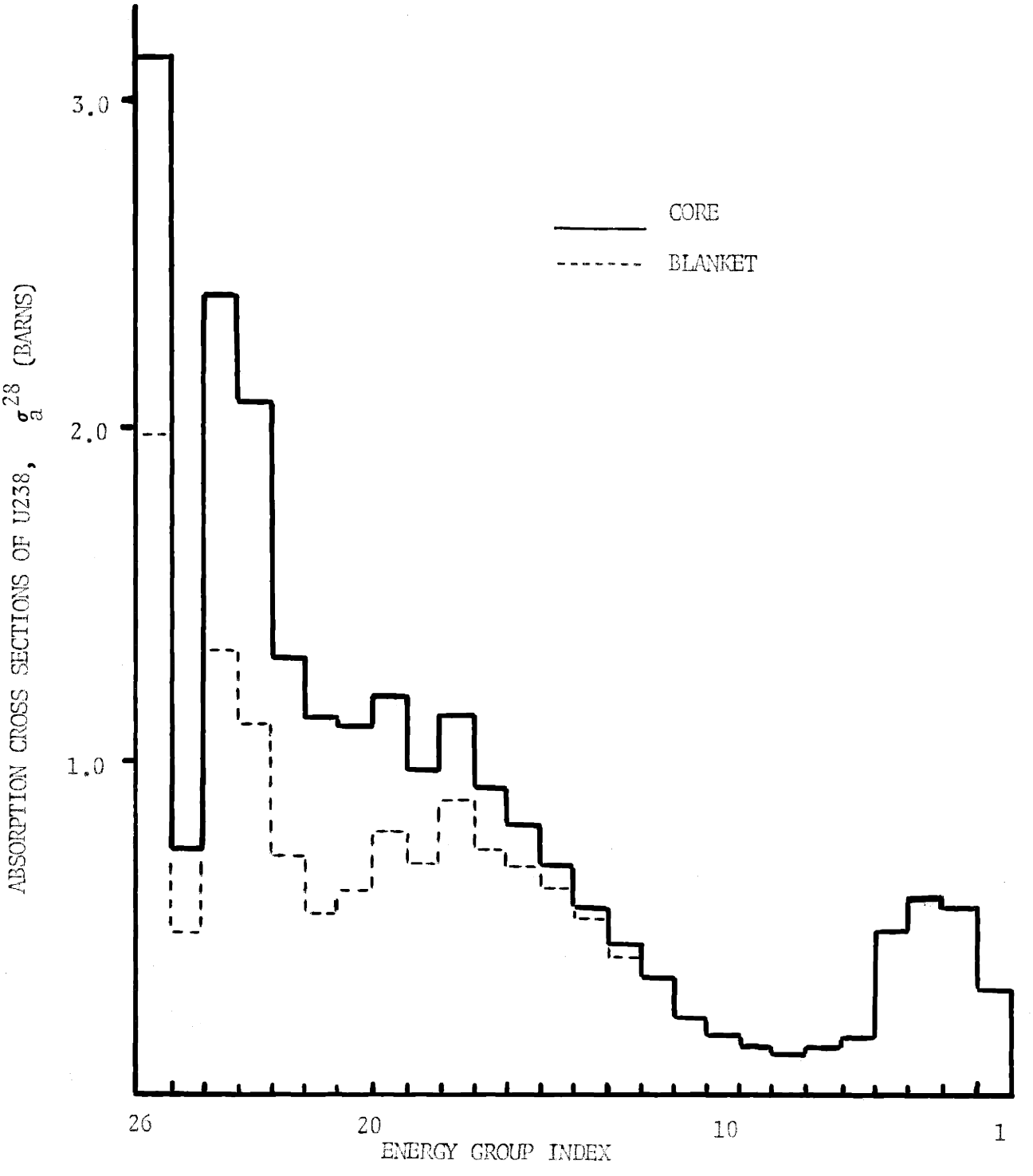

FIG. 3.14 26-GROUP U238 ABSORPTION CROSS SECTIONS FOR CORE AND BLANKET AS GENERATED BY 1DX PROGRAM FROM THE RUSSIAN SET

Because of the relatively hard core spectrum, the core heterogeneity corrections are slight, and the "core" cross-section sets are not greatly different from the infinitely-dilute Russian set. In this section, the blanket heterogeneity effects will be measured relative to core conditions, i.e. the core cross-sections are considered as infinitely dilute. To avoid confusion, the following notation is used in this section:

$\sigma(j,k)$		a local cross-section found by collapsing the multigroup parent set j over the local spectrum from a multigroup physics computation in which multigroup set k was used as input for the blanket cross-sections.
j or k	=	He . . . heterogeneity-corrected blanket parent multigroup set
	=	Ho . . . homogeneous (infinitely dilute) core parent multigroup set
$\phi(k)$		local neutron flux, from a multigroup physics computation in which multigroup cross-section set k was used as input for the blanket cross-sections.

Figure 3.15 displays σ_a^{28} (Ho, He) and σ_a^{28}(He, He) as functions of radial position along the midplane of the reference reactor(#1) at time zero. The blanket heterogeneity effect, σ_a^{28} (Ho, He) - σ_a^{28}(He,He) is seen to increase with depth into the blanket, due to spectrum softening with depth.

Heterogeneity affects blanket fissile production in two opposing ways:

(a) the lower effective U238 microscopic capture cross-section, σ_c^{28}, depresses the U238 to Pu239 conversion rate, leading to lower bred fissile Pu inventories;

(b) viewing blanket neutronics as an attenuation process, in a macroscopic sense, the lower effective microscopic absorption cross-sections (the most significant being U238) results in higher blanket macroscopic fluxes, tending to increase the U238 capture rate and bred fissile inventories.

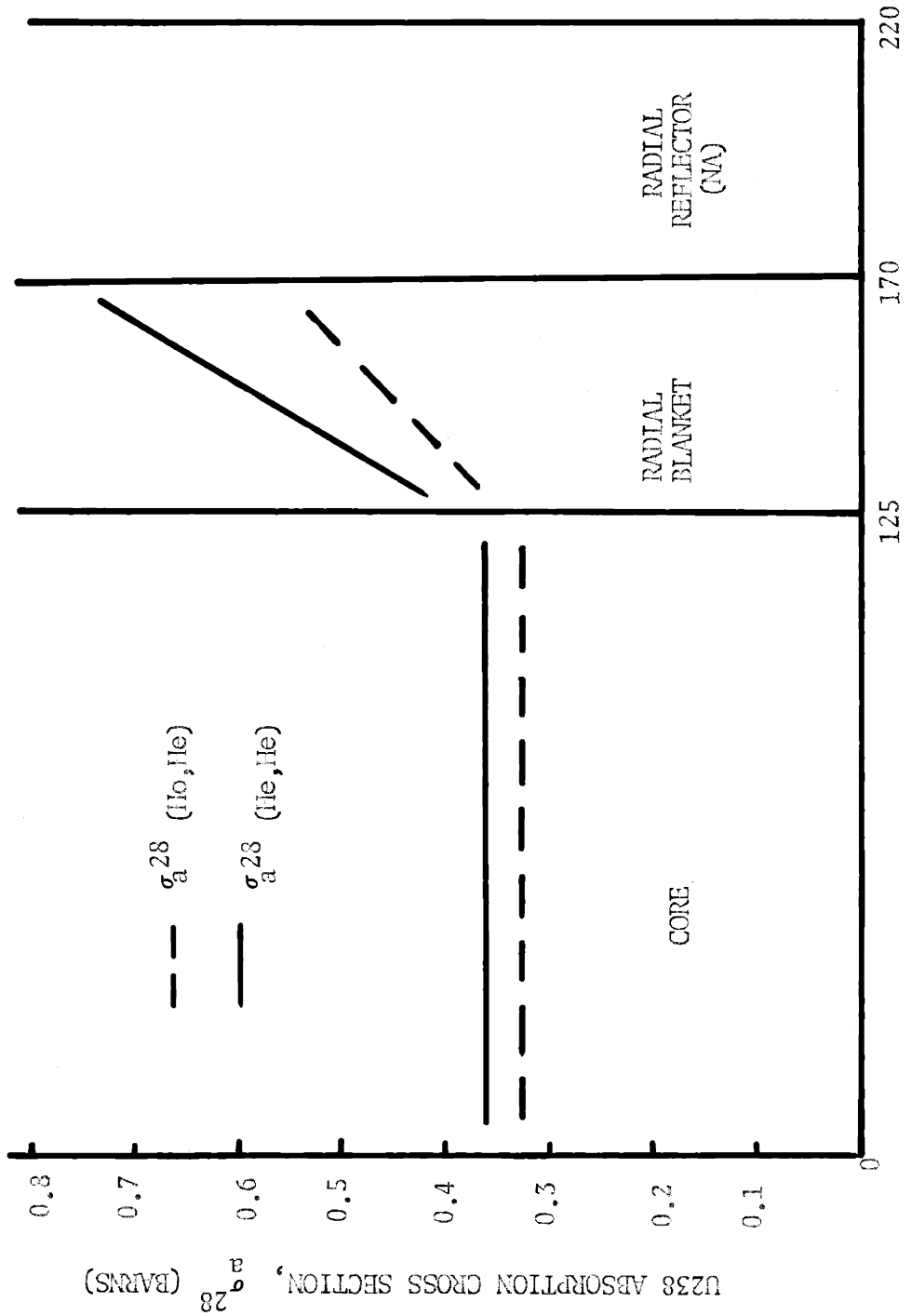

FIG. 3.15 SPECTRUM-WEIGHTED ONE-GROUP U238 ABSORPTION CROSS SECTIONS AS FUNCTIONS OF RADIAL POSITION

Of the two opposing effects, (a) dominates and heterogeneity influences blanket breeding adversely.

To separate and quantify these effects, three parallel SAM radial blanket calculations were performed, using as local input

(1) σ (Ho, He) , ϕ (He)

(2) σ (He, He) , ϕ (He)

(3) σ (Ho, Ho), ϕ (Ho) .

Comparison of (1) and (2) provides a measure of effect (a), the depressed U238 capture cross-section. The overall net effect, on fissile breeding, is shown by comparing (2) and (3). Two separate multigroup physics computations, with the 2DB program, generated the local $\{\sigma, \phi\}$ data - one using "He" in the radial blanket, and the other using "Ho" in the radial blanket. The reference reactor configuration, Figure 3.3, was assumed in both computations. Spatial detail for depletion purposes and for purposes of inputting cross-sections and fluxes to SAM, was the same as in the studies of Section 3.4. Table 3.9 shows the local U238 capture rate data in zone #8 (see Figure 3.3) for the three SAM calculations.

The overall radial blanket depletion results, by the three SAM calculations, are compared in Figure 3.16. Comparing (1) and (2) isolates effect (a), that of the depressed σ_c^{28}. The discrepancy in discharge Pu239 inventory is about 20%, resulting in a discrepancy of about 20% in material credit. Effect (a) is offset significantly by effect (b), as can be seen by comparing (1) and (3). The overall self-shielding effect on Pu239 discharge - the combined effects (a) and (b) - is seen by comparing (2) and (3). Self-shielding reduces discharge Pu239 content by about 10%.

TABLE 3.9

U238 CAPTURE DATA ILLUSTRATING RADIAL BLANKET HETEROGENEITY EFFECT

	σ_c^{28}	ϕ	$\sigma_c^{28}\phi$
(1) σ_c^{28}(Ho,He)			
ϕ(He)	0.447	1.879	0.840
(2) σ_c^{28}(He,He)			
ϕ(He)	0.374	1.879	0.703
(3) σ_c^{28}(Ho,Ho)			
ϕ(Ho)	0.4168	1.778	0.740

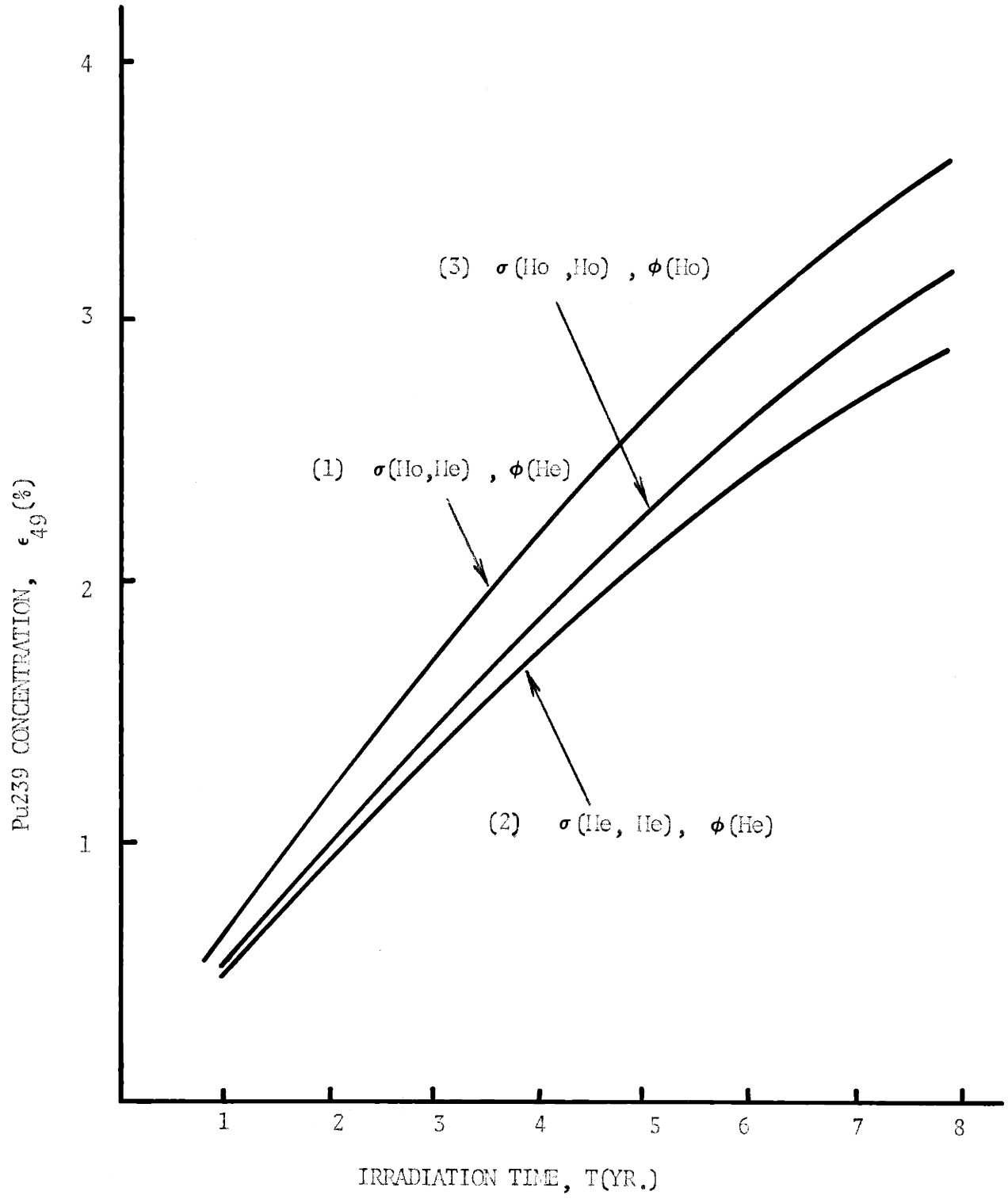

FIG. 3.16 EFFECT OF HETEROGENEITY CORRECTION ON RADIAL BLANKET DEPLETION RESULTS

3.8 SUMMARY

A fast breeder reactor fuel depletion method, suitable for survey, ranking, and sensitivity studies, is established and tested in this Chapter. This method, labeled the Semi-Analytic Method (SAM), assumes that local spectra and fluxes do not vary with irradiation time. These assumptions are tested by comparing SAM results with those of multigroup (26 group) and one group time step depletion calculations. These assumptions are found to have negligible effect on core depletion results (error in discharge composition is less than 0.1%). Error in blanket depletion results is tolerable for purposes of comparative studies: less than 4% in axial blanket results, and about 10% in radial blanket results. Batch fuel management is assumed in the test calculations, thus placing maximum strain on the constant flux, constant spectrum assumptions. Of these two assumptions (which result in opposing errors), the constant flux assumption is found to be the most significant.

SAM results in a computer time savings of about 90%, and is selected for application to the case studies of Chapter 5. As applied in this report, SAM is restricted to fixed fuel schemes, i.e. batch or scatter fuel management.

A further limitation of SAM is that it does not yield reactivity history, since only one physics (multigroup) computation is performed per configuration per fuel lifetime. This is not considered a serious restriction in the sensitivity and comparative studies for which it is intended.

Effects of heterogeneity corrections on blanket depletion results are also examined in this chapter. Blanket heterogeneity is found to reduce fissile discharge inventory by about 10% for irradiation times of interest (2-7 years).

CHAPTER 4

INTEGRATED DEPLETION-ECONOMICS MODEL, SELECTION OF REFERENCE LMFBR, REFERENCE LMFBR FUEL ECONOMICS

4.1 INTRODUCTION

Fast breeder reactor fuel cost analysis and fuel depletion methods were discussed separately in Chapters 2 and 3, respectively. The "cash flow method (CFM)" was selected for cost analysis; the "semi-analytic method (SAM)" using neutronic data from a single multigroup calculation (per reactor configuration) was selected for the depletion model.

The purposes of the present chapter are:

1. to combine these two models into a procedure (Section 4.2) useful for scoping, survey, and sensitivity studies;

2. to compare the selected LMFBR reference configuration to other 1000 MWe LMFBR reference designs (Section 4.3); and

3. to apply the integrated depletion-economics model to the reference economic environment (Section 4.4).

Section 4.2 summarizes the calculational procedure used in the remainder of the report. Section 4.4 serves as an illustration of the procedure, while establishing the base case around which the case studies and sensitivity studies of Chapter 5 are performed. Also, the effect of core enrichment zoning on blanket fuel economics is estimated in Section 4.4.

4.2 INTEGRATED DEPLETION-ECONOMICS MODEL

Figure 4.1 is a schematic of the integrated depletion-economics model. The step-by-step procedure is described below.

1. The reactor configuration is set in accordance with normal

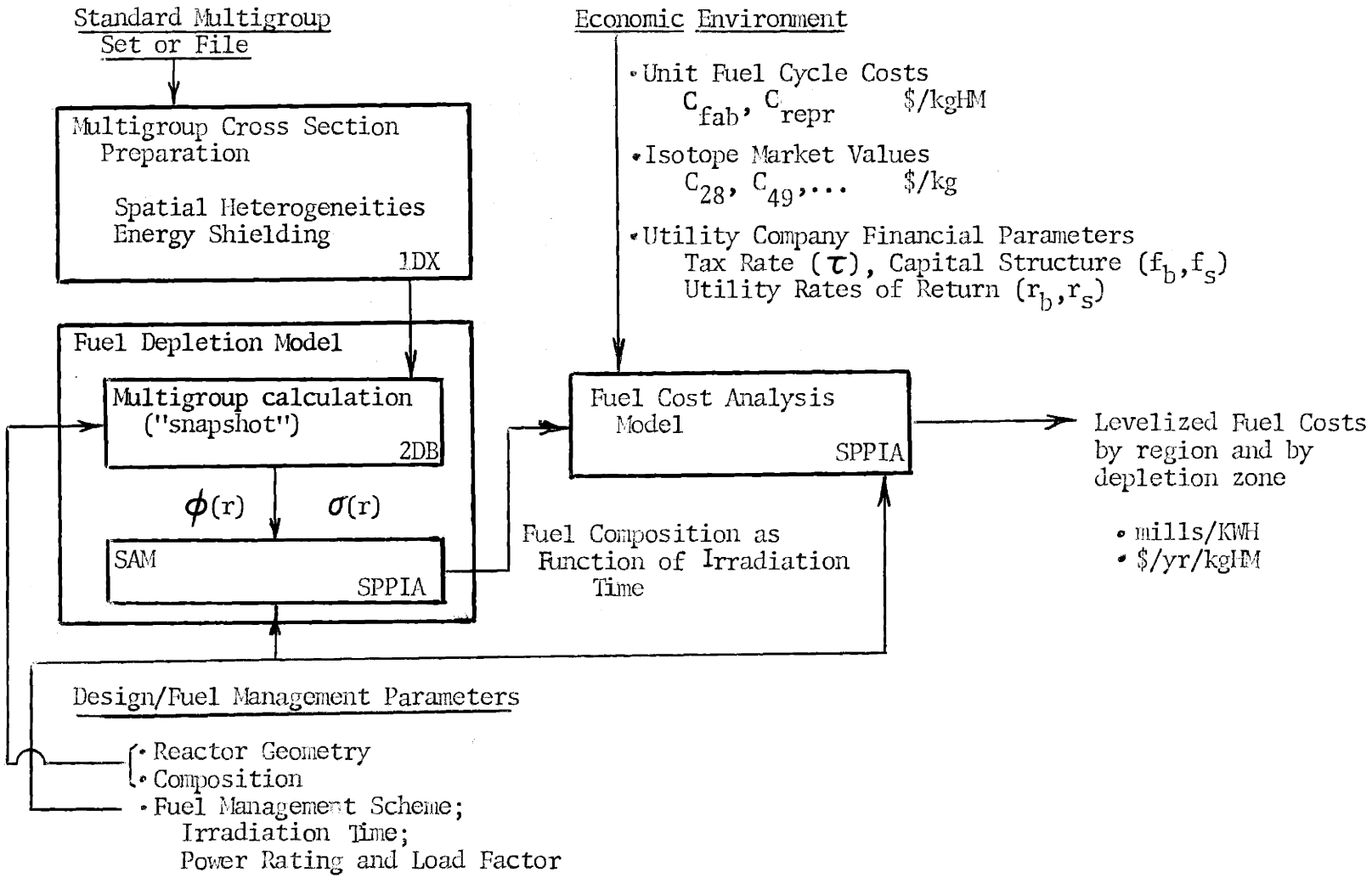

FIG. 4.1 INTEGRATED DEPLETION-ECONOMICS MODEL

design procedures which need not be the subject of detailed discussion here.

(a) Geometry (shape) and dimensions are established.

(b) Initial compositions of the major regions - core, axial blanket, radial blanket, reflectors - are selected. Reactor geometry and composition are of course chosen to be compatible in terms of achieving criticality, and beginning-of-life (BOL) excess reactivity needed to achieve the rated burnup.

(c) Reactor power rating is specified, satisfying maximum local power density constraints and the desired power shape criteria at the point in life considered, typically BOL.

Depletion Calculation

2. Each major fuel-bearing region is subdivided into depletion zones. Depletion zones should be sufficiently numerous to give the detailed space-dependent depletion information desired and to account for large flux gradients and spectrum variations.

3. A single "snapshot" physics computation is performed to obtain $\phi(r, E)$. A standard multigroup program such as ANISN (46) or 2DB (26) may be used for this purpose. The program 2DB was used throughout the present study. In the present study, BOL nuclide inventories are used in the "snapshot" calculation. Flux shape and local spectra are used to obtain zone flux magnitudes, $\tilde{\phi}$,normalized to rated reactor power, and zone one-group cross sections:

$$\sum_{\text{zones}} \left(V \quad \tilde{\phi} \quad \Sigma_f \right)_{\text{zone}} = \text{Rated Reactor Power}$$

$$\sigma = \sum_g \tilde{\phi}_g \quad \sigma_g \; / \; \tilde{\phi}$$

$$\tilde{\phi} = \sum_g \tilde{\phi}_g \qquad (4\text{-}1)$$

where $\tilde{\phi}$ is the zone flux (total, integrated over energy and zone volume) at rated reactor power, V is the zone volume, Σ_f is the total macroscopic fission cross section for the zone, $\tilde{\phi}_g$ is the zone flux in energy group g.

Input to the multigroup physics computation includes, in addition to reactor configuration information, a multigroup cross section set. This multigroup set could be obtained from a cross section processing program such as 1DX (27) or MC^2 (39), making appropriate corrections, regionally, on a standard set or file, for self-shielding. Multigroup cross section data used in this report consisted of the 26 group Russian set (48), 1DX-corrected (27, 81) for the core and blanket.

4. Zone fluxes and zone cross sections, found in step 3, and plant load factor (L) are input to the "semi-analytic depletion method (SAM)" calculation, Equations (3-9), to obtain zone compositions as a function of flux time, burnup, and irradiation time. The load factor is used to scale the fluxes for Equations (3-7)and (3-9):

$$\phi = L\ \tilde{\phi} \tag{4-2}$$

Equations (3-9) yield the zone number densities at irradiation time T: $N_{28}(T)$, $N_{49}(T)$, ..., $N_{42}(T)$. The nuclide number densities are converted to masses by equations of the form

$$M_i(T) = N_i(T)\ V\ \frac{\tilde{M}_i}{N_{av}} \tag{4-3}$$

where

$M_i(T)$ = mass of nuclide i in the depletion zone at irradiation time T, kg;

V = zone volume, liters;

$\tilde{M}_i$ = atomic mass of nuclide i;

N_{av} = Avogadro 's number

Since many economics parameters are normalized to mass of heavy metals (U, Pu) loaded, it is convenient to define the nuclide fractions

$$\epsilon_i(T) = M_i(T) / M^0_{HM} \tag{4-4}$$

where

M^0_{HM} = mass of heavy metals (U, Pu) loaded in zone

$= M^0_{28} + M^0_{49} + \ldots + M^0_{42}$

5. Zone masses may be summed over an annular region which is batch or scatter-managed to obtain the masses discharged from fuel lots irradiated in that region:

$$\left[M_i(T)\right]_{\substack{\text{annular}\\\text{region}}} = \sum_k \left[M_i(T)\right]_{\text{zone k}}$$

$$\left[\epsilon_i(T)\right]_{\substack{\text{annular}\\\text{region}}} = \frac{\left[M_i(T)\right]_{\text{annular region}}}{\left[M^0_{HM}\right]_{\text{annular region}}} \tag{4-5}$$

Cost Calculations

6. The following economics parameters are set:

. Unit fuel processing costs, dollars per kg of heavy metal,

C_{fab}, C_{repr} [\$/kg HM]

. Isotope market values, dollars per kg of isotope,

$C_{28}, C_{49}, \ldots, C_{42}$ [\$/kg]

. Financial parameters

Tax rate (τ)

Capital structure (f_b, f_s)

Utility rates of return (r_b, r_s)

7. Using the economics parameters of step 6 and the nuclide masses from step 4 (local, depletion zone) or step 5 (annular region), fuel costs are calculated from the CFM cost equations developed in Chapter 2.

The levelized cost of electricity (mills/KWH) associated with a depletion zone or annular region is given by

$$\overline{e} = \frac{1000}{E} M_{HM}^{0} \left[\frac{(C_{28}\epsilon_{28}^{0} + C_{49}\epsilon_{49}^{0} + \ldots)}{T} F^{mp}(T) \right. \quad \text{(material purchase)}$$

$$+ \frac{C_{fab} F^{fab}(T)}{T} \quad \text{(fabrication)}$$

(4-6)

$$+ \frac{C_{repr} F^{repr}(T)}{T} \quad \text{(reprocessing)}$$

$$\left. - \frac{(C_{28}\epsilon_{28}(T) + C_{49}\epsilon_{49}(T) + \ldots)}{T} F^{mc}(T) \right] \quad \text{(material credit)}$$

where M_{HM}^{0}, ϵ_{28}^{0}, ϵ_{49}^{0}, ..., $\epsilon_{28}(T)$, $\epsilon_{49}(T)$, ... are either depletion zone quantities (step 4) or annular region quantities (step 5). Other terms in Equation (4-6) are defined below:

E = electrical energy produced by the plant per year, $\frac{\text{kwhe}}{\text{yr}}$

1000 = conversion factor, mills/dollar

$F^{q}(T)$ = carrying charge factor for cost component q, defined such that

Total cost (q) = direct cost (q) x $F^{q}(T)$
carrying charge (q) = direct cost (q) x $[F^{q}(T)-1]$.

The cost components of Equation (4-6) above correspond to chronological events in the fuel cycle, e.g. material purchase → fabrication → (irradiation) → reprocessing → material credit. Costs may be restructured as desired, e.g.

material costs = material, direct + material, carrying charge
="burnup cost" + "inventory cost"

processing costs = fabrication + reprocessing
= processing, direct + processing, carrying charge

The bracketed term in Equation (4-6) may be regarded as a figure of merit representing local fuel economic performance, having units of dollars per year per local kilogram of heavy metal loaded.

8. Steps 4 through 7 generate local (by depletion zone), annular region, and major regional (core, axial blanket, radial blanket) depletion and economics results as a function of irradiation time.

The process may be repeated for different economic environments (step 6), using a single set of neutronics data from step 3, that is, the multigroup physics computation need be performed only once per reactor configuration.

A computer program, SPPIA, was developed to perform steps 4, 5, and 7, e.g. to perform SAM depletion calculations and CFM cost calculations, using, as input, the zone neutronic information from step 3 and the economic parameters set in step 6. This program is described in Appendix C.

4.3 REFERENCE LMFBR CONFIGURATION

In order to select a representative LMFBR configuration for blanket case studies, a brief survey was made of U.S. reactor manufacturers' 1000 MWe LMFBR 1964 (65, 64, 67, 68) and 1968 Follow-on (67, 70, 71, 74, 75, 76) designs, the Karlsruhe (77, 78) designs, the reference reactors used in

design calculations for the MIT Blanket Test Facility (60), and reference reactors used in other blanket analytical studies (1, 4, 5). Only uranium-plutonium ceramic fueled reactors were considered. Modular and annular geometries were excluded. Key variables surveyed were those base design parameters which affect blanket fuel economics directly and prominently: core height-to-diameter ratio, core power density, blanket size, and core and blanket compositions. Table 4.1 summarizes this data for the reactors considered, together with the LMFBR reference design adopted for the present studies. The reference LMFBR arrangement is shown in Figure 4.2.

The reference LMFBR adopted is identical to that used in the depletion method studies of Chapter 3. It closely resembles the Karlsruhe designs, and the reference LMFBR used for the MIT Blanket Test Facility design calculations. The two subcases (1, 1') of the reference LMFBR are identical except that 1' has two core enrichment zones while 1 has a single uniform load enrichment.

4.4 REFERENCE LMFBR FUEL ECONOMICS

One-Zone Core

In this section, the procedure outlined in Section 4.2 is applied to the reference LMFBR described in Section 4.3.

The reference economic environment assumed for these calculations is summarized in Table 4.2. This data is representative of base data used in LMFBR design studies (62, 63, 64, 65, 66, 69, 70, 71, 72, 73) and falls within ranges projected for the mature U.S. nuclear fuel cycle economy (18). Unit fuel cycle costs are sensitive to national nuclear fuel cycle throughput and capacity, and are closely coupled to reactor design and operation (fuel pin design, discharge enrichment). Since these concerns lie beyond the purvue of this study, the economic environment is treated parametrically

TABLE 4.1 SURVEY OF LMFBR DESIGNS

1964 1000 MWe LMFBR Designs

		GE Ref.(65,67,68)	CE Ref.(64,67,68)
Core Height	(cm)	60.96	76.2
Diameter	(cm)	356.62	219.46
Height/Diameter		0.1709	0.347
Volume	(liters)	6030	2895
Axial Blanket Thickness x2	(cm)	91.4	91.4
Radial Blanket Thickness	(cm)	38.1	42.6
Core Power Density	(kw_t/liter)	365	695
Core & Axial Blanket Composition			
Fuel	(v/o)	34.8	25.6
Structural Metal	(v/o)	18.8	7.9
Sodium	(v/o)	46.4	66.5
Radial Blanket Composition			
Fuel	(v/o)	50.7	45
Structural Metal	(v/o)	17.2	12
Sodium	(v/o)	32.1	43
Fuel Enrichment Zoning			
No.of Core Enrichment Zones		3	2
Enrichment Zone #		I II III	I II
Load Enrichment	(%)	15.67 17.96 20.24	10.68 15.28
Enrichment Zone Volume	(liters)	2010 2010 2010	1447.5 1447.5

TABLE 4.1 - Continuation

1968 1000 MWe LMFBR Follow-on Designs

		AI Ref.(70,74)	CE Ref.(71,76)	B&W Ref.(69,75)
Core Height	(cm)	127	60.96	88.73
Diameter	(cm)	235	270.36	306.68
Height/Diameter		0.54	0.226	0.29
Volume	(liter)	5506	3498	6516
Axial Blanket Thickness x 2	(cm)	60.96	91.44	71.12
Radial Blanket Thickness	(cm)		30.8	30.8
Core Power Density	(kw_t/liter)	408	608	346
Core&Axial Blanket Composition				
Fuel	(v/o)	31.0	38.63	44.2
Structural Metal	(v/o)	18.9	13.10	16.9
Sodium	(v/o)	50.1	39.98	35.4
Radial Blanket Composition				
Fuel	(v/o)	57.7	52.66	64.3
Structural Metal	(v/o)	13.1	15.01	16.3
Sodium	(v/o)	29.2	32.33	19.5
Fuel Enrichment Zoning				
No.of Core Enrichment Zones		2	2	3
Enrichment Zone #		I II	I II	I II III
Load Enrichment	(%)	11.6 16.0	10.13 12.05	
Enrichment Zone Volume	(liters)			

TABLE 4.1 Continuation

		Karlsruhe Ref. (77)	Karlsruhe (Jansen) Ref. (78)	Forbes Ref. (60)
Core Height	(cm)	95.5	94	95
Diameter	(cm)	286	282	200
Height/Diameter		0.333	0.333	0.475
Volume	(liters)	6132	5868	2983
Axial Blanket Thickness x 2	(cm)	80	80	80
Radial Blanket Thickness	(cm)	45.3	46	45
Core Power Density	(kw_t/liter)	393		
Core & Axial Blanket Composition				
Fuel	(v/o)	30.4	30	35
Structural Metal	(v/o)	19.6	20	15
Sodium	(v/o)	50.0	50	50
Radial Blanket Composition				
Fuel	(v/o)	48.3	50	50
Structural Metal	(v/o)	21.9	20	20
Sodium	(v/o)	29.8	30	30
Fuel Enrichment Zoning				
No. of Core Enrichment Zones		2	2	1 | 2
Enrichment Zone #		I II	I II	I I II
Load Enrichment	(%)	10.66 13.93		12.43 11.54 15.06
Enrichment Zone Volume	(liters)	3066 3066		2983 1462 1521

TABLE 4.1 Continuation

		Klickman Ref.(1)	Hasnain Ref.(4)	Perks Ref.(5)
Core Height	(cm)	105	93	119.38
Diameter	(cm)	131	104	193.04
Height/Diameter		0.801	0.9	0.62
Volume	(liters)	1414	800	3400
Axial Blanket Thickness x 2	(cm)	92	80	122
Radial Blanket Thickness	(cm)	40	45	61
Core Power Density	(kw_t/liter)	443	1000	329
Core & Axial Blanket Composition				
Fuel	(v/o)	50	30	30.8
Structural Metal	(v/o)	14	20	25.0
Sodium	(v/o)	36	50	36.4
Radial Blanket Composition				
Fuel	(v/o)		60	
Structural Metal	(v/o)		18	varied
Sodium	(v/o)		22	
Fuel Enrichment Zoning				
No.of Core Enrichment Zones		1	1	2
Enrichment Zone #		I	I	I II
Load Enrichment	(%)	9.8		17.5 12.93
Enrichment Zone Volume	(liter)	1414		
Plant Rated Thermal Power	(MW_t)	620	800	1200
Plant Rated Electrical Power	(MW_e)	230		500

TABLE 4.1 Continuation

		Reference LMFBR for Present Studies		
Core Height	(cm)	100		
Diameter	(cm)	250		
Height/Diameter		0.4		
Volume	(liters)	4906		
Axial Blanket Thickness x 2	(cm)	80		
Radial Blanket Thickness	(cm)	45		
Core Power Density	(kw_t/liter)	500		
Core & Axial Blanket Composition				
Fuel	(v/o)	30		
Structural Metal	(v/o)	20		
Sodium	(v/o)	50		
Radial Blanket Composition				
Fuel	(v/o)	50		
Structural Metal	(v/o)	20		
Sodium	(v/o)	30		
Fuel Enrichment Zoning				
No.of Core Enrichment Zones		1*	2**	
Enrichment Zone #		I	I	II
Load Enrichment	(%)	14	11	17
Enrichment Zone Volume	(liters)	4906	2540	2366
Plant Rated Thermal Power	(MWt)	2560		
Plant Rated Electrical Power	(MW_e)	1000		

* Reactor #1
** Reactor #1'

QUARTER-CORE VERTICAL SECTION

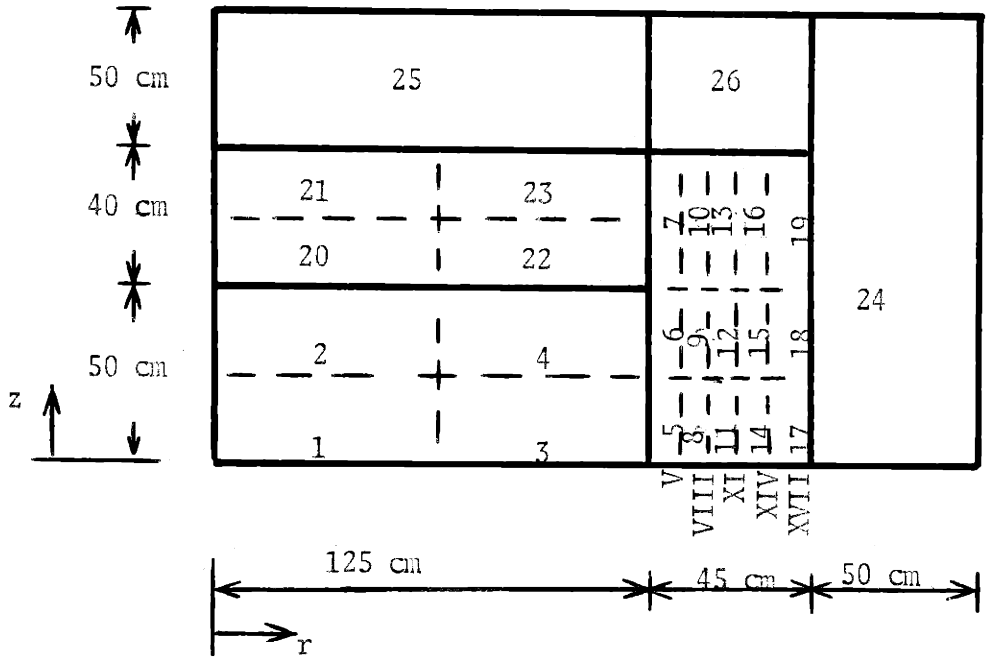

VOLUME FRACTIONS

REGION	CORE	RADIAL BLANKET	AXIAL BLANKET	RADIAL REFL.	AXIAL REFL.	AX.REFL. FOR RAD.BKT.
ZONE	1-4	5-19	20-23	24	25	26
SODIUM	0.50	0.30	0.50	1.00	0.50	0.30
OXIDE	0.30*	0.50	0.30	0	0	0
SS CR-FE-NI	0.20	0.20	0.20	0	0.50	0.70

* INITIAL CORE ENRICHMENT = 14%

FIG. 4.2 REFERENCE LMFBR CONFIGURATION (REACTOR #1)

TABLE 4.2

REFERENCE ECONOMIC ENVIRONMENT

Unit Fuel Processing Costs — $/kg HM

	Core	Axial Blanket	Radial Blanket
Fabrication (C_{fab})	314	80	69
Reprocessing (C_{repr})	31.5	31.5	31.5

Isotope Market Values — $/kg

U238	(C_{28})	0
Pu239	(C_{49})	10,000
Pu240	(C_{40})	0
Pu241	(C_{41})	10,000
Pu242	(C_{42})	0

Financial Parameters

Income Tax Rate (τ)		0.5
Capital Structure		
Bond(Debt) Fraction	(f_b)	0.5
Stock (Equity) Fraction	(f_s)	0.5
Rates of Return		
Bonds	(r_b)	0.07
Stocks	(r_s)	0.125
Discount Rate *	(x)	0.08

* $x = (1-\tau)r_b f_b + r_s f_s$

in Chapter 5, where the sensitivity of LMFBR fuel costs (mills/KWHe) to economic environment is estimated.

Table 4.3 lists pre-irradiation, irradiation, and post-irradiation times assumed for these reference calculations. Table 4.4 summarizes the reference plant power data.

Figures 4.3, 4.4, and 4.5 show fuel costs (mills/KWHe) versus irradiation time for the reference LMFBR (#1) core, axial blanket, and radial blanket. Batch fuel management of each of these regions is assumed. The reference one-zone core irradiation time of two years corresponds to an average core burnup of 102,000 MWD_t/MT. Core fuel cost at this exposure is seen to be 0.97 mills/KWHe. It is assumed, for practical reasons, that the axial blanket must be operated on the same fueling schedule as the core, i.e. two year irradiation time. The optimum irradiation time for the axial blanket, under the reference economic environment, is about two years (Figure 4.4). At two years, the axial blanket fuel cost is -0.141 mills/KWHe, a net revenue.

Unlike the axial blanket, the irradiation time for the radial blanket may be fixed independently of the core. Figure 4.5 shows its "breakeven" irradiation time to be about three years. Its optimum irradiation time is about six years, corresponding to a fuel cost of -0.036 mills/KWHe, (-8.1 $/yr./kg HM), a net revenue.

Comparing the fuel economics of the axial and radial blankets, one notes: (a) the relatively low net revenue provided by the radial blanket at its optimum irradiation time, i.e. 8.1 $/yr./kgHM for the radial blanket vs. 100 $/yr./kgHM for the axial blanket; and (b) the relatively "sluggish" behavior of the radial blanket, i.e. the radial blanket is slow in reaching its maximum net revenue. The comparatively poor radial blanket performance is the result of its relatively

TABLE 4.3 REFERENCE FUEL CYCLE TIMING

Region	Scheme	Pre-Irradiation Times (yr.)		Irradiation Time (yr.)	Post-Irradiation Times (yr.)	
		Material Purchase	Fabrication		Reprocessing	material credit
core	batch	0.5	0.5	2	0.5	0.5
axial blanket	batch	0.5	0.5	2	0.5	0.5
radial blanket	batch	0.5	0.5	variable	0.5	0.5

TABLE 4.4

REFERENCE PLANT POWER PARAMETERS

Plant Rated Power, electrical	1000 MWe
Plant Thermal Efficiency (η)	39%
Plant Load Factor (L)	83%

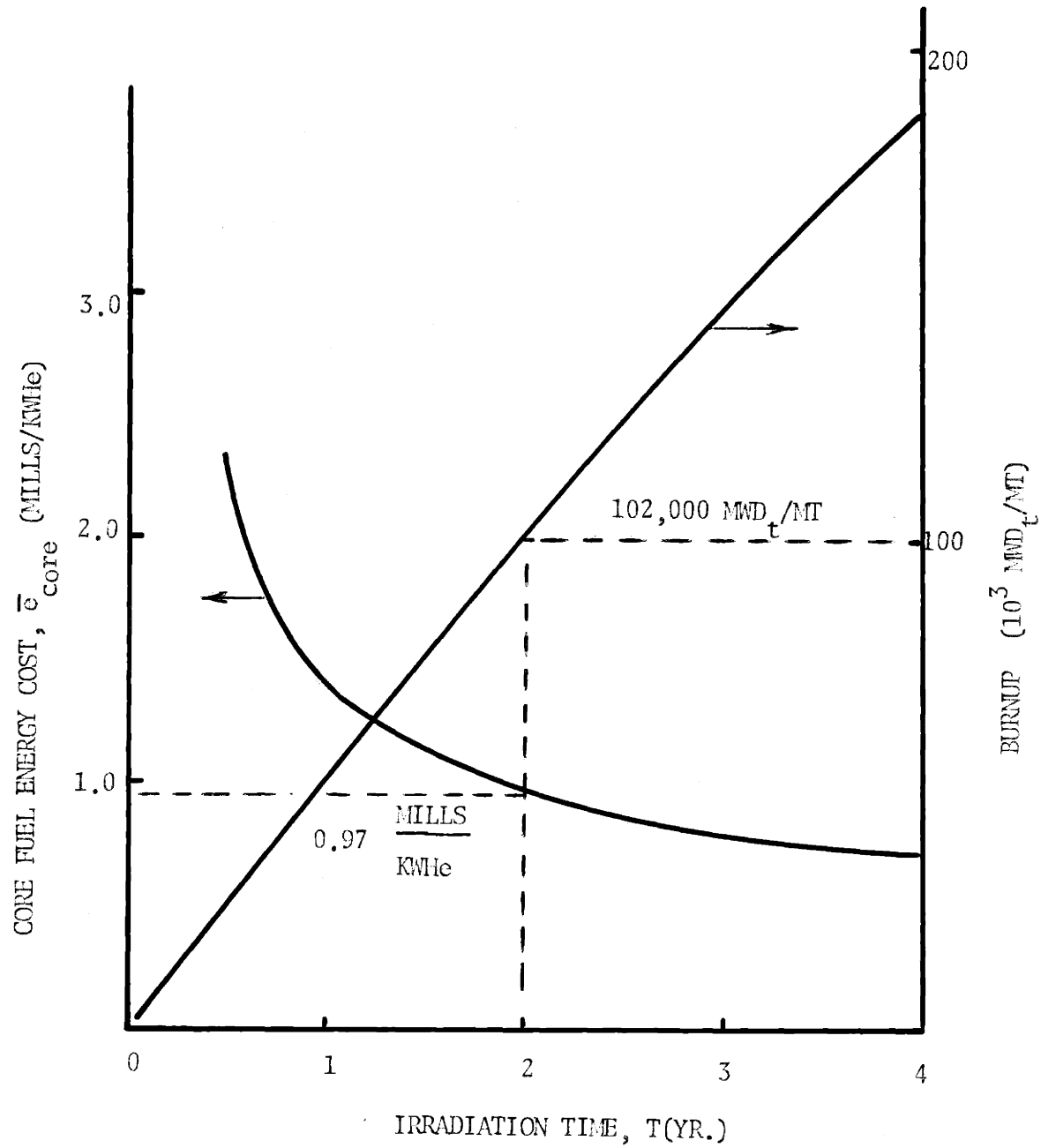

FIG. 4.3 REFERENCE LMFBR CORE FUEL ENERGY COST AS A FUNCTION OF EXPOSURE

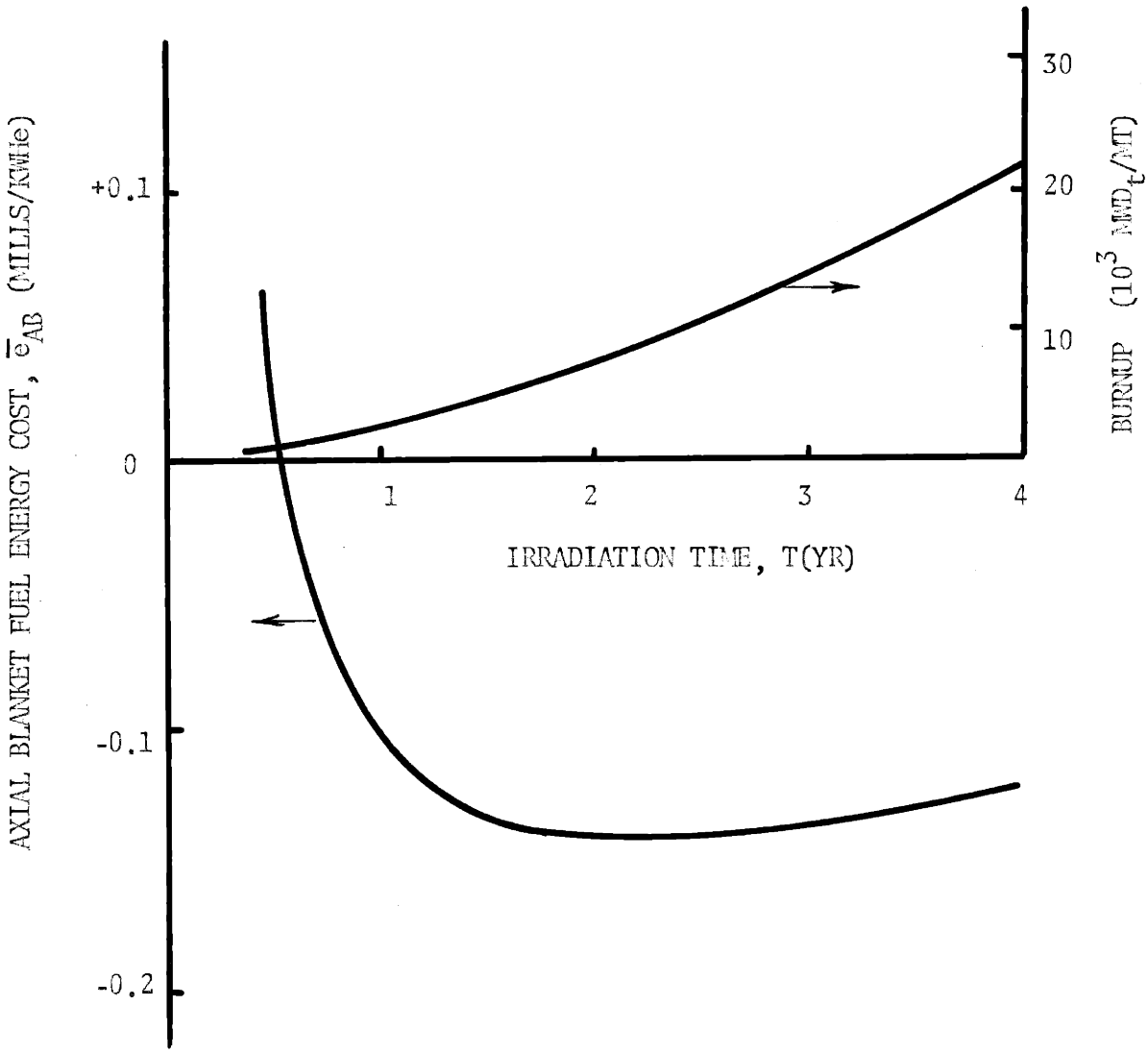

FIG. 4.4 REFERENCE LMFBR AXIAL BLANKET FUEL ENERGY COST AS A FUNCTION OF EXPOSURE

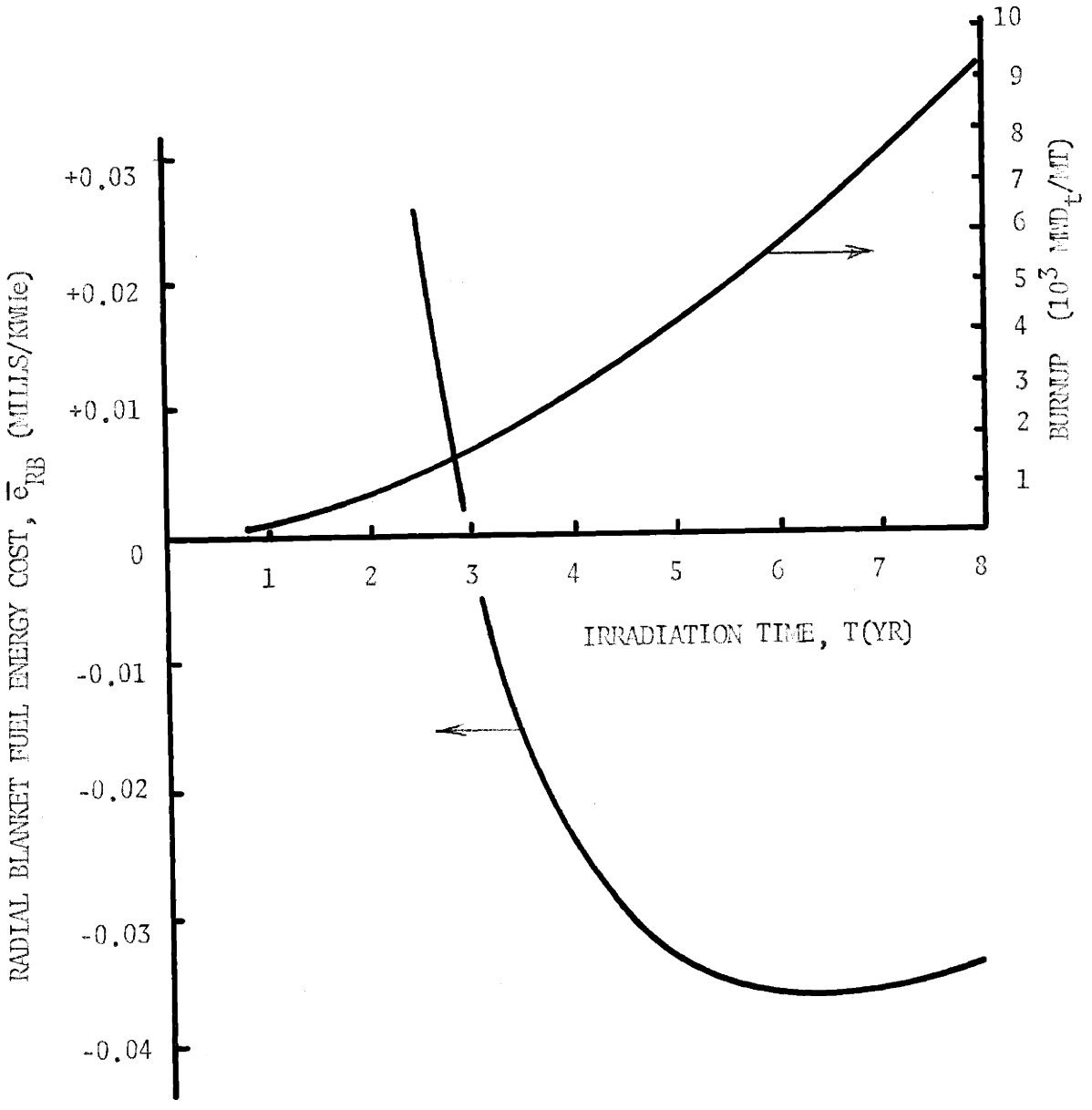

FIG. 4.5 REFERENCE LMFBR RADIAL BLANKET FUEL COST AS A FUNCTION OF EXPOSURE

low average neutron flux (axial leakage predominates) and its somewhat harder spectrum (the radial blanket contains less sodium per unit volume).

Figures 4.6, 4.7 and 4.8 display the reference LMFBR (#1) radial blanket neutronic and fuel economic spatial characteristics. Figure 4.6 shows ϕ, σ_c^{28}, and $\phi\sigma_c^{28}$ as functions of radial position along the mid-plane (Z=0) determined by the 2DB computation, step 3, Section 4.2. Figure 4.7 shows the resulting local fuel economic performance ($/yr/kgHM) versus irradiation time, for the annular regions labeled V, VIII, XI, XIV, and XVII in Figure 4.2. Breakeven and optimum irradiation times increase with distance from the core-blanket interfact because the fissile plutonium buildup is most rapid in the high flux regions near the core. Regions near the core show relatively sharp optima, compared to the regions XIV, XVII deep in the blanket. The optimum irradiation time(6.5years) for the batch-managed radial blanket is indicated by the dotted line. At the optimum, annular region XVII (outermost) incurs a net cost, rather than a net revenue, indicating that the radial blanket,under the economic environment assumed, is too thick.

Figure 4.8 displays the variation of local fuel performance ($/yr/kgHM) with distance from the core, at irradiation times of 2, 4, 6, and 8 years. Net revenue from the entire radial blanket may be identified with the net area under (+) and above (-) the curve. For a two year irradiation, about two-thirds of the 45 cm radial blanket incurs a net cost, i.e. the fissile produced is not enough to offset fabrication, reprocessing, and carrying charges. At 6.5 years, the optimum, the outer one-third (outer row of fuel assemblies) is unprofitable. The slope of the plot ($/yr-kgHM-cm) decreases with irradiation time, as the inner regions pass their optimum irradiation times.

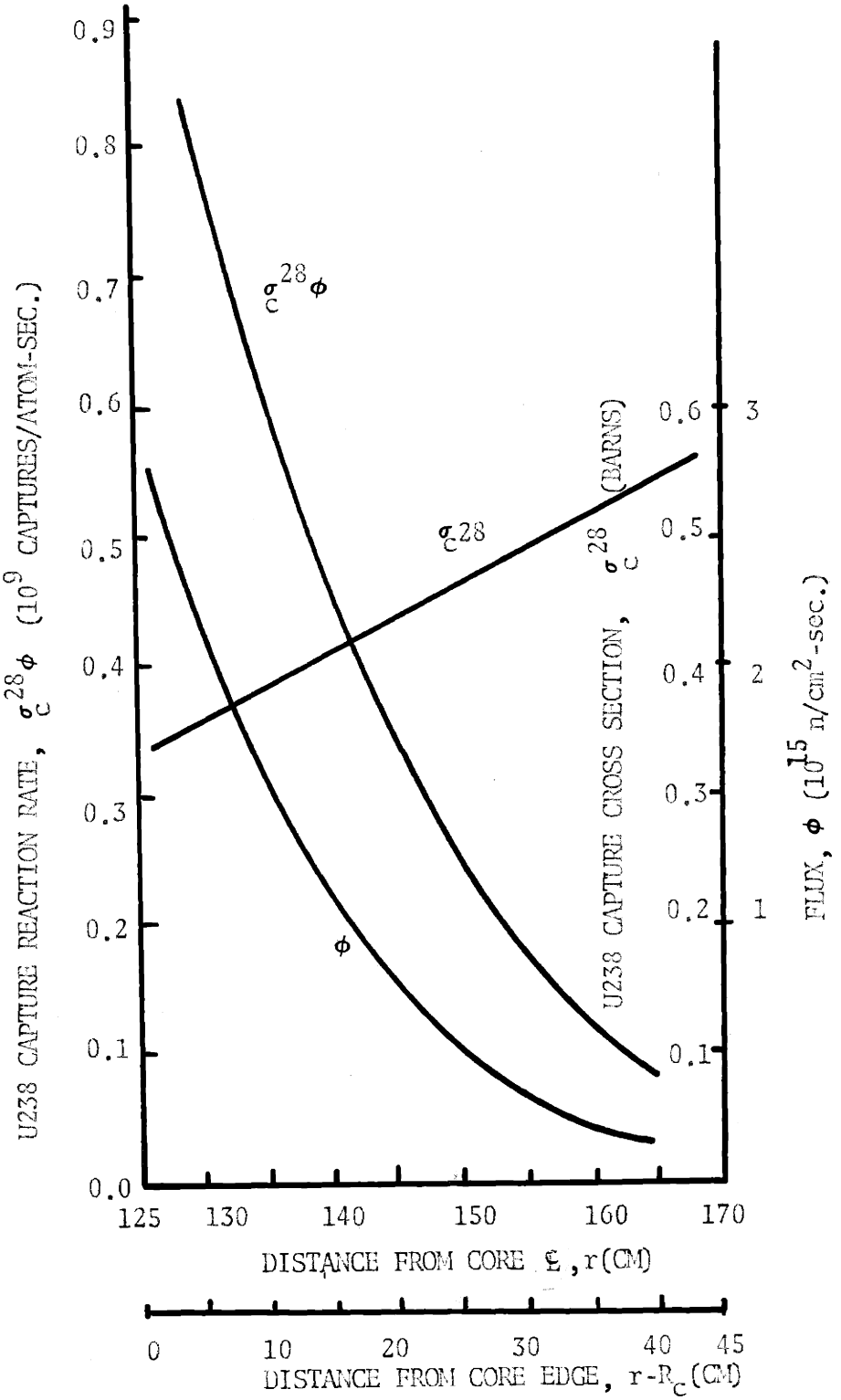

FIG. 4.6 LOCAL NEUTRONICS OF THE REFERENCE LMFBR RADIAL BLANKET

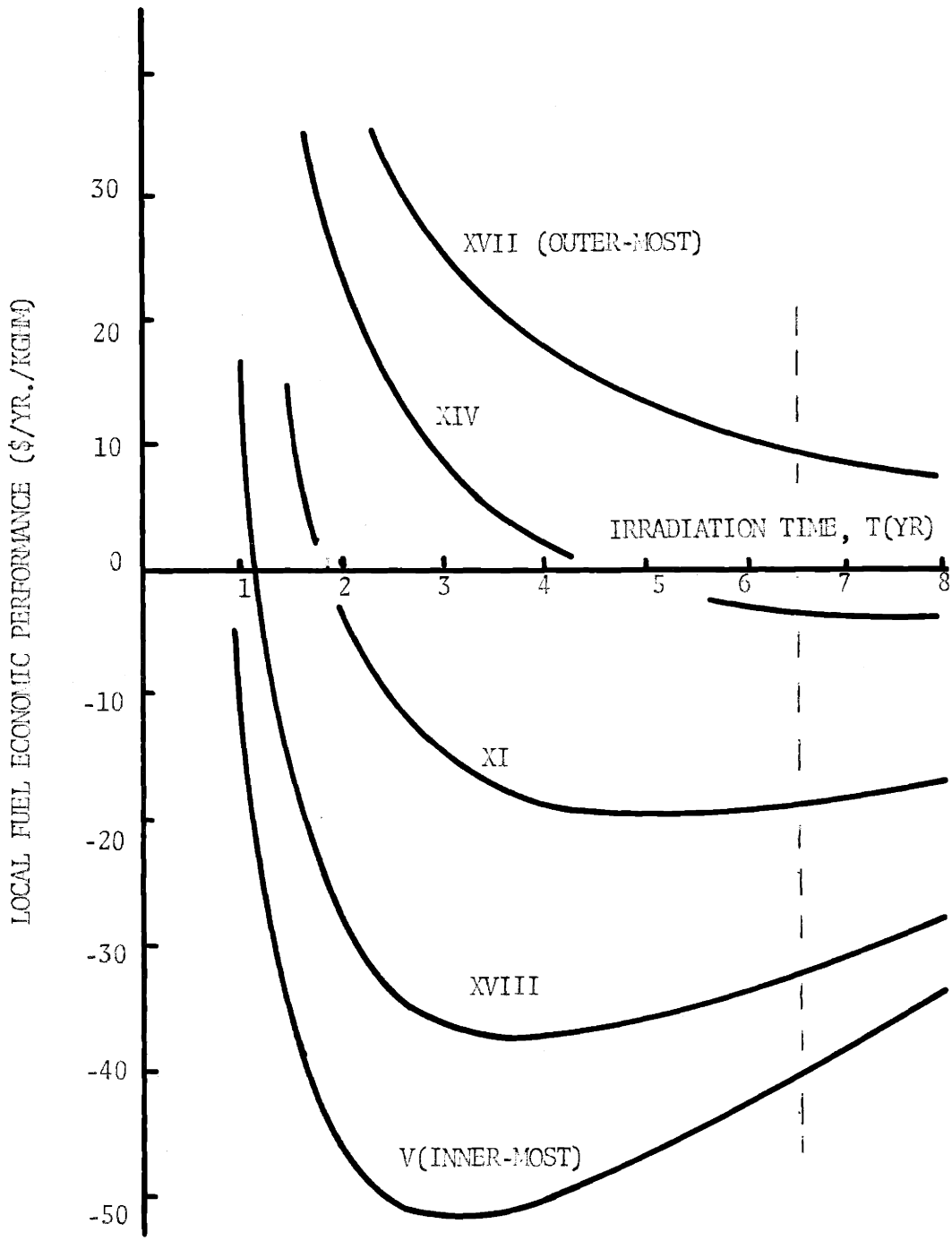

FIG. 4.7 FUEL ECONOMIC PERFORMANCE OF ANNULAR REGIONS IN THE REFERENCE LMFBR RADIAL BLANKET

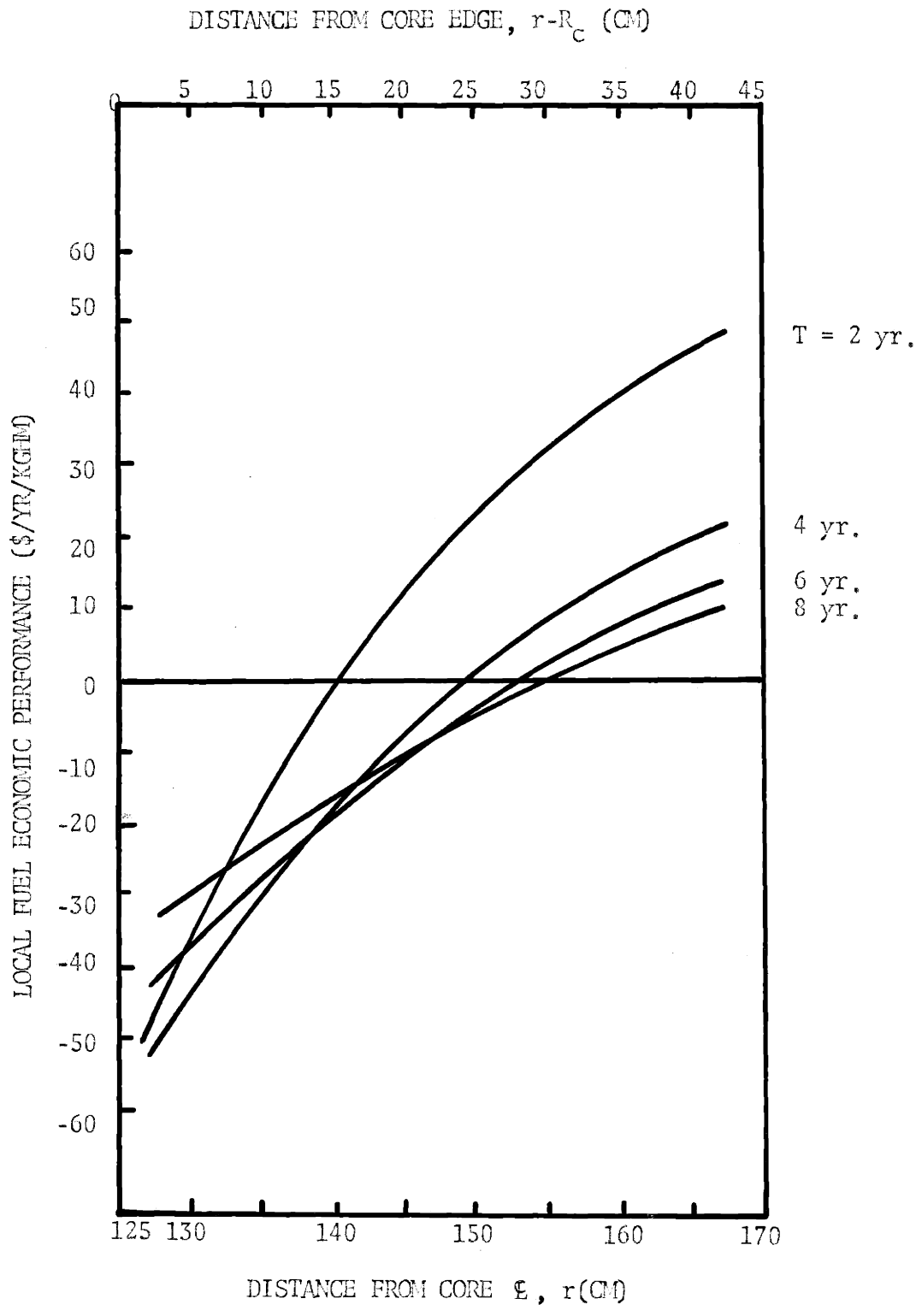

FIG. 4.8 FUEL ECONOMIC PERFORMANCE AS A FUNCTION OF RADIAL POSITION IN THE REFERENCE LMFBR RADIAL BLANKET

One Versus Two Core Enrichment Zones

In addition to its advantages to core economics (53), core enrichment zoning enhances blanket breeding by increasing blanket flux. In order to estimate the effect of core enrichment zoning on blanket depletion economics, a two-zone core reactor (Reactor #1') was compared to the one-zone core reactor (Reactor #1) evaluated above. In this comparison, core fissile inventory loaded, rated reactor power, and core size were fixed.

Since both rated power and core size are held fixed, the effect of power flattening on core fuel depletion economics (either more allowable power, or a smaller core and lower critical mass are possible) are not accounted for. Also unaccounted for is the inventory cost of the additional fissile mass required for k_{eff}-equivalence with the one zone core reactor. These two unaccounted for effects tend to cancel. Since primary interest here is the blanket fuel economics, the adjustments in core conditions are not deemed necessary, although the net improvement in core fuel economics may, because core fuel costs (mills/KWHe) dominate, be more significant than the increased blanket revenue.

The comparison is shown in Table 4.5. When the core is zoned as prescribed, radial blanket revenue increases by about 150%, the axial blanket revenue by about 6%. Taken together, the incremental improvement in blanket revenue is about 0.07 mills/KWHe, a savings of the order of 5 to 10% in total reactor fuel cost.

4.5 SUMMARY

The fuel economics and depletion methods established in Chapters 2 and 3, respectively, are combined in this Chapter to form a simple step-by-step procedure. (Appendix C describes the computer program, SPPIA, developed to perform the fuel economics-depletion computations.)

TABLE 4.5

EFFECT OF CORE ENRICHMENT ZONING ON BLANKET FUEL ECONOMICS

	Reactor #1 (1-zone core)	Reactor #2 (2-zone core)	
Core			
Enrichment Zone #	-	I	II
Zone Enrichment, %	14	11	17
Zone Volume, liters	4906	2540	2366
Average Enrichment, %	14	14	
Radial Blanket			
Fuel Cost, mills/KWHe	-0.036		-0.093
Optimum Irradiation Time, years	6.5		4.5
$\Phi(0,0)/\Phi(125,0)$	6.294		2.831
Axial Blanket			
Fuel Cost, mills/KWHe	-0.141		-0.150
$\Phi(0,0)/\Phi(0,50)$	2.526		2.507
$\Phi(0,0)/\Phi(110,50)$	7.297		3.759

A reference 1000 MWe LMFBR configuration, representative of those used in current design studies, is specified; the depletion-economics model is applied to this reference design. Major characteristics of FBR depletion-economics are noted. The beneficial effect of core enrichment zoning on blanket fuel economics is demonstrated.

CHAPTER 5

1000 MWe LMFBR CASE STUDIES

5.1 INTRODUCTION

In this chapter, the calculational procedure outlined in Section 4.1 is applied to a number of case studies. Objectives of these case studies are:

(1) to determine the effects, on reactor fuel economic performance, of radial blanket thickness and radial reflector material;

(2) to determine the economic advantage of operating each radial blanket region (annular) on its own local optimum irradiation schedule; and

(3) to examine the sensitivity of core, axial blanket, and radial blanket fuel energy costs (mills/KWHe) to the economic environment.

Radial blanket thickness and radial reflector are varied, as shown in Table 5.1. All other design parameters - core and axial blanket geometry and compositions, and radial blanket composition - are held fixed at reference reactor values given in Section 4.3, i.e. Reactor #1. Core and axial blanket fuel power costs (mills/KWHe) are found to be quite insensitive to radial blanket thickness and choice of radial reflector material (Section 5.2), and are thus ignored in evaluating the radial blanket configurations. Results of the radial blanket thickness - radial reflector material case studies are presented in Section 5.3.

The assumption of a one-zone core in these studies penalizes radial blanket economics in all cases considered. Thus, the absolute values of net radial blanket revenue (in mills/KWHe) of individual configurations should not be taken as representative or typical. However, comparative

TABLE 5.1 CASE DEFINITIONS

Reactor Configuration #	Radial Blanket Thickness (cm)	Radial Reflector Material
1 (reference)	45	Na
1A	30	Na
1B	15	Na
2	45	Be metal
2A	30	Be metal
2B	15	Be metal

conclusions and trends demonstrated by these studies are unaffected by the one-zone assumption.

Two radial blanket fuel management schemes are compared in Section 5.4: (a) "whole blanket" management, in which all blanket fuel sees the same irradiation time, the optimum for the blanket as a whole; and (b) "regional"management, in which each annular region is exposed to its own local optimum irradiation time. In either case, fuel sees only one position in the reactor.

The sensitivity of core, axial blanket, and radial blanket fuel power costs to changes in the economic environment is evaluated in Section 5.5. Also, simple linear forms of the cost equations are obtained in Section 5.5.

5.2 EFFECTS OF RADIAL BLANKET THICKNESS AND RADIAL REFLECTOR MATERIAL ON CORE AND AXIAL BLANKET FUEL DEPLETION ECONOMICS

Assessment of the economic (energy costs) effects of radial configuration design changes may be simplified considerably by ignoring their influence on core and axial blanket fuel depletion economics, that is by considering only the radial blanket depletion economics. For the reference geometry selected (H/D = 0.4), one would expect such changes in core and axial blanket fuel economic performance to be small because of the relatively small radial leakage from the core. That these changes are smaller, by orders of magnitude, than the simultaneous changes in radial blanket fuel depletion economics, is demonstrated in this section.

Changes in radial blanket thickness and/or radial reflector material can affect core and axial blanket fuel economics in two ways: (1) by affecting the core fissile inventory required for criticality, and thereby affecting core inventory cost; and (2) by perturbing the flux magnitude and spectra in the core and axial blanket, causing changes in

depletion and material credit results.

(1) Core inventory cost is closely proportional to $yT\epsilon$, where y is the carrying charge rate (per annum), T is the time the fissile material is in the possession of the utility company, and ϵ is the critical enrichment. Thus the fractional change in core inventory cost, Inv.(mills/KWHe), caused by a change in critical enrichment is given by

$$\frac{\Delta \text{Inv.}}{\text{Inv.}} = \frac{\Delta \epsilon}{\epsilon}$$

or

$$\frac{\Delta \text{Inv.}}{\text{Inv.}} \simeq 5 \frac{\Delta K}{K}$$

where the expression[1]

$$\frac{\Delta K}{K} \simeq 0.2 \frac{\Delta \epsilon}{\epsilon}$$

has been used.

To illustrate the insensitivity of core inventory cost to radial configuration changes, Cases 1 (45 cm radial blanket with Na radial reflector) and 2B (15 cm radial blanket with Be radial reflector) are compared. From a reactivity point of view, these are the two most disparate cases. The multigroup physics computations for the two cases showed that for the same core fissile content, their values of K_{eff} differ by less than 0.0002. Thus

$$\frac{\Delta \text{Inv.}}{\text{Inv.}} = 5 \times \frac{0.0002}{1.0} = 0.001.$$

The core inventory cost (Inv.) for Case 1 is 0.4147 mills/KWHe. Thus

---

1. From the 26G-TSD calculation for Reactor #1 (no fission products).

$$\Delta \text{Inv.} = \text{Inv.} \times \frac{\Delta \text{Inv.}}{\text{Inv.}} \simeq 0.4147 \times 0.001$$

$$\simeq 0.00042 \text{ mills/KWHe}$$

The difference in optimum radial blanket fuel costs between the two cases is 0.05 mills/KWHe[1], which dwarfs the difference in core inventory costs. Of the six Na and Be reflected cases considered (Table 5.1), the minimum difference between radial blanket fuel costs is found to be 0.004 mills/KWHe (Cases 1 and 2)[1], which is an order of magnitude greater than the maximum difference in core inventory costs.

(2) To illustrate the insensitivity of core and axial blanket fuel costs to the changes in flux shape and spectra occasioned by a radial configuration change, Table 5.2 shows the fuel costs of core, axial blanket and radial blanket for Cases 1 and 2B. The core results do not include the core inventory correction (0.0004 mills/KWHe) estimated above.

To summarize, core and axial blanket fuel depletion-economics is quite insensitive to choice of radial reflector material and radial blanket thickness:

(1) $\Delta \bar{e}_{RB} \gg \Delta \text{Inv.}_{core}$

(2) $\Delta \bar{e}_{RB} \gg \Delta \bar{e}_{core}$, $\Delta \bar{e}_{AB}$

For this reason, only the radial blanket fuel economic performance was considered in ranking the reactor configurations of Table 5.1.

5.3 RADIAL BLANKET THICKNESS AND RADIAL REFLECTOR MATERIAL

Reducing the radial blanket thickness has several effects on the radial blanket fuel economic performance:

---

1. Section 5.3.

TABLE 5.2

EFFECTS OF RADIAL CONFIGURATION CHANGES

ON CORE AND AXIAL BLANKET FUEL COSTS

Reactor Configuration #	Radial Blanket Thickness (cm)	Radial Reflector Material	$\bar{e}_{RB}$	$\bar{e}_{core}$	$\bar{e}_{AB}$
1	45	Na	-0.03635	0.96975	-0.14130
2B	15	Be	-0.08687	0.96981	-0.14176
		(2B-1) =	-0.05052	0.00006*	-0.00046

* Does not include core inventory correction.

(a) fabrication and reprocessing costs for the region eliminated are saved;

(b) the plutonium which would have been bred in the region eliminated is forfeited;

(c) the breeding performance ($\overline{\sigma_c^{28} \phi}$) of the remaining radial blanket is improved, by bringing the high-albedo and moderating reflector nearer to the high flux regions of the blanket; and

(d) coolant pumping power requirements for the radial blanket are reduced. These effects suggest that an economic optimum thickness may exist.

Radial reflector composition influences radial blanket fuel economic performance through

(e) improved albedo, i.e. a beneficial effect on neutron economy through flux enhancement in the blanket, as well as overall flux flattening; and

(f) improved moderating ratio, softening radial blanket spectra and enhancing capture by U238.

Other economic considerations associated with choice of reflector material and reflector design are:

(g) radial reflector coolant pumping requirements;

(h) radial reflector material purchase and fabrication costs and exposure limits; and

(i) shielding performance of the radial reflector.

The economic consequences of changes in (d) radial blanket coolant pumping requirements, (g) radial reflector coolant pumping requirements, (h) radial reflector material and fabrication costs, and exposure limits, and (i) radial reflector shielding performance, are currently being investigated by others at MIT (13). The studies reported here embrace only

the depletion-economics considerations listed above, (a), (b), (c), (e), and (f). Further, the depletion-economics comparisons are biased toward the exotic moderating reflector: a solid reflector (100 V/o Be metal) is assumed. A real reflector would probably consist of clad BeO, with as much as 20 V/o required for coolant. Also, the costs of the Be reflector are not included in the tradeoff study.

Figure 5.1 shows the radial blanket fuel costs (mills/KWHe) as functions of irradiation time for the cases 1, 2, 1A, 2A, 1B, and 2B defined in Table 5.1. The reference economic environment, Tables 4.2 and 5.4, was assumed. Table 5.3 summarizes the optimum irradiation times, fuel costs, fissile plutonium breeding rates, and discharge fissile plutonium inventories in both reference and more favorable economic environments defined in Table 5.4. Figure 5.2 summarizes the radial blanket fuel costs (at optimum irradiation time) for the six combinations of radial blanket thickness and radial reflector material, under the two economic environments.

Several features are noted in the results presented in Figure 5.1 and Table 5.3.

(1) The importance of reflector material choice, with respect to blanket fuel economics, decreases with increased blanket thickness. Choice of beryllium results in an improvement in blanket revenue of about 60% over sodium, for a 15 cm radial blanket. For a 45 cm blanket, the improvement is only about 8%.

(2) For either sodium or beryllium reflectors, reducing the blanket thickness always reduces the plutonium bred by the blanket, i.e. effect (c) mentioned above is not sufficient to offset effect (b).

(3) Optimum irradiation time decreases with decreased radial blanket thickness.

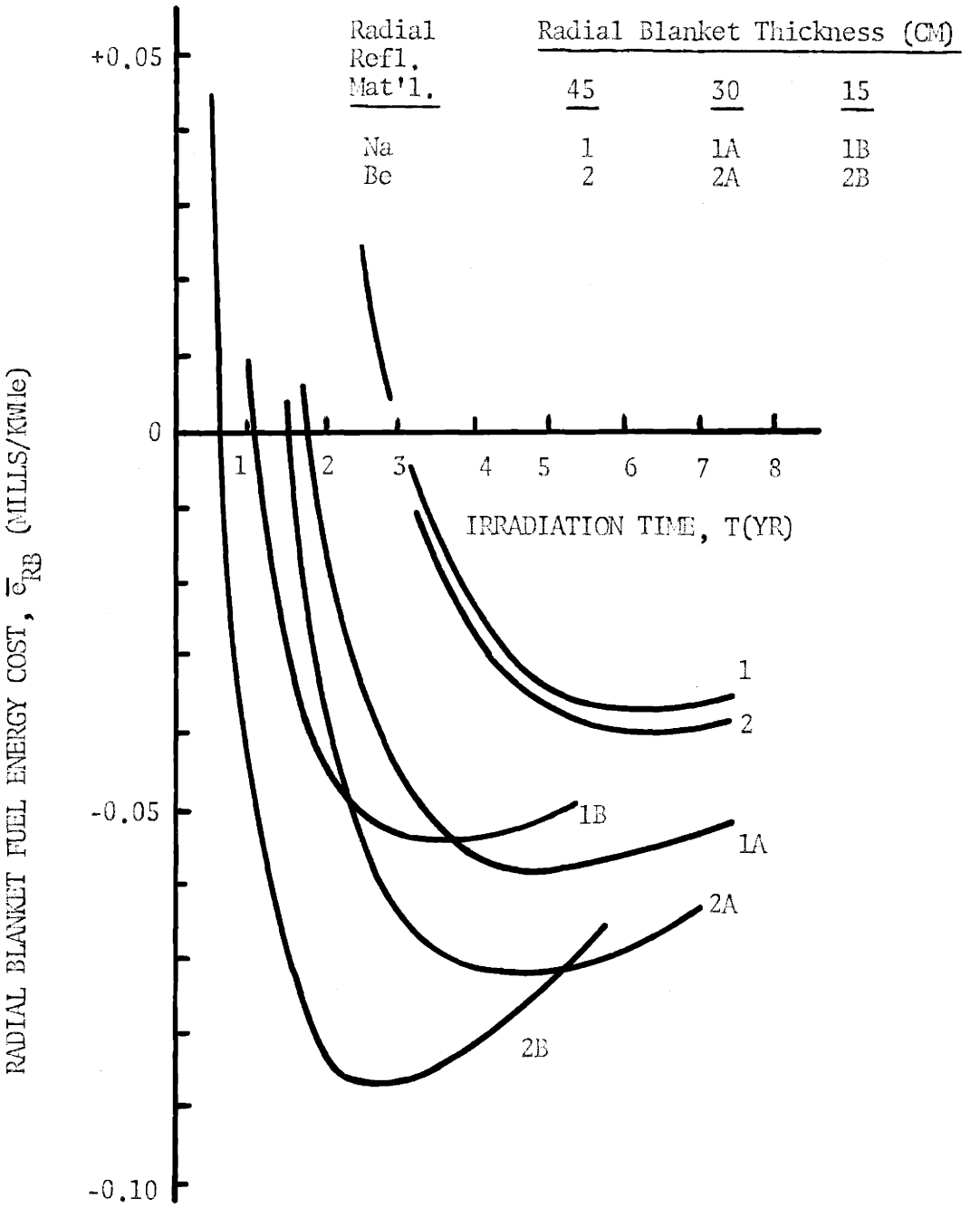

FIG. 5.1 EFFECT OF RADIAL BLANKET THICKNESS AND RADIAL REFLECTOR MATERIAL ON RADIAL BLANKET FUEL ECONOMICS

TABLE 5.3

EFFECT OF RADIAL BLANKET THICKNESS AND RADIAL REFLECTOR MATERIAL ON RADIAL BLANKET FUEL ECONOMICS

Config-uration #	Radial Blanket Thickness (cm)	Radial Reflector Material	M_{49}/T @ T=2yr (kg/yr)	Reference Economic Environment: Topt (yr)	Reference Economic Environment: $\bar{e}_{RB}$ @ Topt (mills/KWHe)	Reference Economic Environment: M_{49} @ Topt (kg)	More Favorable Economic Environment: Topt (yr)	More Favorable Economic Environment: $\bar{e}_{RB}$ @ Topt (mills/KWHe)	More Favorable Economic Environment: M_{49} @ Topt (kg)
1	45	Na	158	6-1/2	-0.037	825	3-1/2	-0.237	512
2	45	Be-metal	160	6-1/2	-0.040	845	3-1/2	-0.243	521
1A	30	Na	141	4-3/4	-0.058	596	2-1/2	-0.242	342
2A	30	Be-metal	157	4-1/2	-0.072	610	2-1/2	-0.279	380
1B	15	Na	97	3-1/2	-0.055	304	2	-0.188	194
2B	15	Be-metal	130	2-3/4	-0.087	308	1-1/2	-0.276	205

TABLE 5.4

REFERENCE AND MORE FAVORABLE

ECONOMIC ENVIRONMENTS

	Reference	More Favorable
Radial Blanket Fabrication Cost, $/kgHM	69	40
Radial Blanket Reprocessing Cost, $/kgHM	31.50	31.50
Fissile Market Value, $/kg	10,000	20,000
Discount Rate, %	8	8

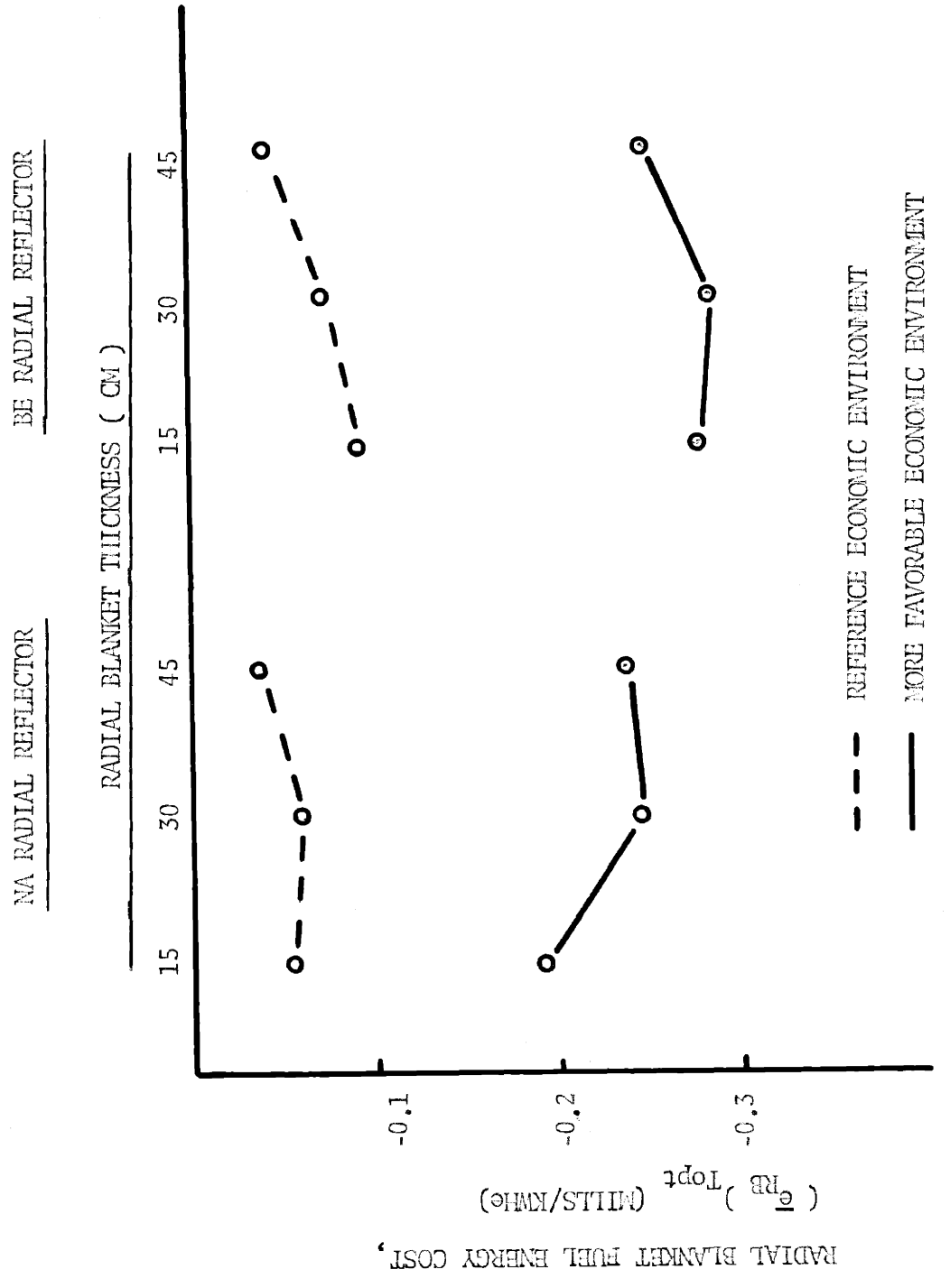

FIG. 5.2 EFFECT OF ECONOMIC ENVIRONMENT ON OPTIMUM RADIAL BLANKET THICKNESS

(4) The effect of the choice of radial reflector material on the optimum irradiation time is more pronounced the thinner the blanket.

(5) Optimum irradiation time decreases as the economic environment improves.

(6) In the reference economic environment, the sodium reflected radial blanket displays a weak optimum thickness between 15 and 30 cm. For the beryllium reflected radial blanket, the optimum, if it exists, is between 0 and 15 cm, that is, the 15 cm beryllium reflected blanket is superior to the 30 and 45 cm blankets, owing to effect (c) above.

The increment of 15 cm is a representative thickness for a row of fuel subassemblies. LMFBR operators may have the option of adding or subtracting radial blanket rows in accordance with current economic conditions - fissile market value, fabrication and reprocessing costs, etc. Thicker radial blankets are indicated when (i) fabrication and reprocessing costs decreases, and/or (ii) fissile market value increases, as seen in Figure 5.2.

Figures 5.3 and 5.4 show the local neutronics obtained from the multigroup "snapshot" physics computations (2DB). In Figure 5.3 the beginning of fuel life capture reaction rate per U238 atom, $\sigma_c^{28}\phi$, is plotted along the radial blanket midplane (z=0). Breeding performance, for a particular case, may be associated qualitatively with the area under that case's $\sigma_c^{28}\phi$ vs. r curve. The improvement of the breeding performance of inner regions by reducing the blanket thickness, effect (c) above, is noted. This effect is quite weak for the sodium reflected blanket, e.g. $\sigma_c^{28}\phi$ in the inner 15 cm of radial blanket is insensitive to the location of the radial reflector. However, the improvement is quite pronounced for the Be reflected blanket, and the advantage of the Be reflector (over the Na reflector) is seen to increase as blanket thickness decreases.

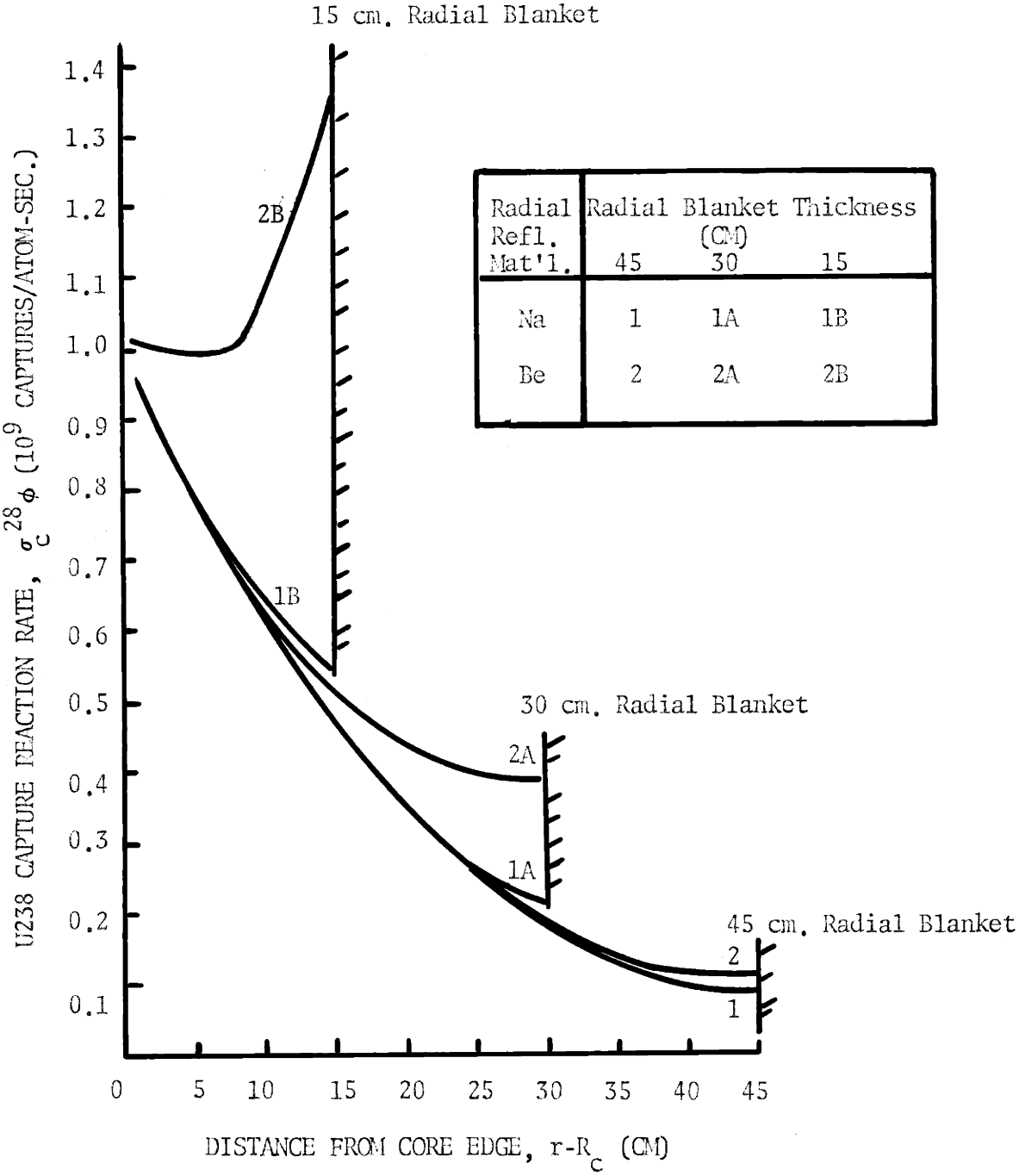

FIG. 5.3 LOCAL U238 CAPTURE REACTION RATES ($\sigma_c^{28}\phi$) FOR VARIOUS RADIAL BLANKET THICKNESSES AND RADIAL REFLECTOR MATERIALS

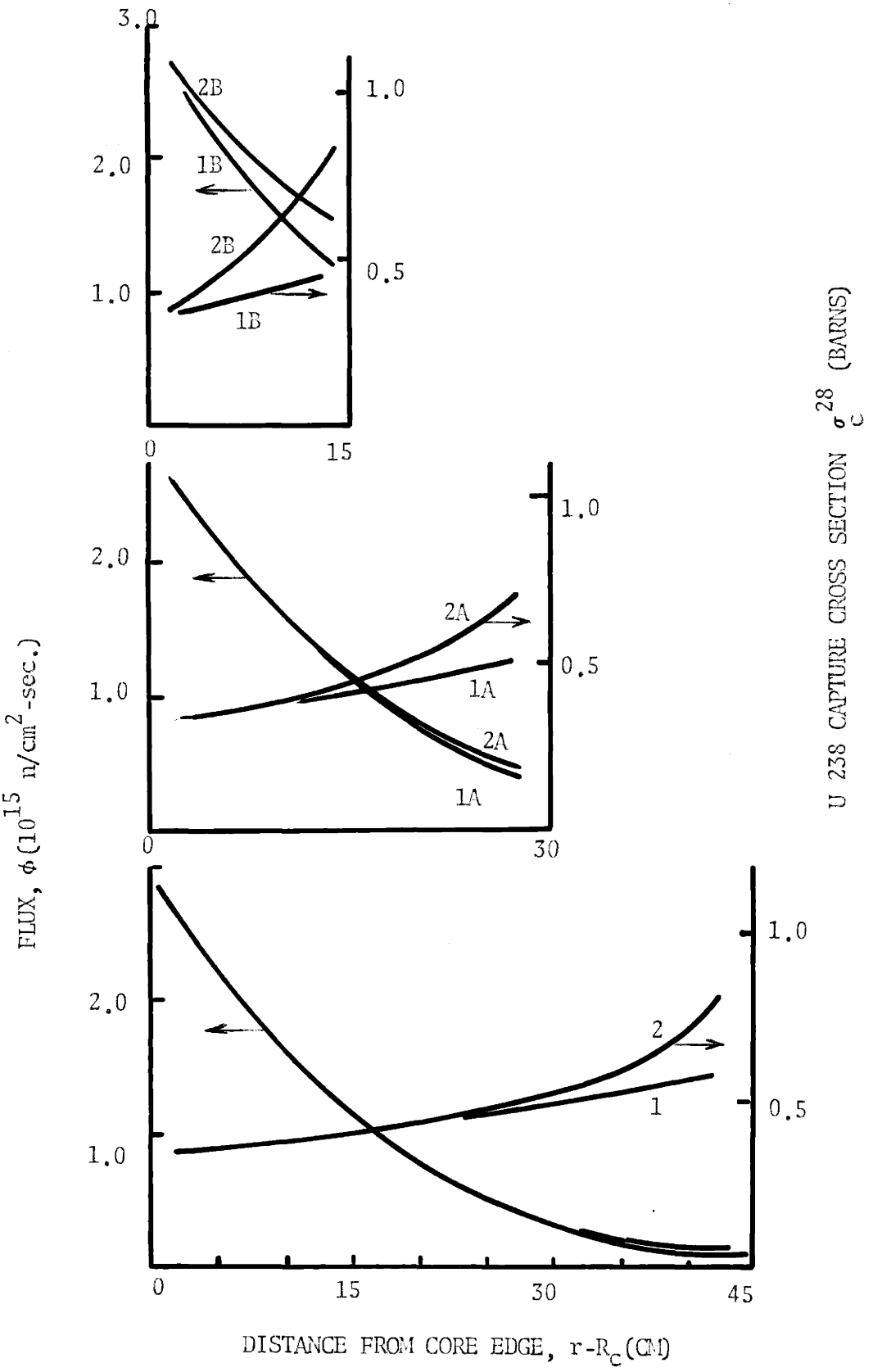

FIG. 5.4 LOCAL NEUTRONICS IN THE RADIAL BLANKET

Figure 5.4 shows the resolution of the U238 capture rate into its components, σ_c^{28} and ϕ. Both reflective (blanket ϕ) and moderating (blanket σ_c^{28}) properties of Be are superior to those of Na.

5.4 RADIAL BLANKET FUEL MANAGEMENT SCHEMES

Case studies discussed elsewhere in this report assume that all radial blanket fuel sees the same irradiation time, the optimum for the blanket as a whole. From Figure 4.7, the optimum irradiation times of the annular regions range from about three years for the innermost region to about ten years for the outermost. At the "whole blanket" irradiation time of 6.5 years, the inner regions are past their optimum, while outer regions are under-exposed.

Clearly, an improvement in radial blanket performance would result if each annular region were irradiated to its own local optimum exposure. This scheme is labeled "regional" management in this report. Table 5.5 compares the radial blanket fuel energy costs (mills/KWHe) under whole blanket and regional management schemes. The regional scheme improves blanket profit by about 30%. Other advantages of the regional scheme, not implicit in Table 5.5, are power flattening and reduction of power buildup in the inner regions over an irradiation cycle.

Other fuel management schemes proposed for FBR radial blankets are:

- out-in (4)
- in-out (10, 73), and
- fuel assembly rotation (10)

The out-in scheme has been evaluated by Hasnain and Okrent (4) for a somewhat smaller reactor (800 liter core) than the reference reactor

TABLE 5.5

WHOLE BLANKET VS. REGIONAL

FUEL MANAGEMENT SCHEMES

Reactor Configuration	Radial Blanket Fuel Energy Costs (mills/KWHe)	
	Whole Blanket Management	Regional Management
#1 (reference): 45 cm radial blanket; Na radial reflector	-0.0364	-0.0494
#2: 45 cm radial blanket; Be radial reflector	-0.0394	-0.0519

assumed in the present study. In this scheme, fresh fuel is loaded in the outermost blanket region, then moved inward in the following consecutive cycles, and discharged, finally, from the innermost region. The fuel economic advantage of out-in management, relative to batch and scatter schemes, is that uniformity of discharge composition may be achieved. However, Hasnain and Okrent found little fuel economic advantage in this scheme. A major engineering advantage is that local power density change with time is lessened, thereby reducing orificing control requirements. The out-in scheme would not, however, be expected to assist in power flattening.

Although it was not demonstrated quantitatively in their study, Hasnain and Okrent (4) argued that in-out management would be uneconomic, due to the holdup of bred plutonium. Froelich (10) has shown that in-out management has a strong power flattening effect, as well as reducing the power swing of radial blanket fuel over an irradiation cycle.

Froelich (10) has also shown that rotation of fuel assemblies implements power flattening and decreases power swing.

Advantages and disadvantages of various radial blanket fuel management options are summarized in Table 5.6.

5.5 SENSITIVITY OF FUEL ENERGY COSTS TO THE ECONOMIC ENVIRONMENT

5.5.1 Introduction

The purpose of this section is to examine the sensitivity of the reference LMFBR (Reactor #1) fuel energy costs (mills/KWHe) to changes in economic environment.

Unit costs ($/kgHM, $/kg fissile), credits ($/kg fissile), and carrying charges throughout the nuclear fuel cycle are ultimately transferred to the utility company, burdened to the production of electricity, and, together

TABLE 5.6 RADIAL BLANKET FUEL MANAGEMENT SCHEMES

Fuel Management Scheme	References	Advantages	Disadvantages
1. Fixed-Fuel Schemes			
A. Batch and Scatter			
(1) Whole Blanket Management	(this report)	.simplicity	.non-uniform burnup .power tilt across blanket
(2) Regional Management	(69,70,71, 72,73), (this report)	.power flattening .more uniform burnup than whole blanket management; local optima achieved	. complexity
B. Batch	(this report)	.simplicity	.more severe power swing than scatter management
C. Scatter	(69,70,71, 72,73), (this report)	. reduces power swing	
2. Moving-Fuel Schemes			
A. Out-in	(4)	.uniform burnup .reduction in power swing	.aggravates power tilt across blanket
B. In-out	(10,73)	.uniform burnup .reduction in power swing .power flattening	

with utility company carrying charges, borne by the electricity consumer via a levelized price (cost) of electricity in mills/KWHe. These unit costs, credits, and carrying charges are determined largely by factors outside the scope of this report, e.g. supply-demand effects in the market place, technical-economic characteristics of fuel cycle processes, fuel processing capacities and throughputs, availability and structure of capital, fuel element design, etc. Thus, in this report, the following variables are regarded as comprising the "economic environment" and are treated in parametric fashion, as input to the depletion-economics calculations:

unit costs for fabrication and reprocessing, C_{fab} and C_{repr}, in dollars per kilogram of heavy metal (U + Pu);

nuclide market values, C_{28}, C_{49}, ... ,C_{42} in dollars per kilogram of the respective nuclide;

utility company financial paramters i.e. tax rate (τ), capital structure (f_b, f_s) and rates of return (r_b, r_s) from which the discount rate (x) may be determined, $x = (1-\tau)r_b f_b + r_s f_s$.

In the sensitivity studies reported below, the economic parameters were varied over the ranges shown in Table 5.7. Reference values are shown in parentheses. Reference values of C_{fab} and C_{repr} are typical of those projected for oxide-fueled LMFBR's by the USAEC Fuel Recycle Task Force (18), and of those assumed in the several 1000 MWe LMFBR design studies. Reference values of the utility company financial parameters, leading to a reference discount rate of 8%, are typical of those of the Commonwealth Edison Company in the late 1960's (82).

The fuel energy costs (mills/KWHe) associated with the major regions (core, axial blanket, radial blanket) were computed by the procedure

TABLE 5.7

RANGES OF ECONOMIC ENVIRONMENT PARAMETERS *

Unit Processing Costs [$/kgHM]	
Fabrication (C_{fab})	
Core	150-(314)-330
Axial Blanket	20-(80)-314
Radial Blanket	20-(69)-100
Reprocessing (C_{repr})	
Core	15-(31)-60
Axial Blanket	15-(31)-60
Radial Blanket	15-(31)-60
Nuclide Market Values [$/kg]	
Fertile (C_{28}, C_{40})	0
Fissile (C_{49}, C_{41})	5000-(10,000)-25,000
Utility Company Financial Parameters	
Income Tax Rate (τ)	(0.5)
Discount Rate (x)	0.06-(0.08)-0.10

* Reference values are given in parentheses ( ).

outlined in Section 4.1. Each economic parameter was varied individually, holding all other parameters fixed at their reference values.

5.5.2 Core and Axial Blanket

Figures 5.5 through 5.12 display the behavior of reference reactor core and axial blanket fuel energy costs as the economic environment is varied around the reference environment.

Since the core and axial blanket irradiation times are fixed by the core burnup limit, core and axial blanket fuel energy cost equations can be reduced to convenient linear forms. From Equation (4-6), the fuel energy cost associated with region s (core, axial blanket,or radial blanket) is given by

$$\begin{aligned}\bar{e}_s &= \bar{e}_{fab,s} + \bar{e}_{repr,s} + \bar{e}_{matl,s} \\ &= \frac{1000\, M^0_{HM}}{ET} \left[C_{fab,s} F_{fab}(T) + C_{repr,s} F_{repr}(T) \right. \\ &\qquad \left. + C_{fiss} \left(\epsilon^0_s F_{mp}(T) - \epsilon_s(T) F_{mc}(T) \right) \right] \end{aligned} \tag{5-1}$$

With irradiation time (T) fixed, Equation (5-1) reduces to a linear expression in the unit costs $C_{fab,s}$, $C_{repr,s}$, C_{fiss}:

$$\bar{e}_s = a_{fab,s} C_{fab,s} + a_{repr,s} C_{repr,s} + a_{matl,s} C_{fiss} \tag{5-2}$$

where the constants $\{a_{q,s}\}$ are given by

$$a_{q,s} = \left(\frac{\bar{e}_{q,s}}{C_{q,s}} \right)_x = \left(\frac{\bar{e}_{q,s}}{C_{q,s}} \right)_0 = \frac{1000}{ET} M^0_{HM}\, g(T) \ .$$

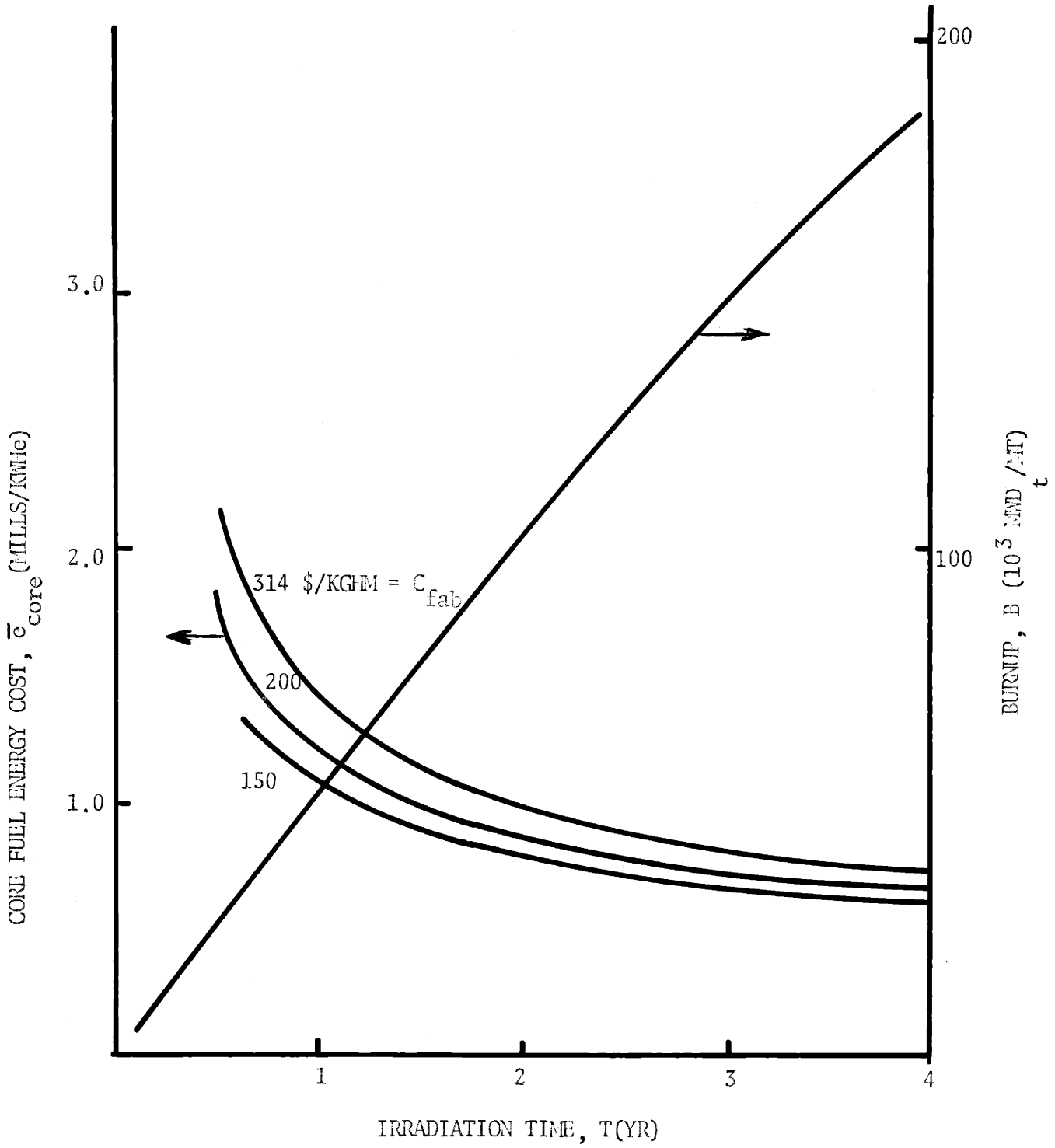

FIG. 5.5 EFFECT OF UNIT FABRICATION COST ON CORE FUEL ENERGY COST

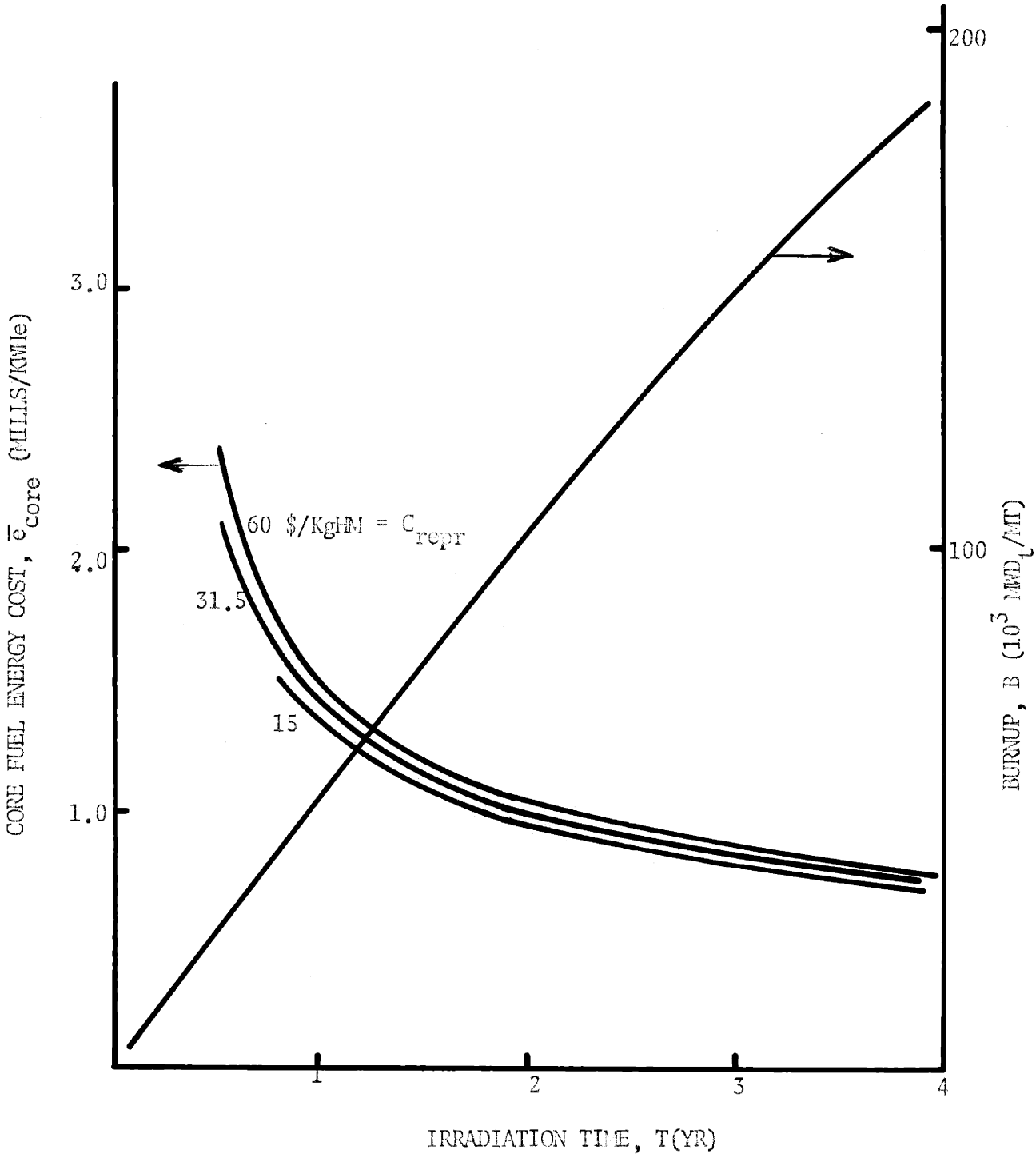

FIG. 5.6 EFFECT OF UNIT REPROCESSING COST ON CORE FUEL ENERGY COST

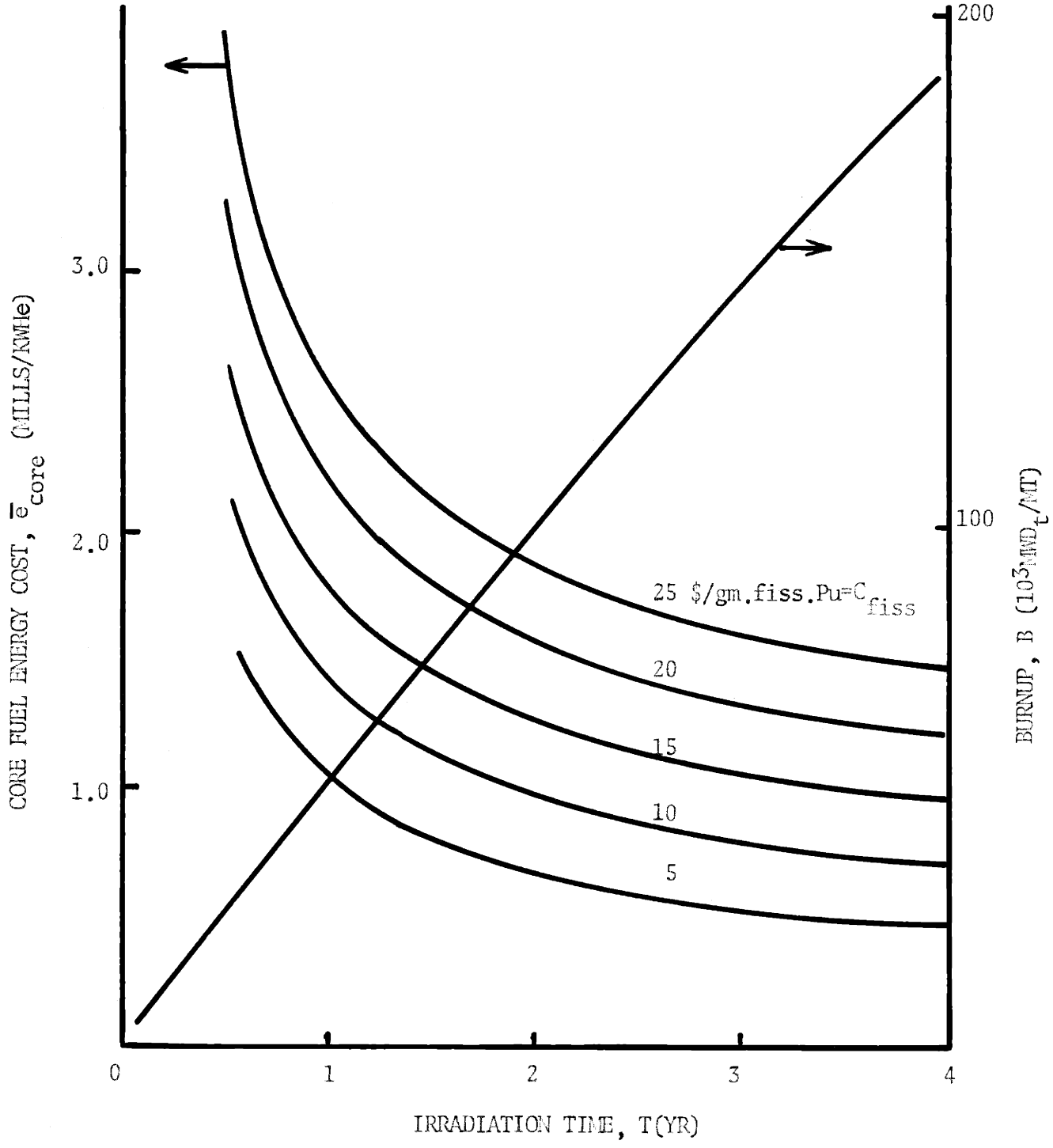

FIG. 5.7 EFFECT OF FISSILE PLUTONIUM PRICE ON CORE FUEL ENERGY COST

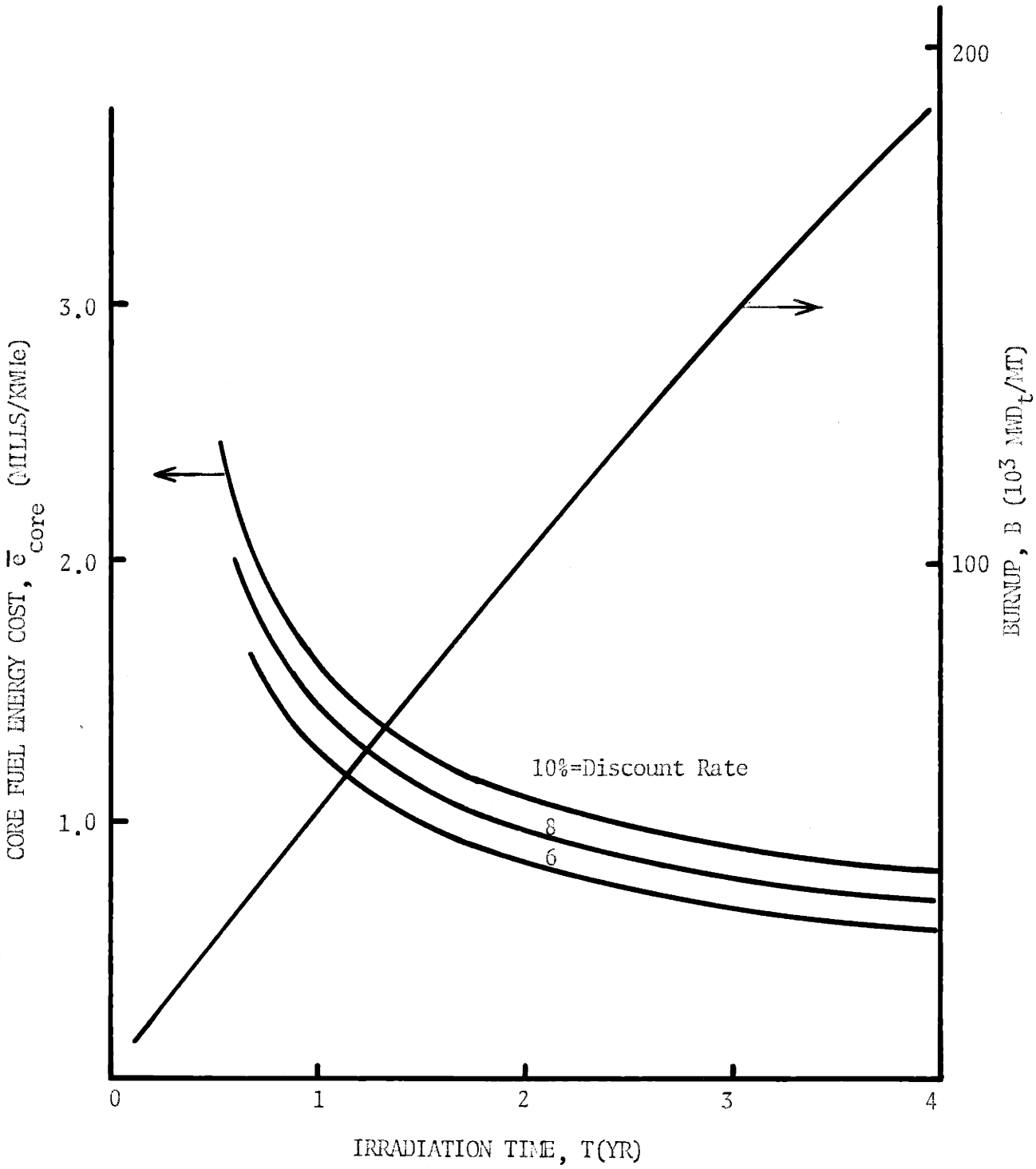

FIG. 5.8 EFFECT OF DISCOUNT RATE ON CORE FUEL ENERGY COST

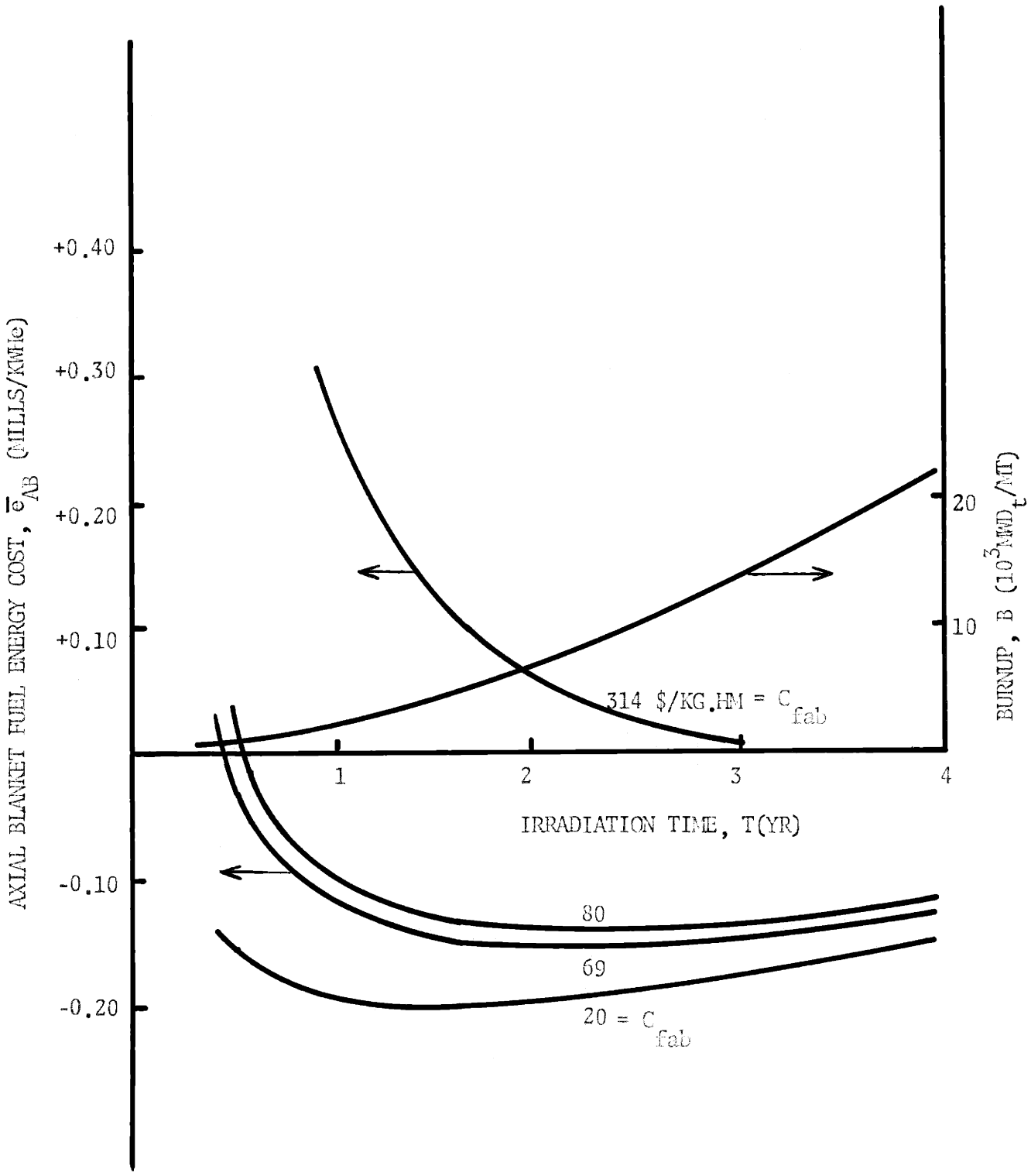

FIG. 5.9 EFFECT OF UNIT FABRICATION COST ON AXIAL BLANKET FUEL ENERGY COST

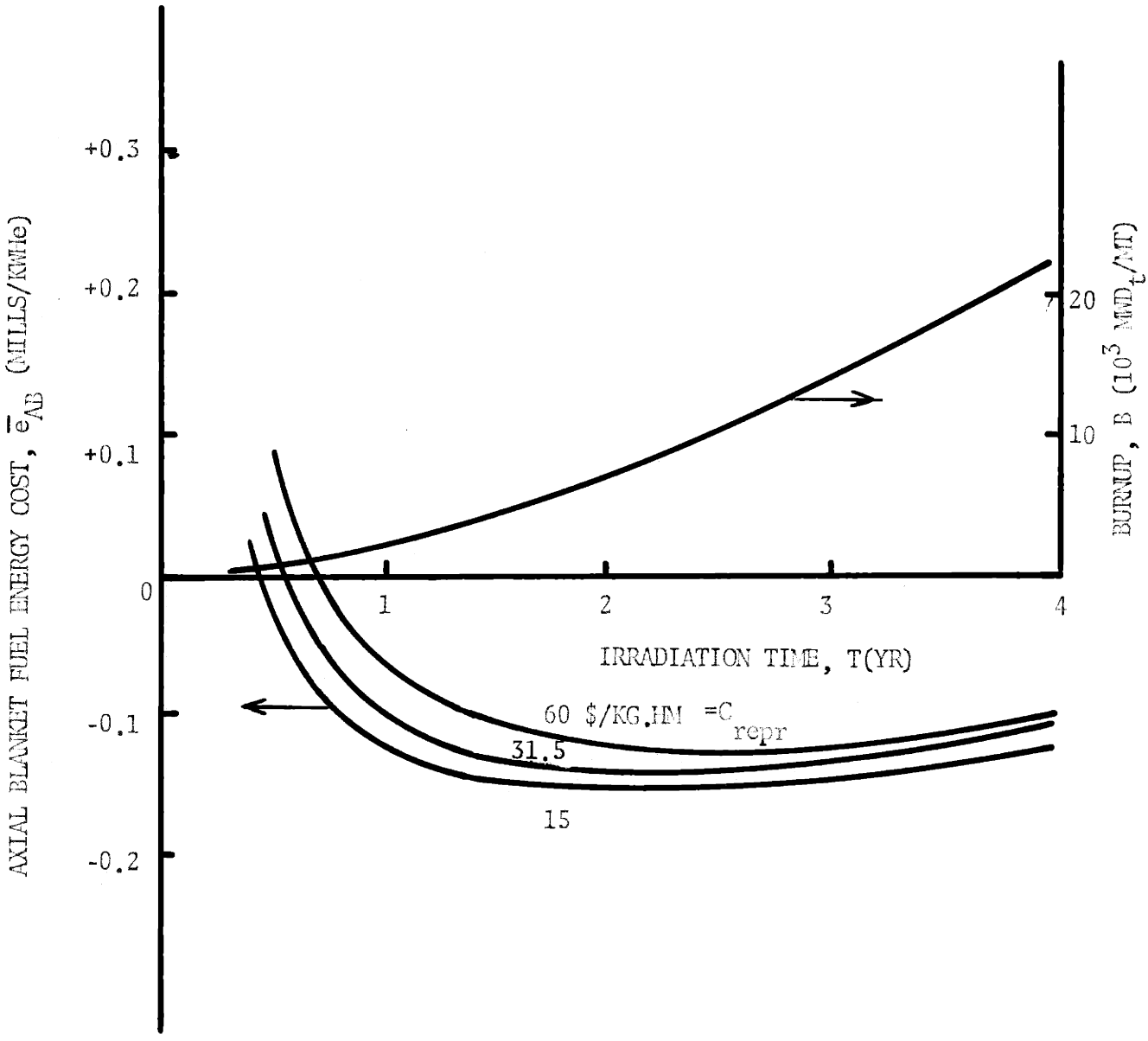

FIG. 5.10 EFFECT OF UNIT REPROCESSING COST ON AXIAL BLANKET FUEL ENERGY COST

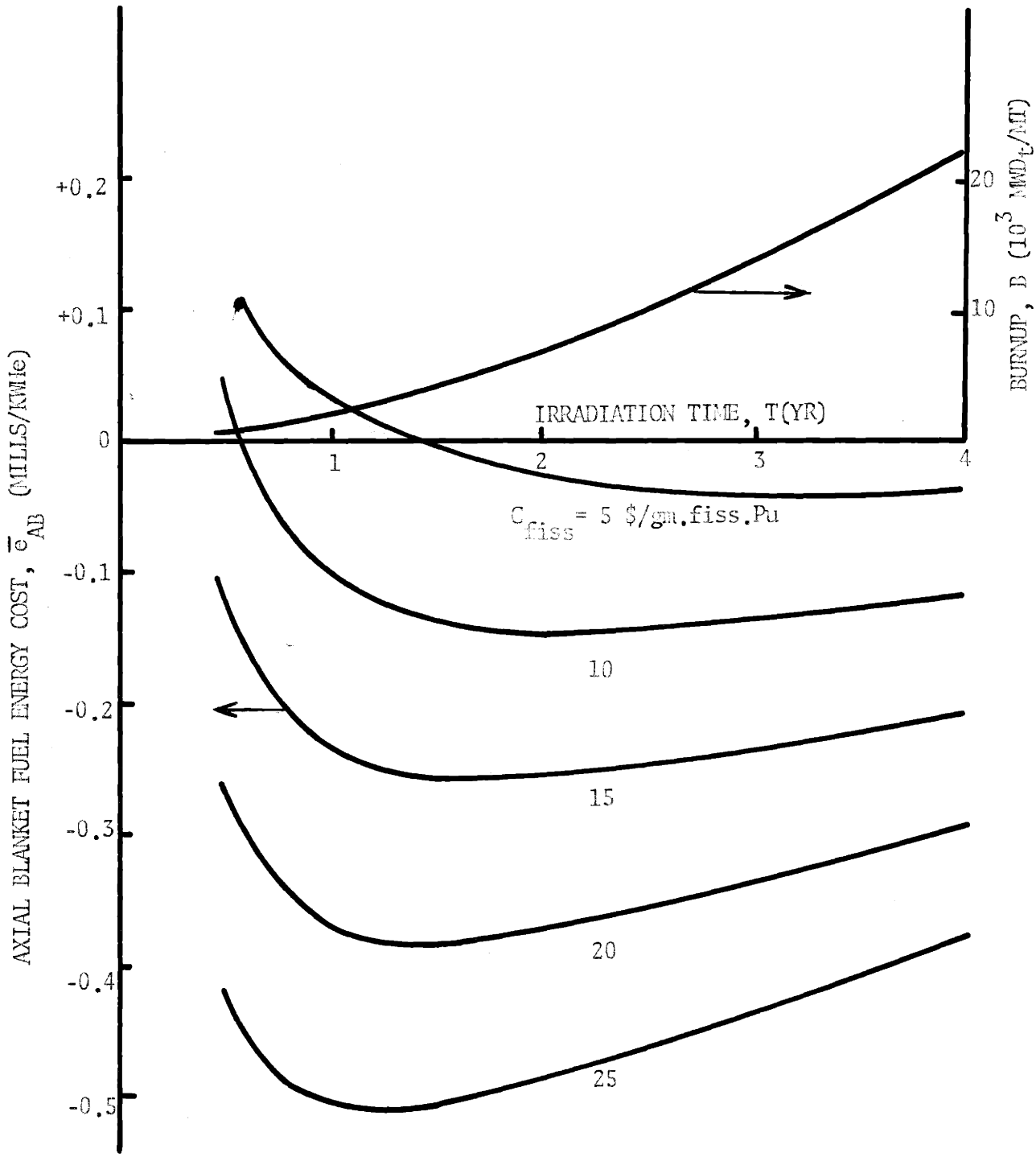

FIG. 5.11 EFFECT OF FISSILE PLUTONIUM PRICE ON AXIAL BLANKET FUEL ENERGY COST

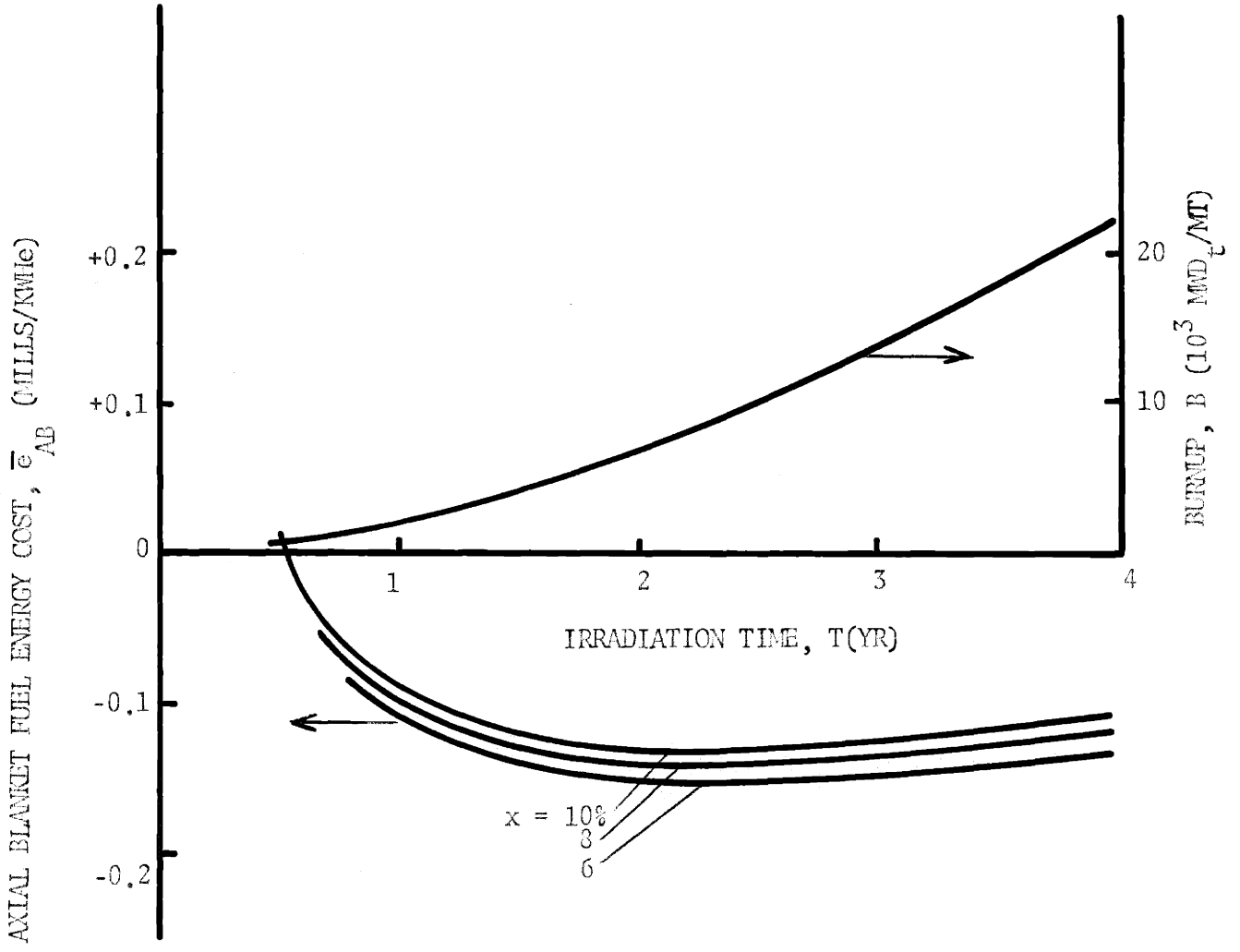

FIG. 5.12 EFFECT OF DISCOUNT RATE ON AXIAL BLANKET FUEL ENERGY COST

The subscript q denotes the cost component (fabrication, reprocessing, material); the subscript 0 denotes the reference economic condition, while x refers to an arbitrary economic condition.

Core and axial blanket irradiation time is set by the burnup limit of the core, in this case, 2 years, corresponding to an average core burnup of 102,000 MWD_t/MT. Equation (5-2) for the core is

$$\bar{e}_{core} = 1.09 \times 10^{-3} C_{fab,core} + 0.784 \times 10^{-3} C_{repr,core} + 0.06027 \times 10^{-3} C_{fiss} . \quad (5\text{-}3)$$

For the axial blanket,

$$\bar{e}_{AB} = 0.872 \times 10^{-3} C_{fab,AB} + 0.625 \times 10^{-3} C_{repr,AB} - 0.02307 \times 10^{-3} C_{fiss} \quad (5\text{-}4)$$

A "sensitivity coefficient", $(A_{q,s})_0$, is defined, to measure the sensitivity of $\bar{e}_s$ to changes in parameter $C_{q,s}$ from its reference value, all other parameters remaining fixed at their reference values:

$$(A_{q,s})_0 = \left(\frac{C_{q,s}}{\bar{e}_s}\right)_0 \frac{\partial \bar{e}_s}{\partial C_{q,s}}$$

$$= \frac{\Delta \bar{e}_s/(\bar{e}_s)_0}{\Delta C_{q,s}/(C_{q,s})_0}$$

$$= \left(\frac{C_{q,s}}{\bar{e}_s}\right)_{a_{q,s}} = \left(\frac{\bar{e}_{q,s}}{\bar{e}_s}\right)_0 \quad (5\text{-}5)$$

Values of $(A_{q,s})_0$ for the core and axial blanket are summarized in Table 5.8. For both the core and axial blanket, the material (fissile) component dominates, i.e. energy costs are most sensitive to C_{fiss}. Fabrication is the next most important component, followed by reprocessing.

Changes in $\bar{e}_s$ due to simultaneous changes in several economic parameters may be computed by linear superposition:

$$\Delta \bar{e}_s = a_{fab,s} \Delta C_{fab,s} + a_{repr,s} \Delta C_{repr,s} + a_{matl,s} \Delta C_{fiss}$$

or (5-6)

$$\frac{\Delta \bar{e}_s}{\bar{e}_s} = A_{fab,s} \frac{\Delta C_{fab,s}}{C_{fab,s}} + A_{repr,s} \frac{\Delta C_{repr,s}}{C_{repr,s}} + A_{fiss} \frac{\Delta C_{fiss}}{C_{fiss}}$$

5.5.3 Radial Blanket

Figures 5.13 through 5.16 display the behavior of radial blanket fuel power costs as the economic environment is varied around the reference environment. The optimum irradiation time (Topt) is seen to decrease as C_{fiss} increases, as $C_{fab,RB}$ decreases, as $C_{repr,RB}$ decreases, or as the discount rate (x) increases.

Unlike the axial blanket, the radial blanket may be fuel-managed independently of the core. The radial blanket may thus be irradiated to its optimum exposure, which occurs somewhat beyond the two year core burnup limit. One is concerned, then, with the sensitivity of the optimum radial blanket fuel energy cost, $(\bar{e}_{RB})_{Topt}$, to the economic environment.

The optimum irradiation time, Topt, is an implicit function of the economic environment. Hence, the fuel energy cost expression (5-1) does not reduce exactly to a linear form (5-2) in the unit costs C_{fab}, C_{repr},

TABLE 5.8

CORE AND AXIAL BLANKET SENSITIVITY COEFFICIENTS, $(A_{q,s})_0$*

q ↓ s →	Core	Axial Blanket
Fabrication	0.357	-0.495 **
Reprocessing	0.025	-0.140 **
Material	0.628	1.635
	1.000	1.000

$$* \ (A_{q,s})_0 = \frac{\bar{e}_s \ / \ (\bar{e}_s)_0}{C_{q,s}/(C_{q,s})_0}$$

** These terms are negative because $(\bar{e}_{AB})_0$ is negative.

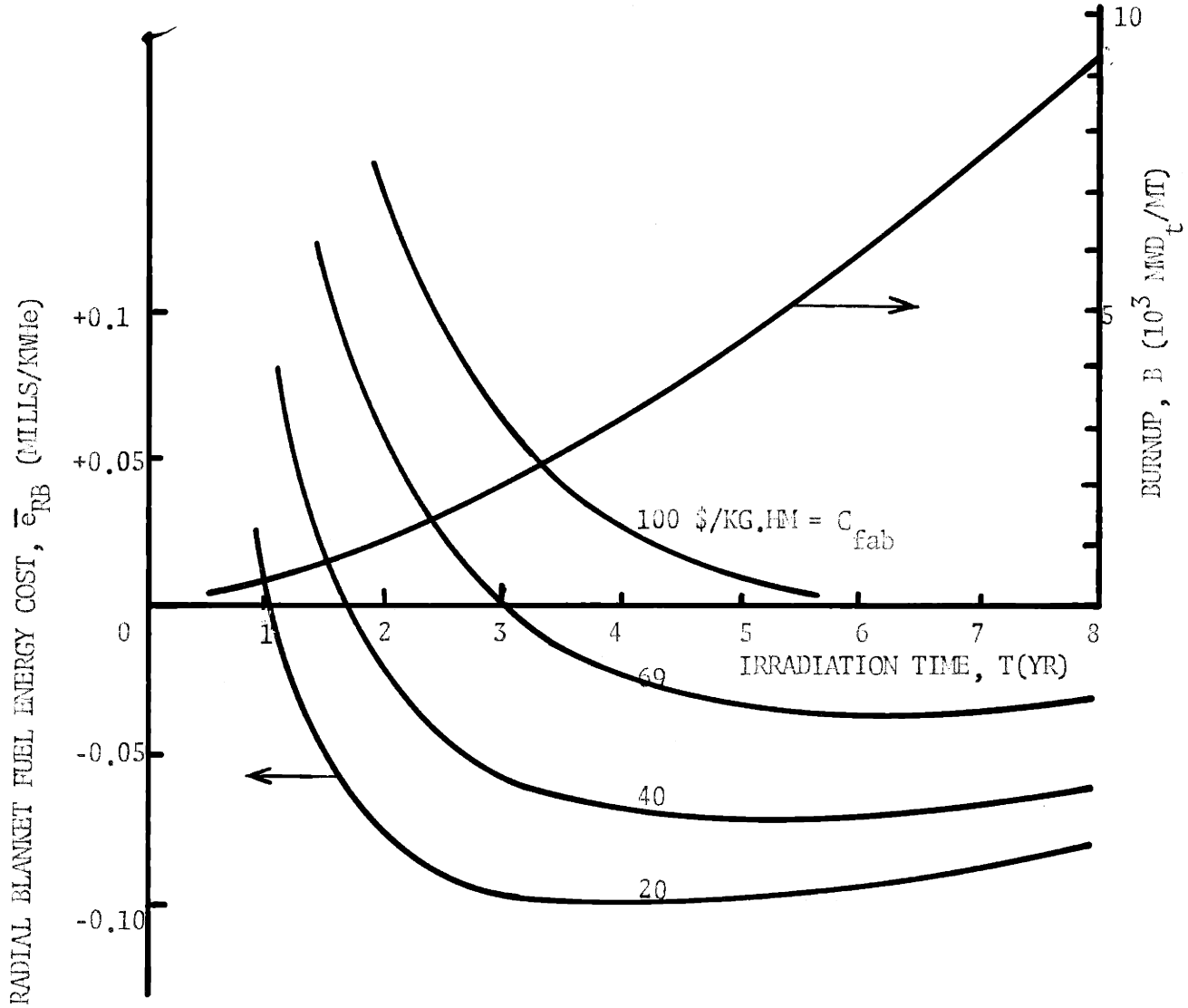

FIG. 5.13 EFFECT OF UNIT FABRICATION COST ON RADIAL BLANKET FUEL ENERGY COST

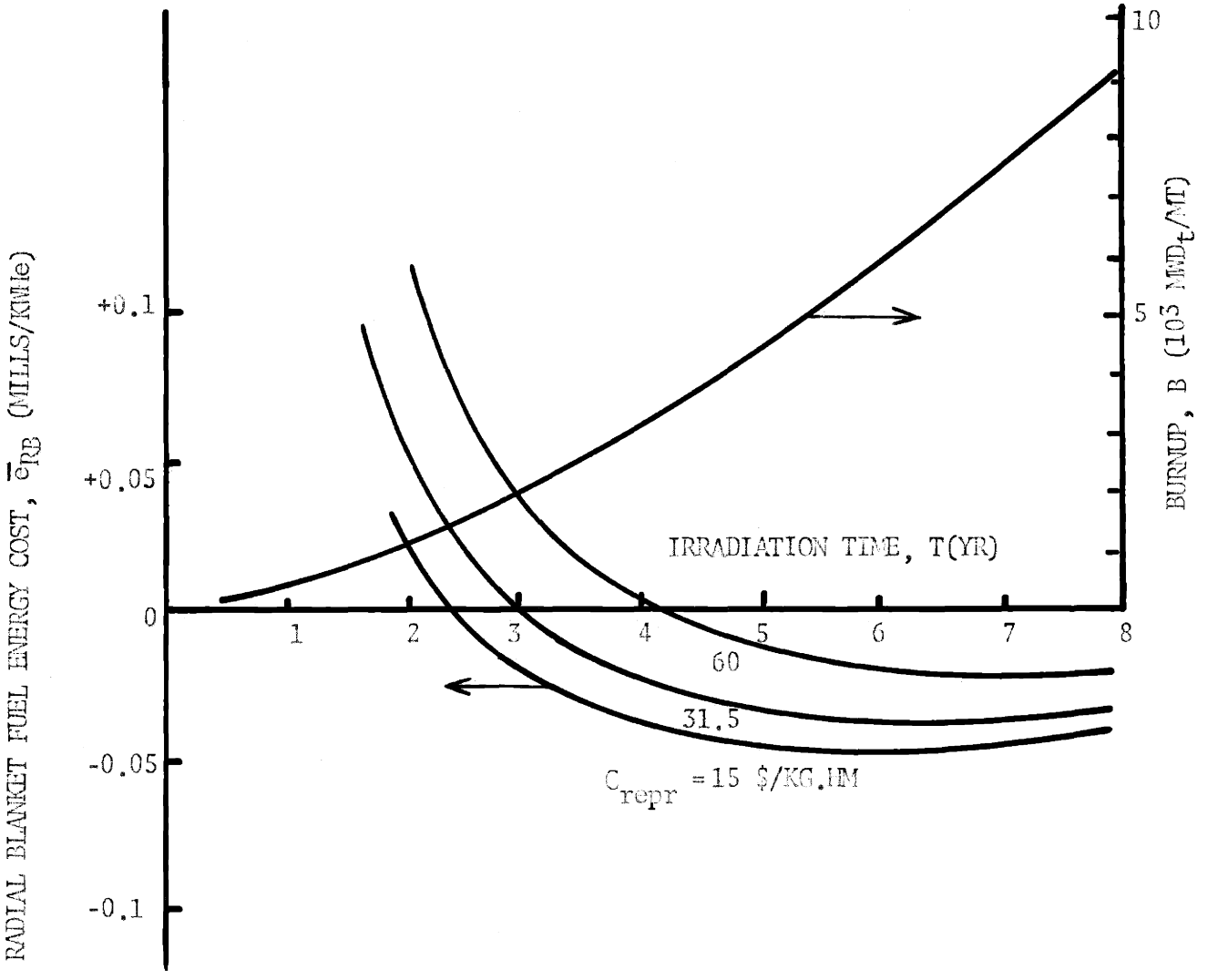

FIG. 5.14 EFFECT OF UNIT REPROCESSING COST ON RADIAL BLANKET FUEL ENERGY COST

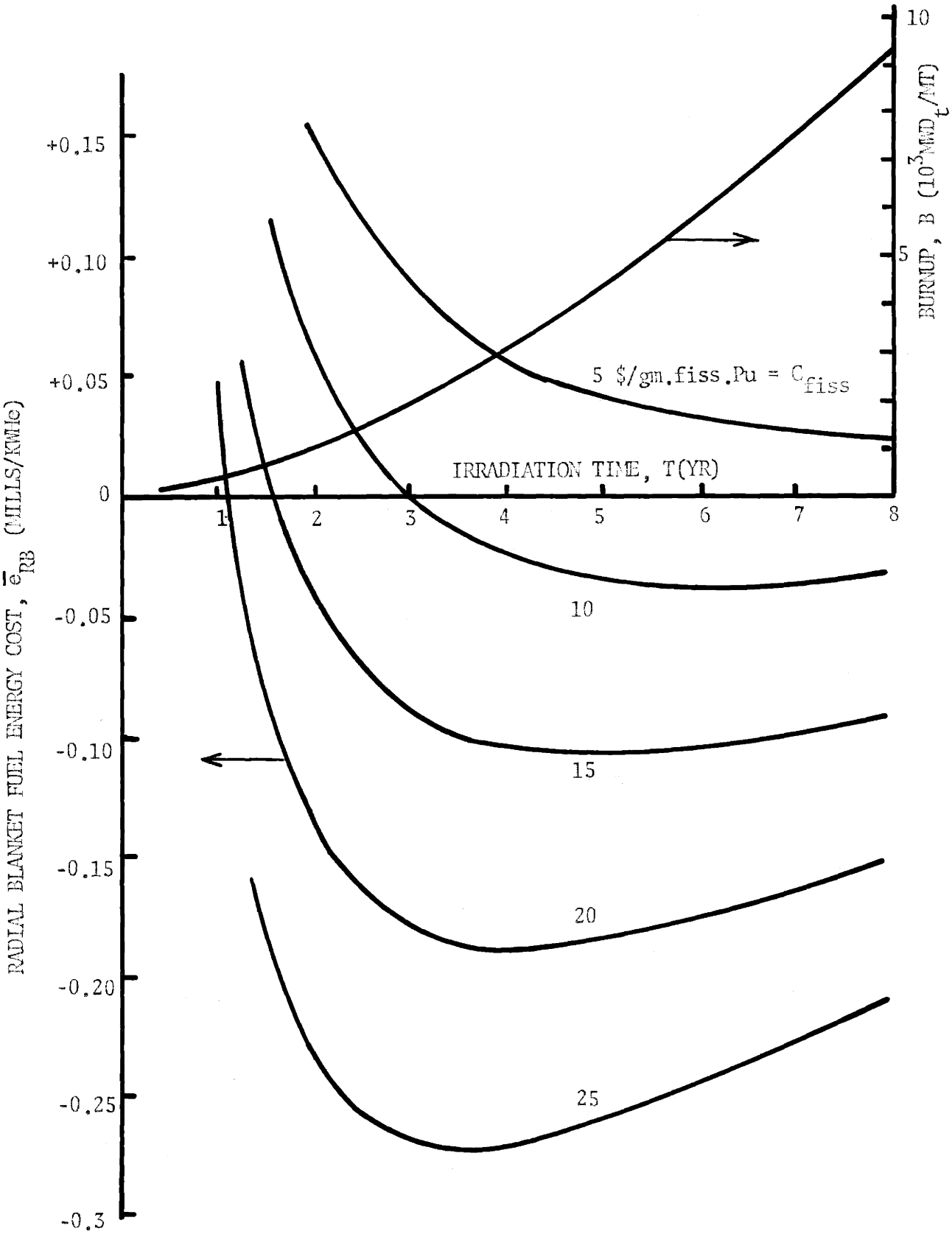

FIG. 5.15 EFFECT OF FISSILE PLUTONIUM PRICE ON RADIAL BLANKET FUEL ENERGY COST

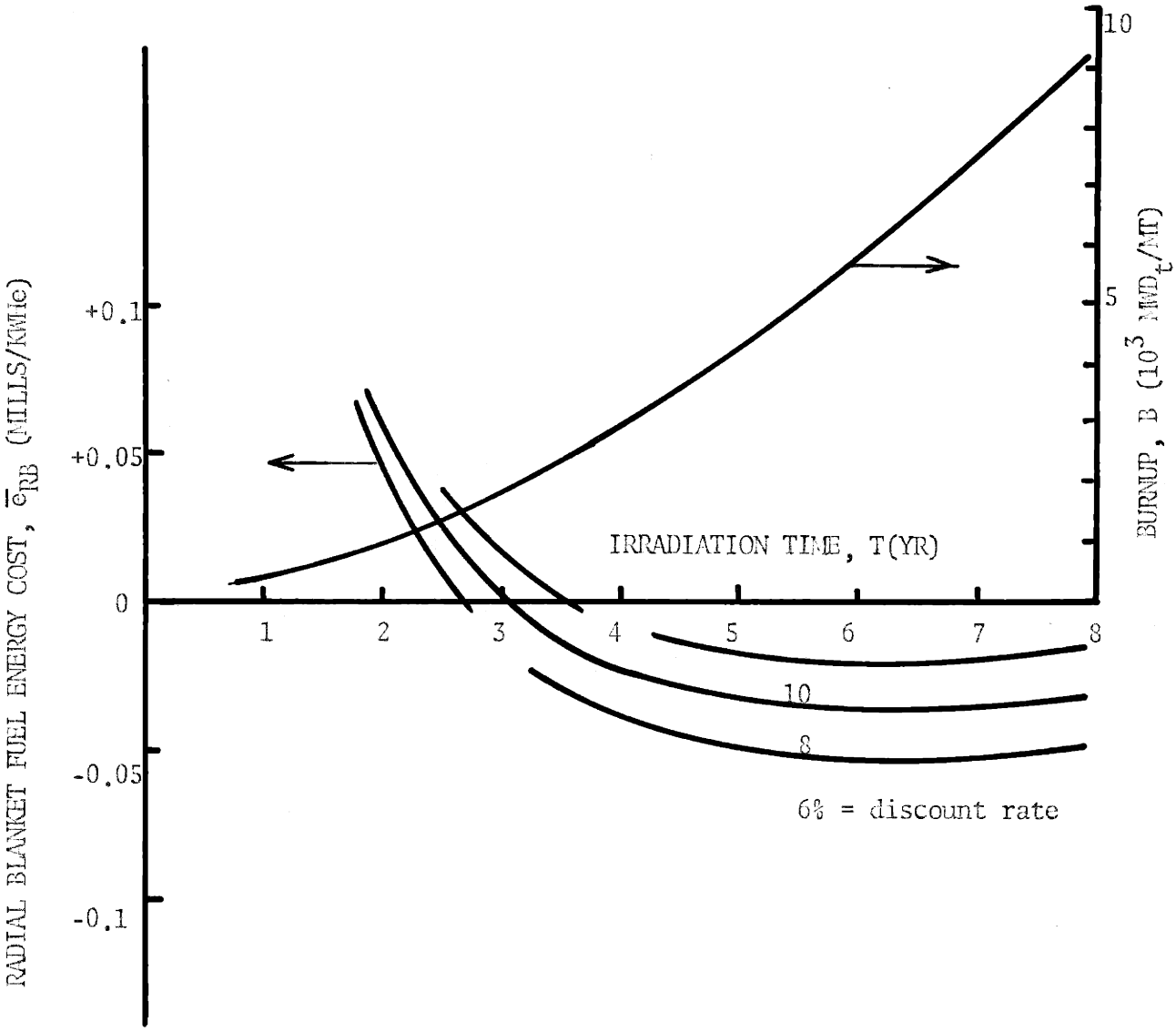

FIG. 5.16 EFFECT OF DISCOUNT RATE ON RADIAL BLANKET FUEL ENERGY COST

C_{fiss} as is the case for core and axial blanket. However, plots of $(\bar{e}_{RB})_{Topt}$ versus the unit costs, Figures 5.17, 5.18 and 5.19 show that $(\bar{e}_{RB})_{Topt}$ is nearly linear in C_{fab}, C_{repr}, and C_{fiss}.

For small perturbations in the economic environment (ΔC) the assumption of linearity is especially good. This is shown by the broken lines in Figures 5.17, 5.18 and 5.19, which represent linearizations at the reference conditions, e.g.

$$(\bar{e}_{RB})_{Topt} = \left(\frac{\bar{e}_{fab,RB}}{C_{fab,RB}}\right)_{0,Topt} C_{fab,RB} + (\bar{e}_{repr,RB})_{0,Topt} + (\bar{e}_{matl,RB})_{o,Topt} \qquad (5\text{-}7)$$

The constants of proportionality, $\left(\frac{\bar{e}_{q,RB}}{C_{fab,RB}}\right)_{0,Topt}$, in units of 10^{-3} kg/KWHe are

$$\left(\frac{\bar{e}_{fab,RB}}{C_{fab,RB}}\right)_{0,Topt} = 1.154 \times 10^{-3}$$

$$\left(\frac{\bar{e}_{repr,RB}}{C_{repr,RB}}\right)_{0,Topt} = 0.519 \times 10^{-3}$$

$$\left(\frac{\bar{e}_{matl,RB}}{C_{fiss,RB}}\right)_{0,Topt} = -0.0132 \times 10^{-3}$$

A composite linear form, analogous to Equation (5-2), valid near reference economic conditions, is

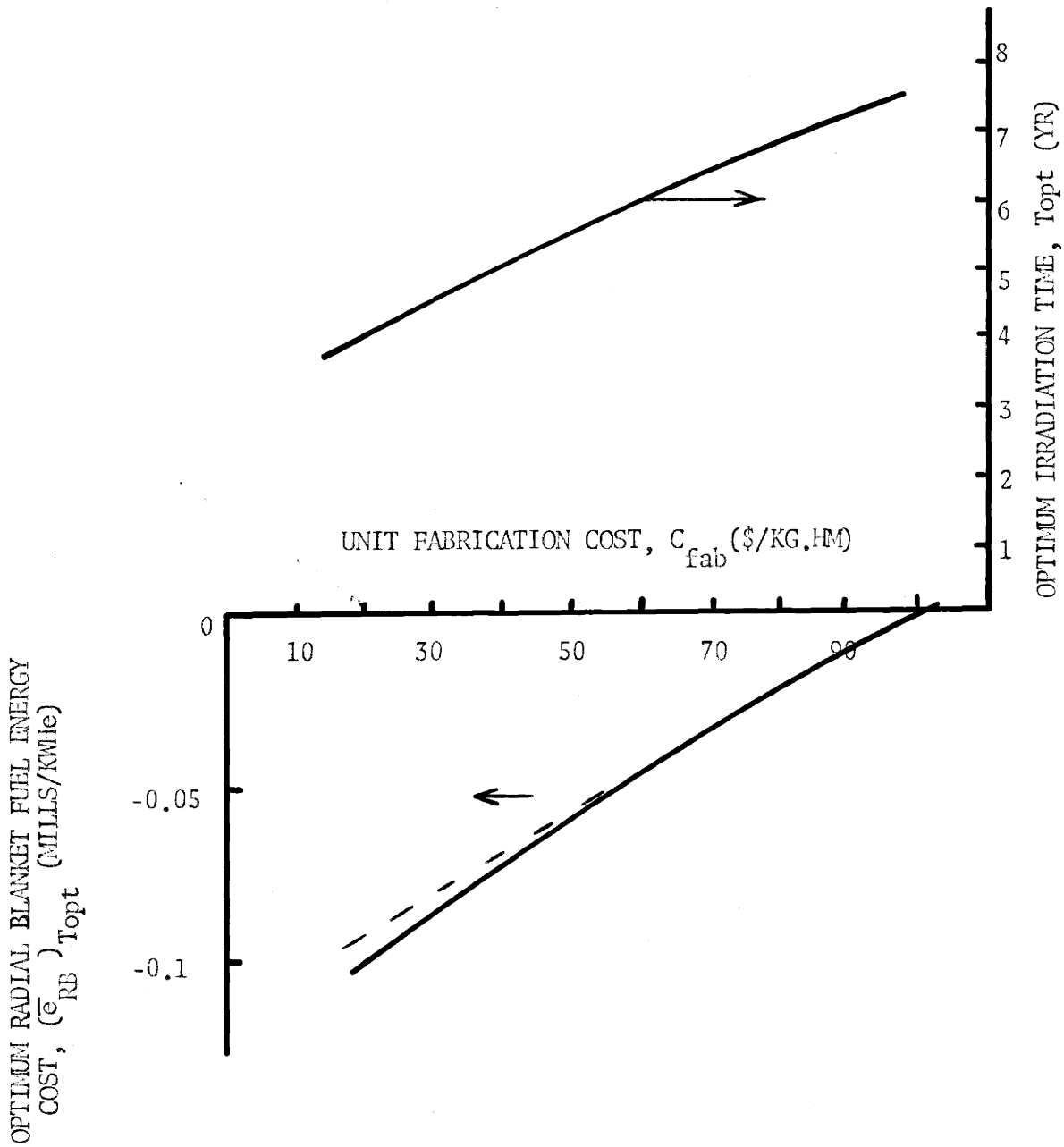

FIG. 5.17 SENSITIVITY OF OPTIMUM RADIAL BLANKET FUEL ENERGY COST TO UNIT FABRICATION COST

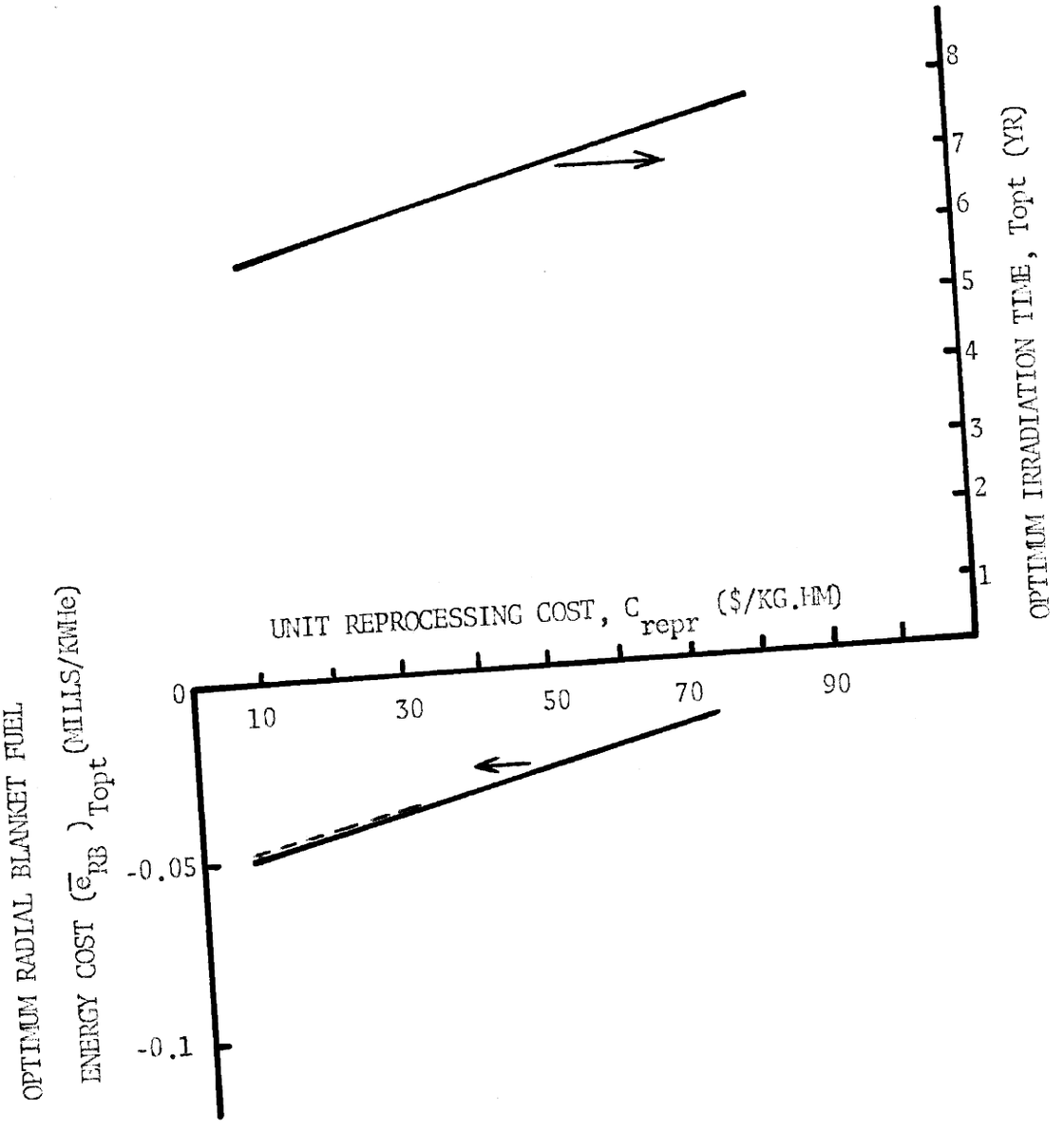

FIG. 5.18 SENSITIVITY OF OPTIMUM RADIAL BLANKET FUEL ENERGY COST TO UNIT REPROCESSING COST

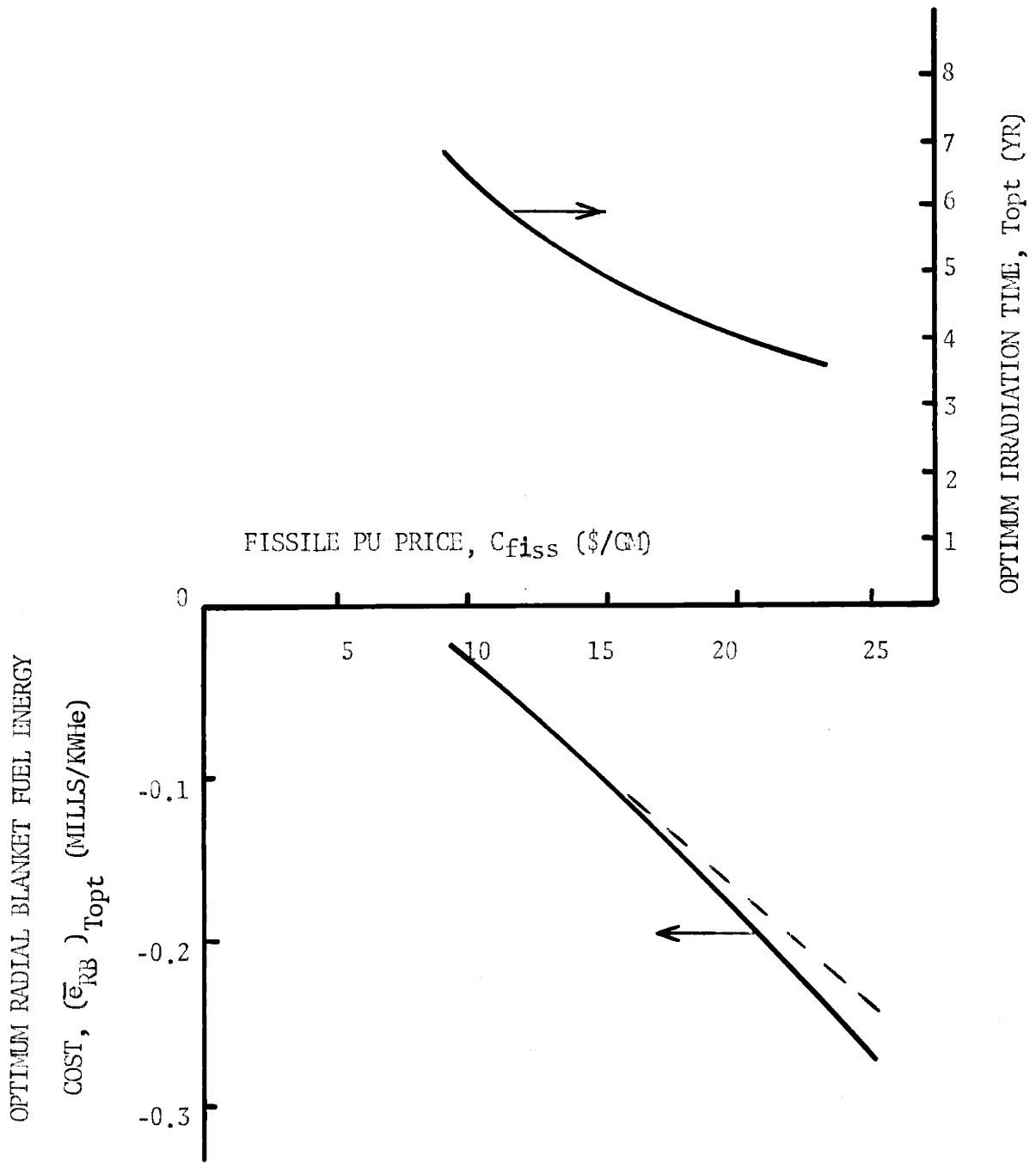

FIG.5.19 SENSITIVITY OF OPTIMUM RADIAL BLANKET FUEL ENERGY COST TO FISSILE PLUTONIUM PRICE

$$(\bar{e}_{RB})_{Topt} = a_{fab,RB}C_{fab,RB} + a_{repr,RB}C_{repr,RB} + a_{matl,RB}C_{fiss}$$

$$= \left(\frac{\bar{e}_{fab,RB}}{C_{fab,RB}}\right)_{0,Topt} C_{fab,RB} + \left(\frac{\bar{e}_{repr,RB}}{C_{repr,RB}}\right)_{0,Topt} C_{repr,RB}$$

$$+ \left(\frac{\bar{e}_{matl,RB}}{C_{fiss}}\right)_{0,Topt} C_{fiss}$$

$$= 1.154\text{x}10^{-3}\, C_{fab,RB} + 0.519\text{x}10^{-3}\, C_{repr,RB}$$

$$-0.0132\text{x}10^{-3}\, C_{fiss} \,. \qquad (5\text{-}8)$$

Values of the radial blanket sensitivity coefficients, defined as in Section 5.5.2, are given in Table 5.9. Optimum radial blanket fuel energy cost is seen to be most sensitive to fissile price, and least sensitive to unit reprocessing cost.

5.5.4 Fissile Market Price and the Economic Potential of LMFBR Blankets

In Sections 5.5.2 and 5.5.3, core, axial blanket, and radial blanket fuel energy costs were found to be most sensitive to fissile market price (C_{fiss}). It was also shown that $\bar{e}_{core}$ and $\bar{e}_{AB}$, assuming a fixed irradiation time, are linear in the unit costs $\{C_{q,s}\}$ while $(\bar{e}_{RB})_{Topt}$ is approximately linear in the $\{C_{q,RB}\}$.

Figure 5.20 shows the reactor fuel energy costs as a function of C_{fiss}. The total reactor fuel energy cost is the sum of the energy costs associated with each region:

$$\bar{e}_{reactor} = \bar{e}_{core} + \bar{e}_{AB} + (\bar{e}_{RB})_{Topt} \qquad \frac{\text{mills}}{\text{KWHe}}$$

TABLE 5.9

RADIAL BLANKET SENSITIVITY COEFFICIENTS*, $(A_{q,RB})_{0,Topt}$

q	$(A_{q,RB})_{0,Topt}$
Fabrication	-2.15 **
Reprocessing	-0.44 **
Material (fissile)	+3.59
	1.00

$$* \ (A_{q,RB})_{0,Topt} = \frac{(\Delta \bar{e}_{RB})_{Topt} / (\bar{e}_{RB})_{0,Topt}}{\Delta C_{q,RB} / (C_{q,RB})_{0,Topt}}$$

** These terms are negative because $(\bar{e}_{RB})_{0,Topt}$ is negative.

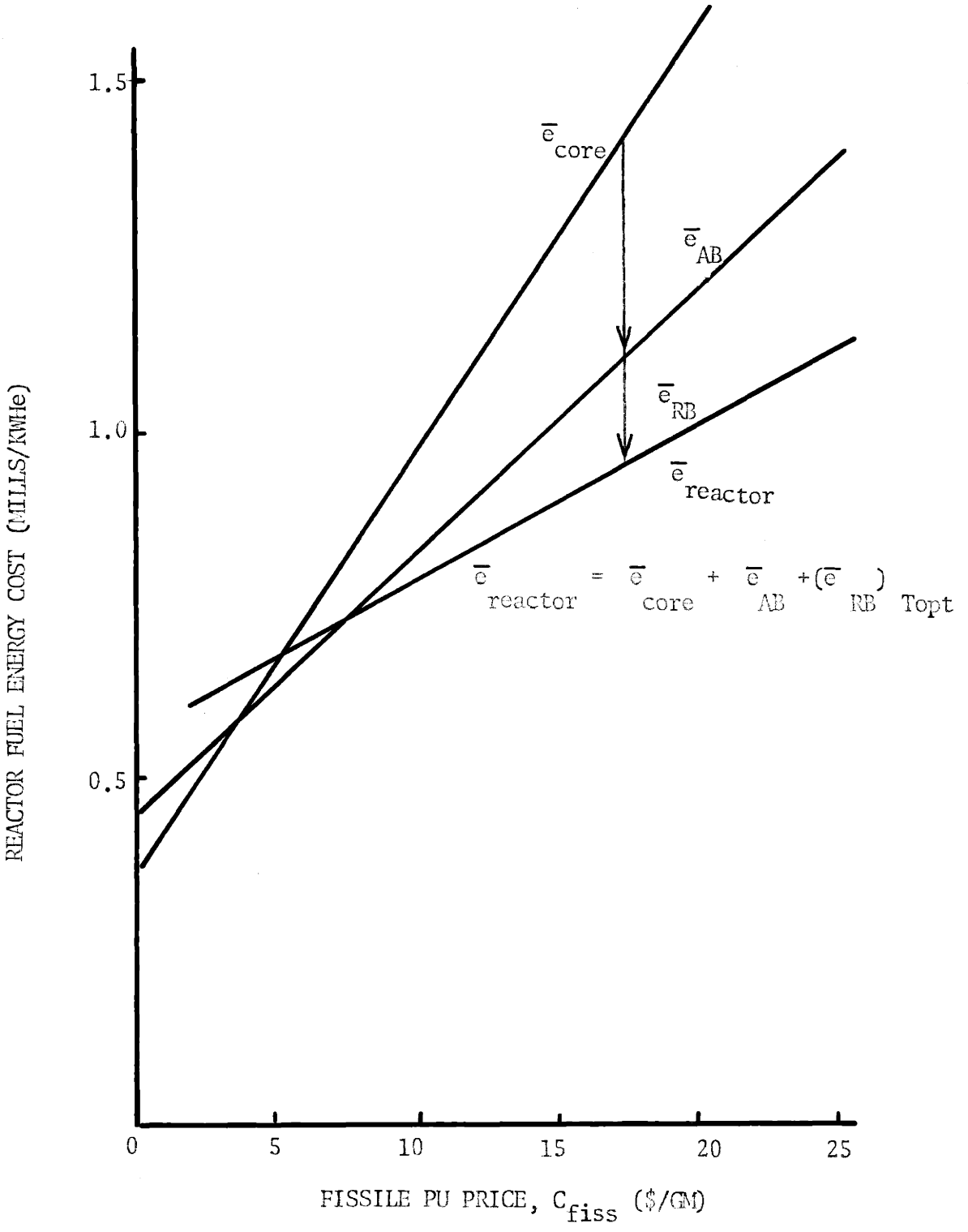

FIG. 5.20 EFFECT OF FISSILE PU PRICE ON TOTAL REACTOR FUEL ENERGY COST

The values of $(\bar{e}_{RB})_{Topt}$ used in constructing Figure 5.20 were taken from actual computed results, Figures 5.19 and 5.15, rather than the linear approximation, Equation (5-8).

Figure 5.20 displays several features:

(a) $\bar{e}_{reactor}$ increases with C_{fiss} despite the fact that the reactor produces more fissile material than it consumes. This is due to the high core fissile inventory cost. An increase in C_{fiss} results in an increase in net direct material revenue, but this advantage is overcome by the increased core inventory costs.

(b) The axial blanket is more profitable than the radial blanket, because the axial blanket sees more neutrons (H/D = 0.4). A two enrichment zone core configuration (Reactor 1', Section 4.4), of course, upgrades radial blanket performance by enhancing radial leakage.

(c) Below $C_{fiss} \simeq 8$ \$/gm, the blankets are of marginal importance. As the fissile price increases, the blankets become more viable, substantially offsetting the high core inventory cost.

(d) The axial blanket breakeven point, from Figure 5.20, occurs at 3.88 \$/gm. This is confirmed by solving Equation (5-4) for C_{fiss} with $\bar{e}_{AB} = 0$.

(e) The radial blanket breakeven point, from Figure 5.20, occurs at 7.25 \$/gm. This agrees with the solution of the linear approximation, Equation (5-8), with $(\bar{e}_{RB})_{Topt} = 0$.

CHAPTER 6

CONCLUSIONS AND RECOMMENDATIONS

In the preceding chapters, a variety of specific conclusions have been reached in regard to a broad spectrum of FBR fuel economic questions. An FBR fuel depletion-economics model was developed and applied to a number of 1000 MWe LMFBR case studies. In this chapter, the specific conclusions, in both the methods development and application phases, are reviewed as a prelude to a discussion of broader issues and recommendations as to the scope and direction of future work.

6.1 CONCLUSIONS

The major conclusions of this study are summarized below.

Depletion-Economics Methods

1. Blankets impose several unique accounting problems: blanket fuel appreciates with irradiation, thus raising certain income tax questions; and the long irradiation times in the radial blanket make the accounting treatment of blanket carrying charges important. Two methods of treating post-irradiation transactions were compared:

Method A. Tax the revenue from sale of fissile material (material credit) as ordinary income, along with electricity revenue; treat reprocessing costs as tax deductible expenses in the year in which they occur;

Method B. Capitalize fissile revenue and reprocessing costs.

Method A results in significantly lower values of levelized fuel costs (mills/KWHe). While the choice between fuel cost accounting methods

has a significant effect on absolute values of energy costs, it does not distort comparative and incremental results, e.g. design rankings, optimization of radial blanket residence times, etc. However, choice of method B would lead to the selection of thinner blankets, since under method B more of the radial blanket is unprofitable.

The question of whether or not to tax fissile revenue must ultimately be resolved by taxing authorities or by common usage. Fast breeder reactors have two major products: electricity and fissile material. Thus it would appear that fissile revenue should properly be taxed as ordinary income, along with the revenue from the sale of electricity. For this reason, method A is recommended for future studies.

2. Several effects complicate the physics-depletion of FBR blankets: spectrum softening with distance from the core-blanket interface; spectrum hardening and flux shift with irradiation; and heterogeneity effects. The two exposure dependent effects - spectrum hardening and flux shift - influence the blanket breeding rate in opposing directions. The flux shift effect dominates. A single multigroup physics computation, to obtain the flux shape and local spectra for depletion calculations, is sufficient for evaluating blanket/reflector design changes, scoping studies, and sensitivity studies. The major source of error in computing fissile buildup by this procedure is the assumption of constant flux over an irradiation cycle.

Corrections (to the U238 capture cross section) for blanket heterogeneity effects influence computed fissile production in two opposing ways: (a) reduction in σ_c^{28}, tending to reduce the bred fissile inventory; and (b) reduction in neutron attenuation, tending to increase blanket fluxes and increase breeding rate. Of these effects, (a) dominates, and heterogeneity leads to a net adverse effect on blanket breeding. For a

typical radial blanket, heterogeneity corrections lead to a reduction in discharge fissile inventories of about 10%.

It was also found that core and axial blanket fuel costs are insensitive to radial blanket/reflector configuration changes.

1000 MWe LMFBR Case Studies

3. Substitution of a moderating reflector (e.g. Be) for the outer radial blanket row/s can improve overall radial blanket economic performance significantly. Choice of radial reflector material, e.g. Be vs. Na has little effect on the fuel economics of thick (~ 45 cm) radial blankets. The relative advantage of a moderating reflector increases as the reflector is moved nearer the high flux zones of the blanket, that is, as the blanket thickness decreases.

4. Reducing blanket thickness (by replacing outer blanket regions with reflector) reduces the bred fissile inventory of the blanket, that is, the plutonium forfeited in the region eliminated is greater than the additional plutonium bred in the remaining region due to its improved breeding performance ($\sigma_c^{28}\phi$). This loss of plutonium revenue is opposed by savings in fabrication and reprocessing costs of the blanket elements eliminated. Radial blanket thickness optimization is weak, i.e. net blanket revenue does not display a sharp peak as radial blanket thickness is reduced from 3 rows to 2 rows to 1 row.

5. Core enrichment zoning, in addition to its advantages to core fuel economics, significantly enhances breeding in the radial blanket, and can increase net radial blanket revenue by a factor of two or more.

6. Optimum radial blanket fuel residence times increase with distance from the core, ranging from approximately 2 years for fuel assemblies nearest the core to about 10 years for fuel in the outer row of a 45 cm

blanket. Thus, if the blanket is irradiated to a single irradiation time (whole blanket management), the optimum irradiation time for the blanket as a whole, then inner blanket fuel is overexposed and the outer blanket fuel is underexposed. Significant improvement ($\sim$ 30% increase in net blanket revenue) results from irradiating each annular region to its own, local optimum irradiation time.

7. For a fixed irradiation time set by the burnup limit of core fuel, core and axial blanket fuel costs (mills/KWHe) are simple linear functions of the unit costs for fabrication, reprocessing ($/kgHM) and fissile material ($/kg fissile). Core and axial blanket fuel costs are most sensitive to fissile value. Fabrication is the next most important component.

Unlike the axial blanket, the radial blanket may be fuel-managed independently of the core, and thus may be irradiated to its optimum exposure which occurs somewhat beyond core residence times. The radial blanket fuel cost (or net revenue) at its optimum irradiation time is an implicit function of the unit costs for fabrication, reprocessing and fissile material, as is the optimum irradiation time. Thus the optimum radial blanket fuel cost is not <u>exactly</u> linear in the unit costs, as is the case for core and axial blanket. However, both the optimum irradiation time and the corresponding radial blanket fuel cost (or net revenue) are <u>approximately</u> linear functions of the unit costs. Optimum radial blanket fuel cost (mills/KWHe) is most sensitive to fissile price.

For increased fissile prices, both blankets (axial and radial) become more important in offsetting the increased core fissile inventory costs.

6.2 RECOMMENDATIONS

1. Blanket Power and Blanket Seeding

The availability of neutrons for fertile-to-fissile conversion is a key factor in blanket economics. Deep in the blanket (far from the core), where neutrons are relatively scarce, the conversion rate may be too low to overcome the rates of increase of fabrication and fissile carrying charges with residence time, resulting in net positive costs for fuel assemblies there. Thus design or fuel manangement options which tend to increase blanket flux have the potential of enhancing blanket economics.

Overall reactor fuel economic performance, represented by the net total fuel costs of core and blankets (mills/KWHe), is improved by increasing blanket power. This statement assumes that the maximum local power density in the core is held fixed.

A scheme which increases both blanket multiplication (and hence blanket flux) and blanket power is the inclusion of fissile material in blanket load fuel, or blanket seeding. Depending on the orificing scheme adopted, other advantages of blanket seeding are increased coolant exit temperatures (reducing the mixed mean temperature degradation) and reduced blanket power-swing over an irradiation cycle. Another incentive for seeding, or some equivalent accomodation, is the desirability of modifying a given blanket so that the theoretically optimum blanket thickness matches the discrete thickness allowed by fixed subassembly dimensions. Blanket seeding has a number of disadvantages, including increased inventory cost, increased pumping power requirements, decreased fertile material load available for conversion, and, in the case of uranium seeding, additional processing charges, for enrichment.

Table 6.1 summarizes the advantages and disadvantages of blanket seeding. A parametric study to examine these tradeoffs in a more quantitative manner is recommended.

Other investigators (12) have shown that reducing the load fissile enrichment from that of natural uranium (0.7% U235) to zero has negligible effect on blanket breeding. Thus substitution of natural uranium for enrichment plant tails (~0.2% U235) would offer no improvement in blanket breeding.

Figure 3.11 shows that the local breeding ratio decreases from greater than unity to below unity as load enrichment is increased from zero (blankets) to about 14% (core), because of the enhanced competition for neutrons by the fissile species. At some intermediate point, the local blanket breeding ratio will be unity. Offsetting the diminished local blanket breeding ratio is the increased blanket flux, which tends to increase net blanket revenue at the local optimum irradiation time and to decrease the local optimum irradiation time.

2. Radial Blanket Fuel Management

The literature search, Appendix D, failed to render a comprehensive, comparative evaluation of alternate fuel management strategies for a fixed reactor configuration. This is perhaps due to the complexity of fuel management calculations and the lack, until recently, of computer programs flexible enough to survey all feasible options with ease. Several recently developed programs promise to be useful for FBR fuel management studies: PHENIX (31), REBUS (32), FUMBLE (45), and 2DBCOST (17). A comparative evaluation of scatter, batch, out-in, and in-out equilibrium radial blanket fuel management schemes is recommended. Table 6.2 gives qualitative advantages and disadvantages of these options.

TABLE 6.1 ADVANTAGES AND DISADVANTAGES OF BLANKET SEEDING

ADVANTAGES	DISADVANTAGES
. Increased blanket multiplication (more neutrons available for fertile-to-fissile conversion)	. For the same fuel volume fraction, slightly less fertile material available for conversion.
."Bonus power". For a fixed local power density limit in the core, increased reactor power.	. Increased blanket coolant pumping requirements.
. Reduced mixed mean temperature degradation from blanket coolant.	. Increased fissile inventory costs.
. Decreased power swing over an irradiation cycle.	. In the case of U235, a possible increase in processing costs (enrichment).

TABLE 6.2 RADIAL BLANKET FUEL MANAGEMENT SCHEMES

Fuel Management Scheme	References	Advantages	Disadvantages
1. Fixed-Fuel Schemes			
A. Batch and Scatter			
(1) Whole Blanket Management	(this report)	.simplicity	.non-uniform burnup .power tilt across blanket
(2) Regional Management	(69), (70), (71), (72), (73) (this report)	. power flattening .more uniform burnup than whole blanket management; local optima achieved.	.complexity
B. Batch	(this report)	.simplicity	.more severe power swing than scatter management.
C. Scatter	(69), (70), (71), (72), (73), (this report)	.reduces power swing	.complexity
2. Moving-Fuel Schemes			
A. Out-in	(4)	.uniform burnup .reduction in power swing	.aggravates power tilt across blanket .large amount of handling per fuel element

TABLE 6.2 (continued)

Fuel Management Schemes	References	Advantages	Disadvantages
B. In-out	(10), (73)	. uniform burnup . reduction in power swing .power flattening	.large amount of handling per fuel element

Once the reactor is in operation, the radial blanket offers the major remaining area of fuel management flexibility. The operator may tailor its size (or number of rows of subassemblies), load composition (enrichment in fissile plutonium or uranium, or possibly the use of fertile thorium), and fuel management scheme to current and projected economic environments. Thus, for example, if higher plutonium prices and/or lower fabrication and reprocessing costs are forecast, he may decide to add a row of subassemblies. Under other conditions, he may elect to alter the radial reflector design, include moderating material in the radial blanket, etc. A recent study (17) has addressed the general problem of optimizing FBR fuel management options in a variable economic environment. Continued effort in this area is recommended, with the aim of parameterizing and simplifying fuel management decision-making.

3. FBR Fuel Management and Design

In-reactor fuel management, particularly that of the blanket, is commonly treated an an after-thought in reactor design. The reactor is designed first; then fuel management is optimized, subject to the configuration selected and its engineering limitations and constraints. Ideally, the tasks of design and of setting the fuel management scheme should be intimately coupled, with the goal of reaching a more "global" optimum.

For example, the power swing (and hence orificing requirements) over an irradiation cycle in a radial blanket region, i, may be diminished by decreasing the fraction, g_i, of fuel replaced in that region per refueling event. This, in turn decreases the region throughput, increases the irradiation time, and increases the fissile inventory in the region, which may affect the net blanket fuel revenue adversely. Similarly, a degree of power flattening across the blanket can be achieved

by dividing the radial blanket into annular regions and assigning them refueling fractions (g_1 , g_2 , ...) which decrease with distance from the core. The design benefits of power shaping should be included explicitly in the analysis of fuel management strategies.

Whatever aspects of blanket fuel management are subjected to further scrutiny should be approached on a more global basis, at the minimum taking into consideration the strong interaction of management schemes and the flow orificing pattern adopted.

Finally, since unit sizes are projected to increase to 2000 MWe and beyond after the year 2000, a more thorough parametric study of blanket performance versus reactor rating is recommended. The reactor size-blanket fuel economics preliminary study in Appendix B identifies some of the design-fuel management issues which should be addressed by such an effort.

APPENDIX A - NOMENCLATURE

Chapter 2 - Nomenclature

Subscripts, Superscripts and Abbreviations.

q	cost component index; mp, fab, repr or mc
mp	material purchase
fab	fabrication
repr	reprocessing
mc	material credit
28	U238
49	Pu239
40	Pu240
41	Pu241
42	Pu242
HM	heavy metal (U + Pu)
CFM	cash flow method
CIM	compound interest method
SIM	simple interest method

Levelized Cost (Price) of Electricity

$\bar{e}$	levelized cost (price) of electricity associated with fuel. Depending on context, the symbol $\bar{e}$ denotes: *total reactor levelized fuel cost (sum over all fuel streams) *levelized fuel cost associated with a given fuel stream (sum over the cost components, q, of the fuel stream).	$\frac{\text{mills}}{\text{KWH}_e}$

Unit Costs

C_{fab}	unit fabrication cost for a given type fuel	$\frac{\$}{\text{kgHM}}$

C_{repr}	unit reprocessing cost for a given type fuel	$\frac{\$}{kgHM}$
C_j	market value of isotope j	$\frac{\$}{kg}$

Annual Quantities for CFM Derivation

E_j	electrical energy generated by the plant, year j	KWHe
V_j	taxable revenue from sources other than the sale of electricity, year j	$
O_j	tax deductable cost, year j	$
D_j	depreciation for tax purposes, year j	$
V'_j	non-taxable revenue, year j	$
Z_j	capitalized cost (new capitalization), year j	$
Y_j	book value (liability to investors) in effect during year j	$
T_j	income tax, year j	$
w(j)	discount factor, $(1+x)^{-j}$	

Costs Associated with a Fuel Lot

z_m^q	direct cost, cost component q, fuel lot m	$
$(z_m^q)^{**}$	carrying charge associated with cost component q, fuel lot m	$
$(z_m^q)^{*}$	total cost associated with component q, fuel lot m;	$

$$= z_m^q + (z_m^q)^{**}$$

Time

t_m^q	time from beginning of plant life to transaction q, fuel lot m	yr.
t_m	time from beginning of plant life to irradiation midpoint of fuel lot m	yr.
T_m	irradiation time of fuel lot m	yr.
T'^q_m	pre-irradiation time, component q, fuel lot m; time between transaction q and start of irradiation	yr.
T''^q_m	post-irradiation time, component q, fuel lot m; time between end of irradiation and transaction q	yr.
T^q_m	time between transaction q of lot m, and midpoint of irradiation	yr.

Financial Parameters

x	discount rate
f_b	fraction of capital from bondholders
f_s	fraction of capital from stockholders
r_b	bondholders' rate of return
r_s	stockholders' rate of return
τ	income tax rate
F^q_m	carrying charge factor associated with cost component q, fuel lot m; $(z^q_m)^*/z^q_m$
y_q	carrying charge rate associated with cost component q

Fuel Composition

$M_{28}(T)$, $M_{49}(T)\ldots$	Mass of indicated nuclide after irradiation	kg
M^o_{28}, $M^o_{49},\ldots$	Initial mass of indicated nuclide	kg

$\in(T)$ Fissile concentration after irradiation time T,

$$M_{49}(T) + M_{41}(T)/M^0_{HM}$$

$\in_0$ Initial fissile concentration (enrichment),

$$M^0_{49} + M^0_{41} / M^0_{HM}$$

Chapter 3 - Nomenclature

$\sigma^j_{k,e}$	microscopic cross-section for event e, energy group k, nuclide j	barns
σ^j_e	spectrum averaged one group cross-section, event e, nuclide j	barns

$$\sum_{k=1}^{n} \phi_k \sigma^j_{k,e} / \sum_{k=1}^{n} \phi_k$$

ϕ_k	neutron flux in energy group k	n/cm^2sec
ϕ	total flux,	n/cm^2sec

$$\sum_{k=1}^{n} \phi_k$$

N_j	atom density, nuclide j	$atoms/cm^3$
N^0_j	initial atom density, nuclide j	$atoms/cm^2$
θ	flux time	

$$\equiv \int^t \phi(t')\, dt'$$

Appendix B - Nomenclature

R_c	core radius	cm
V_c	core volume	liter
B^2_c	critical core buckling	cm^{-2}
$\in_c$	critical core enrichment	

b_i	internal breeding ratio, fissile production rate in core / fissile destruction rate in core	
b_x	external breeding ratio, fissile production rate in blanket / fissile destruction rate in core	
$\theta_{c,ox}$	oxide volume fraction in core	
$\theta_{b,ox}$	oxide volume fraction in blanket	
f	fraction of reactor thermal power produced in blanket	
$\Delta M_{c,49}(T_c)$	change in core Pu239 inventory during core irradition time Tc	kg
$M^0_{c,49}$	initial core Pu239 inventory	kg
$\Delta M_{b,49}(T_b)$	change in blanket Pu239 inventory during blanket irradiation time Tb	kg
$\bar{e}_{c,proc}$	levelized core processing (fabrication + reprocessing) cost, including carrying charges	mills / KWHe
$\bar{e}_{b,proc}$	levelized blanket processing (fabrication + reprocessing) cost, including carrying charges	mills / KWHe
$\bar{e}_{c,BU}$	levelized core burnup (direct material) cost, including material purchase and material credit	mills / KWHe
$\bar{e}_{c,Inv.}$	levelized core inventory cost (material carrying charge)	mills / KWHe
$\bar{e}_{b,mat}$	levelized blanket material cost (revenue), including carrying charge	mills / KWHe
$\bar{e}_c$	total levelized core fuel cost, $\bar{e}_{c,proc} + \bar{e}_{c,BU} + \bar{e}_{c,Inv.}$	mills / KWHe
$\bar{e}_b$	total levelized blanket fuel cost $\bar{e}_{b,proc} + \bar{e}_{b,mat}$	mills / KWHe
$\bar{e}$	total levelized reactor fuel cost $\bar{e}_c + \bar{e}_b$	mills / KWHe

APPENDIX B

REACTOR SIZE AND BLANKET FUEL ECONOMICS

B.1 INTRODUCTION

Very large reactors (> 1000 MWe), advantaged by economics of scale, have been predicted. For example, the EEI "Fast Breeder Reactor Report" (58) suggests that light water reactors and fast breeder reactors may have unit ratings in excess of 2000 MWe by the year 1990. The purpose of this appendix is to examine relationships between FBR core size (or power rating) and FBR blanket fuel economics.

As core size is increased, (holding shape fixed), core neutron leakage (per core fission) and external breeding ratio decrease. Net blanket revenue (plutonium credit less fabrication and reprocessing costs), per unit of power, decreases. At the same time, core critical enrichment decreases, resulting in lower core fissile inventory costs. With a higher fertile concentration in the core, the internal breeding ratio is enhanced, diminishing the burnup (direct material) component of core fuel energy cost. Indeed, for a sufficiently large core, the internal breeding ratio exceeds unity and the burnup component becomes a revenue.

For these reasons, the economic importance of the blanket tends to decrease with reactor size. In fact, it may be worthwhile, for a sufficiently large core, to substitute a non-breeding reflector for the breeding blanket. This would eliminate fabrication and reprocessing costs, although this advantage may be offset by the cost of the added reflector. In addition, the core neutron economy may be improved, provided the reflector has superior neutronic properties compared to the breeding blanket,[1]

1. Design studies for the FFTF (84) have shown that Ni is superior to a breeding blanket, as a core reflector.

resulting in even lower critical enrichment (lower core inventory cost) and higher internal breeding ratio (lower burnup cost). If the reflector is merely sodium coolant, it need not be fabricated or cooled in situ and blanket fabrication costs and pumping requirements are eliminated. Against these advantages of a non-breeding reflector must be weighed its obvious disadvantage - the loss of blanket plutonium revenue.

The arguments above are largely academic. First, the core shape was assumed to be held fixed as core size increases. In reality, high leakage geometries (e.g. pancake, annular) may be required for large cores to enhance the negative component of the sodium void coefficient. Another reason for spoiling large core geometry is to hold the internal breeding rate near unity, thus minimizing reactivity control requirements, control systems costs, and parasitic loss of neutrons available otherwise for breeding.

The purpose of this appendix is to examine some of these qualitative arguments in a semi-quantitative way. Using simple, one energy group, spherical geometry neutronics equations, the fuel economics of reactors with and without blankets were compared as core size (power rating) is increased. Three cases are considered:

Case A: Spherical core with a breeding blanket, assuming no Pu239 burnup in the blanket[1];

Case A*: Spherical core with a breeding blanket, corrected for Pu239 burnup in the blanket, blanket power fraction = 0.1[1];

Case B: Spherical core with a sodium reflector (no breeding blanket).

---

1. Case A*, a refinement of Case A, is included to examine the effect of blanket burnup on overall energy costs (mills/KWHe).

The spherical core size limit for a negative sodium void coefficient (50% sodium loss) have been determined in an extensive parametric study by Terasawa, et.al. (55). This limit is indicated in the results of Section B.3.

B.2 EQUATIONS

B.2.1 Summary

The neutron balance, depletion, and economics working equations used in this study are summarized in Table B.1. Major assumptions are listed in Table B.2. Table B.3 gives the region compositions and one group physics data. Table B.4 presents the economic data. Residence times and power-related parameters are given in Table B.5. The equations of Table B.1 are used as follows:

1. For a given core volume (V_c), the core critical buckling (B_c^2) is found by solving the transcendental critical Equation (B-4A) or (B-4B).

2. With this value of critical buckling, critical core enrichment (ϵ_c) is computed, using Equation (B-15). Critical mass ($M^0_{c,49}$) may also be computed at this time, from ϵ_c and V_c, using Equation (B-17).

3. The internal breeding ratio (b_i), a function of ϵ_c, is determined from Equation (B-20). The external breeding ratio (b_x), a function of both ϵ_c and B_c, is found from Equation (B-24).

4. Masses of Pu239 discharged from core and blanket ($M_{c,49}$, $M_{b,49}$) are found from Equations (B-36) and(B-37) respectively, with the known values of V_c, ϵ_c, b_i and b_x. This step may be by-passed since the economics equations incorporate (B-36) and(B-37).

5. Core and blanket levelized fuel energy costs are determined from Equations (B-48) through (B-78), with the values of ϵ_c, b_i and b_x

TABLE B.1 - SUMMARY OF WORKING EQUATIONS

Neutronic and Depletion Equations

(a) Critical Core Buckling:

$$6.24V_c^{1/3} B_c \cot 6.24 V_c^{1/3} B_c = -0.3V_c^{1/3} - 0.1915 \quad \text{(Case A,A*)} \quad \text{(B-4A)}$$

$$= -0.04815V_c^{1/3} - 1.4561 \quad \text{(Case B)} \quad \text{(B-4B)}$$

(b) Critical Core Enrichment:

$$\epsilon_c = 0.0651 + 62.76 B_c^2 \quad \text{(Case A,A*,B)} \quad \text{(B-15)}$$

(c) Critical Core Mass:

$$M^0_{c,49} = 2.64 V_c \epsilon_c \quad \text{(Case A,A*,B) (kg)} \quad \text{(B-17)}$$

(d) Breeding Ratios:

$$b_i = 0.1255 \left(\frac{1-\epsilon_c}{\epsilon_c}\right) \quad \text{(Case A,A*,B)} \quad \text{(B-20)}$$

$$b_x = 76.19 B_c^2 / \epsilon_c \quad \text{(Case A)} \quad \text{(B-24)}$$

(e) Discharge Pu239 Mass

$$M_{c,49} = 2.64 V_c \epsilon_c + 0.3250 (b_i - 1) V_c \quad \text{(Case A,A*,B) (kg)} \quad \text{(B-36)}$$

$$M_{b,49} = 0.975 b_x V_c \quad \text{(Case A)} \quad \text{(B-37)}$$

Cost Equations

(f) Core

$$\text{Burnup, } \bar{e}_{c,BU} = -1.16 (b_i - 1) \quad \text{(Case A,B) (mills/KWHe)} \quad \text{(B-48)}$$

Inventory, $\bar{e}_{c,inv} = 3.335\ \epsilon_c + 0.1250\ (b_i - 1)$ . . . . . (Case A,B) . . (mills/KWHe). (B-49)

Processing, $\bar{e}_{,c,proc} = 0.3964$ . . . . . (Case A,B) . . (mills/KWHe). (B-50)

(g) Blanket

Material, $\bar{e}_{b,mat} = -0.886\ b_x$. . . . . (Case A) . . . (mills/KWHe). (B-60)

Processing, $\bar{e}_{b,proc} = 0.2555$ . . . . . (Case A) . . . (mills/KHWe) .(B-61)

Corrections for Blanket Pu239 Burnup (Case A*)

(e)* Discharge Pu239 Mass (Blanket):

$M^*_{b,49} = 0.8\ M_{b,49} = 0.78\ b_x\ V_c$ . . . . . (Case A*). . . . (kg). . . . (B-69)

(f)* Core Cost Equations:

$\bar{e}^*_{c,BU} = 0.9\ \bar{e}_{c,BU}$ . . . . . (Case A*). . . (mills/KWHe). (B-75)

$\bar{e}^*_{c,inv} = 0.9\ \bar{e}_{c,inv}$ . . . . . (Case A*). . . (mills/KWHe). (B-76)

$\bar{e}^*_{c,proc} = 0.9\ \bar{e}_{c,proc}$. . . . . (Case A*) .. . (mills/KWHe). (B-77)

(g)* Blanket Cost Equations:

$\bar{e}^*_{b,mat} = 0.72\ \bar{e}_{b,mat}$ . . . . . (Case A*). . . (mills/KWHe). (B-79)

$\bar{e}^*_{b,proc} = 0.9\ \bar{e}_{b,proc}$ . . . . . (Case A*). . . (mills/KWHe). (B-78)

Total Fuel Energy Cost Equations

Core: $\bar{e}_c = \bar{e}_{c,BU} + \bar{e}_{c,inv} + \bar{e}_{c,proc}$ . . . . . (Case A,B) . . (mills/KWHe)

$\bar{e}_c^* = \bar{e}_{c,BU}^* + \bar{e}_{c,inv}^* + \bar{e}_{c,proc}^*$ . . . . . (Case A*) . . . (mills/KWHe)

Blanket: $\bar{e}_b = \bar{e}_{b,mat} + \bar{e}_{b,proc}$ . . . . . (Case A) . . . (mills/KWHe)

$\bar{e}_b^* = \bar{e}_{b,mat}^* + \bar{e}_{b,proc}^*$ . . . . . (Case A*) . . . (mills/KWHe)

Reactor: $\bar{e} = \bar{e}_c$ . . . . . (Case B) . . . (mills/KWHe)

$\bar{e} = \bar{e}_c + \bar{e}_b$ . . . . . (Case A) . . . (mills/KWHe)

$\bar{e}^* = \bar{e}_c^* + \bar{e}_b^*$ . . . . . (Case A*) . . . (mills/KWHe)

Plant Power Rating

$Pe = 0.2\ V_c$ . . . . . (Case A,B) . . (MWe) . . . . . (B-64)

$Pe^* = 0.222\ V_c$ . . . . . (Case A*) . . . (MWe) . . . . . (B-65)

(V_c in liters)

TABLE B.2 - ASSUMPTIONS

1. Geometry
   - . Spherical core
   - . Infinite outer region (for criticality calculation)
   - . Blanket Volume = 3 x core volume (for blanket processing cost calculation)

2. For Case A, there is no Pu239 burnup in the blanket (blanket power fraction is zero).*

   For Case A*, Pu 239 burnup in the blanket is accounted for (blanket power fraction is 0.1).*

3. Core rated power density is independent of core size.

4. No fissile material is loaded in the blanket.

5. Core and blanket have the same one group cross sections (no spectral effects).

6. No higher isotopes of Plutonium are considered.

7. Core enrichment is uniform (no zoned enrichment scheme).

8. Increased control requirements for internal breeding ratios substantially above unity are ignored.

9. There are no sodium void coefficient restrictions on the size of a spherical core.

* For blanket irradiation times near six years, U238 fission provides about 15% of blanket energy.

TABLE B.3 - REGION COMPOSITIONS AND ONE-GROUP DATA

Region	Nuclide	Volume Fraction	Theoretical Atom Density $\left(\frac{\text{atom}}{\text{barn-cm}}\right)$	σ_a (barns)	$\nu\sigma_f$ (barns)	σ_t (barns)	η	Composite Parameters
Core	U238(oxide)	0.3	0.024	0.35	0.14	7.65	0.4	D_c=core diff. coeff $\simeq$ 1.65cm
	Pu239(oxide)		0.025	2.36	5.66	8.0	2.4	$\Sigma_{a,p}$=non-fuel
	Na	0.55	0.025	0.0016		3.29		absorption
	Fe	0.15	0.085	0.010		2.50		$\simeq$0.0002 cm^{-1}
Blanket	U238(oxide)	0.6	0.024	0.35	0.14	7.65	0.4	D_b=blanket diff. coeff. $\simeq$ 1.966 cm
(Case A,	Na	0.2	0.025	0.0016		3.29		
A*)	Fe	0.2	0.085	0.010		2.50		X_b=0.04 cm^{-2}
Na Reflec-	Na	1.0	0.024	0.0016		3.29		D_b=4.05 cm
tor (case B)								X_b=0.00314 cm^{-2}

TABLE B.4 - ECONOMICS DATA

Pu239	(C_{49})	$10,000 $/kg Pu239
Fabrication Costs		
core	($C_{c,fab}$)	314 $/kgHM (Pu+U)
Blanket	($C_{b,fab}$)	69
Reprocessing Costs		
core	($C_{c,repr}$) . . .	31.5 $/kgHM (Pu + U)
Blanket	($C_{b,repr}$) . . .	31.5
Utility Company Financial Paramters		
Income Tax Rate	(τ)	0.5
Capital Structure		
Bond Fraction	(f_b)	0.5
Stock Fraction	(f_s)	0.5
Rates of Return		
Bonds	(r_b)	0.07
Stocks	(r_s)	0.125
Discount Rate*	(x)	
* $x = (1-\tau) f_b r_b + r_s f_s$	. . . .	0.08

TABLE B.5 - PLANT POWER RELATED PARAMETERS AND BATCH FUEL TIMING

Rated Core Power Density	(q''')	500 kw_t/liter
Plant Load Factor	(L)	0.8
Net Thermal Efficiency	(η)	0.4
Fuel Irradiation Times		
core	(T_c)	2 years
blanket	(T_b)	6 years
Pre and Post-Irradiation Times (core and Blanket)		
material purchase	(T'_{mp})	0.5 years
fabrication	(T_{fab})	0.5
reprocessing	(T''_{repr})	0.5
material credit	(T''_{mc})	0.5

determined above.

B.2.2 Derivation of Equations

B.2.2.1 Neutronic and Depletion Equations

Critical Core Buckling

The one-group criticality equation for a spherical core surrounded by an infinite outer region is

$$B_c R_c \cot B_c R_c = 1 - \frac{D_b}{D_c} (X_b R_c + 1) \qquad \text{(B-1)}$$

where

B_c^2 = (critical core buckling)

$$= \frac{k_{\infty_c} - 1}{L_c^2} = \frac{1}{D_c} [\upsilon \Sigma_{f,c} - \Sigma_{a,c}] ,$$

$$X_b^2 = \frac{1 - k_{\infty_b}}{L_b^2} = -B_b^2 = \frac{1}{D_b} [\Sigma_{a,b} - \upsilon \Sigma_{f,b}] ,$$

R_c ≡ core radius

D_i ≡ diffusion coefficient, region i

$\Sigma_{f,i}$ ≡ macroscopic fission cross section, region i

$\Sigma_{a,i}$ ≡ macroscopic absorption cross section, region i

υ ≡ neutron yield per fission

subscript i = c (core)

= b (outer region)

The "outer region (b)" is either a breeding blanket (Case A) or a sodium reflector (Case B). In the latter case, the outer region is not a multiplying medium, and $X_b^2 = 1/L_b^2$, as usual.

The core radius expressed in terms of core volume (V_c) is given by

$$R_c = (3/4 \ \pi \ V_c)^{1/3}$$

$$= 6.24 \ V_c^{1/3} \qquad \text{(B-2)}$$

where V_c is in liters, and R_c is in centimeters. Equation (B-1) thus becomes

$$B_c(6.24 \ V_c^{1/3}) \cot B_c(6.24 \ V_c^{1/3}) = - \frac{D_b}{D_c} [X_b(6.24 \ V_c^{1/3}) + 1] \qquad \text{(B-3)}$$

Using the data of Table 6.3, Equation (B-3) becomes

$$6.24 \ V_c^{1/3} \ B_c \cot\left(6.24 \ V_c^{1/3} \ B_c\right) = -0.3 \ V_c^{1/3} - 0.1915 \text{..Case A} \qquad \text{(B-4A)}$$

$$= -0.04815 \ V_c^{1/3} - 1.4561 \text{ Case B} \qquad \text{(B-4B)}$$

Critical Core Enrichment

For a given core volume, the transcendental Equation (B-4A) or (B-4B) is solved for critical core buckling, by trial and error, or graphically. An expression relating critical core enrichment (ϵ_c) and critical core buckling is developed below.

The core diffusion equation, for criticality, is

$$D_c \nabla^2 \phi - \Sigma_{a,c} \phi + \upsilon \Sigma_{f,c} \phi = 0 \qquad \text{(B-5)}$$

or

$$\nabla^2 \phi + B_c^2 \phi = 0$$

where

$$B_c^2 = \frac{\upsilon \Sigma_{f,c} - \Sigma_{a,c}}{D_c}$$

or

$$-D_c B_c^2 - \Sigma_{a,c} + \upsilon \Sigma_{f,c} = 0 \qquad \text{(B-6)}$$

But

$$\nu \Sigma_{f,c} = \nu_{28} \Sigma_{f,c,28} + \nu_{49} \Sigma_{f,c,49}$$

$$= \eta_{28} \Sigma_{a,c,28} + \eta_{49} \Sigma_{a,c,49} \qquad \text{(B-7)}$$

where the subscripts 28 and 49 denote U238 and Pu239 respectively. Substituting (B-7) into (B-6),

$$\eta_{28} \Sigma_{a,c,28} + \eta_{49} \Sigma_{a,c,49} = \Sigma_{a,c} + D_c B_c^2 \qquad \text{(B-8)}$$

Letting

$\Sigma_{a,c,p}$ ≡ non-fuel, macroscopic absorption cross section in the core,

the total core macroscopic cross section is given by

$$\Sigma_{a,c} = \Sigma_{a,c,28} + \Sigma_{a,c,49} + \Sigma_{a,c,p} \qquad \text{(B-9)}$$

Substituting (B-9) into (B-8) one obtains

$$(\eta_{28}-1) \Sigma_{a,c,28} + (\eta_{49} - 1) \Sigma_{a,c,49}$$

$$= \Sigma_{a,c,p} + D_c B_c^2 \qquad \text{(B-10)}$$

The heavy metals uranium and plutonium have approximately the same theoretical number densities in the form of oxides (Table B.3). Thus their macroscopic cross sections may be expressed in terms of enrichment, as follows:

$$\Sigma_{a,c,49} = N_{49}^* \epsilon_c \theta_{c,ox} \sigma_{a,49} \qquad \text{(B-11)}$$

$$\Sigma_{a,c,28} = N_{28}^* (1 - \epsilon_c) \theta_{c,ox} \sigma_{a,28} \qquad \text{(B-12)}$$

where

N_{49}^{*} , N_{28}^{*} ≡ theoretical number densities of Pu239 and U238 in the form of oxides, atoms/barn-cm

ϵ_c ≡ critical core enrichment

≡ Pu239 number density/(Pu239 number density + U238 number density)

$\theta_{c,ox}$ ≡ volume fraction of oxide in core (B-13)

$\sigma_{a,49}$ ≡ Pu239 microscopic absorption cross section, barns

$\sigma_{a,28}$ ≡ U238 microscopic absorption cross section, barns.

Substituting (B-11) and (B-12) into (B-10) and solving for critical core enrichment,

$$\epsilon_c = \frac{\Sigma_{a,c,p} + D_c B_c^2 - (\eta_{28}-1)\, N_{28}^{*}\, \theta_{c,ox}\, \sigma_{a,28}}{(\eta_{49}-1)\, N_{49}^{*}\, \theta_{c,ox}\, \sigma_{a,49} - (\eta_{28}-1)\, N_{28}^{*}\, \theta_{c,ox}\, \sigma_{a,28}} \quad \text{(B-14)}$$

Assuming the representative values

$$\Sigma_{a,c,p} = 0.0002 \quad cm^{-1}$$

$$\theta_{c,ox} = 0.3$$

and using the one group data of Table B.3, Equation (B-14) becomes

$$\epsilon_c = 0.0651 + 62.76\, B_c^2 \quad \text{(B-15)}$$

Critical Core Mass (Pu239)

Equation (B-15) is used to determine the critical core enrichment, using the critical core buckling found from Equation (B-4A) or (B-4B). Critical core mass (Pu239), $M_{c,49}^{0}$, may be computed from enrichment as follows:

$$M^0_{c,49} = \epsilon_c M_{c,HM} = \epsilon_c V_c \theta_{c,ox} \varphi_{ox} C \qquad \text{(B-16)}$$

where

M^0_{49} ≡ critical core fissile mass (kg)

φ_{ox} ≡ oxide density ≃ 10 (kg HM oxide/liter HM oxide)

C ≡ 0.88 (kg HM/kg HM oxide)

$M_{c,HM}$ = mass of heavy metal (U + Pu) in the core (kg).

For an oxide volume fraction of 0.3,

$$M_{c,49} = 2.64\ V_c \epsilon_c$$
$$M_{c,HM} = 2.64\ V_c \qquad \text{(B-17)}$$

Breeding Ratios

The Pu239 inventories in discharged core and blanket fuel are to be expressed in terms of internal (core) and external (blanket) breeding ratios, respectively. Internal breeding ratio (b_i) is defined as

$$b_i \equiv \frac{\text{Pu239 production rate in the core}}{\text{Pu239 consumption rate in the core}} \qquad \text{(B-18)}$$

Thus

$$b_i = \frac{N_{c,28}\ \sigma_{c,28}}{N_{c,49}\ \sigma_{a,49}} = \frac{1-\epsilon_c}{\epsilon_c}\ \frac{\sigma_{c,28}}{\sigma_{a,49}} \qquad \text{(B-19)}$$

where

$\sigma_{c,28}$ ≡ U238 microscopic capture cross section

$\sigma_{a,49}$ ≡ Pu239 microscopic absorption cross section.

Using the cross section data of Table B.3,

$$b_i = 0.1255\ \frac{1-\epsilon_c}{\epsilon_c} \qquad \text{(B-20)}$$

The external breeding ratio (b_x) is defined as follows:

$$b_x \equiv \frac{\text{Pu239 production rate in the blanket}}{\text{Pu239 consumption rate in the core}} \qquad \text{(B-21)}$$

Thus,

$$b_x = \left\{\frac{\text{core neutron leakage rate}}{\text{Pu239 consumption rate in core}}\right\} \cdot \left\{\frac{\text{U238 capture rate in the blanket}}{\text{core neutron leakage rate}}\right\} \qquad \text{(B22)}$$

Assuming no leakage from the outer face of the blanket, and no blanket multiplication,

$$b_x = \left(\frac{D_c B_c^2}{N_{49}^* \epsilon_c \theta_{c,ox} \sigma_{a,49}}\right) \cdot \left(\frac{\Sigma_{c,b,28}}{\Sigma_{a,b}}\right) \qquad \text{(B-23)}$$

where

$\Sigma_{c,b,28}$ = U238 macroscopic capture cross section in the blanket

$\Sigma_{a,b}$ ≡ total macroscopic absorption cross section in the blanket

Using the data of Tabe B.3,

$$b_x = 76.19 \frac{B_c^2}{\epsilon_c} \qquad \text{(B-24)}$$

Discharge Pu239 Inventories

The change in core Pu239 inventory over the fuel lifetime in the core is given by

$$\Delta M_{c,49}(T_c) \equiv M_{c,49}(T_c) - M^0_{c,49}$$

$$= (\text{Pu239 atom production rate} - \text{Pu239 atom consumption rate})_{core} \times T_c \, G$$

$$= \left(\frac{\text{Pu239 atom production rate}}{\text{Pu239 atom consumption rate}} \times \frac{\text{Pu239 atom consumption rate}}{\text{total fission rate}} \times \text{total fission rate} \right)_{core} \times T_c \, G$$

$$- \left(\frac{\text{Pu239 atom consumption rate}}{\text{total fission rate}} \times \text{total fission rate} \right)_{core} \times T_c G$$

$$= b_i \left(\frac{1+\alpha_{49}}{1+\delta_c} \right) \frac{(1-f)\,LQ}{EPF} T_c \, G$$

$$- \left(\frac{1+\alpha_{49}}{1+\delta_c} \right) \frac{(1-f)\,LQ}{EPF} T_c \, G$$

$$= \left(\frac{1+\alpha_{49}}{1+\delta_c} \right) \frac{(1-f)\,LQ}{EPF} T_c \, G \, (b_i - 1) \,, \qquad \text{B-25)}$$

where

$\Delta M_{c,49}(T_c)$ ≡ change in core Pu239 inventory over fuel lifetime, kg

$M_{c,49}(T_c)$ ≡ discharge Pu239 inventory, core, kg.

$\alpha_{49} \equiv \sigma_{c,49} / \sigma_{f,49}$

$\delta_c \equiv N_{c,28} \, \sigma_{f,28} / N_{c,49} \, \sigma_{f,49}$

f ≡ fraction of reactor power produced in the blanket

Q ≡ rated reactor thermal power, kw_t

$T_c \equiv$ fuel residence time in core, years

$L \equiv$ plant load factor

$G \equiv 39.67 \times 10^{-26}$ kg Pu239/atom Pu239

$EPF \equiv$ energy per fission $= 1.016 \times 10^{-21}$ kw-yr/fission

Evaluating the constant, G/EPF, and substituting

$$\Delta M_{c,49}(T_c) = \frac{1 + \alpha_{49}}{1 + \delta_c} (1-f)\, LQ\, T_c\, (b_i - 1) \times 3.9045 \times 10^{-4} \quad \text{(B-26)}$$

Letting

$$\frac{1 + \alpha_{49}}{1 + \delta_c} \simeq 1.04 \quad \text{(B-27)}$$

and assuming negligible blanket power,

$$f \simeq 0, \quad \text{(B-28)}$$

equation (B-26) becomes

$$\Delta M_{c,49}(T_c) = LQT_c\, (b_i - 1) \times 4.06 \times 10^{-4} \quad \text{(B29)}$$

A similar development for the blanket yields

$$\Delta M_{b,49}(T_b) \equiv M_{b,49}(T_b) - M^0_{b,49} \quad \text{(B-30)}$$

$$= \left[b_x(1-f)\left(\frac{1+\alpha_{49}}{1+\delta_c}\right) - f\left(\frac{1+\alpha_{49}}{1+\delta_b}\right)\right] T_b LQ \times 3.9045 \times 10^{-4}$$

where

$\Delta M_{b,49}(T_b)$ ≡ change in blanket Pu239 inventory over fuel lifetime, kg

$M^0_{b,49}$ ≡ load Pu239 inventory in blanket kg

$M_{b,49}(T_b)$ ≡ discharge Pu239 inventory, blanket kg

$\delta_b \equiv N_{b,28}\ \sigma_{f,28} / N_{b,49}\ \sigma_{f,49}$

T_b ≡ fuel residence time in blanket kg

Using Equations (B-27) and B-28), Equation (B-30) reduces to

$$\Delta M_{b,49}(T_b) = LQT_b\ b_x \times 4.06 \times 10^{-4} \qquad \text{(B-31)}$$

Rated thermal power (Q) is given by

$$Q = q'''_c\ V_c$$

where q'''_c is the rated core thermal power density in kw_t/liter. Equations (B-29) and (B-31) become

$$\Delta M_{c,49}(T_c) = Lq'''_c V_c T_c (b_i - 1) \times 4.06 \times 10^{-4} \qquad \text{(B-32)}$$

and

$$\Delta M_{b,49}(T_b) = Lq'''_c V_c T_b\ b_x \times 4.06 \times 10^{-4} \qquad \text{(B-33)}$$

Using the values for q'''_c, L, T_c and T_b from Table B.5, Equations (B-32) and (B-33) become

$$\Delta M_{c,49} = 0.325\ (b_i - 1)\ V_c \qquad \text{(B-34)}$$

$$\Delta M_{b,49} = 0.975\ b_x\ V_c \qquad \text{(B-35)}$$

The Pu239 inventory changes during irradiation were defined above as

$$\Delta M_{c,49}(T_c) = M_{c,49}(T_c) - M^0_{c,49}$$

$$\Delta M_{b,49}(T_b) = M_{b,49}(T_b) - M^0_{b,49}$$

Combining these definitions with (B-34) and (B-35), using Equation (B-17) for $M^0_{c,49}$, and assuming that no Pu239 is loaded in the blanket, one obtains

$$M_{c,49} = 2.64\ V_c\ \epsilon_c + 0.325\ (b_i - 1)\ V_c \qquad \text{(B-36)}$$

and

$$M_{b,49} = 0.975\ b_x\ V_c \qquad \text{(B-37)}$$

B.2.2.2 Economics Equations

The expressions for levelized unit energy costs (mills/KWHe) associated with regions under batch management are derived in Chapter 2. The following cost components are identified with each region: material purchase, fabrication, reprocessing, and material credit. Each of these components are further subdivided into direct and carrying charge subcomponents, such that for region "s", component "q",

$$(\text{cost})_{s,q} = (\text{direct cost})_{s,q}\ F_q\ (T_s) \qquad \text{(B-38)}$$

$$(\text{carrying charge})_{s,q} = (\text{direct cost})_{s,q}\,(F_q(T_s) - 1)$$

$$= (\text{direct cost})_{s,q}\ f_q\ (T_s) \qquad \text{(B-39)}$$

where $F_q(T_s)$ is a carrying charge factor emerging from the levelizing process and T_s is the residence time of region "s" fuel. Expressions for the carrying charge factors are derived in terms of utility company financial parameters in Chapter 2.

For the purposes of this study, the cost components and subcomponents are re-aggregated as follows:

(1) core direct material components (direct material purchase and direct material credit) are combined to form the core "burnup" or "depletion" component, $\bar{e}_{c,BU}$ (mills/KWHe);

(2) carrying charges associated with the core material components (material purchase and material credit) are combined to form the core "inventory" component, $\bar{e}_{c,inv}$(mills/KWHe);

(3) core fabrication and reprocessing components (including their direct and carrying charges) are combined to form the core "processing" component, $\bar{e}_{c,proc}$ (mills/KWHe);

(4) blanket material components (including their direct and carrying charges) are combined to form the blanket material component, $\bar{e}_{b,mat}$ (mills/KWHe); and

(5) blanket fabrication and reprocessing components (including their direct and carrying charges) are combined to form the blanket "processing" component, $\bar{e}_{b,proc}$ (mills/KWHe).

Core Fuel Energy Costs

From the cost equations derived in Chapter 2, the core fuel energy costs defined above are given by

$$\bar{e}_{c,BU} = \frac{1000}{ET_c} C_{49} \Delta M_{c,49}(T_c) = \frac{1000}{ET_c} C_{49} [M^0_{c,49} - M_{c,49}(T_c)] \quad \text{(B-40)}$$

$$\bar{e}_{c,inv} = \frac{1000}{ET_c} C_{49} [M^0_{c,49} f_{mp}(T_c) - M_{c,49}(T_c) f_{mc}(T_c)] \quad \text{(B-41)}$$

$$\bar{e}_{c,proc} = \frac{1000}{ET_c} M_{c,HM} [C_{c,fab} F_{fab}(T_c) + C_{c,repr} F_{repr}(T_c)] \quad \text{(B-42)}$$

where

$E \equiv$ electric energy produced per year, kwhe/year

$$= 8760 \eta L q^m_c V_c \quad \text{(B-43)}$$

$\eta \equiv$ net thermal efficiency, kw_e/kw_t

Chapter 2 gives expressions for the carrying charge factors, F(=1+f), in terms of utility company financial parameters:

$$f_{mp}(T_c) = F_{mp}(T_c) - 1$$

$$= \frac{1}{1-\tau}\left[(1+x)^{T'_{mp}+1/2T_c} - \tau \right] - 1 \qquad \text{(B-44)}$$

$$f_{mc}(T_c) = F_{mc}(T_c) - 1$$

$$= (1+x)^{-(T''_{mc}+1/2T_c)} - 1 \qquad \text{(B-45)}$$

$$F_{fab}(T_c) = \frac{1}{1-\tau}\left[(1+x)^{T'_{fab}+1/2T_c} - \tau \right] \qquad \text{(B-46)}$$

$$F_{repr}(T_c) = (1+x)^{-(T''_{repr}+1/2T_c)} \qquad \text{(B-47)}$$

Using the data of Tables B.4 and B.5,

$$f_{mp}(T_c=2) = 0.2445$$
$$f_{mc}(T_c=2) = -0.1089$$
$$F_{fab}(T_c=2) = 1.2445$$
$$F_{repr}(T_c=2) = 0.8911$$

Further, using Equations (B-36), (B-17) and the data of Tables B.4 and B.5, Equations (B-40), (B-41), and (B-42) become

$$\bar{e}_{c,BU} = -1.16\,(b_i-1) \qquad \text{(B-48)}$$

$$\bar{e}_{c,inv} = 3.335\,\epsilon_c + 0.1260\,(b_i-1) \qquad \text{(B-49)}$$

$$\bar{e}_{c,proc} = 0.3964 \qquad \text{(B-50)}$$

The total fuel energy cost associated with the core, $\bar{e}_c$, is given by

$$\bar{e}_c = \bar{e}_{c,BU} + \bar{e}_{c,inv} + \bar{e}_{c,proc}$$

$$= 3.335 \in_c - 1.034 \ (b_i - 1) + 0.3964 \qquad \text{(B-51)}$$

Blanket Fuel Energy Costs

From the cost equations derived in Chapter 2, the blanket fuel energy costs defined above are

$$\bar{e}_{b,mat} = \frac{1000}{ET_b} \ C_{49} \ [M^0_{b,49} \ F_{mp}(T_b) - M_{b,49}(T_b) \ F_{mc}(T_b) \ ] \qquad \text{(B-52)}$$

$$\bar{e}_{b,proc} = \frac{1000}{ET_b} \ M_{b,HM} \ [\ C_{b,fab} \ F_{fab}(T_b) + C_{b,repr} \ F_{repr}(T_b) \ ] \qquad \text{(B-53)}$$

where E is given by Equation (B-43).

From Chapter 2,

$$F_{mp}(T_b) = \frac{1}{1-\tau}[\ (1+x)^{T'_{mp}+1/2T_b} - \tau \ ] \qquad \text{(B-54)}$$

$$F_{mc}(T_b) = (1+x)^{-(T''_{mc} + 1/2T_b)} \qquad \text{(B-55)}$$

$$F_{fab}(T_b) = \frac{1}{1-\tau} \ [\ (1+x)^{T'_{fab}+1/2T_b} - \tau \ ] \qquad \text{(B-56)}$$

$$F_{repr}(T_b) = (1+x)^{-(T''_{repr}+1/2T_b)} \qquad \text{(B-57)}$$

Using the data of Tables B.4 and B.5,

$$F_{mp}(T_b=6) = 1.6175$$
$$F_{mc}(T_b=6) = 0.7641$$
$$F_{fab}(T_b=6) = 1.6175$$
$$F_{repr}(T_b=6) = 0.7641$$

For the purposes of estimating blanket processing costs, the blanket volume is assumed to be three times the core volume,

$$V_b = 3\ V_c\ ; \tag{B-58}$$

and

$$M_{b,HM} = 3\ V_c\ \theta_{b,ox}\ \varphi_{ox}\ C$$

where

$\theta_{b,ox}$ ≡ oxide volume fraction, blanket

φ_{ox} ≡ oxide density

C ≡ 0.88 (kgHM/ kgHM oxide)

Further it is assumed that no Pu239 is loaded in the blanket,

$$M^{0}_{b,49} = 0 \tag{B-59}$$

Using Equations (B-54), (B-55), (B-43), (B-59), the material carrying charges factor above, and data from Tables B.4 and B.5, Equation (B-52) becomes

$$\bar{e}_{b,mat} = -0.886\ b_x \tag{B-60}$$

Using Equations (B-56), (B-57), (B-43), the processing carrying charge factors above, and data from Tables B.4 and B.5, Equation (B-53) becomes

$$\bar{e}_{b,proc} = 0.2555 \tag{B-61}$$

The total fuel energy cost associated with the blanket, $\bar{e}_b$, is given by

$$\bar{e}_b = \bar{e}_{b,mat} + \bar{e}_{b,proc}$$

$$= -0.886\ b_x + 0.2555 \tag{B-62}$$

B.2.2.3 Rated Power and Core Volume

Core rated thermal power is given by

$$Q = q_c''' V_c \qquad kw_t$$

where q_c^m is the rated core power density in kw_t/liter and V_c is the core volume in liters. If the blanket is assumed to produce negligible power (Case A), then plant rated electrical power, P_e, in MWe is

$$P_e = \eta Q \times 10^{-3} = \eta q_c''' V_c \times 10^{-3} \qquad MWe \qquad (B\text{-}63)$$

where η is the net thermal efficiency. For rated core power density of 500 kw_t/liter and a net thermal efficiency of 40%,

$$P_e = 0.2\ V_c \qquad MWe \qquad (B\text{-}64)$$

If the blanket is assumed to produce 10% of the total thermal power (Case A*), then plant rated electrical power, P_e^*, is

$$P_e^* = 0.22\ V_c \qquad MWe \qquad (B\text{-}65)$$

B.2.3.4 Corrections for the Blanket Pu239 Burnup Assumption: Case A*

In deriving the equations above, it was assumed that there was no burnup of Pu239 in the blanket, i.e. that blanket power contribution was approximately zero, and that all of the bred Pu239 was available at end of blanket fuel life.

The assumption has several effects on fuel energy costs. For the same core power rating, the cost components $\bar{e}_{c,BU}$, $\bar{e}_{c,inv}$, $\bar{e}_{c,proc}$, and $\bar{e}_{b,proc}$ are over estimated, since the total delivered energy E, in the denominators of the cost equations, is underestimated. The assumption effects the blanket material component, $\bar{e}_{b,mat}$, a revenue, in two ways, both tending toward an overestimation of this revenue: the total delivered

energy E is underestimated (denominator) and the discharge Pu239 inventory $M_{b,49}$ (numerator) is overestimated.

Corrections for the assumption are developed in this section. Numerical comparisons of Cases A and A* are given in Section B.4.

Correction Factors for Blanket Discharge Pu239 Inventory

The assumption in question causes the blanket Pu239 discharge inventory to be overestimated. To compensate for this, a correction factor (C F) is defined

$$CF \equiv M^*_{b,49}(T_b) \,/\, M_{b,49}(T_b) \tag{B-66}$$

where

$M_{b,49}(T_b)$ ≡ blanket Pu239 discharge inventory assuming no Pu239 burnup (Case A).

$M^*_{b,49}(T_b)$ ≡ blanket Pu239 discharge inventory, allowing for Pu239 burnup (Case A*)

The correction factor CF is estimated by two methods below.

Method (1)

The "true" discharge inventory, $M^*_{b,49}(T_b)$, is given by Equation (B-30) while the assumed discharge inventory $M_{b,49}(T_b)$ is found by setting blanket power fraction (f) equal to zero in Equation (B-30). Using Equation (B-30) and Equation (B-66),

$$CF = 1\text{-}f - (f/b_x)\left[(1 + \delta_c)/(1 + \delta_b)\right] \tag{B-67}$$

The parameters δ_c and δ_b are given by

$$\delta_c = \frac{N_{c,28}}{N_{c,49}} \frac{\sigma_{f,28}}{\sigma_{f,49}} = \frac{1-\epsilon_c}{\epsilon_c} \frac{\sigma_{f,28}}{\sigma_{f,49}} \tag{B-68}$$

and

$$\delta_b = \frac{N_{b,28}}{N_{b,49}} \frac{\sigma_{f,28}}{\sigma_{f,49}} = \frac{1-\epsilon_b}{\epsilon_b} \frac{\sigma_{f,28}}{\sigma_{f,49}}$$

where ϵ_b is some representative Pu239 fraction in the blanket, i.e. at midpoint of an equilibrium cycle. Letting

$$\epsilon_c \simeq 0.15$$

$$\epsilon_b \simeq 0.02$$

and using the cross section data of Table B.3, one finds

$$\frac{1 + \delta_c}{1 + \delta_b} = 0.5$$

Assuming an external breeding ratio (b_x) of ~ 0.5 and a blanket power fraction (f) of ~ 10%,

$$CF \simeq 0.8 \qquad \text{(B-69)}$$

Method (2)

The U238, Pu239 population equations, in terms of flux time (θ), are

$$\frac{dN_{b,28}}{d\theta} + \sigma_{c,28} N_{b,28} = 0$$

$$\frac{dN_{b,49}}{d\theta} + \sigma_{a,49} N_{b,49} = \sigma_{c,28} N_{b,28}$$

Assuming $N^0_{b,49} = 0$, and that $\sigma_{a,49} N_{b,49} \neq 0$, the solution for $N_{b,49}$ is

$$N^*_{b,49} = N^0_{b,28} \frac{\sigma_{c,28}}{\sigma_{a,49} - \sigma_{a,28}} \exp(-\sigma_{a,28}\theta)\left[1 - \exp(-[\sigma_{a,49} - \sigma_{a,28}]\theta)\right] \qquad \text{(B-70)}$$

(Case A*)

The solution, assuming that $N^0_{b,49} = 0$ and that $\sigma_{a,49} N_{b,49} = 0$, is

$$N_{b,49} = N^{0}_{b,28} \quad \frac{\sigma_{c,28}}{\sigma_{a,28}} \quad [\ 1\text{-exp}\ (-\sigma_{a,28}\theta)\ ] \qquad \text{(B-71)}$$

(Case A)

Thus,

$$CF = \frac{N^{*}_{b,49}}{N_{b,49}} = \frac{e^{-\sigma_{a,28}\theta} - e^{-\sigma_{a,49}\theta}}{1 - e^{-\sigma_{a,28}\theta}} \qquad \text{(B-72)}$$

For a blanket flux of 10^{15} n/cm^2 sec and irradiation time of six years,

$$\theta \simeq 1.9 \times 10^{23} \quad \text{n/cm}^2$$

Using the cross section data of Table B.3,

$$CF \simeq 0.76 \qquad \text{(B-73)}$$

which is in rough agreement with the CF computed by the first method.

Corrections to the Economic Equations

A blanket power fraction of 10% and blanket discharge Pu239 correction factor (CF) of 0.80 are assumed (Method 1).

Quantities with a superscript asterisk (*) denote Case A* (with blanket burnup) values; those without asterisks denote Case A (without blanket Pu239 burnup).

With f=10%,

$$E^{*} = E/0.9 \qquad \text{(B-74)}$$

and

$$\bar{e}^{*}_{c,BU} = 0.9\ \bar{e}_{c,BU} \qquad \text{(B-75)}$$

$$\bar{e}^{*}_{c,inv} = 0.9\ \bar{e}_{c,inv} \qquad \text{(B-76)}$$

$$\bar{e}^{*}_{c,proc} = 0.9\ \bar{e}_{c,proc} \tag{B-77}$$

$$\bar{e}^{*}_{b,proc} = 0.9\ \bar{e}_{b,proc} \tag{B-78}$$

The blanket material component is corrected both for E and $M_{b,49}$

$$\bar{e}^{*}_{b,mat} = (0.9)\ (0.8)\ \bar{e}_{b,mat} = 0.72\ \bar{e}_{b,mat} \tag{B-79}$$

B.3 SAMPLE CALCULATION

Table B.6 presents sample calculations for Cases A, A* and B, for a core of 4000 liters.

B.4 RESULTS

Neutronics

Principal neutronics results are given in Figures B.1 and B.2. Core critical enrichments for Cases A, A* (breeding blanket) and Case B (sodium reflector) are plotted versus core volume in Figure B.1. Breeding ratios are shown as a function of core volume in Figure B.2. Enrichments and breeding ratios are independent of the blanket burnup assumption, with core volume as the independent variable. Another scale is shown to relate core volume to plant power rating.

As expected, critical enrichment and external breeding ratio decrease with core size, while internal breeding ratio increases. Case B (sodium reflector) enjoys slightly lower critical enrichment than Cases A, A* (breeding blanket). The lower critical enrichment of Case B improves its internal breeding ratio, but not enough to offset the sacrifice of external breeding.

TABLE B.6 - SAMPLE CALCULATIONS

	CASE(1)		
	A	A*	B
Core Volume, V_c(liters)	4000	4000	4000
Reactor Power Rating, Pe(MWe)	800	890	800
Critical Buckling, $B_c^2(cm^{-2})$	0.0007156	0.0007156	0.000552
Critical Enrichment, ϵ_c	0.1096	0.1096	0.0994
Critical Mass, $M^0_{c,49}$(kg)	1155	1155	1050
Internal Breeding Ratio, b_i	1.0198	1.0198	1.1367
External Breeding Ratio, b_x	0.4976	0.4976	-
Total Breeding Ratio, b	1.5174	1.5174	1.1367
Discharge Pu239			
Core(T_c=2yr), $M_{c,49}$(kg)	1181	1181	1228
Blanket(T_b=6yr), $M_{b,49}$(kg)	1940	1550	-
Fuel Energy Costs (mills/KWHe):			
Core Burnup, $\bar{e}_{c,BU}$	-0.0229	-0.0203	-0.1585
Core Inventory, $\bar{e}_{c,inv}$	0.3675	0.3300	0.3490
Core Processing, $\bar{e}_{c,proc}$	0.3964	0.357	0.3964
Core Total, $\bar{e}_c$	0.7410	0.666	0.5869
Blanket Material, $\bar{e}_{b,mat}$	-0.441	-0.318	-
Blanket Processing, $\bar{e}_{b,proc}$	0.2555	0.230	-
Blanket Total, $\bar{e}_b$	-0.1855	-0.088	-
Reactor Total, $\bar{e}$	0.5555	0.4805	0.5869

(1) Case A: Spherical core with breeding blanket (No Pu239 burnup in blanket)
Case A*: Spherical core with breeding blanket (with Pu239 burnup in blanket)
Case B: Spherical core with sodium reflector

FIG. B.1 CRITICAL CORE ENRICHMENT AS A FUNCTION OF CORE VOLUME

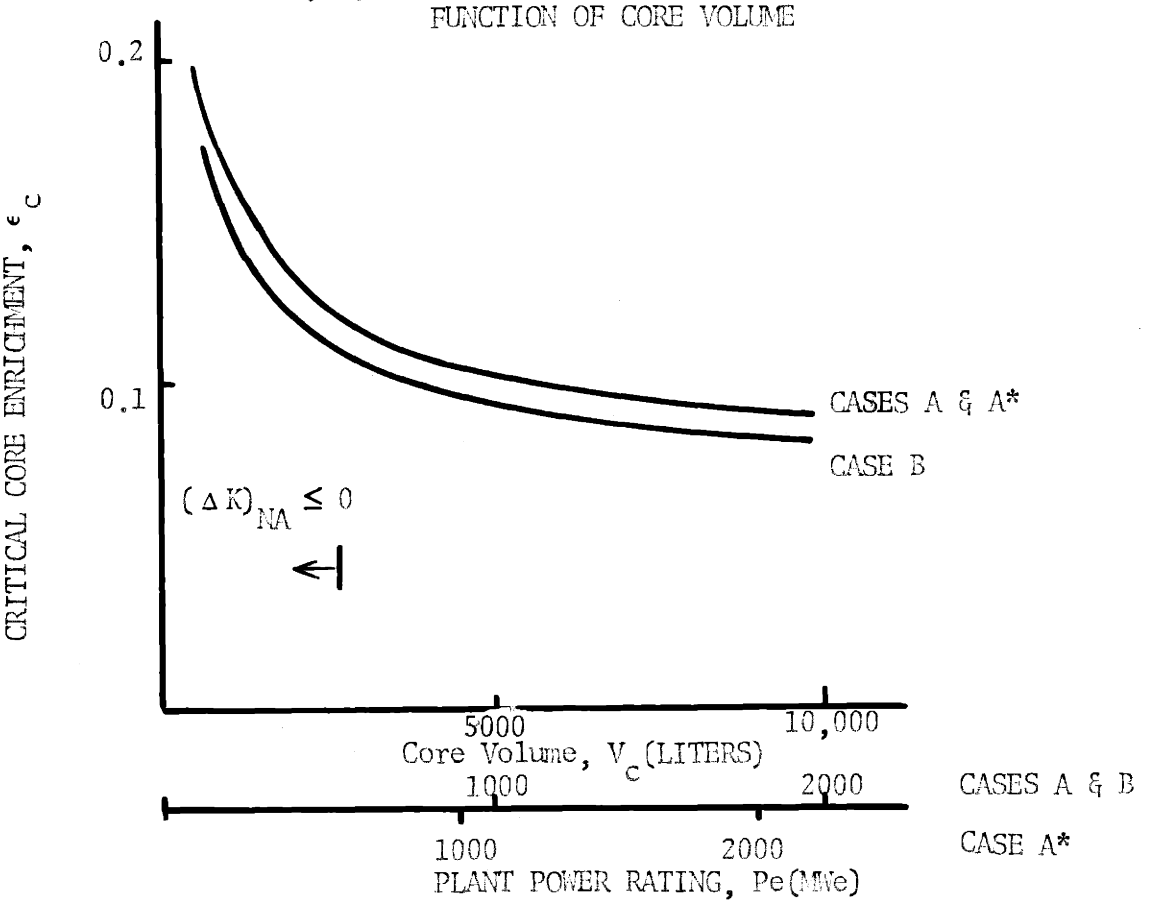

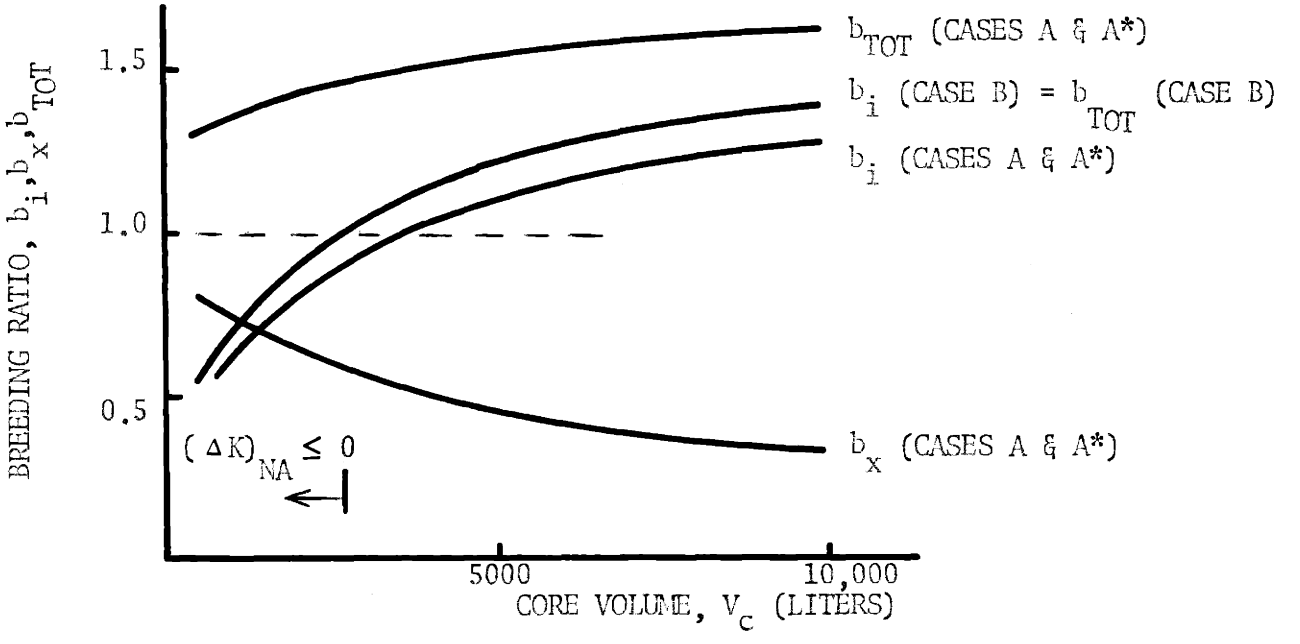

FIG. B.2 BREEDING RATIOS AS FUNCTION OF CORE VOLUME

Case A versus Case A*:

Effect of Blanket Pu239 Burnup Assumption

The "no blanket power" (no blanket burnup) assumption affects energy costs (mills/KWHe) in several ways. For the same core power rating,

(a) the core fuel cost components (burnup, inventory and processing) are overestimated since the total energy delivered, in the denominators of the cost equations, is underestimated;

(b) the blanket processing component is similarly overestimated;

(c) the blanket material component, a revenue, is overestimated because the discharge Pu239 inventory is overestimated and the total energy delivered is underestimated.

Figures B.3 and B.4 show the effects (on energy costs) of the "no blanket power" assumption. In Figure B.3, the assumption is seen to lead to an overprediction, $\bar{e}_{TOT} > \bar{e}^*_{TOT}$, of order 0.05 mills/KWHe. This is not insignificant compared to the effects of the radial design and management changes demonstrated in Chapter 5. Figure B.4 compares the blanket costs (net revenues), with and without the "no blanket power" assumption. The assumption is seen to favor blanket revenue significantly, $\bar{e}_b < \bar{e}_b^*$. This bias is, however, offset by the overestimation of core fuel costs.

Cases A, A* versus Case B:

A Breeding Blanket versus A Sodium Reflector

Figure B.5 shows the total reactor fuel energy costs as functions of plant power rating, for cases A, A* and B. The breeding blanket is seen to be advantageous to about 1350 MWe (Case A), or to about 1600 MWe (Case A*). The indifference points are not sharp and definitive, owing to the similarity of the slopes of the curves; a slight change in the economic environment could have a large effect on the indifference point. Beyond

FIG. B.3 EFFECT OF BLANKET BURNUP (POWER FRACTION) ASSUMPTION ON REACTOR FUEL ENERGY COSTS

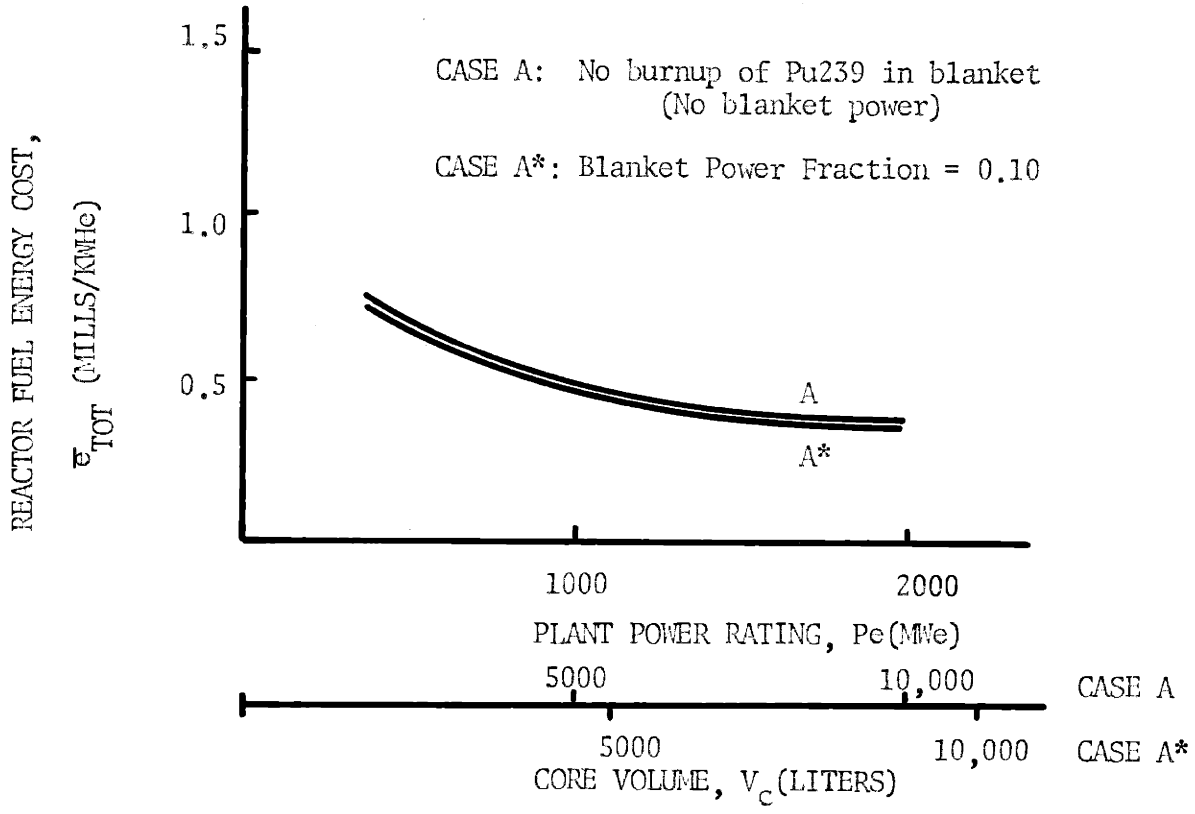

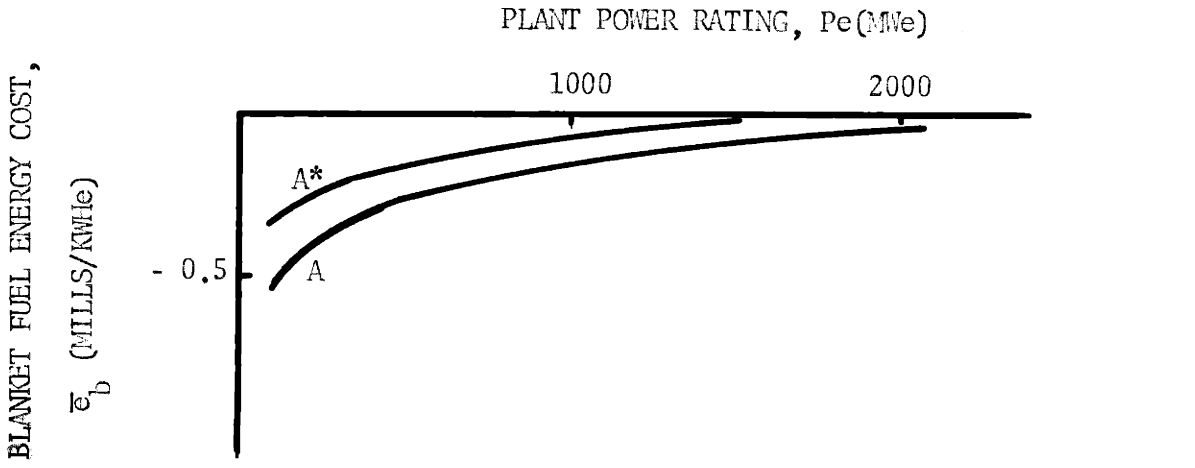

FIG. B.4 EFFECT OF BLANKET BURNUP (POWER FRACTION) ASSUMPTION ON BLANKET FUEL ENERGY COSTS

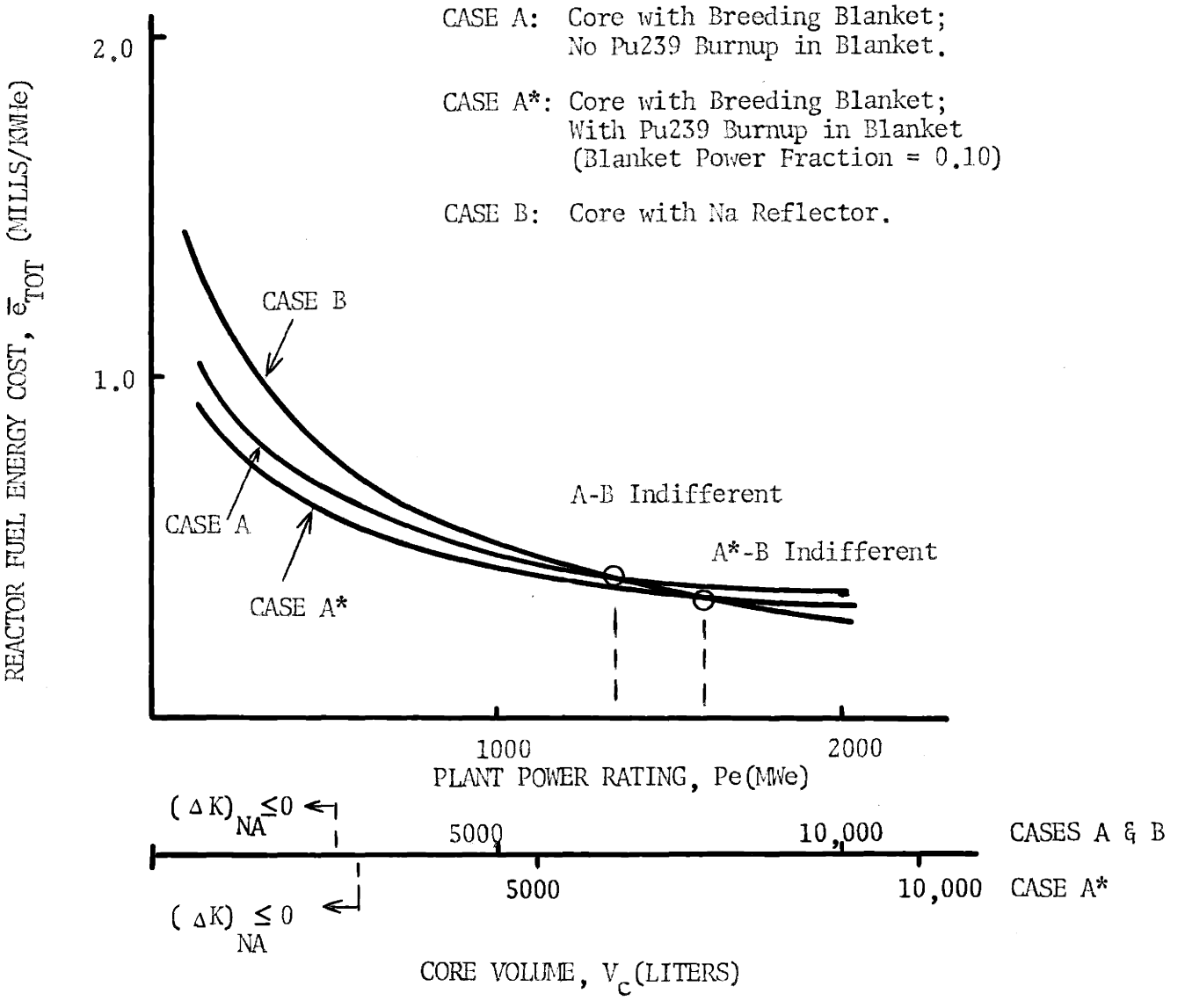

FIG. B.5 REACTOR FUEL ENERGY COSTS WITH AND WITHOUT A BREEDING BLANKET

the indifference points, the advantage of the reflector-only configuration is very slight.

The fuel-economic advantages and disadvantages of substituting a non-breeding reflector for a breeding blanket, in large LMFBRs, are summarized qualitatively in Table B.7, and are shown quantitatively, component-by-component, in Figures B.6 and B.7.

Figure B.6 shows the total core fuel energy costs for Cases A and B. The difference $\Delta \bar{e}_c$ is the savings in core fuel energy cost occasioned by the substitution of a sodium reflector for the breeding blanket. The savings is seen to increase with core size. Figure B.7 disaggregates the core fuel savings, $\Delta \bar{e}_c$, into its components $\Delta \bar{e}_{c,inv}$ and $\Delta \bar{e}_{c,BU}$. The improvement is seen to result largely from the burnup component savings, $\Delta \bar{e}_{c,BU}$ (higher internal breeding ratio), the inventory savings $\Delta \bar{e}_{c,Inv.}$ being practically negligible.

Offsetting the core savings $\Delta \bar{e}_c$ is the loss of net blanket revenue, $\Delta \bar{e}_b$, as shown in Figure B.7.

Core Size and the Sodium Void Coefficient

Terasawa et.al. (55) have performed parametric studies similar to the study described above. As in the present study, spherical geometry was adopted. The Terasawa study was confined to LMFBR neutronics and involved sodium void and Doppler coefficients, in addition to the variables of the present study, e.g. core volume, critical enrichment, breeding ratios, etc.

Of particular interest are their results concerning enrichment (core size), sodium void coefficient, and internal breeding ratio. The studies reveal that for a sodium volume fraction above about 10% (structure $\simeq$ 15%, fuel $\leq$ 75%), it is impossible to have both (a) an internal breeding ratio above unity and (b) a negative sodium void coefficient (50% sodium loss). For a fuel volume fraction of 30% (assumed in present studies),

TABLE B.7 - ADVANTAGES AND DISADVANTAGES OF SUBSTITUTING A SODIUM REFLECTOR FOR A BREEDING BLANKET

Advantages	Disadvantages
CORE	
1. Lower core inventory cost due to lower critical enrichment; $\Delta \bar{e}_{c,\,inv}$	
2. Higher internal breeding performance (lower burnup cost) due to lower critical enrichment; $\Delta \bar{e}_{c,BU}$	
OUTER REGION	
3. No processing costs $\longleftarrow \Delta \bar{e}_b \longrightarrow$	4. No external breeding

FIG. B.6 CORE FUEL ENERGY COSTS FOR REACTORS WITH AND WITHOUT BREEDING BLANKETS

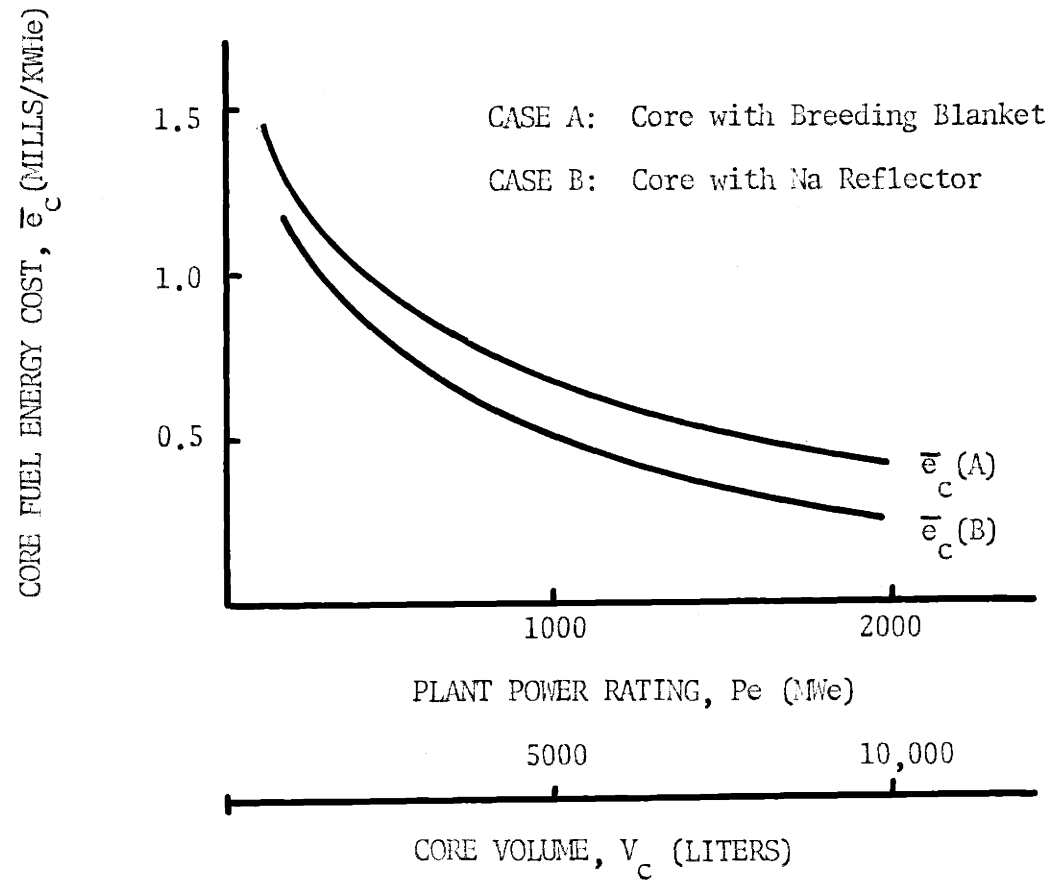

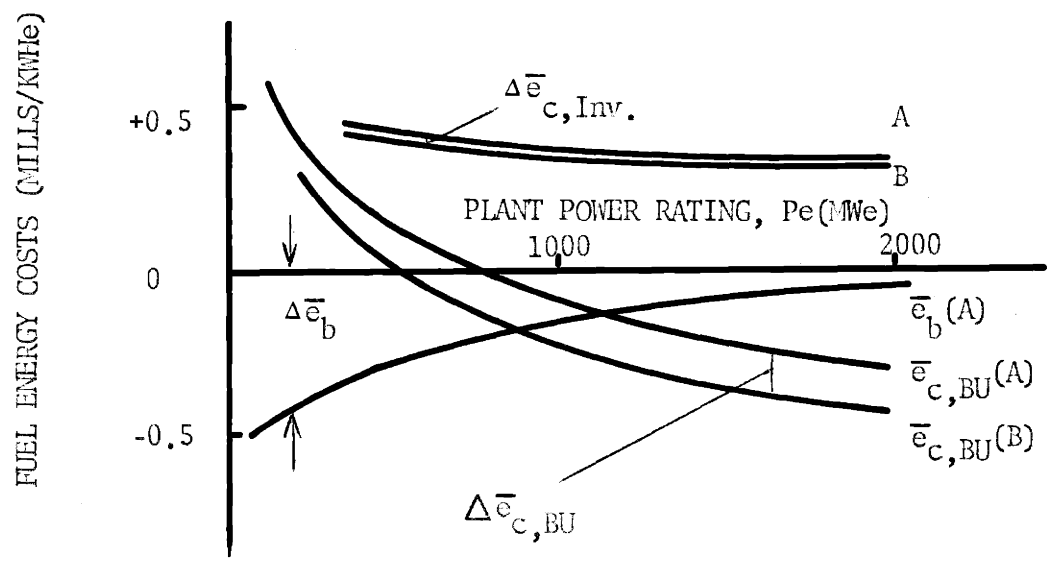

FIG. B.7 FUEL ENERGY COST COMPONENTS FOR REACTORS WITH AND WITHOUT BREEDING BLANKETS

(a) $b_i \geq 1$ for $\epsilon_c \leq 0.107$

(b) $(\Delta k)_{Na} \leq 0$ for $\epsilon_c \geq 0.12$

where Terawawa's atom ratio, E'_c (= Pu239/U238), has been converted to enrichment ϵ_c (= Pu239/Pu239+U238). The threshold (a) for b_i=1 is confirmed by the present study, Figures B.1 and B.2.

From Figure B.1, the enrichment (b) of 12% occurs at a core volume of 2700 liters, or reactor power rating of 540 MWe (case A) or 600 MWe (Case A*). Thus, from Figure B.5, the breeding blanket cases are preferable to the sodium reflector case, for conservatively permissible values of sodium void coefficient (≤ 0). For core volumes greater than 2700 liters, core geometry may be altered to increase leakage, to maintain a negative sodium void coefficient. This would favor external breeding.

Discussion

Several major assumptions were adopted in this study - not only to simplify the analysis, but also to provide a net bias against the blanket concept:

(1) Minimum leakage geometry (spherical) was assumed throughout the range of core volumes considered. In actual design, the core geometry may have to be "spoiled" to enhance the negative component of the sodium void coefficient in large FBRs .

(2) It was assumed that blanket volume was three times core volume. Thus while the leakage decreases as core size increases, the blanket continues to be charged with constant processing charge per unit energy delivered. In actual design practice, the blanket size would be optimized, and one would expect the blanket-to-core volume ratio to decrease with core size.

(3) In Case A, blanket power (blanket Pu239 burnup) was neglected. This assumption was seen to disfavor the blanket concept.

(4) Blanket cross sections were assumed to be the same as for the core. In reality, blanket spectra will be softer, favoring external breeding.

(5) A one zone core was assumed. An optimal material loading pattern would call for some multi-zone enrichment scheme, with outer core zones having higher load enrichments, (52, 53), tending to increase blanket flux.

(6) The study did not account for increased control costs and control absorption neutronic penalties associated with increasing internal breeding ratio substantially above unity.

In spite of these penalties, the blanket concept is seen to be economically desireable (over the no-blanket configuration) to an "indifference point" somewhat over 1000 MWe. Beyond this "indifference point", the advantage of the sodium reflector (no blanket) configuration is very slight.

APPENDIX C

SPP1A, A DEPLETION-ECONOMICS PROGRAM FOR FAST BREEDER REACTORS

C.1 DESCRIPTION OF PROGRAM

The program SPP1A performs depletion-economics calculations for fast breeder reactors under fixed-element fuel management schemes, i.e. batch or scatter management. Input includes fuel cycle cost information and the neutronics data (local fluxes and spectrum-weighted cross sections) from a single physics compution. The program uses the "Semi-Analytic Depletion Method (SAM)" described in Chapter 3 to obtain local nuclide concentrations as functions of irradiation time. The cash flow equations developed in Chapter 2 are used to compute local and aggregate fuel costs in mills/KWHe, \$/yr/kgHM, and \$/kgHM as functions of irradiation time. Chapter 4 gives a step-by-step procedure for using the FBR fuel depletion-economics model embodied in SPP1A.

Local fluxes and cross sections may be taken from a multigroup physics program run for the reactor configuration assumed. Using these local ϕ's and σ's, SPP1A solves for time-dependent concentrations in Equations (3-9). The cost equations (2-30), (2-33), and (2-34) are then used to obtain local (by depletion zone), annular-regional, and major regional (i.e. core, axial blanket, radial blanket) fuel costs as functions of irradiation time.

C.2 INPUT INSTRUCTIONS

Table C.1 describes the input data for SPP1A. Control constants and economic data for a single computer run are given on cards 1 through 9. Neutronic data for each depletion zone are provided by cards 10 through 14, each zone having an individual set 10-14.

TABLE C.1

SPP1A INPUT

Variable	Columns	Format	Description
CARD 1			
ID(11)	1-66	11A6	Identification card.
CARD 2			
NCASE	1-6	I6	The number of depletion zones.
NVR	7-12	I6	The number of contiguous depletion zones per region,e.g. annular region. Although each zone is depleted individually, discharge compositions and economics are computed by regions which may consist of more than one zone.
NPRINT	13-18	I6	If NPRINT=0, print out of zone depletion and economics results is omitted. Only region results are printed. If NPRINT= 1, both zone and region results are printed.
CARD 3			
NTS	1-6	I6	The number of time steps. Depletion and economics results are printed out after each time step.
CARD 4			
DT	1-12	F12.8	Duration of a time step, full power days.
CARD 5			
EFF	1-12	F12.8	Net thermal efficiency.
CARD 6			
F$KGHM	1-10	F10.2	Unit fabrication cost, $/KGHM
R$KGHM	11-20	F10.2	Unit reprocessing cost, $/KGHM
S$KG49	21-30	F10.2	Price of Pu239, $/KG Pu239

Variable	Columns	Format	Description
CARD 6 (continued)			
S$KG28	31-40	F10.2	Price of U238, $/KG U238
S$KG40	41-50	F10.2	Price of Pu240, $/KG Pu240
S$KG41	51-60	F10.2	Price of Pu241, $/KG Pu241
S$KG42	61-70	F10.2	Price of Pu242, $/KG Pu242
CARD 7			
TAX	1-12	F12.8	Income tax rate
BDRTE	13-24	F12.8	Bondholders' rate of return
BDFRN	25-36	F12.8	Bond Fraction
SKRTE	37-48	F12.8	Stockholders' rate of return
SKFRN	49-60	F12.8	Stock fraction
CARD 8			
SLF	1-12	F12.8	Plant load factor
CAPMWE	13-24	F12.8	Plant rated capacity, MWe
CARD 9			
TFPRE	1-12	F12.8	Time prior to beginning of irradiation that fabrication cash flow occurs, years.
TMPPRE	13-24	F12.8	Time prior to beginning of irradiation that material purchase cash flow occurs, years.
TRPPST	25-36	F12.8	Time after end of irradiation that reprocessing cash flow occurs, years.
TMCPST	37-48	F12.8	Time after end of irradiation that material credit occurs, years.

Note: There are NCASE sets of Cards 10-14, each set corresponding to a single depletion zone. Zone neutronic data is provided on Cards 10-14.

CARD 10			
SIGA28	1-12	F12.8	U238 microscopic absorption cross section, barns.

Variable	Colums	Format	Description
CARD 10 (continued)			
SIGF28	13-24	F12.8	U238 microscopic fission cross section, barns.
SIGA49	25-36	F12.8	Pu239 microscopic absorption cross section, barns
SIGF49	37-48	F12.8	Pu239 microscopic fission cross section, barns
CARD 11			
SIGA40	1-12	F12.8	Pu240 microscopic absorption cross section, barns
SIGF40	13-24	F12.8	Pu240 microscopic fission cross section, barns
SIGA41	25-36	F12.8	Pu241 microscopic absorption cross section, barns
SIGF41	37-48	F12.8	Pu241 microscopic fission cross section, barns
SIGA42	49-60	F12.8	Pu242 microscopic absorption cross section, barns
SIGF42	61-72	F12.8	Pu242 microscopic fission cross section, barns
CARD 12			
FLUX	1-12	F12.8	Neutron flux, 10^{15} n/cm^2-sec
CARD 13			
U28NO	1-12	F12.8	Initial U238 atom density, atoms/barn-cm
P49NO	13-24	F12.8	Initial Pu239 atom density, atoms/barn-cm
P40NO	25-36	F12.8	Initial Pu240 atom density, atoms/barn-cm
P41NO	37-48	F12.8	Initial Pu241 atom density, atoms/barn-cm
P42NO	49-60	F12.8	Initial Pu242 atom density, atoms/barn-cm
CARD 14			
VOL	1-12	F12.8	Zone volume, liters

C.3 SAMPLE PROBLEM

This section describes an SPP1A computer run for the reference LMFBR radial blanket (Figure 4.2).

The radial blanket is divided into fifteen depletion zones. These depletion zones were combined to form five annular regions, three depletion zones per annular region. Figure C.1 shows the input data card deck. The reference economic environment, Table 4.2, is assumed. Depletion zone neutronic data is taken from a 26 energy group multigroup computation using the program 2DB. Figure C.2 is SPP1A printed output giving composition and economics results for the innermost annular region (V) at an irradiation time of 3 years. The same computer run yields similar printed output for each of the NTS irradiation intervals, for each of the annular regions. Depletion-economics of each depletion zone can be obtained as well, by setting the control constant NPRINT equal to or greater than unity. Table C.2 interprets the variable names and table headings appearing in printed output.

FIG. C.1 SPP1A SAMPLE PROBLEM INPUT DECK

```
SPP1A SAMPLE PROBLEM:   REFERENCE RAD BLANKET (SPP1A#1.03)
   15      3      0
   16
  150.00
  0.388198      10.00
  69.00    31.50      10000.0    0.0    0.0    0.0    0.0
  0.5      0.07       0.5        0.125  0.5
  0.823    1000.0
  0.5      0.5        0.5        0.5
 0.3669    0.02363    3.016      2.246
  1.151    0.2557     4.613      3.844      0.8939     0.1784
 2.5735
 0.0109 E 00
 200.28
 0.3752    0.0258     3.153      2.325
 1.223     0.2483     4.881      4.057      0.9499     0.1714
 1.778
 0.0109 E 00
  200.28
  0.4479   0.009459   4.512      3.112
  1.961    0.167      7.653      6.298      1.508      0.09461
 0.5483
 0.0109 E 00
  320.44
  0.3905   0.01610    3.400      2.463
  1.343    0.2131     5.379      4.453      1.036      0.1378
 1.87895
 0.0109 E 00
```

FIG. C.1 SPPIA SAMPLE PROBLEM INPUT DECK - CONTINUATION

```
208.14
0.3991      0.01531     3.558       2.555
 1.431      0.2070      5.687       4.700       1.103       0.1321
1.30035
0.0109 E 00
208.14
 0.4669     0.007158    4.868       3.321
 2.174      0.1512      8.381       6.891       1.662       0.07968
0.40861
0.0109 E 00
333.00
 0.4251     0.009883    3.980       2.797
 1.657      0.1731      6.530       5.375       1.271       0.1001
1.13375
0.0109 E 00
439.82
 0.4339     0.009347    4.159       2.903
 1.762      0.1686      6.884       5.662       1.350       0.09584
0.7874
0.0109 E 00
439.82
 0.4954     0.004854    5.429       3.651
 2.510      0.1336      9.535       7.836       1.911       0.06311
0.255475
0.0109 E 00
703.72
 0.4734     0.005180    4.875       3.321
 2.170      0.1382      8.310       6.815       1.658       0.06721
```

FIG. C.1 SPPIA SAMPLE PROBLEM INPUT DECK - CONTINUATION

```
0.53545
0.0109 E 00
471.24
 0.4822      0.004876     5.082       3.445
 2.298       0.1351       8.730       7.160       1.754       0.06436
0.37464
0.0109 E 00
471.24
 0.5371      0.002824     6.343       4.193
 3.069       0.1157       11.44       9.409       2.326       0.04632
0.127945
0.0109 E 00
753.98
 0.5328      0.002663     6.248       4.138
 2.985       0.1146       11.11       9.104       2.279       0.04518
0.197415
0.0109 E 00
 765.76
 0.5436      0.002481     6.548       4.317
 3.176       0.1122       11.75       9.635       2.419       0.04301
0.141005
0.0109 E 00
 765.76
 0.5990      0.001527     8.023       5.197
 4.101       0.1002       15.09       12.44       3.097       0.03223
0.05346
0.0109 E 00
 1225.22
```

FIG. C.2 SPPIA SAMPLE PROBLEM PRINTED OUTPUT (PARTIAL)

```
                                                RTIMEY        TIMED
                                                2.99605656        900.0000
     AFT              AEFTOT           ABNUP          APFRN
    0.11294E 00      0.23992E 05      0.77238E 04     0.10348E-01
     AU28M            AP49M            AP40M          AP41M          AP42M
    0.29754E 04      0.99274E 02      0.60680E 01     0.27195E 00    0.97431E-02
     A28MR            A49MR            A40MR          A41MR          A42MR              EPS
     0.05788616       0.03195970       0.00195349      0.00008755     0.00000314        0.03204725
   CCFMP        CCFF         CCFRP        CCFMC
   0.3324451    0.3324451   -0.1425308   -0.1425308
   CCFMP        CCFF         CCFRPB       CCFMCB
   0.3324451    0.3324451   -0.2850618   -0.2850618

POWER COSTS (MILLS/KWH)
  MATPUR          FAB          REPR(A)      MATCRE(A)        TOTALS(A)         REPR(B)      MATCRE(B)        TOTALS(B)
  0.0          0.00992267    0.00452992   -0.04596025      -0.03150767      0.00452992   -0.04596025      -0.03150767      DIRECT
  0.0          0.00329874   -0.00064565    0.00655075       0.00920384     -0.00129131    0.01310151       0.01510894      CARCHG
  0.0          0.01322141    0.00388426   -0.03940950      -0.02230383      0.00323861   -0.03285874      -0.01639873      TOTALS
    MATERIAL                          PROCESSING                        TOTALS                          METHOD(A)
       DIR(BU)       -0.04596025          DIR          0.01445259       -0.03150767 DIRECT
       CARCHG(INV)    0.00655075          CARCHG       0.00265309        0.00920384 CARCHG
       TOTMAT        -0.03940951          TOTPROC      0.01710568       -0.02230383 TOTALS
    MATERIAL                          PROCESSING                        TOTALS                          METHOD(B)
       DIR(BU)       -0.04596025          DIR          0.01445259       -0.03150767 DIRECT
       CARCHG(INV)    0.01310151          CARCHG       0.00200744        0.01510894 CARCHG
       TOTMAT        -0.03285875          TOTPROC      0.01646002       -0.01639872 TOTALS

POWER COSTS ($/YR/KGHMLOADED)
  MATPUR          FAB          REPR(A)      MATCRE(A)        TOTALS(A)         REPR(B)      MATCRE(B)        TOTALS(B)
        0.0         23.03         10.51      -106.67           -73.13            10.51      -106.67           -73.13      DIRECT
        0.0          7.66         -1.50        15.20            21.36            -3.00        30.41            35.07      CARCHG
        0.0         30.69          9.02       -91.47           -51.77             7.52       -76.26           -38.06      TOTALS
    MATERIAL                          PROCESSING                        TOTALS                          METHOD(A)
       DIR(BU)          -106.67          DIR          33.54            -73.13 DIRECT
       CARCHG(INV)        15.20          CARCHG        6.16             21.36 CARCHG
       TOTMAT            -91.47          TOTPROC      39.70            -51.77 TOTALS
    MATERIAL                          PROCESSING                        TOTALS                          METHOD(B)
       DIR(BU)          -106.67          DIR          33.54            -73.13 DIRECT
       CARCHG(INV)        30.41          CARCHG        4.66             35.07 CARCHG
       TOTMAT            -76.26          TOTPROC      38.20            -38.06 TOTALS

POWER COSTS ($/KGHMLOADED)
  MATPUR          FAB          REPR(A)      MATCRE(A)        TOTALS(A)         REPR(B)      MATCRE(B)        TOTALS(B)
        0.0         69.00         31.50      -319.60          -219.10            31.50      -319.60          -219.10      DIRECT
        0.0         22.94         -4.49        45.55            64.00            -8.98        91.10           105.06      CARCHG
        0.0         91.94         27.01      -274.04          -155.10            22.52      -228.49          -114.03      TOTALS
    MATERIAL                          PROCESSING                        TOTALS                          METHOD(A)
       DIR(BU)          -319.60          DIR         100.50           -219.10 DIRECT
       CARCHG(INV)        45.55          CARCHG       18.45             64.00 CARCHG
       TOTMAT            -274.04          TOTPROC     118.95           -155.10 TOTALS
    MATERIAL                          PROCESSING                        TOTALS                          METHOD(B)
       DIR(BU)          -319.60          DIR         100.50           -219.10 DIRECT
       CARCHG(INV)        91.10          CARCHG       13.96            105.06 CARCHG
       TOTMAT            -228.49          TOTPROC     114.46           -114.03 TOTALS


    MATCRE/MATPUR+FAB+REPR
```

TABLE C.2

INTERPRETATION OF SPP1A PRINTED OUTPUT

Variable	Description	Units
RTIMEY	Actual irradiation time	years
TIMED	Irradiation time in full power days	days
ABNUP	Burnup in the annular region	MWD/MTHM
APFRN	Fraction of total reactor power supplied by the annular region	
	Nuclide Masses:	
AU28M	Mass of U238 in annular region after irradiation	kg
AP49M	Mass of Pu239 in annular region after irradiation	kg
AP40M AP41M AP42M	Masses of Pu239,241,242 in annular region after irradiation	kg
AHMKGL	Initial mass of heavy metal (U+Pu)	kg
	Nuclide Fractions:	
A28MR	AU28M/AHMKGL	
A49MR	AP49M/AHMKGL	
A40MR	AP49M/AHMKGL	
A41MR	AP41M/AHMKGL	
A42MR	AP42MR/AHMKGL	
EPS	Fissile Mass/Initial Mass of Heavy Metal	

Label or Heading	Description
MATPUR	Material Purchase Component
FAB	Fabrication Component
REPR(A)	Reprocessing Component (Tax Method A)

Label or Heading	Description
REPR(B)	Reprocessing Component (Tax Method B)
MATCRE(A)	Material Credit Component (Tax Method A)
MATCRE(B)	Material Credit Component (Tax Method B)
DIR	Direct Component
CACHG	Carrying Charge Component
TOTMAT	Total Material Component (Burnup+Inventory)
TOTPROC	Total Processing Component (fabrication+reprocessing, including their carrying charges)

C.4 FORTRAN LISTING

The SPPLA FORTRAN listing is given on the following pages.

```
C      SPP1-A ..... 'SPECIAL PURPOSE PROGRAM  1-A'                          CARD0001
C                                                                           CARD0002
C      FAST BREEDER REACTOR FUEL DEPLETION AND ECONOMICS CALCULATIONS        CARD0003
C      FBR BLANKET TEST FACILITY, MASSACHUSETTS INSTITUTE OF TECHNOLOGY      CARD0004
C      S.T. BREWER, M.J. DRISCOLL, E.A. MASON                               CARD0005
C         *          *          *          *          *          *           CARD0006
C      GIVEN ECONOMIC PARAMETERS AND LOCAL PHYSICS DATA THIS PROGRAM         CARD0007
C      COMPUTES LOCAL, ANNULAR-REGIONAL, AND REGIONAL (CORE,                 CARD0008
C      AXIAL BLANKET,RADIAL BLANKET)  FUEL COSTS AS FUNCTIONS OF             CARD0009
C      IRRADIATION TIME  UNDER SCATTER OR BATCH FUEL MANAGEMENT SCHEMES.     CARD0010
C         *          *          *          *          *          *           CARD0011
                                                                            CARD0012
       DIMENSION  AU28M(30),AP49M(30),AP40M(30),AP41M(30),AP42M(30)         CARD0013
       DIMENSION  AMPD(30),AFBD(30),ARPD(30),AMCD(30),ADT(30),              CARD0014
      1           AMPCC(30),AFBCC(30),ARPCC(30),AMCCC(30),ACCT(30),         CARD0015
      2           AMPTT(30),AFBTT(30),ARPTT(30),AMCTT(30),AT(30)            CARD0016
       DIMENSION  FAMPD(30),FAFBD(30),FARPD(30),FAMCD(30),FADT(30),         CARD0017
      1           FAMPCC(30),FAFBCC(30),FARPCC(30),FAMCCC(30),FACCT(30),    CARD0018
      2           FAMPTT(30),FAFBTT(30),FARPTT(30),FAMCTT(30),FAT(30)       CARD0019
       DIMENSION  AEFTOT(30),ABNUP(30),SFTV(30),AFT(30)                     CARD0020
                                                                            CARD0021
       DIMENSION   ARPCCB(30),ARPTTB(30),AMCCCB(30),AMCTTB(30),             CARD0022
      1   ACCTB(30),ATB(30)                                                 CARD0023
       DIMENSION   FARPCB(30),FAMCCB(30),FACCTB(30),FARPTB(30),             CARD0024
      1  FAMCTB(30),FATB(30)                                               CARD0025
       DIMENSION  A28MR(30),A49MR(30),A40MR(30),A41MR(30),A42MR(30),        CARD0026
      1  EPS(30)                                                           CARD0027
       DIMENSION  ABU(30),AINV(30),AINVB(30),AMAT(30),AMATB(30),APRSD(30)   CARD0028
      1  ,APRSC(30),APRST(30),APRSCB(30),AAT(30),AATB(30),AADT(30),        CARD0029
      2  AACCT(30),AACCTB(30)                                              CARD0030
       DIMENSION  APRSTB(30)                                                CARD0031
       DIMENSION  ID(11)                                                    CARD0032
       DOUBLE PRECISION  ID                                                 CARD0033
                                                                            CARD0034
                                                                            CARD0035
C      FORMATS FOR READ CARD INPUT                                          CARD0036
```

```
    1  FORMAT(3I6)                                                          CARD0037
    2  FORMAT(4F12.8)                                                       CARD0038
   22  FORMAT(6F12.8)                                                       CARD0039
    3  FORMAT(F12.8)                                                        CARD0040
    4  FORMAT(5F12.8)                                                       CARD0041
    5  FORMAT(F12.8)                                                        CARD0042
    6  FORMAT(I6)                                                           CARD0043
    7  FORMAT(F12.8)                                                        CARD0044
   21  FORMAT(2F12.8)                                                       CARD0045
   31  FORMAT(7F10.2)                                                       CARD0046
   41  FORMAT(5F12.8)                                                       CARD0047
   51  FORMAT(2F12.8)                                                       CARD0048
   61  FORMAT(4F12.8)                                                       CARD0049
C                                                                           CARD0050
                                                                            CARD0051
                                                                            CARD0052
      PRINT 4442                                                            CARD0053
 4442 FORMAT(///99H PROGRAM "SPP1A" * * * * FBR BLANKET TEST FACILITY, M    CARD0054
     1IT * * * * S.T.BREWER, M.J.DRISCOLL, E.A.MASON)                       CARD0055
      PRINT 4443                                                            CARD0056
 4443 FORMAT(//18X,63H FAST BREEDER REACTOR FUEL DEPLETION AND ECONOMICS    CARD0057
     1 CALCULATIONS)                                                        CARD0058
      READ 4444,(ID(I),I=1,11)                                              CARD0059
 4444 FORMAT(11A6)                                                          CARD0060
      PRINT 4445,(ID(I),I=1,11)                                             CARD0061
      PRINT 400                                                             CARD0062
 4445 FORMAT(////24H PROBLEM IDENTIFICATION:, 11A6)                         CARD0063
                                                                            CARD0064
      PRINT 411                                                             CARD0065
                                                                            CARD0066
C     READ AND PRINT CARD INPUT DATA:                                       CARD0067
C       CONTROL CONSTANTS; ECONOMIC AND POWER PARAMETERS                    CARD0068
      READ 1, NCASE,NVR,NPRINT                                              CARD0069
      PRINT 2010                                                            CARD0070
 2010 FORMAT(1X,6H NCASE,3X,4H NVR,1X,7H NPRINT)                            CARD0071
      PRINT 2011, NCASE,NVR,NPRINT                                          CARD0072
```

```
2011 FORMAT(1X,2I6,1X,I6)                                                    CARD0073
                                                                             CARD0074
     READ 6, NTS                                                             CARD0075
     READ 7, DT                                                              CARD0076
     READ 21,EFF,DENOX                                                       CARD0077
     READ 31,F$KGHM,R$KGHM,S$KG49,S$KG28,S$KG40,S$KG41,S$KG42                CARD0078
     READ 41,TAX,BDRTE,BDFRN,SKRTE,SKFRN                                     CARD0079
     READ 51,SLF,CAPMWE                                                      CARD0080
     READ 61,    TFPRE,TMPPRE,TRPPST,TMCPST                                  CARD0081
     PRINT 406                                                               CARD0082
 406 FORMAT(3X,4H NTS)                                                       CARD0083
     PRINT 416, NTS                                                          CARD0084
 416 FORMAT(1X,I6)                                                           CARD0085
     PRINT 407                                                               CARD0086
 407 FORMAT(3X,3H DT)                                                        CARD0087
     PRINT 417,DT                                                            CARD0088
 417 FORMAT(1X,F12.8)                                                        CARD0089
     PRINT 500                                                               CARD0090
 500 FORMAT(1X,19H COST ANALYSIS DATA)                                       CARD0091
     PRINT 598                                                               CARD0092
 598 FORMAT(4X,4H EFF,4X,6X,6H DENOX)                                        CARD0093
     PRINT 599, EFF,DENOX                                                    CARD0094
 599 FORMAT(1X,2F12.6)                                                       CARD0095
     PRINT 531                                                               CARD0096
 531 FORMAT(3X,7H F$KGHM,2X,3X,7H R$KGHM,2X,3X,7H S$KG49,                    CARD0097
    1  2X,3X,7H S$KG28,2X,3X,7H S$KG40,2X,3X,7H S$KG41,2X,3X,7H S$KG42)      CARD0098
     PRINT 532,F$KGHM,R$KGHM,S$KG49,S$KG28,S$KG40,S$KG41,S$KG42              CARD0099
 532 FORMAT(1X,2F12.8,5F12.2)                                                CARD0100
     PRINT 541                                                               CARD0101
 541 FORMAT(3X,4H TAX,5X,3X,6H BDRTE,3X,3X,6H BDFRN,3X,3X,6H SKRTE,3X,       CARD0102
    1 3X,6H SKFRN)                                                           CARD0103
     PRINT 542, TAX,BDRTE,BDFRN,SKRTE,SKFRN                                  CARD0104
 542 FORMAT(1X,5F12.8)                                                       CARD0105
     PRINT 551                                                               CARD0106
 551 FORMAT(3X,4H SLF,5X,3X,7H CAPMWE)                                       CARD0107
     PRINT 552,SLF,CAPMWE                                                    CARD0108
```

```
  552 FORMAT(1X,F12.8,F12.1)                                              CARD0109
      PRINT 561                                                           CARD0110
  561 FORMAT(3X,6H TFPRE,3X,2X,7H TMPPRE,3X,2X,7H TRPPST,3X,2X,           CARD0111
     1 7H TMCPST)                                                         CARD0112
      PRINT 562,TFPRE,TMPPRE,TRPPST,TMCPST                                CARD0113
  562 FORMAT(1X,4F12.8)                                                   CARD0114
                                                                          CARD0115
C     INITIALIZE                                                        CARD0116
      DO 10001  J = 1,30                                                CARD0117
      AU28M(J)  =  0.0                                                  CARD0118
      AP49M(J)  =  0.0                                                  CARD0119
      AP40M(J)  =  0.0                                                  CARD0120
      AP41M(J)  =  0.0                                                  CARD0121
      AP42M(J)  =  0.0                                                  CARD0122
       AMPD(J)  =  0.0                                                  CARD0123
      FAMPD(J)  =  0.0                                                  CARD0124
       AFBD(J)  =  0.0                                                  CARD0125
      FAFBD(J)  =  0.0                                                  CARD0126
       ARPD(J)  =  0.0                                                  CARD0127
      FARPD(J)  =  0.0                                                  CARD0128
       AMCD(J)  =  0.0                                                  CARD0129
      FAMCD(J)  =  0.0                                                  CARD0130
       ADT(J)  =  0.0                                                   CARD0131
      FADT(J)  =  0.0                                                   CARD0132
       AMPCC(J)  =  0.0                                                 CARD0133
      FAMPCC(J)  =  0.0                                                 CARD0134
       AFBCC(J)  =  0.0                                                 CARD0135
      FAFBCC(J)  =  0.0                                                 CARD0136
       ARPCC(J)  =  0.0                                                 CARD0137
      FARPCC(J)  =  0.0                                                 CARD0138
       AMCCC(J)  =  0.0                                                 CARD0139
      FAMCCC(J)  =  0.0                                                 CARD0140
       ACCT(J)  =  0.0                                                  CARD0141
      FACCT(J)  =  0.0                                                  CARD0142
       AMPTT(J)  =  0.0                                                 CARD0143
      FAMPTT(J)  =  0.0                                                 CARD0144
```

```
 AFBTT(J)   =   0.0                                                     CARD0145
FAFBTT(J)   =   0.0                                                     CARD0146
 ARPTT(J)   =   0.0                                                     CARD0147
FARPTT(J)   =   0.0                                                     CARD0148
 AMCTT(J)   =   0.0                                                     CARD0149
FAMCTT(J)   =   0.0                                                     CARD0150
 AT(J)   =   0.0                                                        CARD0151
FAT(J)   =   0.0                                                        CARD0152
ARPCCB(J) =  0.0                                                        CARD0153
ARPTTB(J) =  0.0                                                        CARD0154
AMCCCB(J) =  0.0                                                        CARD0155
AMCTTB(J) =  0.0                                                        CARD0156
ACCTB(J) =  0.0                                                         CARD0157
ATB(J) =  0.0                                                           CARD0158
FARPCB(J) =  0.0                                                        CARD0159
FAMCCB(J) =  0.0                                                        CARD0160
FACCTB(J) =  0.0                                                        CARD0161
FARPTB(J) =  0.0                                                        CARD0162
FAMCTB(J) =  0.0                                                        CARD0163
FATB(J) =  0.0                                                          CARD0164
A28MR(J)   =   0.0                                                      CARD0165
A49MR(J)   =   0.0                                                      CARD0166
A40MR(J)   =   0.0                                                      CARD0167
A41MR(J)   =   0.0                                                      CARD0168
A42MR(J)   =   0.0                                                      CARD0169
EPS(J)   =   0.0                                                        CARD0170
                                                                        CARD0171
ABU(J) =  0.0                                                           CARD0172
AINV(J)   =   0.0                                                       CARD0173
AINVB(J)   =   0.0                                                      CARD0174
AMAT(J)   =   0.0                                                       CARD0175
AMATB(J)   =   0.0                                                      CARD0176
APRSD(J)   =   0.0                                                      CARD0177
APRSC(J)   =   0.0                                                      CARD0178
APRST(J)   =   0.0                                                      CARD0179
APRSCB(J)   =   0.0                                                     CARD0180
```

```
      APRSTB(J)  =  0.0                                                  CARD0181
      AAT(J)  =  0.0                                                     CARD0182
      AATB(J)  =  0.0                                                    CARD0183
      AADT(J)  =  0.0                                                    CARD0184
      AACCT(J)  =  0.0                                                   CARD0185
      AACCTB(J)  =  0.0                                                  CARD0186
      AEFTOT(J)  =  0.0                                                  CARD0187
      ABNUP(J)  =  0.0                                                   CARD0188
      SFTV(J)  =  0.0                                                    CARD0189
      AFT(J)  =  0.0                                                     CARD0190
10001 CONTINUE                                                           CARD0191
                                                                         CARD0192
                                                                         CARD0193
      NCOUNT  =  0.0                                                     CARD0194
      AHMKGL  =  0.0                                                     CARD0195
      ATHMLD  =  0.0                                                     CARD0196
      AVOL  =  0.0                                                       CARD0197
                                                                         CARD0198
      AU28MO = 0.0                                                       CARD0199
      AP49MO = 0.0                                                       CARD0200
      AP40MO = 0.0                                                       CARD0201
      AP41MO = 0.0                                                       CARD0202
      AP42MO = 0.0                                                       CARD0203
      IAR =  0                                                           CARD0204
                                                                         CARD0205
C                                                                        CARD0206
C     CASE LOOP                                                          CARD0207
C     EACH CASE IS A ZONE OR A LOT OF FUEL                               CARD0208
      DO 10 I = 1,NCASE                                                  CARD0209
      NCOUNT  =  NCOUNT  +  1                                            CARD0210
C     READ CARD INPUT FOR CASE # I :  PHYSICS DATA                       CARD0211
      READ 2, SIGA28,SIGF28,SIGA49,SIGF49                                CARD0212
      READ 22, SIGA40,SIGF40,SIGA41,SIGF41,SIGA42,SIGF42                 CARD0213
      READ 3, FLUX                                                       CARD0214
      READ 4, U28NO,P49NO,P40NO,P41NO,P42NO                              CARD0215
      READ 5, VOL                                                        CARD0216
```

```
      PRINT 400                                                                 CARD0217
      PRINT 400                                                                 CARD0218
  400 FORMAT(1H1)                                                               CARD0219
      PRINT 401                                                                 CARD0220
  401 FORMAT(8H CASE NO)                                                        CARD0221
      PRINT 101,I                                                               CARD0222
  101 FORMAT(I6///)                                                             CARD0223
C     PRINT OUT INPUT DECK  IMAGE                                               CARD0224
      PRINT 411                                                                 CARD0225
  411 FORMAT(12X,17H INPUT DECK IMAGE)                                          CARD0226
      PRINT 4111                                                                CARD0227
 4111 FORMAT(1X,23H PHYSICS-DEPLETION DATA)                                     CARD0228
      PRINT 420                                                                 CARD0229
  420 FORMAT(3X,7H SIGA28,2X,3X,7H SIGF28,2X,3X,7H SIGA49,3X,7H SIGF49)         CARD0230
      PRINT 20, SIGA28,SIGF28,SIGA49,SIGF49                                     CARD0231
   20 FORMAT(1X,4F12.8)                                                         CARD0232
      PRINT 367                                                                 CARD0233
  367 FORMAT(3X,7H SIGA40,2X,3X,7H SIGF40,2X,                                   CARD0234
     1   3X,7H SIGA41,2X,3X,7H SIGF41,2X,                                       CARD0235
     2   3X,7H SIGA42,2X,3X,7H SIGF42)                                          CARD0236
      PRINT 368, SIGA40,SIGF40,SIGA41,SIGF41,SIGA42,SIGF42                      CARD0237
  368 FORMAT(1X,6F12.8)                                                         CARD0238
      PRINT 413                                                                 CARD0239
  413 FORMAT(3X,5H FLUX)                                                        CARD0240
      PRINT 403, FLUX                                                           CARD0241
  403 FORMAT(1X,F12.8)                                                          CARD0242
      PRINT 404                                                                 CARD0243
  404 FORMAT(3X,6H U28NO,2X,3X,6H P49NO,2X,3X,6H P40NO,2X,3X,6H P41NO,          CARD0244
     1       2X,3X,6H P42NO)                                                    CARD0245
      PRINT 414, U28NO,P49NO,P40NO,P41NO,P42NO                                  CARD0246
  414 FORMAT(1X,5F12.8)                                                         CARD0247
      PRINT 405                                                                 CARD0248
  405 FORMAT(3X,4H VOL)                                                         CARD0249
      PRINT 415,VOL                                                             CARD0250
  415 FORMAT(1X,F12.8)                                                          CARD0251
C                                                                               CARD0252
```

```
C       CALCULATE CONSTANT PARAMETERS (OUTSIDE THE TIME LOOP)                    CARD0253
        CONSTA = (SIGA28-SIGF28)/(SIGA49-SIGA28)                                 CARD0254
        CONSTB = U28NO*CONSTA                                                    CARD0255
        CB1 = (SIGA49-SIGF49)/(SIGA40-SIGA28)                                    CARD0256
        CB2 = (SIGA49-SIGF49)/(SIGA40-SIGA49)                                    CARD0257
        BETA1 = P40NO-(U28NO*CONSTA*CB1-U28NO*CONSTA*CB2+P49NO*CB2)              CARD0258
        CC1 = (SIGA40-SIGF40)/(SIGA41-SIGA28)                                    CARD0259
        CC2 = (SIGA40-SIGF40)/(SIGA41-SIGA49)                                    CARD0260
        CC3 = (SIGA40-SIGF40)/(SIGA41-SIGA40)                                    CARD0261
        BETA2 = P41NO-(U28NO*CONSTA*CB1*CC1-U28NO*CONSTA*CB2*CC2                 CARD0262
       1   +P49NO*CB2*CC2+BETA1*CC3)                                             CARD0263
        CD1 = (SIGA41-SIGF41)/(SIGA42-SIGA28)                                    CARD0264
        CD2 = (SIGA41-SIGF41)/(SIGA42-SIGA49)                                    CARD0265
        CD3 = (SIGA41-SIGF41)/(SIGA42-SIGA40)                                    CARD0266
        CD4 = (SIGA41-SIGF41)/(SIGA42-SIGA41)                                    CARD0267
        BETA3 = P42NO-(U28NO*CONSTA*CB1*CC1*CD1-U28NO*CONSTA*CB2*CC2*CD2         CARD0268
       1   +P49NO*CB2*CC2*CD2 + BETA1*CC3*CD3 + BETA2*CD4)                       CARD0269
                                                                                 CARD0270
        PRINT 600                                                                CARD0271
  600   FORMAT(1H1)                                                              CARD0272
        PRINT 601                                                                CARD0273
  601   FORMAT(1X,15H OUTPUT FOLLOWS///)                                         CARD0274
        PRINT 602                                                                CARD0275
  602   FORMAT(3X,7H CONSTA)                                                     CARD0276
        PRINT 102,CONSTA                                                         CARD0277
  102   FORMAT(1X,E15.5)                                                         CARD0278
        PRINT 1801                                                               CARD0279
 1801   FORMAT(6X,4H CB1,5X,6X,4H CB2,5X,6X,6H BETA1)                            CARD0280
        PRINT 802, CB1,CB2,BETA1                                                 CARD0281
  802   FORMAT(1X,3E15.5)                                                        CARD0282
        PRINT 803                                                                CARD0283
  803   FORMAT(6X,4H CC1,5X,                                                     CARD0284
       1       6X,4H CC2,5X,                                                     CARD0285
       2       6X,4H CC3,5X,                                                     CARD0286
       3       6X,6H BETA2)                                                      CARD0287
        PRINT 1804,  CC1,CC2,CC3,BETA2                                           CARD0288
```

```
 1804 FORMAT(1X,4E15.5)                                                  CARD0289
      PRINT 805                                                          CARD0290
  805 FORMAT(6X,4H CD1,5X,6X,4H CD2,5X,                                  CARD0291
     1       6X,4H CD3,5X,6X,4H CD4,5X,6X,6H BETA3)                      CARD0292
      PRINT 806,CD1,CD2,CD3,CD4,BETA3                                    CARD0293
  806 FORMAT(1X,5E15.5)                                                  CARD0294
                                                                         CARD0295
C     DOLLAR COST PER LOT                                              CARD0296
      U28MO=U28NO*VOL*395.25                                             CARD0297
      P49MO=P49NO*VOL*396.92                                             CARD0298
      P40MO = P40NO*VOL*398.62                                           CARD0299
      P41MO = P41NO*VOL*400.28                                           CARD0300
      P42MO = P42NO*VOL*401.96                                           CARD0301
      HMKGLD = U28MO + P49MO + P40MO + P41MO + P42MO                     CARD0302
      FAB$L = HMKGLD*F$KGHM                                              CARD0303
      REPR$L = HMKGLD*R$KGHM                                             CARD0304
      SMP$L = P49MO*S$KG49  +  U28MO*S$KG28  +  P40MO*S$KG40     +       CARD0305
     1   P41MO*S$KG41  +  P42MO*S$KG42                                   CARD0306
                                                                         CARD0307
      PRINT 920                                                          CARD0308
  920 FORMAT(4X,6H U28MO,5X,4X,6H P49MO,5X,4X,6H P40MO,5X,4X,6H P41MO,5X CARD0309
     1  ,4X,6H P42MO,5X,5X,7H HMKGLD)                                   CARD0310
      PRINT 921, U28MO,P49MO,P40MO,P41MO,P42MO,HMKGLD                    CARD0311
  921 FORMAT(1X,6F15.5)                                                  CARD0312
                                                                         CARD0313
      PRINT 922                                                          CARD0314
  922 FORMAT(3X,6H SMP$L,3X,3X,6H FAB$L,3X,3X,7H REPR$L)                 CARD0315
      PRINT 923, SMP$L,FAB$L,REPR$L                                      CARD0316
  923 FORMAT(1X,3F12.2)                                                  CARD0317
                                                                         CARD0318
                                                                         CARD0319
      VFOX = HMKGLD/(VOL*DENOX*0.88)                                     CARD0320
      PRINT 901                                                          CARD0321
  901 FORMAT(1X,5H VFOX)                                                 CARD0322
      PRINT 902, VFOX                                                    CARD0323
  902 FORMAT(1X,F12.8)                                                   CARD0324
```

```
C       LEVELIZING PARAMETERS                                                   CARD0325
        TAXF1 = 1.0/(1.0-TAX)                                                   CARD0326
        TAXF2 = TAX/(1.0-TAX)                                                   CARD0327
        DISRTE = (1.0-TAX)*BDRTE*BDFRN  + SKRTE*SKFRN                           CARD0328
C       ACTUAL ANNUAL ENERGY PRODUCED BY REACTOR PLANT(KWH/YEAR)                CARD0329
        AARPE = SLF*CAPMWE*1000.0*8760.0                                        CARD0330
                                                                                CARD0331
                                                                                CARD0332
        AARPT = AARPE/EFF                                                       CARD0333
        PRINT 611                                                               CARD0334
  611   FORMAT(//3X,7H DISRTE)                                                  CARD0335
        PRINT 612, DISRTE                                                       CARD0336
  612   FORMAT(1X,F12.8)                                                        CARD0337
        PRINT 621                                                               CARD0338
  621   FORMAT(//3X,6H AARPE,6X,3X,6H AARPT)                                    CARD0339
        PRINT 622, AARPE,AARPT                                                  CARD0340
  622   FORMAT(1X,2E15.5)                                                       CARD0341
        PRINT 400                                                               CARD0342
C                                                                               CARD0343
C       TIME LOOP                                                               CARD0344
        N = NTS                                                                 CARD0345
        DO 100  J=1,N                                                           CARD0346
        TJ = J                                                                  CARD0347
C       EQUIVALENT FULL POWER TIME                                              CARD0348
        TIMED = TJ*DT                                                           CARD0349
        TIME = TIMED*86400.0                                                    CARD0350
C       CALCULATE U238, PU239, PU240, PU241, PU242                              CARD0351
C         ZONE ATOM DENSITIES (ATOMS/BARN-CM), MASSES (KG)                      CARD0352
        FT = FLUX*TIME*(1.00E-09)                                               CARD0353
        TMFN1 = (EXP(-FT*SIGA28))*(1.0-EXP(-FT*(SIGA49-SIGA28)))                CARD0354
        P49N = (CONSTB*TMFN1)+(P49N0*EXP(-SIGA49*FT))                           CARD0355
        P49M = P49N*VOL*396.92                                                  CARD0356
        U28N = U28N0*EXP(-SIGA28*FT)                                            CARD0357
        U28M = U28N*VOL*395.25                                                  CARD0358
        P40N = U28N0*CONSTA*CB1*EXP(-SIGA28*FT)                                 CARD0359
     1   -U28N0*CONSTA*CB2*EXP(-SIGA49*FT)                                      CARD0360
```

```
     2    +P49NO*CB2*EXP(-SIGA49*FT)                                          CARD0361
     3    +BETA1*EXP(-SIGA40*FT)                                              CARD0362
      P40M = P40N*VOL*398.62                                                  CARD0363
      P41N = U28NO*CONSTA*CB1*CC1*EXP(-SIGA28*FT)                             CARD0364
     1    -U28NO*CONSTA*CB2*CC2*EXP(-SIGA49*FT)                               CARD0365
     2    +P49NO*CB2*CC2*EXP(-SIGA49*FT)                                      CARD0366
     3    +BETA1*CC3*EXP(-SIGA40*FT)                                          CARD0367
     4    +BETA2*EXP(-SIGA41*FT)                                              CARD0368
      P41M = P41N*VOL*400.28                                                  CARD0369
      P42N = U28NO*CONSTA*CB1*CC1*CD1*EXP(-SIGA28*FT)                         CARD0370
     1    -U28NO*CONSTA*CB2*CC2*CD2*EXP(-SIGA49*FT)                           CARD0371
     2    +P49NO*CB2*CC2*CD2*EXP(-SIGA49*FT)                                  CARD0372
     3    +BETA1*CC3*CD3*EXP(-SIGA40*FT)                                      CARD0373
     4    +BETA2*CD4*EXP(-SIGA41*FT)                                          CARD0374
     5    +BETA3*EXP(-SIGA42*FT)                                              CARD0375
      P42M  =  P42N*VOL*401.96                                                CARD0376
C     ACTUAL (REAL) TIME   (YEARS)                                            CARD0377
      RTIMEY = TIMED/(365.0*SLF)                                              CARD0378
                                                                              CARD0379
      IF(NPRINT.LT.1)  GO TO 1401                                             CARD0380
      PRINT 400                                                               CARD0381
      PRINT 713                                                               CARD0382
  713 FORMAT(50X,7H RTIMEY)                                                   CARD0383
      PRINT 703, RTIMEY                                                       CARD0384
  703 FORMAT(50X,F12.8)                                                       CARD0385
 1401 CONTINUE                                                                CARD0386
                                                                              CARD0387
C     PARAMETERS RELATED TO ZONE ENERGY AND POWER                             CARD0388
C      1. ATOMS FISSIONED IN REGION(LOT)                                      CARD0389
      AFIS49= SIGF49*VOL*((EXP(-SIGA49*FT)-1.0)*((CONSTB-P49NO)/SIGA49)       CARD0390
     1   -(EXP(-SIGA28*FT)-1.0)*(CONSTB/SIGA28))*(1.00E+27)                   CARD0391
      AFIS28= SIGF28*VOL*(U28NO/SIGA28)*(1.0-EXP(-SIGA28*FT))*(1.00E+27)      CARD0392
      AFISTT=AFIS49+AFIS28                                                    CARD0393
C      2. FISSION ENERGY RELEASED IN REGION(LOT)    (MWDT)                    CARD0394
      EF49=(3.715)*(1.00E-22)*AFIS49                                          CARD0395
      EF28=(3.715)*(1.00E-22)*AFIS28                                          CARD0396
```

```
      EFTOT=EF49+EF28                                                    CARD0397
C      3. NUMBER OF PU239 ATOMS CONSUMED IN REGION(LOT)                  CARD0398
      ACON49=AFIS49*(SIGA49/SIGF49)                                      CARD0399
C      4. NUMBER OF PU239 ATOMS BRED IN REGION(LOT).                     CARD0400
      ABRD49=AFIS28*((SIGA28-SIGF28)/SIGF28)                             CARD0401
C      5. REGION(LOT) TIME INTEGRAL BREEDING RATIO...                    CARD0402
C              PU239 BRED IN REGION/PU239 CONSUMED IN REGION             CARD0403
      BR1=ABRD49/ACON49                                                  CARD0404
C      6.ACTUAL THERMAL ENERGY RELEASED BY REACTOR DURING IRRADIATION    CARD0405
C             OF THIS LOT(REGION)          (MWDT)                       CARD0406
      TERTR=AARPT*RTIMEY/(24.0*1000.0)                                   CARD0407
C      7. FRACTION OF REACTOR THERMAL ENERGY RELEASED IN THIS REGION(LOT) CARD0408
      PERNL=EFTOT/TERTR                                                  CARD0409
C      8. BURNUP IN REGION (LOT)       (MWDT/MT OF HM LOADED)            CARD0410
      THMLD = HMKGLD/1000.0                                              CARD0411
      BURNUP = EFTOT/THMLD                                               CARD0412
C      9. REGION (LOT) THERMAL POWER AT TIME OF DISCHARGE (RTIMEY)       CARD0413
C           AT RATED PLANT CAPACITY          (MWT)                       CARD0414
      PDMW49=3.715*P49N*SIGF49*FLUX*VOL*(86400.0)*(1.00E-04)             CARD0415
      PDMW28=3.715*U28N*SIGF28*FLUX*VOL*(86400.0)*(1.00E-04)             CARD0416
      PDTOT=PDMW49+PDMW28                                                CARD0417
C      10. REGION (LOT) THERMAL POWER DENSITY AT TIME OF DISCHARGE       CARD0418
C           (RTIMEY)   AT RATED PLANT CAPACITY     (KWT/LITER)          CARD0419
      PDENSD=PDTOT*1000.0/VCL                                            CARD0420
C      11.  ACTUAL (AT LOAD FACTOR)  REGION (LOT)  TIME AVERAGED         CARD0421
C           POWER DENSITY              (KWT/LITER)                       CARD0422
      PDENSA=(EFTOT*SLF*1000.0)/(VOL*TIMED)                              CARD0423
                                                                         CARD0424
      IF(NPRINT.LT.1)  GO TO 1402                                        CARD0425
      PRINT 603                                                          CARD0426
  603 FORMAT(///5X,6H TIMED,4X,                                          CARD0427
     1          6X,3H FT,6X,                                            CARD0428
     2          4X,6H TMFN1,5X,                                         CARD0429
     3          5X,5H U28N,5X,                                          CARD0430
     4          5X,5H U28M,5X,                                          CARD0431
     5          5X,5H P49N,5X,                                          CARD0432
```

```
     6          5X,5H P49M)                                                    CARD0433
      PRINT 613,  TIMED,FT,TMFN1,U28N,U28M,P49N,P49M                          CARD0434
  613 FORMAT(1X,7E15.5)                                                       CARD0435
      PRINT 467                                                               CARD0436
  467 FORMAT(5X,5H P40N,5X,5X,5H P41N,5X,5X,5H P42N)                          CARD0437
      PRINT 468,P40N,P41N,P42N                                                CARD0438
  468 FORMAT(1X,3E15.5)                                                       CARD0439
      PRINT 469                                                               CARD0440
  469 FORMAT(5X,5H P40M,5X,5X,5H P41M,5X,5X,5H P42M)                          CARD0441
      PRINT 470, P40M,P41M,P42M                                               CARD0442
  470 FORMAT(1X,3E15.5)                                                       CARD0443
                                                                              CARD0444
      PRINT 697                                                               CARD0445
  697 FORMAT(4X,7H AFIS49,4X,4X,7H AFIS28,4X,4X,7H AFISTT)                    CARD0446
      PRINT 698,AFIS49,AFIS28,AFISTT                                          CARD0447
  698 FORMAT(1X,3E15.5)                                                       CARD0448
      PRINT 688                                                               CARD0449
  688 FORMAT(4X,5H EF49,6X,4X,5H EF28,6X,4X,6H EFTOT)                         CARD0450
      PRINT 689, EF49,EF28,EFTOT                                              CARD0451
  689 FORMAT(1X,3E15.5)                                                       CARD0452
      PRINT 677                                                               CARD0453
  677 FORMAT(4X,7H ACON49,4X,4X,7H ABRD49,4X,11X,4H BR1)                      CARD0454
      PRINT 678,ACON49,ABRD49,BR1                                             CARD0455
  678 FORMAT(1X,3E15.5)                                                       CARD0456
      PRINT 671                                                               CARD0457
  671 FORMAT(4X,6H TERTR,5X,4X,6H PFRNL,5X,4X,7H BURNUP)                      CARD0458
      PRINT 672, TERTR, PFRNL,BURNUP                                          CARD0459
  672 FORMAT(1X,3E15.5)                                                       CARD0460
      PRINT 673                                                               CARD0461
  673 FORMAT(4X,7H PDMW49,4X,4X,7H PDMW28,4X,4X,6H PDTOT)                     CARD0462
      PRINT 674, PDMW49,PDMW28,PDTOT                                          CARD0463
  674 FORMAT(1X,3E15.5)                                                       CARD0464
      PRINT 675                                                               CARD0465
  675 FORMAT(4X,7H PDENSD,4X,4X,7H PDENSA)                                    CARD0466
      PRINT 676,PDENSD,PDENSA                                                 CARD0467
  676 FORMAT(1X,2E15.5)                                                       CARD0468
```

```
 1402 CONTINUE                                                                  CARD0469
                                                                                CARD0470
                                                                                CARD0471
C      CALCULATE POWER COSTS  (MILLS/KWHE)                                     CARD0472
C      POWER COSTS, DIRECT (MILLS/KWH)                                         CARD0473
       TPPE = 1000.0/(AARPE*RTIMEY)                                            CARD0474
C       MATERIAL PURCHASE                                                      CARD0475
       PCMPD = SMP$L*TPPE                                                      CARD0476
C       FAB                                                                    CARD0477
       PCFBD = FAB$L*TPPE                                                      CARD0478
C       REPROCESSING                                                           CARD0479
       PCRPD = REPR$L*TPPE                                                     CARD0480
C       MATERIAL CREDIT                                                        CARD0481
       SMC$L = P49M*S$KG49  + U28M*S$KG28 + P40M*S$KG40 + P41M*S$KG41          CARD0482
      1     + P42M*S$KG42                                                     CARD0483
                                                                              CARD0484
       IF(NPRINT.LT.1)  GO  TO 1403                                           CARD0485
       PRINT 301                                                              CARD0486
  301  FORMAT(3X,6H SMC$L)                                                    CARD0487
       PRINT 302,SMC$L                                                        CARD0488
  302  FORMAT(1X,F12.2)                                                       CARD0489
       PRINT 2222                                                             CARD0490
 1403  CONTINUE                                                               CARD0491
       PCMCD = -SMC$L*TPPE                                                    CARD0492
C      POWER COSTS,CARRYING CHARGES (MILLS/KWH)                                CARD0493
C      MATERIAL PURCHASE                                                       CARD0494
       TMP = 0.5*RTIMEY + TMPPRE                                              CARD0495
       DISFMP = 1.0/((1.0+DISRTE)**(-TMP))                                    CARD0496
       CCFMP = TAXF1*DISFMP  -  TAXF2  -  1.0                                 CARD0497
       PCMPCC =  (PCMPD)*(CCFMP)                                              CARD0498
       PCMPTT =  PCMPD + PCMPCC                                               CARD0499
C       FAB                                                                   CARD0500
       TFB = 0.5*RTIMEY  +  TFPRE                                             CARD0501
       DISFF = 1.0/((1.0+DISRTE)**(-TFB))                                     CARD0502
       CCFF = TAXF1*DISFF  - TAXF2  -  1.0                                    CARD0503
       PCFBCC = (PCFBD)*(CCFF)                                                CARD0504
```

```
      PCFBTT =  PCFBD + PCFBCC                                          CARD0505
C     REPROCESSING                                                      CARD0506
      TRP =  -(0.5*RTIMEY + TRPPST)                                     CARD0507
      DISFRP = 1.0/((1.0+DISRTE)**(-TRP))                               CARD0508
      CCFRP = DISFRP  -  1.0                                            CARD0509
      PCRPCC = (PCRPD)*(CCFRP)                                          CARD0510
      PCRPTT =  PCRPD + PCRPCC                                          CARD0511
      CCFRPB = TAXF1*DISFRP - TAXF2 - 1.0                               CARD0512
      PCRPCB = (PCRPD)*(CCFRPB)                                         CARD0513
      PCRPTB = PCRPD + PCRPCB                                           CARD0514
C     MATERIAL CREDIT                                                   CARD0515
      TMC = -(0.5*RTIMEY + TMCPST)                                      CARD0516
      DISFMC = 1.0/((1.0+DISRTE)**(-TMC))                               CARD0517
      CCFMC = DISFMC - 1.0                                              CARD0518
      PCMCCC =  (PCMCD)*(CCFMC)                                         CARD0519
      PCMCTT =  PCMCD + PCMCCC                                          CARD0520
      CCFMCB = TAXF1*DISFMC - TAXF2 - 1.0                               CARD0521
      PCMCCB = (PCMCD)*(CCFMCB)                                         CARD0522
      PCMCTB = PCMCD + PCMCCB                                           CARD0523
                                                                        CARD0524
C     TOTALS                                                            CARD0525
C     DIRECT                                                            CARD0526
      PCDT=PCMPD+PCFBD+PCRPD+PCMCD                                      CARD0527
C     CARRYING CHARGE                                                   CARD0528
      PCCCT=PCMPCC+PCFBCC+PCRPCC+PCMCCC                                 CARD0529
      PCCCTB = PCMPCC + PCFBCC + PCRPCB + PCMCCB                        CARD0530
C     GRAND TOTAL                                                       CARD0531
      PCT=PCDT+PCCCT                                                    CARD0532
      PCTB = PCDT + PCCCTB                                              CARD0533
                                                                        CARD0534
      IF(NPRINT.LT.1)  GO TO 1404                                       CARD0535
      PRINT 303                                                         CARD0536
  303 FORMAT(3X,6H CCFMP,3X,3X,5H CCFF,4X,3X,6H CCFRP,3X,3X,6H CCFMC)   CARD0537
      PRINT 304,CCFMP,CCFF,CCFRP,CCFMC                                  CARD0538
  304 FORMAT(1X,4F12.7)                                                 CARD0539
      PRINT 30310                                                       CARD0540
```

```
30310 FORMAT(3X,6H CCFMP,3X,3X,5H CCFF,4X,3X,7H CCFRPB,2X,3X,7H CCFMCB)          CARD0541
      PRINT 3041, CCFMP,CCFF,CCFRPB,CCFMCB                                      CARD0542
 3041 FORMAT(1X,4F12.7)                                                         CARD0543
      PRINT 800                                                                 CARD0544
  800 FORMAT(//24H POWER COSTS (MILLS/KWH))                                     CARD0545
      PRINT 804                                                                 CARD0546
      PRINT 814,PCMPD,PCFBD,PCRPD,PCMCD,PCDT,PCRPD,PCMCD,PCDT                   CARD0547
      PRINT 815,PCMPCC,PCFBCC,PCRPCC,PCMCCC,PCCCT,PCRPCB,PCMCCB,PCCCTB          CARD0548
      PRINT 816,PCMPTT,PCFBTT,PCRPTT,PCMCTT,PCT,PCRPTB,PCMCTB,PCTB              CARD0549
                                                                                CARD0550
 1404 CONTINUE                                                                  CARD0551
C                                                                               CARD0552
                                                                                CARD0553
C     SUM OR AVERAGE OVER ZONES TO OBTAIN ANNULAR REGION RESULTS                CARD0554
      AU28M(J)  =  AU28M(J)  +  U28M                                            CARD0555
      AP49M(J)  =  AP49M(J)  +  P49M                                            CARD0556
      AP40M(J)  =  AP40M(J)  +  P40M                                            CARD0557
      AP41M(J)  =  AP41M(J)  +  P41M                                            CARD0558
      AP42M(J)  =  AP42M(J)  +  P42M                                            CARD0559
                                                                                CARD0560
      AMPD(J)  =  AMPD(J)  +  PCMPD                                             CARD0561
      AMPCC(J)  =  AMPCC(J)  +  PCMPCC                                          CARD0562
      AMPTT(J)  =  AMPTT(J)  +  PCMPTT                                          CARD0563
      AFBD(J)  =  AFBD(J)  +  PCFBD                                             CARD0564
      AFBCC(J)  =  AFBCC(J)  +  PCFBCC                                          CARD0565
      AFBTT(J)  =  AFBTT(J)  +  PCFBTT                                          CARD0566
      ARPD(J)  =  ARPD(J)  +  PCRPD                                             CARD0567
      ARPCC(J)  =  ARPCC(J)  +  PCRPCC                                          CARD0568
      ARPTT(J)  =  ARPTT(J)  +  PCRPTT                                          CARD0569
      AMCD(J)  =  AMCD(J)  +  PCMCD                                             CARD0570
      AMCCC(J)  =  AMCCC(J)  +  PCMCCC                                          CARD0571
      AMCTT(J)  =  AMCTT(J)  +  PCMCTT                                          CARD0572
      ADT(J)  =  ADT(J)  +  PCDT                                                CARD0573
      ACCT(J)  =  ACCT(J)  +  PCCCT                                             CARD0574
      AT(J)  =  AT(J)  +  PCT                                                   CARD0575
                                                                                CARD0576
```

```
      ARPCCB(J) = ARPCCB(J) + PCRPCB                                    CARD0577
      ARPTTB(J) = ARPTTB(J) + PCRPTB                                    CARD0578
      AMCCCB(J) = AMCCCB(J) + PCMCCB                                    CARD0579
      AMCTTB(J) = AMCTTB(J) + PCMCTB                                    CARD0580
      ACCTB(J) = ACCTB(J) + PCCCTB                                      CARD0581
      ATB(J) = ATB(J) + PCTB                                            CARD0582
                                                                        CARD0583
      SFTV(J) = SFTV(J) + FT*VOL                                        CARD0584
                                                                        CARD0585
      AEFTOT(J) = AEFTOT(J) + EFTOT                                     CARD0586
  100 CONTINUE                                                          CARD0587
C                                                                       CARD0588
                                                                        CARD0589
      AHMKGL = AHMKGL + HMKGLD                                          CARD0590
                                                                        CARD0591
      ATHMLD = AHMKGL/ 1000.0                                           CARD0592
      AVOL = AVOL + VOL                                                 CARD0593
      CONV1 = 1.0/AHMKGL                                                CARD0594
      AU28MO = AU28MO + U28MO                                           CARD0595
      AP49MO = AP49MO + P49MO                                           CARD0596
      AP40MO = AP40MO + P40MO                                           CARD0597
      AP41MO = AP41MO + P41MO                                           CARD0598
      AP42MO = AP42MO + P42MO                                           CARD0599
      A28MRO = AU28MO*CONV1                                             CARD0600
      A49MRO = AP49MO*CONV1                                             CARD0601
      A40MRO = AP40MO*CONV1                                             CARD0602
      A41MRO = AP41MO*CONV1                                             CARD0603
      A42MRO = AP42MO*CONV1                                             CARD0604
      EPSO = A49MRO + A41MRO                                            CARD0605
                                                                        CARD0606
      IF(NCOUNT.LT.NVR) GO TO 10                                        CARD0607
      IAR = IAR + 1                                                     CARD0608
                                                                        CARD0609
      PRINT 400                                                         CARD0610
      PRINT 1001                                                        CARD0611
 1001 FORMAT(3X,23H ANNULAR REGION RESULTS)                             CARD0612
```

```
      PRINT 1002                                                        CARD0613
 1002 FORMAT(//6X,4H IAR)                                               CARD0614
      PRINT 1003, IAR                                                   CARD0615
 1003 FORMAT(6X,I2)                                                     CARD0616
      PRINT 2001                                                        CARD0617
 2001 FORMAT(//5X,5H AVOL,5X,4X,7H AHMKGL)                              CARD0618
      PRINT 2002,  AVOL, AHMKGL                                         CARD0619
 2002 FORMAT(1X,2E15.5)                                                 CARD0620
      PRINT 2222                                                        CARD0621
      PRINT 1004                                                        CARD0622
      RTIMEY = 0.0                                                      CARD0623
      TIMED = 0.0                                                       CARD0624
      PRINT 1005, RTIMEY, TIMED                                         CARD0625
      PRINT 1006                                                        CARD0626
      PRINT 1007, AU28MO,AP49MO,AP40MO,AP41MO,AP42MO                    CARD0627
      PRINT 10071                                                       CARD0628
      PRINT 1107,A28MRO,A49MRO,A40MRO,A41MRO,A42MRO,EPSO                CARD0629
                                                                        CARD0630
      CONV  =  AARPE/(1000.0*AHMKGL)                                    CARD0631
                                                                        CARD0632
      DO 10000   J=1,NTS                                                CARD0633
      FAMPD(J)  =  AMPD(J)*CONV                                         CARD0634
      FAMPCC(J)  =  AMPCC(J)*CONV                                       CARD0635
      FAMPTT(J)  =  AMPTT(J)*CONV                                       CARD0636
      FAFBD(J)  =  AFBD(J)*CONV                                         CARD0637
      FAFBCC(J)  =  AFBCC(J)*CONV                                       CARD0638
      FAFBTT(J)  =  AFBTT(J)*CONV                                       CARD0639
      FARPD(J)  =  ARPD(J)*CONV                                         CARD0640
      FARPCC(J)  =  ARPCC(J)*CONV                                       CARD0641
      FARPTT(J)  =  ARPTT(J)*CONV                                       CARD0642
      FAMCD(J)  =  AMCD(J)*CONV                                         CARD0643
      FAMCCC(J)  =  AMCCC(J)*CONV                                       CARD0644
      FAMCTT(J)  =  AMCTT(J)*CONV                                       CARD0645
      FADT(J)  =  ADT(J)*CONV                                           CARD0646
      FACCT(J)  =  ACCT(J)*CONV                                         CARD0647
      FAT(J)  =  AT(J)*CONV                                             CARD0648
```

```
      FARPCB(J) = ARPCCB(J)*CONV                                        CARD0649
      FAMCCB(J) = AMCCCB(J)*CONV                                        CARD0650
      FACCTB(J) = ACCTB(J)*CONV                                         CARD0651
      FATB(J) = ATB(J)*CONV                                             CARD0652
      FARPTB(J) = ARPTTB(J)*CONV                                        CARD0653
      FAMCTB(J) = AMCTTB(J)*CONV                                        CARD0654
                                                                        CARD0655
                                                                        CARD0656
C     OTHER GROUPINGS OF COSTS                                          CARD0657
      ABU(J) = AMPD(J) + AMCD(J)                                        CARD0658
      AINV(J) = AMPCC(J) + AMCCC(J)                                     CARD0659
      AINVB(J) = AMPCC(J) + AMCCCB(J)                                   CARD0660
      AMAT(J) = ABU(J) + AINV(J)                                        CARD0661
      AMATB(J) = ABU(J) + AINVB(J)                                      CARD0662
      APRSD(J) = AFBD(J) + ARPD(J)                                      CARD0663
      APRSC(J) = AFBCC(J) + ARPCC(J)                                    CARD0664
      APRST(J) = APRSD(J) + APRSC(J)                                    CARD0665
      APRSCB(J) = AFBCC(J) + ARPCCB(J)                                  CARD0666
      APRSTB(J) = APRSD(J) + APRSCB(J)                                  CARD0667
      AAT(J)  =  AMAT(J) + APRST(J)                                     CARD0668
      AATB(J) = AMATB(J) + APRSTB(J)                                    CARD0669
      AADT(J) = ABU(J) + APRSD(J)                                       CARD0670
      AACCT(J) = AINV(J) + APRSC(J)                                     CARD0671
      AACCTB(J) = AINVB(J) + APRSCB(J)                                  CARD0672
                                                                        CARD0673
      AFT(J)  =  SFTV(J)/AVCL                                           CARD0674
                                                                        CARD0675
                                                                        CARD0676
      ABNUP(J)  =  AEFTOT(J)/ATHMLD                                     CARD0677
                                                                        CARD0678
      A28MR(J) = AU28M(J)*CONV1                                         CARD0679
      A49MR(J) = AP49M(J)*CONV1                                         CARD0680
      A40MR(J) = AP40M(J)*CONV1                                         CARD0681
      A41MR(J) = AP41M(J)*CONV1                                         CARD0682
      A42MR(J) = AP42M(J)*CONV1                                         CARD0683
      EPS(J) = A49MR(J)  +  A41MR(J)                                    CARD0684
```

```
      TJ  =  J                                                          CARD0685
      TIMED =  TJ*DT                                                    CARD0686
      RTIMEY  =  TIMED/(365.0*SLF)                                      CARD0687
      TIME  =  TIMED*86400.0                                            CARD0688
      PRINT 400                                                         CARD0689
      PRINT 1004                                                        CARD0690
 1004 FORMAT(45X,7H RTIMEY,6X,6H TIMED)                                 CARD0691
      PRINT 1005,  RTIMEY,TIMED                                         CARD0692
 1005 FORMAT(44X,F12.8,3X,F12.4)                                        CARD0693
                                                                        CARD0694
      TERTR = AARPT*RTIMEY/(24.0*1000.0)                                CARD0695
      APFRN  =  AEFTOT(J)/TERTR                                         CARD0696
      PRINT 2003                                                        CARD0697
 2003 FORMAT(5X,4H AFT,6X,4X,7H AEFTOT,4X,4X,6H ABNUP,5X,               CARD0698
     1  4X,6H APFRN)                                                   CARD0699
      PRINT 2004,AFT(J),AEFTOT(J),ABNUP(J),APFRN                        CARD0700
 2004 FORMAT(1X,4E15.5)                                                 CARD0701
                                                                        CARD0702
      PRINT 1006                                                        CARD0703
 1006 FORMAT(5X,6H AU28M,4X,5X,6H AP49M,4X,                             CARD0704
     1     5X,6H AP40M,4X,5X,6H AP41M,4X,5X,6H AP42M)                   CARD0705
      PRINT 1007,  AU28M(J),AP49M(J),AP40M(J),AP41M(J),AP42M(J)         CARD0706
 1007 FORMAT(1X,5E15.5)                                                 CARD0707
                                                                        CARD0708
      PRINT 10071                                                       CARD0709
10071 FORMAT(4X,6H A28MR,5X,4X,6H A49MR,5X,4X,6H A40MR,5X,              CARD0710
     1  4X,6H A41MR,5X,4X,6H A42MR,5X,5X,6X,4H EPS)                    CARD0711
      PRINT 1107,A28MR(J),A49MR(J),A40MR(J),A41MR(J),A42MR(J),EPS(J)    CARD0712
 1107 FORMAT(1X,5F15.8,5X,F15.8)                                        CARD0713
                                                                        CARD0714
      TMP = 0.5*RTIMEY  +  TMPPRE                                       CARD0715
      DISFMP = 1.0/((1.0+DISRTE)**(-TMP))                               CARD0716
      CCFMP  =  TAXF1*DISFMP  -  TAXF2  -  1.0                          CARD0717
      TFB = 0.5*RTIMEY  +  TFPRE                                        CARD0718
      DISFF = 1.0/((1.0+DISRTE)**(-TFB))                                CARD0719
                                                                        CARD0720
```

```
      CCFF =  TAXF1*DISFF -TAXF2  -  1.0                                CARD0721
      TRP  =  -(0.5*RTIMEY  +  TRPPST)                                  CARD0722
      DISFRP  =  1.0/((1.0+DISRTE)**(-TRP))                             CARD0723
      CCFRP = DISFRP - 1.0                                              CARD0724
      CCFRPB  =  TAXF1*DISFRP - TAXF2 - 1.0                             CARD0725
      TMC = -(0.5*RTIMEY + TMCPST)                                      CARD0726
      DISFMC = 1.0/((1.0+DISRTE)**(-TMC))                               CARD0727
      CCFMC = DISFMC - 1.0                                              CARD0728
      CCFMCB = TAXF1*DISFMC - TAXF2 - 1.0                               CARD0729
      PRINT 303                                                         CARD0730
      PRINT 304,CCFMP,CCFF,CCFRP,CCFMC                                  CARD0731
      PRINT 30310                                                       CARD0732
      PRINT 3041,CCFMP,CCFF,CCFRPB,CCFMCB                               CARD0733
                                                                        CARD0734
      PRINT 1008                                                        CARD0735
 1008 FORMAT(//24H POWER COSTS (MILLS/KWH))                             CARD0736
      PRINT 804                                                         CARD0737
      PRINT 814,AMPD(J),AFBD(J),ARPD(J),AMCD(J),ADT(J),ARPD(J),AMCD(J),  CARD0738
     1  ADT(J)                                                          CARD0739
      PRINT 815,AMPCC(J),AFBCC(J),ARPCC(J),AMCCC(J),ACCT(J),ARPCCB(J),  CARD0740
     1   AMCCCB(J),ACCTB(J)                                             CARD0741
      PRINT 816,AMPTT(J),AFBTT(J),ARPTT(J),AMCTT(J),AT(J),ARPTTB(J),    CARD0742
     1  AMCTTB(J),ATB(J)                                                CARD0743
                                                                        CARD0744
                                                                        CARD0745
      PRINT 3030                                                        CARD0746
      PRINT 3032,  ABU(J),APRSD(J),AADT(J)                              CARD0747
      PRINT 3033,AINV(J),APRSC(J),AACCT(J)                              CARD0748
      PRINT 3034,  AMAT(J),APRST(J),AAT(J)                              CARD0749
      PRINT 3031                                                        CARD0750
      PRINT 3032,  ABU(J),  APRSD(J),AADT(J)                            CARD0751
      PRINT 3033,AINVB(J),APRSCB(J),AACCTB(J)                           CARD0752
      PRINT 3034,  AMATB(J),APRSTB(J),AATB(J)                           CARD0753
                                                                        CARD0754
      PRINT 1013                                                        CARD0755
 1013 FORMAT(//30H POWER COSTS ($/YR/KGHMLOADED))                       CARD0756
```

```
 PRINT 804                                                              CARD0757
 PRINT 1014, FAMPD(J),FAFBD(J),FARPD(J),FAMCD(J),FADT(J),               CARD0758
1  FARPD(J),FAMCD(J),FADT(J)                                           CARD0759
 PRINT 1015, FAMPCC(J),FAFBCC(J),FARPCC(J),FAMCCC(J),FACCT(J),          CARD0760
1    FARPCB(J),FAMCCB(J),FACCTB(J)                                     CARD0761
 PRINT 1016, FAMPTT(J),FAFBTT(J),FARPTT(J),FAMCTT(J),FAT(J),            CARD0762
1    FARPTB(J),FAMCTB(J),FATB(J)                                       CARD0763
                                                                        CARD0764
                                                                        CARD0765
 ABU(J) = ABU(J)*CONV                                                   CARD0766
 AINV(J) = AINV(J)*CONV                                                 CARD0767
 AINVB(J) = AINVB(J)*CONV                                               CARD0768
 AMAT(J) = AMAT(J)*CONV                                                 CARD0769
 AMATB(J) = AMATB(J)*CONV                                               CARD0770
 APRSD(J) = APRSD(J)*CONV                                               CARD0771
 APRSC(J)  =  APRSC(J)*CONV                                             CARD0772
 APRST(J) = APRST(J)*CONV                                               CARD0773
 APRSCB(J) = APRSCB(J)*CONV                                             CARD0774
 APRSTB(J) = APRSTB(J)*CONV                                             CARD0775
 AAT(J) = AAT(J)*CONV                                                   CARD0776
 AATB(J) = AATB(J)*CONV                                                 CARD0777
 AADT(J) = AADT(J)*CONV                                                 CARD0778
 AACCT(J) = AACCT(J)*CONV                                               CARD0779
 AACCTB(J) = AACCTB(J)*CONV                                             CARD0780
                                                                        CARD0781
                                                                        CARD0782
 PRINT 3030                                                             CARD0783
 PRINT 3042, ABU(J),APRSD(J),AADT(J)                                    CARD0784
 PRINT 3043, AINV(J),APRSC(J),AACCT(J)                                  CARD0785
 PRINT 3044, AMAT(J),APRST(J),AAT(J)                                    CARD0786
 PRINT 3031                                                             CARD0787
 PRINT 3042, ABU(J),APRSD(J),AADT(J)                                    CARD0788
 PRINT 3043, AINVB(J), APRSCB(J),AACCTB(J)                              CARD0789
 PRINT 3044, AMATB(J),APRSTB(J),AATB(J)                                 CARD0790
                                                                        CARD0791
                                                                        CARD0792
```

```
2222 FORMAT(//5X,80H METHOD(A): (MATCRE-REPR) IS TAXED.     METHOD(B):      CARD0793
    1(MATCRE-REPR) IS CAPITALIZED.)                                         CARD0794
 804 FORMAT(2X,7H MATPUR,3X,4X,4H FAB,4X,3X,8H REPR(A),1X,2X,               CARD0795
    1  10 H MATCRE(A),3X,4X,10H TOTALS(A),7X,8H REPR(B),1X,2X,             CARD0796
    2   10H MATCRE(B),3X,4X,10H TOTALS(B))                                  CARD0797
 814 FORMAT(1X,4F12.8,4X,F12.8,5X,2F12.8,4X,F12.8,5X,7H DIRECT)             CARD0798
 815 FORMAT(1X,4F12.8,4X,F12.8,5X,2F12.8 ,4X,F12.8,5X,7H CARCHG)            CARD0799
 816 FORMAT(1X,4F12.8,4X,F12.8,5X,2F12.8,4X,F12.8,5X,7H TOTALS)             CARD0800
1014 FORMAT(1X,4F12.2,4X,F12.2,5X,2F12.2,4X,F12.2,5X,7H DIRECT)             CARD0801
1015 FORMAT(1X,4F12.2,4X,F12.2,5X,2F12.2,4X,F12.2,5X,7H CARCHG)             CARD0802
1016 FORMAT(1X,4F12.2,4X,F12.2,5X,2F12.2,4X,F12.2,5X,7H TOTALS)             CARD0803
                                                                            CARD0804
3030 FORMAT(3X,9H MATERIAL,18X,3X,11H PROCESSING,16X,3X,7H TOTALS,20X,      CARD0805
    1     10H METHOD(A))                                                    CARD0806
3031 FORMAT(3X,9H MATERIAL,18X,3X,11H PROCESSING,16X,3X,7H TOTALS,20X,      CARD0807
    1     10H METHOD(B))                                                    CARD0808
3032 FORMAT(6X,8H DIR(BU),4X,F12.8,6X,4H DIR,8X,F12.8,6X,F12.8,             CARD0809
    1 7H DIRECT)                                                            CARD0810
3033 FORMAT(6X,12H CARCHG(INV),F12.8,6X,7H CARCHG,5X,F12.8,6X,F12.8,        CARD0811
    1 7H CARCHG)                                                            CARD0812
3034 FORMAT(6X,7H TOTMAT,5X,F12.8,6X,8H TOTPROC,4X,F12.8,6X,F12.8,          CARD0813
    1 7H TOTALS)                                                            CARD0814
                                                                            CARD0815
3042 FORMAT(6X,8H DIR(BU),4X,F12.2,6X,4H DIR,8X,F12.2,6X,F12.2,             CARD0816
    1 7H DIRECT)                                                            CARD0817
3043 FORMAT(6X,12H CARCHG(INV),F12.2,6X,7H CARCHG,5X,F12.2,6X,F12.2,        CARD0818
    1  7H CARCHG)                                                           CARD0819
3044 FORMAT(6X,7H TOTMAT,5X,F12.2,6X,8H TOTPROC,4X,F12.2,6X,F12.2,          CARD0820
    1  7H TOTALS)                                                           CARD0821
                                                                            CARD0822
                                                                            CARD0823
     PRINT 4013                                                             CARD0824
4013 FORMAT(//27H POWER COSTS ($/KGHMLOADED))                               CARD0825
     FAMPD(J) = FAMPD(J)      * RTIMEY                                      CARD0826
     FAFBD(J) = FAFBD(J)      * RTIMEY                                      CARD0827
     FARPD(J) = FARPD(J)      * RTIMEY                                      CARD0828
```

```
      FAMCD(J) = FAMCD(J)       * RTIMEY                                CARD0829
      FADT(J) = FADT(J)         * RTIMEY                                CARD0830
      FAMPCC(J) = FAMPCC(J)     * RTIMEY                                CARD0831
      FAFBCC(J) = FAFBCC(J)     * RTIMEY                                CARD0832
      FARPCC(J) = FARPCC(J)     * RTIMEY                                CARD0833
      FAMCCC(J) = FAMCCC(J)     * RTIMEY                                CARD0834
      FACCT(J) = FACCT(J)    * RTIMEY                                   CARD0835
      FARPCB(J)=FARPCB(J)       * RTIMEY                                CARD0836
      FAMCCB(J) = FAMCCB(J)     * RTIMEY                                CARD0837
      FACCTB(J) = FACCTB(J)     * RTIMEY                                CARD0838
      FAMPTT(J) = FAMPTT(J)     * RTIMEY                                CARD0839
      FAFBTT(J) = FAFBTT(J)     * RTIMEY                                CARD0840
      FARPTT(J) = FARPTT(J)     * RTIMEY                                CARD0841
      FAMCTT(J) = FAMCTT(J)     * RTIMEY                                CARD0842
      FAT(J) = FAT(J)           * RTIMEY                                CARD0843
      FARPTB(J) = FARPTB(J)     * RTIMEY                                CARD0844
      FAMCTB(J) = FAMCTB(J)     * RTIMEY                                CARD0845
      FATB(J) = FATB(J)         * RTIMEY                                CARD0846
      ABU(J) = ABU(J)           * RTIMEY                                CARD0847
      AINV(J) = AINV(J)*RTIMEY                                          CARD0848
      AINVB(J) = AINVB(J)       * RTIMEY                                CARD0849
      AMAT(J) = AMAT(J)         * RTIMEY                                CARD0850
      AMATB(J) = AMATB(J)       * RTIMEY                                CARD0851
      APRSD(J) = APRSD(J)       * RTIMEY                                CARD0852
      APRSC(J) = APRSC(J)       * RTIMEY                                CARD0853
      APRST(J) = APRST(J)       * RTIMEY                                CARD0854
      APRSCB(J) = APRSCB(J)     * RTIMEY                                CARD0855
      APRSTB(J) = APRSTB(J)     * RTIMEY                                CARD0856
      AAT(J) = AAT(J)           * RTIMEY                                CARD0857
      AATB(J) = AATB(J)         * RTIMEY                                CARD0858
      AADT(J) = AADT(J)         * RTIMEY                                CARD0859
      AACCT(J) = AACCT(J)       * RTIMEY                                CARD0860
      AACCTB(J) = AACCTB(J)     * RTIMEY                                CARD0861
      PRINT 804                                                         CARD0862
      PRINT 1014, FAMPD(J),FAFBD(J),FARPD(J),FAMCD(J),FADT(J),          CARD0863
     1  FARPD(J),FAMCD(J),FADT(J)                                       CARD0864
```

```
      PRINT 1015, FAMPCC(J),FAFBCC(J),FARPCC(J),FAMCCC(J),FACCT(J),          CARD0865
     1    FARPCB(J),FAMCCB(J),FACCTB(J)                                      CARD0866
      PRINT 1016, FAMPTT(J),FAFBTT(J),FARPTT(J),FAMCTT(J),FAT(J),            CARD0867
     1    FARPTB(J),FAMCTB(J),FATB(J)                                        CARD0868
      PRINT 3030                                                            CARD0869
      PRINT 3042, ABU(J),APRSD(J),AADT(J)                                   CARD0870
      PRINT 3043, AINV(J),APRSC(J),AACCT(J)                                 CARD0871
      PRINT 3044, AMAT(J),APRST(J),AAT(J)                                   CARD0872
      PRINT 3031                                                            CARD0873
      PRINT 3042, ABU(J),APRSD(J),AADT(J)                                   CARD0874
      PRINT 3043, AINVB(J), APRSCB(J),AACCTB(J)                             CARD0875
      PRINT 3044, AMATB(J),APRSTB(J),AATB(J)                                CARD0876
                                                                            CARD0877
      RMCD  =  FAMCD(J)/(FAMPD(J)+FAFBD(J)+FARPD(J))                        CARD0878
      RMCT = FAMCTT(J)/(FAMPTT(J)+FAFBTT(J)+FARPTT(J))                      CARD0879
      RMCTB = FAMCTB(J)/(FAMPTT(J)+FAFBTT(J)+FARPTB(J))                     CARD0880
      PRINT 8210                                                            CARD0881
 8210 FORMAT(//5X,23H MATCRE/MATPUR+FAB+REPR)                               CARD0882
      PRINT 8211                                                            CARD0883
 8211 FORMAT(3X,7H DIRECT,2X,3X,7H TOT(A),2X,3X,7H TOT(B))                  CARD0884
      PRINT 8212, RMCD,RMCT,RMCTB                                           CARD0885
 8212 FORMAT(1X,3F12.6)                                                     CARD0886
                                                                            CARD0887
      AU28M(J)  =  0.0                                                      CARD0888
      AP49M(J)  =  0.0                                                      CARD0889
      AP40M(J)  =  0.0                                                      CARD0890
      AP41M(J)  =  0.0                                                      CARD0891
      AP42M(J)  =  0.0                                                      CARD0892
       AMPD(J)  =  0.0                                                      CARD0893
      FAMPD(J)  =  0.0                                                      CARD0894
       AFBD(J)  =  0.0                                                      CARD0895
      FAFBD(J)  =  0.0                                                      CARD0896
       ARPD(J)  =  0.0                                                      CARD0897
      FARPD(J)  =  0.0                                                      CARD0898
       AMCD(J)  =  0.0                                                      CARD0899
      FAMCD(J)  =  0.0                                                      CARD0900
```

```
      ADT(J)   =   0.0                                                  CARD0901
     FADT(J)   =   0.0                                                  CARD0902
      AMPCC(J)   =   0.0                                                CARD0903
     FAMPCC(J)   =   0.0                                                CARD0904
      AFBCC(J)   =   0.0                                                CARD0905
     FAFBCC(J)   =   0.0                                                CARD0906
      ARPCC(J)   =   0.0                                                CARD0907
     FARPCC(J)   =   0.0                                                CARD0908
      AMCCC(J)   =   0.0                                                CARD0909
     FAMCCC(J)   =   0.0                                                CARD0910
      ACCT(J)   =   0.0                                                 CARD0911
     FACCT(J)   =   0.0                                                 CARD0912
      AMPTT(J)   =   0.0                                                CARD0913
     FAMPTT(J)   =   0.0                                                CARD0914
      AFBTT(J)   =   0.0                                                CARD0915
     FAFBTT(J)   =   0.0                                                CARD0916
      ARPTT(J)   =   0.0                                                CARD0917
     FARPTT(J)   =   0.0                                                CARD0918
      AMCTT(J)   =   0.0                                                CARD0919
     FAMCTT(J)   =   0.0                                                CARD0920
      AT(J)   =   0.0                                                   CARD0921
     FAT(J)   =   0.0                                                   CARD0922

     AEFTOT(J)   =   0.0                                                CARD0923
     ABNUP(J)   =   0.0                                                 CARD0924
     SFTV(J)   =   0.0                                                  CARD0925
     AFT(J)   =   0.0                                                   CARD0926

     ARPCCB(J) = 0.0                                                    CARD0927
     ARPTTB(J) = 0.0                                                    CARD0928
     AMCCCB(J) = 0.0                                                    CARD0929
     AMCTTB(J) = 0.0                                                    CARD0930
     ACCTB(J) = 0.0                                                     CARD0931
     ATB(J) = 0.0                                                       CARD0932
     FARPCB(J) = 0.0                                                    CARD0933
     FAMCCB(J) = 0.0                                                    CARD0934
                                                                        CARD0935
                                                                        CARD0936
```

```
      FACCTB(J) = 0.0                                                   CARD0937
      FARPTB(J) = 0.0                                                   CARD0938
      FAMCTB(J) = 0.0                                                   CARD0939
      FATB(J) = 0.0                                                     CARD0940
      A28MR(J)  =  0.0                                                  CARD0941
      A49MR(J)  =  0.0                                                  CARD0942
      A41MR(J)  =  0.0                                                  CARD0943
      A42MR(J)  =  0.0                                                  CARD0944
      EPS(J)  =  0.0                                                    CARD0945
      ABU(J) = 0.0                                                      CARD0946
      AINV(J)  =  0.0                                                   CARD0947
      AINVB(J)  =  0.0                                                  CARD0948
      AMAT(J)  =  0.0                                                   CARD0949
      AMATB(J)  =  0.0                                                  CARD0950
      APRSD(J)  =  0.0                                                  CARD0951
      APRSC(J)  =  0.0                                                  CARD0952
      APRST(J)  =  0.0                                                  CARD0953
      APRSCB(J)  =  0.0                                                 CARD0954
      APRSTB(J)  =  0.0                                                 CARD0955
      AAT(J)  =  0.0                                                    CARD0956
      AATB(J)  =  0.0                                                   CARD0957
      AADT(J)  =  0.0                                                   CARD0958
      AACCT(J)  =  0.0                                                  CARD0959
      AACCTB(J)  =  0.0                                                 CARD0960
                                                                        CARD0961
10000 CONTINUE                                                          CARD0962
                                                                        CARD0963
                                                                        CARD0964
      NCOUNT  =  0.0                                                    CARD0965
      AHMKGL  =  0.0                                                    CARD0966
      ATHMLD  =  0.0                                                    CARD0967
      AVOL  =  0.0                                                      CARD0968
      AU28MO = 0.0                                                      CARD0969
      AP49MO = 0.0                                                      CARD0970
      AP40MO = 0.0                                                      CARD0971
      AP41MO = 0.0                                                      CARD0972
```

```
      AP42MO = 0.0                                                      CARD0973
      APFRN = 0.0                                                       CARD0974
   10 CONTINUE                                                          CARD0975
C                                                                       CARD0976
      STOP                                                              CARD0977
      END                                                               CARD0978
```

APPENDIX D - REFERENCES

1. Klickman, A.E., et.al., "The Design and Economic Evaluation of Fixed Blankets for Fast Reactors", APDA-156 (Aug. 1963)
2. Klickman, A.E., et.al., "The Design and Economic Evaluation of Mobile Blankets for Fast Reactors," APDA-160 (Mar. 1964)
3. Klickman, A.E., et.al., "The Design and Economic Evaluation of Blankets for Fast Reactors", Trans. ANS, Vol. 7 (June 1964)
4. Hasnain, S.D., and D. Okrent, "On the Design and Management of Fast Reactor Blankets", NSE, 9, 314-322 (1961)
5. Perks, M.A. and R.M. Lord "Effects of Axial and Radial Blanket Design on Breeding and Economics", Proceedings of the Conference on Breeding, Economics and Safety in Large Fast Power Reactors, Argonne, Ill., ANL-6792 (December 1963)
6. Golubev, V.I., M.N. Nikolaev, et.al., "The Effect of Reflectors Made of Various Materials on the Increase in the Number of Neutron Captures in the Uranium Blanket of a Fast Reactor", Soviet Atomic Energy 15 #4 (October 1963)
7. Gooch, D.J. and J. Hall, "The Effect of the Core Radial Reflector on Breeding", United Kingdom Atomic Energy Authority, AEEW-M641 (Classified)
8. Smith, D.C.G, "Uncertainties in Fast Reactor Blanket Design", United Kingdom Atomic Energy Authority, AEEW-M640 (Classified)
9. Egleme, M. and A. Michel, "Technical and Economical Optimization of a Uranium Oxide Radial Blanket for a 1000 MW Sodium Cooled Fast Reactor", Kerntechnik 9, Jg. (1967) H.3/4
10. Froelich, R. "Optimal Radial Blanket Fuel Management for an LMFBR", Trans. ANS Vol. 14 (June 1971)

11. Maeder, C., "Optimization of Gas-Cooled Fast Reactor Blankets", NSE 42, 89-11 (1970).

12. Mayer, L., "Blanketoptimierung am Beispiel eines dampfgekühlten Schnellen Brutreaktors", Nukleonik 11, 193 (1968).

Mayer, L., "Studies on the Optimum Design of the Radial Blanket on the Basis of a Steam-Cooled Fast Breeder" EURFNR 377, PSB No. 263/67 (May 18, 1967).

Mayer, L., "Studies on the Optimum Design of the Axial Blanket on the Basis of a Steam-Cooled Fast Breeder", EURFNR-378, PSB No. 271/67 (July 14, 1967).

Mayer L., "Untersuchungen uber das optimale Blanketmanagement am Beispiel eines dampfgekühlten schellen Brutreaktors", PSB - Bericht 241/66.

13. Brown, G., Department of Nuclear Engineering, Massachusetts Institute of Technology, Ph.D. Thesis (in progress).

14. Nunn, S.E. and D.E. Deonigi "Fuel Cycle Parameters of Sodium Cooled Fast Reactors", BNWL-965 (July 1969).

15. Benndorf, K., et.al. "Variations in Certain Major Reactor Parameters of Sodium-Cooled 1000 MWe Fast Reactor, For Investigation into Fuel Costs and Needs", Karlsruhe, KFK568 (July 1967), EURFNR-384.

16. Buttrey, K.,et.al. "Liquid Metal Fast Breeder Reactor Task Force Fuel Cycle Study", NAA-SR-MEMO-12604 (Jan. 1968).

17. Elias, D. and F.J. Munno "Reactor Fuel Management Optimization in a Dynamic Environment", Nuclear Technology 12 (September 1971).

18. "Reactor Fuel Cycle Costs for Nuclear Power Evaluation", USAEC,WASH-1099.

19. Vondy, D.R., "Appendix F: Basis and Certain Features of the Discount Technique", Appendix F of "A Comparative Evaluation of Advanced Converters", ORNL-3686 (January 1965).

20. Benedict, M., Course notes for MIT course 22.27 "Economics of Nuclear Power", Massachusetts Institute of Technology, Spring, 1967, 1968.

21. "Guide for Economic Evaluation of Nuclear Reactor Plant Designs", NUS Corporation, NUS-531 (January 1969).

22. "Guide to Nuclear Power Cost Evaluation", USAEC, TID-7025 (March 1962)

23. "A Uniform Procedure for Use in the Evaluation of Nuclear Power Reactors", Atomic Industrial Forum (September 1959).

24. Dragoumis, P. et.al., "Estimating Nuclear Fuel-Cycle Costs", Nucleonics (January 1966)

25. Geller, L, et.al. "Analyzing Power Costs for Nuclear Plants", Nucleonics 22, 7 (July 1964).

26. Little, W.W. and R.W. Hardie, "2DB User's Manual - Revision #1", BNWL-831 (August 1969) Battelle Northwest Laboratory.

27. Little, W.W. and R.W. Hardie, "1DX, A One-Dimensional Diffusion Code for Generating Effective Nuclear Cross Sections", BNWL-954 (March 1969), Battelle Northwest Laboratory.

28. Little, W.W., R.W. Hardie, L.D. O'Dell and R.B. Kidman, "Fuel management Models and Analysis for the Fast Test Reactor", BNWL-SA-2758 (December 1969), Battelle Northwest Laboratory.

29. Hirons, T.J. and R.D. O'Dell, "Calculational Modeling Effects on Fast Breeder Fuel Cycle Analysis", LA-4187 (September 26, 1969), Los Alamos Scientific Laboratory.

30. Hirons, T.J. and R.E. Alcouffe "Heterogeneity Effects on Large Fast Breeder Fuel Cycle Calculations" Trans ANS 13, 1 (June 1970).

31. Hirons, T.J. and R.D. O'Dell, "PHENIX: A Two-Dimensional Diffusion-Burnup-Refueling Code", NSE (March 1970).

32. Hoover, J. and D.A. Meneley, et.al., "The Fuel Cycle Analysis System, REBUS", NSE (July 1971).

33. Little, W.W., R.W. Hardie, et.al., "Numerical Comparison of Data Processing Codes for Fast Reactors", Trans ANS 12, 1 (June 1969).

34. Little, W.W. and R.W. Hardie, "PYRE - A Multigroup Burnup Code for Fast Reactors", BNWL-54 (April 1965) Battelle Northwest Laboratory.

35. Mayer, L. et.al., "Preliminary Description of the ASB Two-Dimensional Burnup Program Version of the Interatom Program for the IBM 360/65", EURFNR-729, EUR-431d, KFK 1079 (November 1969).

36. Channon, F.R., et.al. "Fast Reactor Fuel Burnup", Nuclear Applications (February 1965).

37. Hoover, L.J. and D.A. Meneley, "The Influence of Neutron Energy Group Structure on Fuel Cycle Analysis of Fast Breeder Reactors", Trans ANS 12, 2(November 1969).

38. Brewer, S.T., M.J. Driscoll and E.A. Mason, "FBR Blanket Depletion Studies - Effect of Number of Energy Groups", Trans ANS (November 1970).

39. Toppel, B.J., A.L. Rago and D.M. O'Shea, "MC^2: A Code to Calculate Multigroup Cross Sections", ANL-7318 (1967) Argonne National Laboratory.

40. Cowan, C.L., et.al., "TDOWN - A Code to Generate Composition and Spatially Dependent Cross Sections", GEAP 13740 (August 1971).

41. Vondy, D.R. "Calculation of Depletion in Nuclear Reactor Cores", Background information for a panel discussion on Comparison of Depletion Calculational Methods for Fuel Cycle Analysis, ANS Meeting June 1970.

42. Hirons, T.J., "Reactor Fuel-Cycle Analysis at Los Alamos Scientific Laboratory," Background information for a panel discussion on Comparison of Depletion Calculational Methods for Fuel Cycle Analysis, ANS meeting June 1970.

43. Rothleder, B.M., "Some Depletion Methods Used at WNES", Background information for a panel discussion on Comparison of Depletion Calculational Methods for Fuel Cycle Analysis, ANS meeting, June, 1970.

44. Sheaffer , M., et.al. "A One-Group Method for Fast Reactor Calculations" MIT-4105-1, MITNE-108 (September 1970).

45. Greebler, P. and C.L. Cowan, "FUMBLE: An Approach to Fast Reactor Fuel Management and Burnup Calculations", GEAP-13599 (February 1971).

46. Engle, W.W., "A User's Manual for ANISN", K-1693 (March 1967).

47. Fowler, T.B., and D.R. Vondy "Nuclear Reactor Core Analysis Code: CITATION", ORNL-TM-2496 Rev. 1 (January 1970).

48. Bondarenko, I.I.,et.al. "Group Constants for Nuclear Reactor Calculations", Consultants Bureau, New York (1964).

49. Yiftah, S., D. Okrent and P.A. Moldauer, "Fast Reactor Cross Sections", Pergamon Press, New York (1960).

50. Hansen, H.E. and W.H. Roach "Six and Sixteen Group Cross Sections for Fast and Intermediate Critical Assemblies", LAMS-2543 (Dec. 1961).

51. Inoue, K., "Fast Reactor Core Design Optimization by Linear Programming", NSE (March 1970).

52. Goldschmidt, P. and J. Quenon, "Minimum Critical Mass in Fast Reactors with Bounded Power Density", NSE (March 1970).

53. Tzanos, C.P., et.al., "Optimization of Material Distributions in Fast Breeder Reactors", MIT-4105-6, MITNE-128 (August 1971).

54. Heusener, G., "Optimization of Sodium-Cooled Fast Breeders by Non-linear Programming Methods", Karlsruhe, KFK 1238, EURFNR-830 (July 1970).

55. Terasawa, S., et.al., "Parametric Studies Leading to the Nuclear Characteristics of the JAERI Design Studies", ANL-7520 (November 1968).

56. Wright, J.H., "Core Design and Performance Considerations of FBR's" Westinghouse Engineer (January 1968).

57. "Electricity Too Cheap to Meter", Nuclear News (October 1968).

58. "Fast Breeder Reactor Report", Edison Electric Institute, EEI Pub. #68-28 (April 1968).

59. "Report of the EEI Reactor Assessment Panel", Edison Electric Institute, EEI Pub #70-30 (April 1970).

60. Forbes, I.A., "Design, Construction, and Evaluation of a Facility for the Similation of Fast Reactor Blankets", MIT-4105-2, MITNE-110, (February 1970).

61. "LMFBR Blanket Physics Project, Progress Report #1", Massachusetts Institute of Technology, MIT-4105-3, MITNE-116 (June 30, 1970).

62. "Large Fast Reactor Design Study", Allis-Chalmers, Atomic Power Development Associates, and Babcock and Wilcox, ACNP-64503 (January 1964)

63. "Feasibility Study of a 1000MWe Sodium-Cooled Fast Reactor", Atomics International, NAA-SR-11378 (June 1965).

64. "Liquid Metal Fast Breeder Reactor Design Study", Combustion Engineering CEND-200 (January 1964).

65. "Liquid Metal Fast Breeder Reactor Design Study", General Electric, GEAP-4418 (January 1964).

66. "Liquid Metal Fast Breeder Reactor Design Study", Westinghouse, WCAP-3251-1 (January 1964).

67. "An Evaluation of Four Design Studies of a 1000 MWe Ceramic Fuel Fast Breeder Reactor", Chicago Operations Office, USAEC, COO-279, December 1, 1964).

68. "An Evaluation of the Atomics International 1000 MWe Fast Breeder Reactor", Chicago Operations Office, USAEC, COO-285 (July 1966).

69. Babcock and Wilcox 1000 MWe LMFBR Follow-on Studies

"1000 MWe Follow-on Study Task I Report", BAW-1316
Vol. 1 Task I Report (June 1967)
Vol. 2 Task I Concept I System Description Report (April 1967)
Vol. 3 Task I Concept II System Description Report (June 1967)
Vol. 4 Task I Concept III System Description Report (July 1967)
Vol. 5 Task I Concept IV System Description Report (August 1967)

"1000 MWe LMFBR Follow-on Study Task II and III FinalReport", BAW-1328
Vol. 1 Summary Description and Cost Estimate (February 1969)
Vol. 2 Conceptual System Design Description (March 1969)
Vol. 3 Conceptual System Design Description (February 1969)
Vol. 4 Trade-Off Studies (November 1968)
Vol. 5 Parametric Studies (January 1969)

"1000 MWe LMFBR Follow-on Study-Control Studies"(December 1968) BAW-1330

"Sodium Parameter Study Code NAPS - Topical Report"(April 1968) BAW-1326

"1000 MWe LMFBR Follow-on Study - Task IV Final Report - Research and Development Requirement" (June 1969) BAW-1331 Vols. I and II.

70. Atomics International 1000 MWe LMFBR Follow-on Studies

"ANL 1000 MWe LMFBR Follow-on Study Task I Report", Vols. 1 and 2 (May 1968), AI-AEC-12765 (rev.).

"1000 MWe LMFBR Follow-on Study Task II Report-Conceptual Systems Design Descriptions", Vols. I, II, III (May 1969), AI-AEC-12791.

"1000 MWe LMFBR Follow-on Study Task III - Conceptual Design Report", Vols. I, II, III, IV, V (June 1969) AI-AEC-12792.

"1000 MWe LMFBR Follow-on Study Task IV Report-Research and Development Requirements", (June 1969), AI-AEC-12793.

71. Combustion Engineering 1000 MWe LMFBR Follow-on Studies

"1000 MWe LMFBR Follow-on Study.Task I Report.Preliminary Studies for a reference Conceptual Design" (December 1967) CEND-322.

"1000 MWe LMFBR Follow-on Study.Task II and III Report.A Conceptual Design" CEND-337
Vol. I Conceptual System Design Descriptions (July 1968)
Vol. II Static Design and Performance Analysis (May 1968)
Vol. III Safety and Control Analyses (September 1968)

"1000 MWe LMFBR Follow-on Study.Task IV Report. A Research and Development Program Needed for the CE Reference Concept". (February 1969) CEND-346.

72. General Electric 1000 MWe LMFBR Follow-on Studies

"Comparison of Two Sodium Cooled 1000 MWe Fast Reactor Concepts. Task I Report of 1000 MWe LMFBR Follow-on Work " (June 1968) GEAP-5618.

"Conceptual Plant Design, System Descriptions, and Costs for a 1000 MWe Sodium-Cooled Fast Reactor. Task II Report of 1000 MWe LMFBR Follow-on Work" (September 1968) GEAP-5678.

"Methods System Optimization, and Safety Studies for a 1000 MWe Sodium-Cooled Fast Reactor. Task III and V Report of 1000 MWe LMFBR Follow-on Work" (February 1969) GEAP-5710.

"Research and Development Requirements for a 1000 MWe Sodium-Cooled Fast Reactor. Task IV Report of 1000 MWe LMFBR Follow-on Work" (April 1969), GEAP-5769.

73. Westinghouse 1000 MWeLMFBR Follow-on Studies

"1000 MWe LMFBR Follow-on Study. Task I Final Report" (June 1968) WARD-2000-33.

"1000 MWe LMFBR Follow-on Study. Task I Topical Report. Moisture Separation or Steam Reheat vs. Sodium Reheat. Plant Cycle Technical and Economic Evaluation". (April 1968) WARD-2000-20.

"1000 MWe LMFBR Follow-on Study. Task I Topical Report. Steam Generator Concept Selection" (January 1968) WARD-2000-22.

"1000 MWe LMFBR Follow-on Study. Task I Topical Report. Survey of State-of-the-Art of Intermediate Heat Exchanges" (March 1968) WARD-2000-23.

"1000 MWe LMFBR Follow-on Study. Task I Topical Report. Evaluation of Vented-to-Coolant Design for Sodium-Bonded Carbide Fuel Rods" (February 1968) WARD-2000-31.

"1000 MWe LMFBR Follow-on Study. Task V Report. Safety Studies" (December 1968) WARD-2000-84.

"1000 MWe LMFBR Follow-on Study. Task IV Report. Research and Development" (March 1969) WARD-2000-90.

"1000 MWe LMFBR Follow-on Study. Tasks II and III Topical Report. Comparison of the Westinghouse 1000 MWe LMFBR Reference Design Calculations Using the Westinghouse 6602-M Data and MC^2 Code with Neutron Cross-Section Data from ENDF/B File" (March 1969) WARD-2000-93.

"1000 MWe LMFBR Follow-on Study. Tasks II and III Topical Report. Cost Optimization and Parametric Studies" (March 1969)WARD-2000-96.

"1000 MWe LMFBR Follow-on Study. Tasks II and III Report. Conceptual Design" (April 1969) WARD-2000-97.

74. Aronstein, R.E., et.al., "Atomics International 1000 MWe LMFBR Follow-on Study Progress Report", Proceedings of the International Conference on Sodium Technology and Large Fast Reactor Design (November 1968) Argonne National Laboratory,ANL-7520 Part II.

75. Croft, M.W., et.al., "Babcockand Wilcox 1000 MWe LMFBR Follow-on Study Reference Design", Proceedings of the International Conference on Sodium Technology and Large Fast Reactor Design (November 1968), Argonne National Laboratory, ANL-7520 Part II.

76. Noyles, R.C., et.al., "Development and Evaluation of the Combustion Engineering Advanced 1000 MWe LMFBR Design", Proceedings of the International Conference on Sodium Technology and Large Fast Reactor Design (November 1968), Argonne National Laboratory ANL-7520 Part II.

77. Hafele, W., et.al., "The Karlsruhe Reference Design of a 1000 MWe Sodium Cooled Fast Breeder Reactor", Proceedings of the Conference on Safety, Fuels and Core Design in Large Fast Power Reactors (October 1965), Argonne National Laboratory, ANL-7120

78. Jansen, A. "The Long Time Behavior of FBR's with Pu-Recycle", Proceedings of the Symposium on Fast Reactor Physics and Related Safety Problems, Karlsruhe (October 1967), Fast Reactor Physics, IAEA (1968).

79. Argonne National Laboratory, 1000 MWe LMFBR Follow-on Study: Evaluation Report, Draft (January 16, 1970).

Vol. I - Summary Report
Vol. II - Plant Design
Vol. III - Research and Development
Vol. IV - Backup and Contractual Material.

80. Koncel, E.F., Commonwealth Edison Company, personal communication December 4, 1969.

81. Little, W.W. and R.W. Hardie, Battelle Northwest Laboratory, personal communications, April, May 1970.

82. Corey, Gordon, Commonwealth Edison Company, Lectures at Massachusetts Institute of Technology:

"Certain Aspects of Current Financial and Regulatory Developments" (April 8, 1969)

"Financial Problems Related to Nuclear Power"(March 5, 1968).

83. Riley, Don, USAEC, Lecture at Massachusetts Institute of Technology (January 1971), Short course on LMFBR Core Design,"Overall Core Design View".

84. Driscoll, M.J., Massachusetts Institute of Technology, personal communication January 1972.